Doctoral theses at NTNU, 2021:391

Silje Marie Smitt

Investigation of integrated CO_2 heat pumping systems for hotels in cold climates

Doctoral thesis

Silje Marie Smitt

ISBN 978-82-326-5228-0 (printed ver.)
ISBN 978-82-326-5738-4 (electronic ver.)
ISSN 1503-8181 (printed ver.)
ISSN 2703-8084 (electronic ver.)

NTNU
Norwegian University of
Science and Technology

NTNU
Norwegian University of
Science and Technology
Thesis for the degree of
Philosophiae Doctor
Faculty of Engineering
Department of Energy and Process Engineering

Doctoral theses at NTNU, 2021:391

NTNU

NTNU
Norwegian University of
Science and Technology

Silje Marie Smitt

Investigation of integrated CO_2 heat pumping systems for hotels in cold climates

Thesis for the degree of Philosophiae Doctor

Trondheim, December 2021

Norwegian University of Science and Technology
Faculty of Engineering
Department of Energy and Process Engineering

NTNU
Norwegian University of
Science and Technology

NTNU
Norwegian University of Science and Technology

Thesis for the degree of Philosophiae Doctor

Faculty of Engineering
Department of Energy and Process Engineering

ISBN 978-82-326-5228-0 (printed ver.)
ISBN 978-82-326-5738-4 (electronic ver.)
ISSN 1503-8181 (printed ver.)
ISSN 2703-8084 (electronic ver.)

Doctoral theses at NTNU, 2021:391

PRINTED IN NORWAY
NO - 1598

NORDIC SWAN ECOLABEL
Printed matter
2041 0731

Printed by Skipnes Kommunikasjon AS

Preface

This doctoral thesis is submitted in partial fulfillment of the requirements for the academic degree *philosophiae doctor* at the Norwegian University of Science and Technology (NTNU), Trondheim, Norway. The work was carried out in the Refrigeration group at the Department of Energy and Process Engineering, under the supervision of Professor Armin Hafner and co-supervised by Professor Trygve Magne Eikevik and Dr. Ignat Tolstorebrov.

This doctoral work was created and financed by NTNU.

Acknowledgments

First of all, this thesis would not have been possible without the support and guidance from my supervisor, Professor Armin Hafner. I am grateful for your advice and good discussions during my many years at NTNU. Your passionate enthusiasm for natural refrigerants is contagious and truly inspiring. Thanks also go to my co-supervisor, Professor Trygve Magne Eikevik, for sharing his experience and for always having an open door to discuss my research, as well as all the big and little things in life. I am truly grateful to my co-supervisor, Dr. Ignat Tolstorebrov, for taking me under his wing and for his continuous involvement and interest in my research work. I very much appreciated our many coffee breaks and heated discussions.

Thanks to all the co-authors of my papers, especially Dr. Ángel Álvarez Pardiñas, for the fruitful collaboration, good advice and critical reviews that improved the standard of the research.

My colleagues at NTNU all contributed to an interesting and encouraging work atmosphere - thank you all for making this journey fun and memorable. Special thanks to my good friends and fellow PhD students Knut Ringstad, Håkon Selvnes, Marcel Ahrens and Ehsan Allymehr - without you, I would have finished the doctoral work a year earlier.

I am forever grateful to my family for their love and support. Thank you to Yacine for always reminding me of the important things in life and for showing great patience while helping me through countless programming challenges dealing with my allegedly ”messy” scripts.

To my mother and number one fan, thank you for encouraging me to try new things and make nontraditional choices. This doctoral thesis is dedicated to you.

Summary

The hotel sector features high thermal demands, often realized through processes that advance the global warming effect. The energy consumption within the hotel sector is high compared to other commercial sectors due to the high number of occupants. Excessive energy use within the hotel sector in cold climates is primarily contributed to the thermal energy production of domestic hot water, space heating and cooling. Moreover, the application of conventional and inefficient thermal energy sources in hotels is extensive. Consequently, an efficient and environmentally friendly solution for thermal energy production is necessary to reduce the specific energy consumption and ensure sustainable growth within the sector.

Heat pump systems satisfy these criteria by reducing energy consumption and operational costs related to thermal energy production. The application of natural and environmentally friendly refrigerants, such as carbon dioxide (CO_2), or R744, has gained much attention as an approach to reduce greenhouse gas emissions from refrigeration, air-conditioning, and heat pump systems. The superior thermodynamic properties of CO_2 enables the application of *integrated* systems, in which a single vapor compression system supplies all major thermal demands of the building. The installation of thermal storage is an effective measure to improve the performance of integrated systems. In hotels, thermal storage in the form of hot water tanks can be applied to reduce peak loads. The potential benefits of applying integrated CO_2 systems with thermal storage in hotels are considerable due to the characteristically substantial hot water demand.

The review of state-of-the-art CO_2 applications, particularly integrated CO_2 systems for heat pump applications, indicate the necessity of further investigation and development of CO_2 systems for hotels. In addition, the review demonstrated that the control strategy for hot water production and storage influences the CO_2 system efficiency considerably.

This research work includes a large-scale investigation of the market potential of integrated CO_2 systems within the Nordic hotel sector, an in-depth performance evaluation of an integrated CO_2 hotel unit, and, finally, numerical evaluations of designs and control strategies to enhance performance.

The large-scale data analysis of Norwegian and Swedish hotels revealed that there is a large market potential for integrated CO_2 systems. The hotel sector is characterized by high energy consumption and related emissions. However, a shift towards sustainable energy sources was observed over the five-year investigated period, indicating interest and willingness to adapt energy-efficient and sustainable thermal solutions. Two of the 140 hotels in the analysis were equipped with integrated CO_2 systems. These hotels demonstrated a reduction in specific energy consumption of approximately 60% in relation to thermal energy production. Thus, hotels that use traditional thermal systems could benefit both economically and in terms of emissions by applying integrated CO_2 systems.

The in-depth investigation of an integrated CO_2 hotel unit with thermal storage illustrated that the thermal energy demand of hot water heating represented more than half the annual heat requirement of the hotel. It was found that a substantial thermal storage is essential to ensure high performance of the integrated CO_2 hotel unit, as it reduces peak loads and enables more flexible operations and charging over extended periods of time. Moreover, the storage of the system was found to be inadequate, as it forced the CO_2 unit to operate under unfavorable conditions to fulfill domestic hot water demands. Thus, the flexibility that the storage provided was not fully utilized with the current traditional hot water charging strategy.

A numerical evaluation of the system mentioned above demonstrated that the overall performance of the hotel's thermal system could be enhanced when applying a low load strategy for charging the domestic hot water storage. The principle of the proposed control strategy was to charge the storage at longer periods of time and at reduced loads, thus utilizing the cold supply water to continuously cool down the CO_2 gas cooler outlet temperature and, by this, enhance performance. Applying this strategy resulted in annual energy savings in the range of 8.4%. Further, three different design concepts for integrated CO_2 units were evaluated in terms of energy consumption, environmental impact and economic viability. The main characteristics of the evaluated designs were single-stage compression, parallel compression, and ejector-supported parallel compression. In addition, two hot water charging strategies were implemented and investigated, namely the reduced load strategy and the traditional approach. Applying continuous charging at low loads enhanced the performance of the system over a wide range of ambient temperatures. It was also revealed that the charging strategy was the least expensive measure to enhance performance. Moreover, considerable emission reductions were achieved when applying integrated CO_2 solutions in place of a boiler and HFC chiller.

In summary, integrated CO_2 systems represent an efficient and environmentally friendly option for thermal energy supply within the hotel sector in cold climates. Integrated heating and cooling loads within the same cycle enable high efficiencies, which can be enhanced by applying a thermal storage. However, the specific thermal storage control strategy can influence overall performance considerably. To enhance performance, charging of the hot water thermal storage should take place at low loads over longer time periods.

Contents

Preface i

Acknowledgments iii

Summary v

Contents xiii

List of tables xiii

List of figures xv

Nomenclature xviii

1 Introduction 1

1.1 Motivation 1

1.2 Research objectives 3

1.3 Thesis contents 3

1.4 List of publications 4

1.4.1 Journal publications 4

1.4.2 Conference papers 5

2 Background **7**

2.1 State-of-the-art transcritical CO_2 applications 7

2.2 State-of-the-art integrated CO_2 systems 15

2.2.1 Supermarket applications 16

2.2.2 Heat pump applications 19

2.3 Development of integrated CO_2 systems for hotels 21

2.3.1 Control strategies for domestic hot water production and storage 22

2.4 Summary 24

3 Methodology **25**

3.1 Data collection and analysis 25

3.1.1 Large-scale data analysis 26

3.1.2 In-depth data analysis 27

Uncertainty 28

3.2 Numerical modeling and simulation 29

3.2.1 Principle of the Modelica language and Dymola platform . . 29

3.2.2 Transient model description 29

3.2.3 Model validation process 33

3.3 Summary 35

4 Summary of research work **37**

4.1 Article I: Energy use and retrofitting potential of heat pumps in cold climate hotels 37

4.2 Article II: Integrated CO_2 system with HVAC and hot water for hotels: Field measurements and performance evaluation 39

4.3 Article III: Performance improvement of integrated CO_2 systems with HVAC and hot water for hotels 40

4.4 Article IV: Evaluation of integrated concepts with CO_2 for heating, cooling and hot water production 41

5 Conclusions **43**

6 Suggestions for further work **47**

References **48**

Appendix **59**

List of tables

3.1 Adjustment factor for climate zones in Norway and Sweden. 27
3.2 Model input demands and temperatures. 30
3.3 Setpoints and control objectives for system components. 32
3.4 Comparison between monitored and simulated SCOPs 34

4.1 Performance indicators when applying the low load hot water storage charging strategy. 40

List of figures

2.1 T-s diagram of ideal vapor-compression cycle. 8

2.2 Illustration of typical heat pumping processes. 15

2.3 Illustration of integrated CO_2 supermarket unit in Trondheim. . . . 17

2.4 Illustration of integrated CO_2 supermarket unit in Italy. 18

2.5 Illustration of integrated CO_2 hotel unit in Italy. 21

2.6 Illustration of hot water circuit and thermal storage tanks. 23

3.1 Hotel climate zones. 27

3.2 Illustration of a numerical model developed for the simulation of integrated CO_2 hotel unit. 31

3.3 Measured and simulated values obtained for nominal week. 33

3.4 Measured and simulated hot water values 34

4.1 Available energy sources, primary and secondary thermal heating systems in all hotels. 38

4.2 Schematic drawing of the integrated CO_2 hotel unit. 39

4.3 COP as a function of ambient temperature for the investigated designs when applying the aggressive DHW charging strategy. 41

Nomenclature

Latin symbols

$\dot{Q}$	heat [W]
$\dot{W}$	work [W]
$\overline{v}$	weighted average
C_p	specific heat capacity [J kg^{-1} K^{-1}]
V	volume [m^3]
E	energy [kWh]
P	pressure [bar]
T	temperature [°C]
t	time [sec]
Y	recorded value

Greek symbols

Δ	difference
ρ	density [kg m^{-3}]
σ	uncertainty

Subscripts

a	ambient temperature
AC	air-conditioning
CW	city water
DF	defrost
DHW	domestic hot water
DHW-R	domestic hot water return
DHW-S	domestic hot water supply
eq	equivalent
h	heating
HP	heat pump

HX	heat exchanger
i	index
m	measured
R	return
RH	radiators
s	simulated
tot	total
VH	ventilation

Abbreviations

AC	air-conditioning
CFC	chlorofluorocarbon
CO_2	carbon dioxide
COP	coefficient of performance
DF	defrost heating
EJ	ejector-supported parallel compression
GWP	global warming potential
HCFC	hydrochlorofluorocarbons
HDD	heating degree days
HFC	hydrofluorocarbons
HFO	hydrofluoroolefins
HPWH	heat pump water heater
HVAC	heating, ventilation, and air-conditioning
IHX	internal heat exchanger
LLC	low load charging
LT	low temperature
MT	medium temperature
PC	parallel compression
PI	proportional–integral
R^2	coefficient of determination
RH	radiators
RRMSE	relative root mean square error
SC	single-stage compression
SCOP	seasonal coefficient of performance
TFA	trifluoroacetic acid
VH	ventilation

1 Introduction

This chapter presents the motivation and main objectives of the doctoral work, thesis structure and list of scientific publications within the scope of this thesis.

1.1 Motivation

Tourism, and thereby hotels, play a crucial role in the European economy. The hotel sector features high energy consumption, which greatly contributes to the global warming effect. According to the EU strategic plan for heating and cooling in buildings, new and sustainable solutions for generating thermal energy must be applied to achieve the 2-degree goal of the Paris Agreement [1]. Presently, buildings account for more than 40% of the total end-use energy consumption in Europe [2]. Approximately 1/3 of this energy consumption and related emissions is connected to the commercial sector [3]. By implementing measures to increase efficiency and manage demands, it is estimated that energy saving of 30% can be achieved within the commercial sector [4, 5]. The European hotel sector has increased during the last decade with an annual market growth between 7 to 13%, and it is expected that the number of international visitors will increase by 43 million annually until 2030 [6, 7].

Hotels are energy-intense buildings due to the nature of their operation and the behavior of occupants [8]. The energy consumption in hotels is high compared to other commercial buildings, such as schools and hospitals [9]. The largest contributor to excessive energy use within the hotel sector is hot water, space heating and cooling. In cold climates, it is estimated that approximately 60% of the total energy consumption in hotels is allocated to heating and cooling [10]. Fossil fuel-fired boilers are still the most applied source of heating in Europe despite high emissions [1]. Heating in Nordic hotels has been highly dominated by electric panels or hydronic

heating through electric boilers due to relatively low electricity prices caused by the availability of renewable energy sources. A majority of hotels apply centralized heating stations, where thermal heat is generated and further transported throughout the building by a secondary hydronic circuit. Excessive use of electrical power by peak heating and the use of low-efficiency air-conditioning (AC) units aggravate the electricity problems society is facing. Existing hotels exhibit the most severe problems of excessively high energy demand rates, inevitably requiring renovations along with retrofitting of thermal systems [11]. To reduce the environmental footprint, legislation and favorable incentives have been introduced in Nordic countries to encourages building owners to adopt sustainable heating solutions [12, 13]. Moreover, the environmental aspect of tourism is becoming important for guests when selecting hotels [8]. Nearly 80% of potential guests believe that renewable energy is important for European tourist accommodations [14]. Yet, reducing the operational cost is undeniably the biggest incentive among hotel owners to introduce environmentally-friendly initiatives [15]. Thus, efficient and sustainable solutions for thermal energy production must be applied to reduce the energy consumption and footprint of this growing sector.

Vapor compression systems are among the most energy-efficient methods of providing heating and cooling in buildings. A significant share of AC and heating systems within the hotel sector apply synthetic refrigerants with high environmental impact. Carbon dioxide (CO_2) is a natural refrigerant with negligible environmental impact and favorable thermodynamic properties and is firmly established in both heating and refrigeration applications. Integrated CO_2 heat pump system is a promising technology for space heating and high-temperature hot water production [16]. In these systems, the heat rejection process occurs at gliding temperatures with a high-temperature difference compared with traditional condensers. Thus, CO_2 is superior in heating processes that require a high-temperature lift, such as hot water production [17]. The potential benefits of applying integrated CO_2 systems in hotels are considerable due to the characteristically substantial hot water demand [18]. CO_2 systems can be implemented with ease and high flexibility as a retrofit solution in existing hotels, where other natural refrigerants are limited due to safety restrictions on account of toxicity and flammability. The installation of thermal storage is an effective measure to improve the performance of integrated CO_2 systems and reduce peak loads. Hence, integrated CO_2 systems for heating and cooling may be a suitable solution to increase hotels' thermal efficiency with minimal environmental impact. The market potential and performance of integrated systems in relation to conventional thermal systems should be investigated to quantify potential savings. In addition, detailed system performance evaluations should be performed to identify measures to increase system performance. Moreover, control strategies and system designs can be further investigated to improve the energy efficiency of integrated CO_2 systems for hotel applications.

1.2 Research objectives

The aim of this work is to ***describe concepts and evaluate the performance of integrated CO_2 systems for hotels in cold climates***. As this research involves the application of a novel concept within a new sector, the focus is partially on investigating the potential market. Additionally, it is necessary to analyze the operation of an integrated CO_2 hotel unit to identify measures that can improve system performance. The main research objective can be divided into the following sub-goals:

- Investigate and quantify thermal energy demands within the hotel sector in cold climates to identify the market potential of integrated CO_2 systems.
- Evaluate the performance of an integrated CO_2 hotel system through operational data to identify measures that can improve energy efficiency.
- Develop, apply and validate transient simulation models to evaluate thermal storage charging strategies.
- Design, develop and evaluate concepts for integrated CO_2 systems with thermal storage for hotels in terms of energy efficiency, environmental impact, and economic feasibility.

1.3 Thesis contents

- **Chapter 1** introduces the background and motivation for the doctoral research work. The first part of the introduction demonstrates the advantages related to installing integrated CO_2 units within the hotel sector. Following are the objectives of the thesis and the list of scientific publications.
- **Chapter 2** reviews the technological status of CO_2 as a refrigerant. The first section describes past, current and future state-of-the-art transcritical CO_2 applications. Furthermore, a state-of-the-art review of integrated CO_2 systems is given. A particular focus is granted to integrated CO_2 systems with heating and cooling capabilities, in addition to thermal storage. The last part of the chapter illustrates the development and challenges related to integrated CO_2 systems in hotels in cold climates.
- **Chapter 3** explains the methodologies applied in the doctoral work, in which the focus is to elaborate on the research methods described in the papers. The first part describes data collection and analysis procedures applied to

perform large-scale and in-depth evaluations of thermal systems. The second part describes the software applied in the numerical investigations, model development and simulation model validation.

- **Chapter 4** presents the main research related to the sub-objectives of the doctoral work, which has been performed based on the four journal articles listed in Section 1.4.1. A brief summary is given for each article.
- **Chapter 5** concludes the thesis by presenting the main results, contributions and value of the research work.
- **Chapter 6** gives suggestions for further work to improve integrated CO_2 heat pumps for hotel applications.

1.4 List of publications

The author of this thesis contributed to four journal articles and four conference papers within the subject of CO_2 applications in hotels. All papers are attached in the appendix. The author contributions for each paper are based on the CRediT classification [19] are given below.

1.4.1 Journal publications

Article I

S. Smitt, I. Tolstorebrov, P. Gullo, Á. Pardiñas, A. Hafner (2021). "Energy use and retrofitting potential of heat pumps in cold climate hotels." In: *Journal of Cleaner Production* 298, 2021, 126799. DOI: 10.1016/j.jclepro.2021.126799

Author contributions: Conceptualization: S. Smitt, I. Tolstorebrov, A. Hafner, Investigation: S. Smitt, Formal analysis: S. Smitt, Writing - Original Draft: S. Smitt, P. Gullo, Á. Pardiñas, Writing - Review and Editing: S. Smitt, I. Tolstorebrov, P. Gullo, Á. Pardiñas, Visualization: S. Smitt, Supervision: I. Tolstorebrov, A. Hafner.

Article II

S. Smitt, I. Tolstorebrov, A. Hafner (2020). "Integrated CO_2 system with HVAC and hot water for hotels: Field measurements and performance evaluation." In: *International Journal of Refrigeration* 116, pp. 59-69. DOI: 10.1016/j.ijrefrig.2020.03.021

Author contributions: Conceptualization: S. Smitt, I. Tolstorebrov, A. Hafner, Investigation: S. Smitt, I. Tolstorebrov, Formal analysis: S. Smitt, Writing - Original Draft: S. Smitt, Writing - Review and Editing: S. Smitt, I. Tolstorebrov, Visualization: S. Smitt, Supervision: I. Tolstorebrov, A. Hafner.

Article III

S. Smitt, I. Tolstorebrov, A. Hafner (2021). "Performance improvement of integrated CO_2 systems with HVAC and hot water for hotels." In: *Thermal Science and Engineering Progress* 23, 1 June 2021, 100869. DOI: 10.1016/j.tsep.2021.100869

Author contributions: Conceptualization: S. Smitt, I. Tolstorebrov, A. Hafner, Investigation: S. Smitt, Software: S. Smitt, Writing - Original Draft: S. Smitt, Writing - Review and Editing: S. Smitt, I. Tolstorebrov, Visualization: S. Smitt, Supervision: I. Tolstorebrov, A. Hafner.

Article IV

S. Smitt, Á. Pardiñas, A. Hafner (2021). "Evaluation of integrated concepts with CO_2 for heating, cooling and hot water production." In *Energies* 14 (14), 4103. DOI: https://doi.org/10.3390/en14144103

Author contributions: Conceptualization: S. Smitt, Á. Pardiñas, A. Hafner, Methodology: S. Smitt, Á. Pardiñas, Software: S. Smitt, Investigation: S. Smitt, Original Draft: S. Smitt, Á. Pardiñas, Writing - Review and Editing: S. Smitt, Á. Pardiñas, A. Hafner, Visualization: S. Smitt, Supervision: Á. Pardiñas, A. Hafner.

1.4.2 Conference papers

The following papers are in the scope of the thesis subject and have been published in international conference proceedings during the doctoral research period.

Paper I

S. Smitt, A. Hafner (2018). "Integrated energy concepts for high performance hotel buildings." In: *Proceedings of the 13th IIR Gustav Lorentzen Conference on Natural Refrigerants*, València, Spain.

Author contributions: Conceptualization: S. Smitt, A. Hafner, Investigation: S. Smitt, Resources: A. Hafner, Writing - Original Draft: S. Smitt, Writing - Review and Editing: S. Smitt, A. Hafner, Visualization: S. Smitt, Supervision: A. Hafner.

Paper II

S. Smitt, A. Hafner, E. Hoksrød (2019). "Presentation of the first combined CO_2 heat pump, air conditioning and hot tap water system for a hotel in Scandinavia." In: *Proceedings of the 8th IIR International Conference on Ammonia and CO_2 Refrigeration Technologies*, Ohrid, North Macedonia.

Author contributions: Conceptualization: S. Smitt, A. Hafner, Investigation: S. Smitt, Resources: E. Hoksrød, Writing - Original Draft: S. Smitt, Writing - Review and Editing: S. Smitt, A. Hafner, Visualization: S. Smitt, Supervision: A. Hafner.

Paper III

S. Smitt, A. Hafner (2019). "Numerical performance investigation of a CO_2 heat pump and refrigeration system for a Nordic hotel." In: *Proceedings of the 25th IIR International Congress of Refrigeration.* Montréal, Canada.

Author contributions: Conceptualization: S. Smitt, A. Hafner, Investigation: S. Smitt, Resources: S. Smitt, A. Hafner, Writing - Original Draft: S. Smitt, Writing - Review and Editing: S. Smitt, A. Hafner, Visualization: S. Smitt, Supervision: A. Hafner.

Paper IV

S. Smitt, I. Tolstorebrov, A. Hafner (2020). "Integrated R744 unit for hotels: Analysis of field data." In: *Proceedings of the 13th IIR Gustav Lorentzen Conference on Natural Refrigerants*, Kyoto (Online), Japan.

Author contributions: Conceptualization: S. Smitt, I. Tolstorebrov, Investigation: S. Smitt, I. Tolstorebrov, Formal analysis: S. Smitt, Writing - Original Draft: S. Smitt, Writing - Review and Editing: S. Smitt, I. Tolstorebrov, Visualization: S. Smitt, Supervision: I. Tolstorebrov, A. Hafner.

2 Background

This chapter reviews the technological background of the doctoral work. The first part review state-of-the-art transcritical CO_2 applications. The second part presents state-of-the-art integrated CO_2 systems, with emphasis on supermarket and heat pump applications. The last part presents challenges related to the development of integrated CO_2 systems for hotels.

2.1 State-of-the-art transcritical CO_2 applications

Carbon dioxide, with molecular formula CO_2 and refrigerant name $R744$, is a working fluid with a history that can be traced back more than 100 years. The first CO_2 refrigeration systems were applied for AC and cold storage from the mid 19_{th} century. In contrast to its rival refrigerants at the time, such as ammonia and sulfur dioxide, CO_2 is neither toxic nor flammable. As a result, CO_2 was preferred in applications where refrigerant exposure to produce and people could occur. However, the first CO_2 refrigeration systems struggled with many challenges, such as compromised cooling capacity at high ambient temperatures, high operating pressure and refrigerant leakage [20]. Thus, the general public opinion reflected the belief that CO_2 was an outdated refrigerant. The "father of industrial refrigeration", Carl von Linde, stated that "...[CO_2] can never reach the efficient performance ratio of ammonia." [21]. The search for new and superior synthetic working fluids started, which resulted in the introduction of the chlorofluorocarbons (CFCs) and hydrochlorofluorocarbons (HCFCs) refrigerants, also known as Freon. By the 1930s, new CO_2 refrigeration systems practically disappeared [20]. This trend continued for more than 50 years until the Montreal and Kyoto protocols were established in 1987 and 1997, respectively. The protocols aimed to phase out synthetic refrigerants that were harmful to the environment. This included the

CFCs and HCFCs refrigerants, which cause severe depletion of the ozone layer, and the newly introduced hydrofluorocarbons (HFCs) refrigerants due to high global warming potential (GWP) [22, 23]. Hardly any interest had been granted to CO_2 refrigeration until its "revival" by Professor Gustav Lorentzen in 1990 when he introduced and patented the transcritical CO_2 cycle [24]. Figure 2.1 principally illustrates the difference between (a) a condensing cycle and (b) a transcritical cycle. Since the transcritical CO_2 cycle operates above the critical point (31 °C, 73.8 bar), a gas cooler in place of a condenser accomplishes the heat rejection by cooling compressed fluid at supercritical high-side pressure. Thus, the heat rejection in the transcritical cycle occurs at gliding temperatures, making it exceptional for applications that require a high-temperature lift, such as hot water heating. Reducing the CO_2 temperature before expansion is imperative to ensure a high cooling capacity, as it limits the amount of vapor (flash gas) after expansion, resulting in a high coefficient of performance (COP).

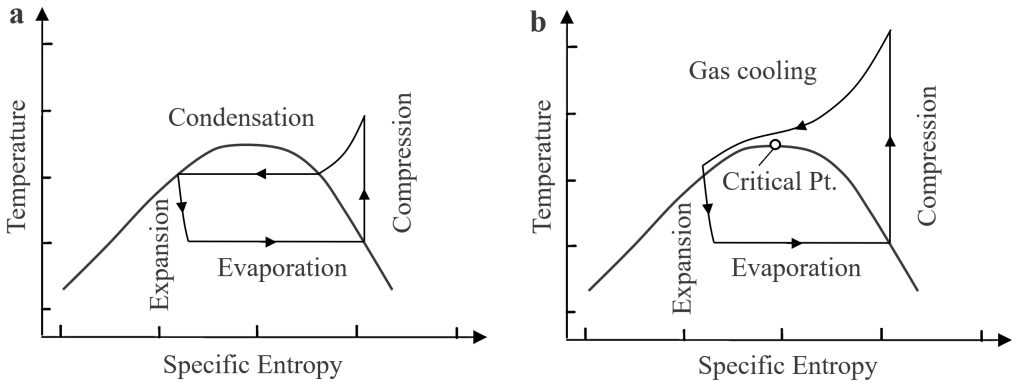

Figure 2.1: T-s diagram of ideal vapor-compression with (a) a condensing cycle and a (b) transcritical cycle.

The operating pressures in CO_2 systems are typically 5–10 times higher than for conventional refrigerant cycles, which results in special requirements for design and equipment. High-side pressure control is crucial in achieving high efficiency in transcritical CO_2 cycles, as both temperature and pressure before expansion highly influence the refrigeration capacity. Furthermore, the COP of any refrigeration cycle depends on the compressor work input and the discharge pressure. The COP of a conventional vapor-compression cycle is reduced as the pressure ratio increases. As demonstrated by Pettersen [25] in 1994, the approach for optimal high-pressure determination is very different in a transcritical cycle. In addition, the high pressure introduces some advantages, such as exceptionally high vapor density and correspondingly high volumetric heating capacity. Consequently, a significantly smaller volume of CO_2 is required in the vapor-compression cycle to

achieve the same heating or refrigeration demand as other refrigerants. This, in turn, allows for the application of smaller components, more compact systems and a considerably lower compressor volume compared to conventional refrigerants [26, 17]. Lorentzen predicted that CO_2 and other natural refrigerants, i.e., hydrocarbons, ammonia, water and air would become essential within future refrigeration and heat pump applications. He advanced this goal by describing strategies to improve CO_2 applications, including multi-stage compression, heat and expansion work recovery [27, 28]. In the following years, considerable research efforts were devoted to CO_2 refrigeration and heat pump applications.

NTNU and SINTEF established the initial research on CO_2, in which the main focus revolved around two applications; mobile AC units and heat pump water heaters (HPWHs). Experimental results demonstrated that a mobile AC unit with CO_2 achieved a comparable system efficiency with that of CFC-12 mobile AC units. These findings were groundbreaking when considering that mobile AC units contributed to about 60% of the CFC emissions within the refrigeration sector at the time [29]. Nekså et al. [30] showed experimentally in 1998 that an HPWH can achieve a COP above 4 when heating water to a temperature of 60 °C. Around the same time, Bredensen et al. [31] measured heat transfer and pressure drop values to validate correlations and adapt simulation tools for CO_2 cycles. The findings were an important contribution to CO_2 heat exchanger design procedures and illustrated that CO_2 evaporators could be designed for high fluid velocities due to the unique relationship between temperature loss and pressure loss ($\Delta T/\Delta P$). For instance, the $\Delta T/\Delta P$ value of ammonia is more than 8 times higher than that of CO_2 at -30 °C (17.2 K/bar vs. 2.1 K/bar). This was significant for the establishment of a new generation of CO_2 refrigeration applications, as new systems could be designed for large pressure drops and enhanced heat transfer. Nekså et al. [32] first introduced the concept of decentralized CO_2 supermarkets in 1998, which included heat recovery from the refrigeration cycle to both space heating and hot water. In the following years, Girotto et al. [33] investigated a CO_2 field-test supermarket installed in Italy, which was found to consume 10% more energy than conventional HFC refrigeration solutions. The authors suggested using a dual-stage compression and suction of the vapor in the liquid receiver to enhance the system performance.

The first comprehensive review on state-of-the-art transcritical CO_2 technology in various refrigeration and heat pump applications was presented by Kim et al. [26] in 2004. The study aimed to evaluate system design issues, methods of high-side pressure control, cycle modifications, component/system design, safety factors, and promising application areas. Pearson [34] later elaborated on the subject by tracing the development of the first CO_2 systems, considers the technical, commercial and social reasons for their slow development and eventual decline. Included in the

review were suggestions for future developments and necessary areas of research and product development required to maximize the potential of CO_2 applications. The consequences, outlook and current options for various types of refrigerants in light of existing international agreements and local control measures were reviewed by Calm [35] in 2008. The newly established 2006 EU fluorinated greenhouse gas (F-gas) directive [36] restricted the use of HFC refrigerants in mobile AC units to refrigerants with GWP values of 150 or less. As a consequence, a new group of synthetic refrigerants was introduced, namely the hydrofluoroolefins (HFOs). These refrigerants were categorized as having zero ozone depletion potential and low GWP. However, many within the research community had adopted the beliefs of Gustav Lorentzen and were concerned about the long-term effects of HFOs, considering the history of its synthetic refrigerant predecessors. Thus, research efforts for the advancements of CO_2 refrigeration, AC and heat pump systems continued over the next decade.

Tremendous technological advances have occurred since then, and plentiful examples demonstrate successful commercialization of CO_2 transcritical systems in several sectors. In the Japanese domestic heat pump market, transcritical CO_2 HPWHs have been commercially available for two decades. Introduced in 2001, over 3 million units of the EcoCute HPWP had been sold by 2011 [37]. Application of CO_2 systems have flourished within the commercial supermarket sector. In 2008, roughly 140 standalone CO_2 supermarket units were installed worldwide. By 2020, more than 35,000 transcritical CO_2 systems existed globally [38]. Currently, CO_2 refrigeration systems are considered the benchmark solution in the European supermarket sector. However, synthetic refrigeration systems still hold the majority market share within heat pump and refrigeration applications. Recent studies and reports have raised concerns regarding the HFO's decomposition product trifluoroacetic acid (TFA). Widespread and long-term application of HFO's can result in TFA accumulating in drinking water, which can have severe effects on human health and the environment [39]. Recently, Holland et al. [40] presented a detailed model of the effects of complete transition from HFC-134a to HFO-1234yf on TFA pollution. A staggering 33-fold increase in global atmospheric TFA is predicted following a complete transition. In addition, a newly published article by Cambell et al. [41] demonstrates that one of the most applied HFOs (HFO-1234ze) in current use ultimately decomposes partially into the refrigerant HFC-23; one of the most potent greenhouse gases known (100-year GWP of 14,800). Thus, advancement of natural refrigerant, such as CO_2, is as imperative today as during the introduction of the first regulations on harmful substances in the 1980s and 1990s.

A great deal of the technological advancements within transcritical CO_2 heat pump and refrigeration systems can be attributed to the development of modern supermarkets. Defining improvements include the application of internal heat exchang-

ers (IHXs), multi-stage compression, parallel compression and ejector technology. Traditionally, IHXs were applied as safety devices in refrigeration plants to prevent liquid from entering the compressor. However, several authors have shown that applying IHXs at various places in the transcritical CO_2 cycle can improve performance significantly. The benefits of applying both inter-stage heat exchangers (intercooler) in combination with an IHX were demonstrated by Cecchinato et al. [42] in a comprehensive investigation of several CO_2 design concepts. Among the evaluated systems were transcritical CO_2 AC systems that incorporated dual-stage compression and throttling with an inter-stage heat exchanger between the compression stages. Substantial energy benefits could be achieved by applying an inter-stage heat exchanger in combination with IHXs. The authors estimated that such configurations could attain average enhancements in COP of close to 30% compared to a single-stage CO_2 refrigerating unit. Torrella et al. [43] later investigated the energy benefits associated with the application of a suction gas IHX in a transcritical CO_2 refrigeration unit at various evaporation temperatures, gas cooler outlet temperatures and high-side pressures. The analysis illustrated that COP and cooling capacity can be increased up to 12% compared to a single-stage system with no IHX. However, the sole implementation of IHXs was not satisfactory in improving the efficiency of the single-stage transcritical CO_2 system enough to compete with state-of-the-art HFC alternatives. Thus, research efforts were invested in reducing compressor input power by applying compression in several stages, eventually leading to the development of the dual-stage (booster) transcritical CO_2 compression system.

The first CO_2 booster unit was installed in Denmark in 2007 as a result of joint academic and industrial efforts [44]. Measurements from the system demonstrated an increase in energy savings and reduction in carbon footprint by respectively 4% and 52% when compared with an HFC-404A system [45]. Ge and Taasou [46] studied parameters that effect the performance of CO_2 booster systems, and found that the COP increased when the intermediate pressure was reduced and flash gas was removed by the high-stage compressor. Sawalha et al. [47] later supported these findings with an analysis of five Swedish supermarkets, in which CO_2 booster designs with and without flash gas removal were evaluated. A combination of long-term operational data and modeling revealed that flash gas removal from the intermediate pressure level enhanced COP by up to 16%, whereas a 2-3 K increase in evaporation temperature contributed to a COP enhancement of up to 14%.

Flash gas removal from an intermediate pressure receiver has become defining in modern CO_2 system design and is applied in various manners today. In conventional CO_2 booster systems, the amount of flash gas removed from the intermediate pressure receiver by the high-stage compressor increases significantly with elevated temperatures before expansion, e.g., in air gas cooler applications at high ambi-

ent temperatures. As illustrated by Gullo et al. [48], compared to an HFC-404A direct expansion unit, the energy efficiency limit experienced with a CO_2 booster system at ambient temperatures of 14 °C and above can be raised to 27 °C by adopting parallel compression. However, as Javerschek et al. [49] emphasized, the advantages related to adopting this solution are dependent on how many hours the parallel compression is employed. Wiedenmann et al. [50] recommended focusing on the design of the auxiliary parallel compressor section in order to suitably select the minimum suction volume rate of the parallel compressor(s). This would enable a considerable increase in the parallel compressor operating time, resulting in enhanced overall performance and increased compressor lifespan. However, the application of auxiliary parallel compressors may pose a challenge due to the relatively large investment cost of compressors compared to other system components. In large commercial systems, the number of required parallel compressors may inflate the investment cost if considerable variations in the heat sink temperature occur.

Pardiñas et al. [51] suggested applying several parallel compressors with pivoting suction ports, i.e., pivoting compressors, to reduce the overall system investment cost. Their work surrounding pivoting compressors was realized with the newly installed full-scale transcritical CO_2 supermarket in the SINTEF/NTNU laboratory facilities, which was introduced by Hafner and Banasiak [52] in 2016. The test facility was designed with high versatility as it permits testing of several system configurations, i.e., booster, ejector supported AC integration and pivoting compressors. The pivoting suction port of the particular compressor refers to the possibility of selecting the suction manifold connection and integrating it in either the base compressor section or the parallel section. The pivoting suction ports can be implemented by applying valves at the suction ports, which can be opened and closed towards the desired pressure level. Consequently, the option of pivoting compressors can decrease the overall number of compressors installed and, as a result, the overall investment cost of the system. In addition, flexibility is significantly enhanced as the integrated system can swiftly adapt the number of compressors assigned to a particular suction group. The concept of pivoting compressors was in 2020 validated in the laboratory facilities at NTNU/SINTEF by Pardiñas et al. [53], in which they concluded that pivoting compressors are primarily beneficial in ejector-supported systems. This was explained by the increase in parallel compressor load due to the vapor ejector that unloaded the base compressors in favor of the parallel compressors. They also found that the investment cost of ejector-supported CO_2 systems with pivoting compressors could be comparable to less sophisticated CO_2 systems. As indicated, integration of two-phase ejectors is immensely beneficial in transcritical CO_2 systems since the large pressure difference between the gas cooler and evaporator offers excellent potential for work recovery of losses associated with convectional isenthalpic expansion.

Significant progress has occurred since the first experimental investigations on transcritical CO_2 ejectors took place in the late 2000s. As reported by Elbel and Lawrence [54], the initial experimental campaigns of ejectors in transcritical CO_2 systems demonstrated COP improvements in the range of 15-30%. Hafner et al. [55] developed the concept of multi-ejectors, in which several ejectors of different sizes are arranged in parallel. Each ejector can be turned on or off independently by the use of solenoid valves in order to achieve different high-side pressures for different operating conditions. Simulation results for multi-ejector integration in a supermarket illustrated that 5-17% improvement in cooling COP could be achieved, dependent on ambient conditions. Several commercialized versions of the multi-ejector exist today, which can cover a cooling load of 0-193 kW in 32 steps (6 kW), making it possible to control the high-side pressure over a large operating range. An extensive review by Gullo et al. [56] found that the application of multi-ejectors can greatly enhance the energy efficiency of commercial transcritical CO_2 systems, especially in warm climates. Hafner et al. [57] presented operational data from an Italian supermarket commissioned in 2014. The transcritical CO_2 refrigeration unit is equipped with multi-ejector supported parallel compression and can cover the entirety of the AC load. The results showed a 15-30% increase in energy-saving when the multi-ejector was utilized to unload the high-stage base compressors in favor of the parallel compressors. Tosato et al. [58] later presented one-year operational data from two additional multi-ejector equipped supermarkets located in Italy. The authors concluded that the systems were reliable and efficient in warm climates but that further operational comparisons to traditional systems were necessary.

Despite its success in the Northern European market, transcritical CO_2 systems are still struggling to become established in southern parts of Europe. The low rate of installations of CO_2 systems in warm European countries can be accredited to the low efficiency experienced at high ambient temperatures. Matthiesen et al. [44] defined this geographical ambient temperature limit as the "CO_2 efficiency equator". However, as pointed out by Minetto et al. [59], the low penetration of CO_2 applications into high ambient temperature markets is mainly due to a few remaining non-technological barriers, such as shortage of CO_2 technicians, little confidence in transcritical CO_2 refrigeration systems, as well as other social and political factors. The next frontier and now key research area within CO_2 refrigeration is applications in warm climates at high ambient temperature conditions.

The demand for thermal energy, in particular cooling, is increasing rapidly in developing countries. It is estimated that an additional 14 billion cooling appliances will be necessary by 2050 to meet demand; four times the current number [60]. Consequently, refrigeration is currently one of the most important and relevant topics in the world, and the advancement of natural refrigerants is crucial to limit climate change [61]. Field-test installations with CO_2 in tropical and arid climate

zones have demonstrated promising results. The first CO_2 transcritical supermarket in the Middle East was built in Amman, Jordan, in 2018. Operational results revealed that a reduction in refrigeration energy demand by more than 30% compared to state-of-the-art HFC installations in the region [62]. Singh et al. [63] demonstrated, through experimental data, that a CO_2 transcritical supermarket test-rig located in Madras, India, could achieve a system COP of 3.1 at ambient temperatures of 40 °C. In 2020, Singh et al. [64] presented numerical simulations of a planned installation of a 140 kW transcritical CO_2 heat pump for a centralized kitchen in Bangalore, India. The heat pump will preheat hot water to 90 °C for steam production while supplying AC cooling for the entire building and utilizing thermal storage to compensate for asynchronous thermal demands. Simulations illustrated that the system could achieve a COP above 6 when operating in combined heating and cooling mode. The total energy consumption is expected to be reduced by 33% compared to the current solution, which will reduce annual $CO_{2\text{-eq}}$ emissions by about 300 tonnes. Thus, application with CO_2 can be successful in warm climates if heat rejection is integrated towards demands within the building or its surroundings.

In addition to geographical advancements, new areas of application for transcritical CO_2 systems have emerged due to the integration of heat recovery from the refrigeration process. Traditionally, heat recovery implementation was applied as an auxiliary function in refrigeration units. As reported in the review by Gullo et al. [65] in 2018, the application of heat recovery has become standard within supermarket refrigeration, as it offers a noteworthy chance further to reduce the energy consumption and carbon footprint of installations. Application of transcritical CO_2 refrigeration systems integrated with heat recovery can lead to satisfactory payback times and thus facilitate the transition of transcritical CO_2 systems in non-traditional sectors. Rogstam [66] presented the the historic development of CO_2 in ice rink applications. He illustrated through recent CO_2 ice rink systems that essentially all-new indoor ice rinks can be self-sufficient with heat when the systems are integrated with heat recovery. Stensli [67] presented the CO_2 refrigeration system installed at the newly built indoor ski arena in Oslo, in which a 2 MW heat pump is applied to recover heat to the district heating network at 75 °C. The overall cooling capacity of the system is 3.5 MW, making it the largest transcritical CO_2 refrigeration system in Norway to date.

CO_2 transcritical systems have unique fluid properties and cycle characteristics that make them applicable in a variety of thermal processes. Since its reintroduction by Gustav Lorentzen in the 1990s, CO_2 systems have undergone a technological leap in terms of applications. Considerable research and industrial efforts have been invested in advancing transcritical CO_2 systems, including optimizing control and operating strategies, improving components and developing innovative system

designs. All these contributions are facilitating the introduction of CO_2 systems to new sectors. Heat recovery from the refrigeration processes has traditionally been applied as an auxiliary function in CO_2 supermarkets. However, as recent works have illustrated, heat recovery enables geographical advancements of the CO_2 cycle to warm climates. In addition, combining heating and cooling within the same cycle enables high efficiency and sufficient payback times, which makes it possible for CO_2 and other natural refrigerants to compete with synthetic refrigerants in non-traditional markets, such as the hotel sector.

2.2 State-of-the-art integrated CO_2 systems

Vapor compression systems are generally categorized according to process functionality, typically divided into two distinctive groups; "heat pump" or "refrigeration" processes, in which the primary function is to provide either heating or cooling, respectively. Combined cycles that incorporate both heating and cooling functionalities, i.e., "heat pumping processes" [68], utilize both sides of the vapor compression cycle. Figure 2.2 illustrates the operation of the refrigeration process, heat pump process and heat pumping process. The refrigeration process extracts heat at the refrigeration temperature and rejects the heat, $\dot{Q}_h$, at ambient temperatures. The utilizable energy from the refrigeration process is the amount of extracted heat, $\dot{Q}_0$. A heat pump process extracts heat, $\dot{Q}_0$, at ambient temperatures and delivers the heat at the heating temperature. Thus, the utilizable amount of energy, $\dot{Q}_h$, is the sum of both extracted heat and supplied work, i.e., $\dot{Q}_0 + \dot{W}$. A heat pumping process combines the two aforementioned processes by utilizing heat at the refrigeration temperature and the heating temperature. Hence, the usable energy is the sum of both the rejected and the extracted heat, $\dot{Q}_h + \dot{Q}_0$, respectively. The value of the utilizable energy can be as large as $2{\cdot}\dot{Q}_0 + \dot{W}$, depending on how much of the refrigerating and heating energy is utilized.

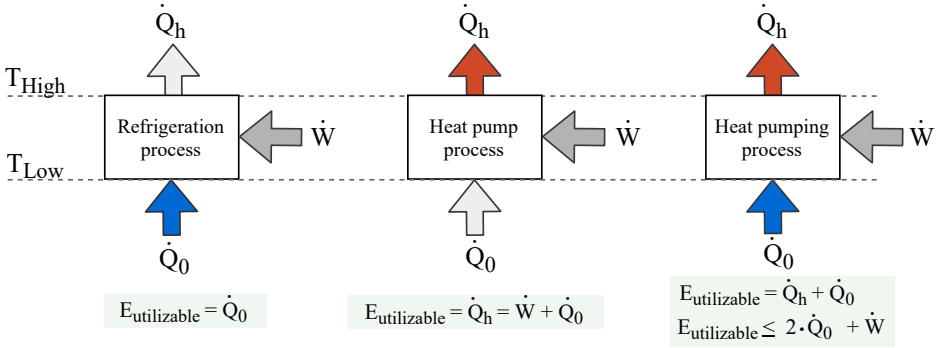

Figure 2.2: Illustration of typical heat pumping processes.

An ”all-in-one” or ”integrated system” is a heat pumping process that integrates refrigeration and heating at different temperatures and loads. There is no official definition of integrated systems, although Hafner and Nekså [69] characterized integrated systems by their ”ability to simultaneously provide refrigeration capacities at various temperature levels, AC, dehumidification, space heating and even DHW at adequate temperature levels”. In contrast to heat recovery from the refrigeration process, a fully integrated system requires active control according to both heating and cooling demands. As follows, it is possible to cover all thermal demands within the building, independent of seasonal loads and ambient temperatures.

Integrated systems are organized into single centralized units, which replace conventional separate refrigeration and heating units. Consequently, centralized systems enable the possibility of surplus heating or cooling export towards nearby buildings or industrial processes. Generally, the total investment, maintenance and operating costs are reduced compared to conventional thermal solutions. Also, the intricacy of system operation and maintenance is reduced on the ownership side, as there is no longer a need for communications between various operation and maintenance crews responsible for their respective heating or refrigeration unit [70]. Integrated solutions with CO_2 are very compact units that require less space compared to applications with conventional refrigerants due to the unique fluid properties of CO_2. Also, CO_2 is a non-toxic and non-flammable refrigerant. Thus, direct heating or cooling towards the source can be applied without secondary safety barriers for leakage prevention. These qualities make CO_2 suitable in applications where other natural refrigerants, such as ammonia and propane, are challenging on account of toxicity and flammability. Thus, integrated CO_2 systems can be implemented with ease and high flexibility as a retrofit solution in existing buildings.

2.2.1 Supermarket applications

It is firmly established that the integrated CO_2 system is an energy-efficient, sustainable and compact solution to provide the entire thermal demand of supermarkets. In recent years, it has become common practice to install integrated systems when applying CO_2 as a refrigerant. Hafner et al. [71] presented an integrated CO_2 supermarket unit installed in Trondheim, Norway, which is illustrated in Figure 2.3. The CO_2 refrigeration unit is a simple dual-stage booster system with evaporation temperatures of -35 and -8 °C for low temperature (LT) freezing and medium temperature (MT) refrigeration cabinets, respectively. The heat from the refrigeration system is rejected through three gas coolers in series, which can alternate heat allocation to different secondary circuits. The system is integrated with floor heating, snow melting, in addition to AC heating and cooling. Thermal storage in the form of hot water tanks and geothermal energy wells is included to compensate for asynchronous thermal demands. Gas cooler 1 is applied to reject heat to a high-temperature circuit, in order to primarily provide ventilation heat-

ing. The second gas cooler supplies heat for the floor heating and snow-melting of store entrances.

At low heating demands during summer, geothermal storage can reduce the refrigerant temperature prior to expansion through gas cooler 3. The geothermal glycol loop is also connected to the ventilation unit and can provide free cooling of the ventilation air. A heat exchanger interface to the CO_2 evaporation can provide additional cooling if needed. During the winter season, geothermal storage can be applied as a heat source to cover the high heating demands through the evaporator at the MT level of the CO_2 refrigeration system. In 2014, Jorschick [72] collected data representative for winter, summer and spring/fall operations. Operational data from spring/fall illustrated that a cooling COP of 3.3 was achieved over the investigated period. In addition, 74% of the surplus heat was recovered.

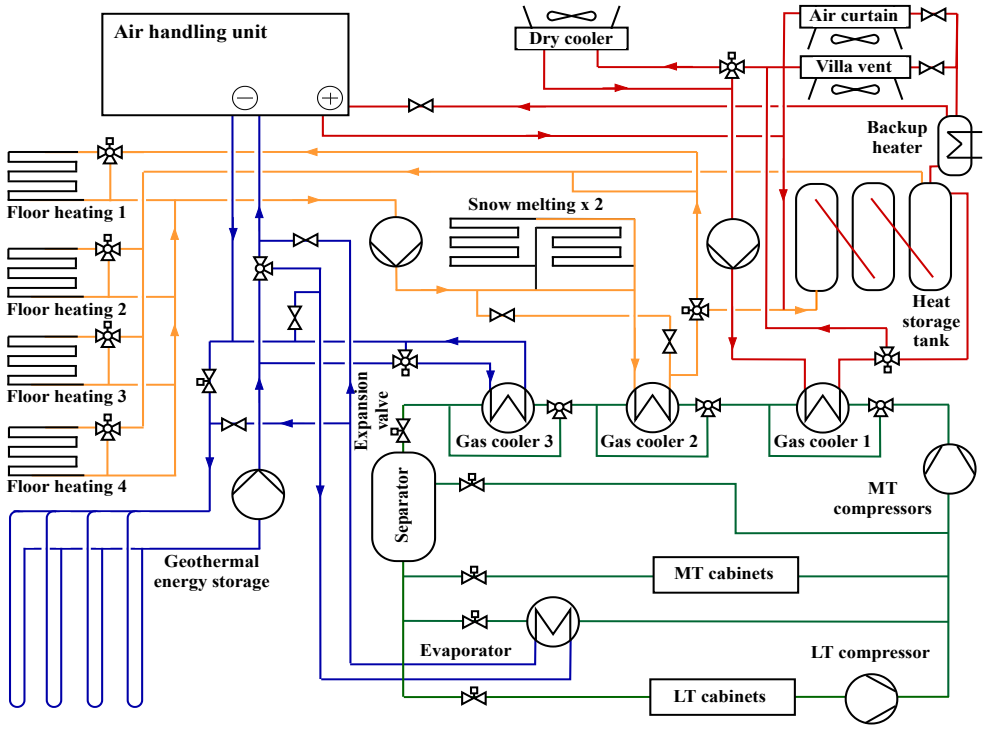

Figure 2.3: Illustration of integrated CO_2 supermarket unit in Trondheim.

Karampour and Sawalha [73] suggested that parallel compression should be adopted for integrated supermarkets in cold climates due to high vapor fraction after expansion and alternatively AC integration during summer operations. Karampour and Sawalha [70] experimentally validated their system design by field measurements collected from a Swedish supermarket in January and July 2014. The system was

able to satisfy the whole AC demand and a large part of the heat recovery for space heating and DHW. Also, COPs during heat recovery were similar or better than those of conventional heat pump units. Polzot et al. [74] suggested an additional air-evaporator at the MT level if heat recovery from refrigeration could not satisfy the thermal demand of the heating system. This solution enables "full integration" of transcritical CO_2 systems in buildings where heating demand can be dominant. In 2018, Karampour and Sawalha [75] investigated state-of-the-art features of integrated transcritical CO_2 booster systems for supermarket applications. Their findings illustrated that two-stage heat recovery, parallel compression, AC integration and flooded evaporation are essential features of integrated CO_2 systems.

Azzolin et al. [76] recently presented an analysis of monitored data from a supermarket system in Italy, illustrated in Figure 2.4. The transcritical CO_2 unit is designed as a booster system with parallel compression and two-stage heat recovery. Two IHXs are installed in the system and can be employed along with active compressors. A notable system feature is the arrangement of the air evaporator and air gas cooler installed in the same framework to reduce system space requirements and investment costs.

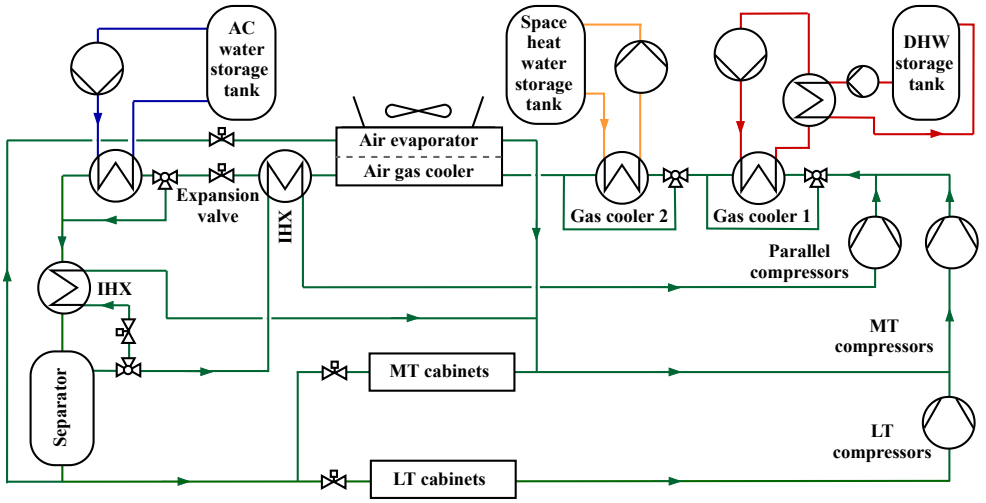

Figure 2.4: Illustration of integrated CO_2 supermarket unit in Italy.

The results from the operational analysis showed that the performance of the CO_2 unit was strongly influenced by the compressor discharge temperature, especially in the summer. They also found that the system efficiency was strongly penalized at high ambient temperatures, despite the implementation of parallel compression, which increased the system capacity and entirely satisfied the AC demand. Dur-

ing winter operations, the system was forced to work in transcritical conditions due to the temperature requirements of DHW and space heating. However, the air-evaporator enabled the CO_2 unit to fully meet both space heating and DHW demands of the supermarket.

2.2.2 Heat pump applications

Integrated CO_2 systems have traditionally been found within the supermarket sector, as illustrated in the previous section. Implementation of integrated CO_2 units, in which their primary function is to serve both heating and cooling requirements, offers a large advantage in buildings and industrial processes that have thermal demands at several temperature levels. In contrast to supermarket application, where the cooling load is usually larger and more stable than the heating demand, cooling and heating demands vary significantly in other commercial buildings. Thus, these systems must be designed to operate in cooling mode, heating mode and combined mode, depending on the thermal envelope of the specific building.

Stene [16] presented a CO_2 heat pump for residential heating in 2005. The gas cooler was partitioned into three parts, which separately served the functions of DHW preheating, space heating and DHW reheating. Thus, the temperature profile of the heated water closely matched that of the CO_2 temperature glide, which was utilized as an advantage to maximize the gliding heat rejection. Moreover, carefully fitting the temperature profile of the different fluids assisted in minimizing CO_2 temperature downstream of the gas cooler, reducing expansion losses and improving performance. Results from the experimental setup demonstrated that the COP was highest for combined mode operation, slightly lower for DHW heating only and lowest when only space heating was applied. Byrne et al. [77] theoretically investigated a CO_2 heat pump layout for simultaneous production of heating and cooling aimed at hotels, luxury dwellings or smaller office buildings. The system design was based on dividing the gas cooler into three parts, with a DHW heat exchanger, a heat exchanger for space heating and a subcooler applied water heating to defrost a backup air evaporator. This air evaporator is necessary to balance the system when the space cooling demand is insufficient to achieve the heating demand. The authors performed a numerical study to compare this heat pump architecture operating with CO_2 and with HFC-407C, and observed that CO_2 could outperform the HFC in terms of environmental impact. However, the results illustrated that the CO_2 heat pump consumed respectively about 4% more energy than the HFC-407C heat pump and 13.2% less electricity in comparison with a standard heat pump in a hotel located in Paris.

Minetto et al. [78] presented a single-stage ejector equipped CO_2 heat pump system for AC space cooling, space heating and DHW. The system was designed to have a flexible operation of secondary circuits, which could alternate the application

of components according to the mode of operation. During summer, the system would connect the AC cooling circuit towards the CO_2 evaporator in order to provide cooling for the building. Heating was then rejected through a connection to an external air-heat exchanger. In winter, the same external air-heat exchanger was connected to the CO_2 evaporator in order to collect heat. Thus, high flexibility of the system was facilitated while reducing the number of necessary components. Applications in Northern Italy resulted in an annual energy saving of about 15% over a conventional solution. Diaby et al. [79] appear as a continuation of the previous work, as the authors present transcritical CO_2 heat pump models for either simultaneous cooling, space heating, DHW or desalination. The numerical results in both cases are satisfactory, and the authors conclude that CO_2 is an exceptionally suited refrigerant for multi-purpose heat pumps compared to conventional refrigerants. Tosato et al. [80] performed an experimental and numerical investigation of a newly developed CO_2 air/water reversible heat pump intended for household applications. The system was evaluated at a range of ambient temperatures (-2.0 to 11.2 °C), and at DHW setpoint temperatures ranging from 60 to 80 °C. The results illustrated that the highest COP was achieved at DHW setpoint temperature of 60 °C, due to an increase in DHW mass flow rate through the gas cooler. However, charging time was significantly reduced at 60 °C when compared with DHW setpoints of 70 and 80 °C.

In 2019, Tosato et al. [81] presented the layout of a CO_2 heat pump installed in a hotel located in Northern Italy intended to provide heating, cooling and DHW. The unit, which is illustrated in Figure 2.5, can apply groundwater as either a heat source or a heat sink to balance thermal demands within the building. For instance, if the building does not request heating, the geothermal energy wells will act as a heat sink and store the surplus heat. An additional heat exchanger can be applied as both a gas cooler and evaporator if needed. The gas cooler pressure is regulated by a two-phase multi-ejector, which works parallel to a high-pressure valve. The system architecture includes ejector-supported two-stage evaporation, which can be applied either as a heat source or for AC production, depending on the operation mode. The first evaporation level is flooded and gravity-driven, while the second one is ejector-driven. Water flows firstly through the gravity-driven heat exchanger, where CO_2 evaporation transpires at the compressor suction pressure. Furthermore, the water is directed to the ejector-driven heat exchanger for additional cooling. This heat exchanger benefits from a lower evaporation pressure, according to the pressure lift provided by the ejector. DHW is produced in a single step and accumulated in two water tanks connected in series to ensure proper stratification. Results from a limited operational period in winter indicated a good efficiency during DHW production. In addition, the benefit of the control strategy resulted in reducing heat pump starts and stops. The authors highlighted that the compressor control strategy during charging should be evaluated to enhance the performance of the

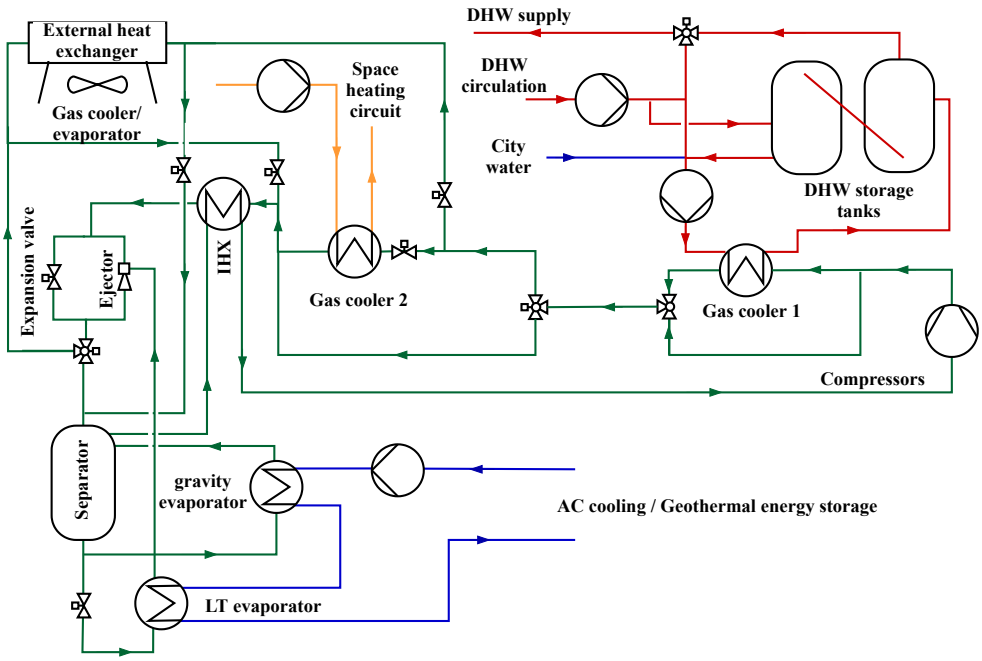

Figure 2.5: Illustration of integrated CO_2 hotel unit in Italy.

system. The potential of evaporation in two stages was not fully evaluated with the available data in Tosato et al. [81]. The first results in summer mode for the aforementioned CO_2 heat pump were presented by Hafner et al. [82] in 2020, showing COPs around 5 when producing chilled water at 7 °C (from 11 °C) and DHW at 60 °C (from 30 °C). The authors concluded that the potential of two-stage evaporation with an ejector would be more advantageous if higher waterside temperature differences were applied in the evaporators.

2.3 Development of integrated CO_2 systems for hotels

As discussed in Section 2.2.2, integrated CO_2 systems can be beneficial in buildings with large thermal demands at several temperature levels. Hotels are such an example, as this type of building typically has large demands for DHW, space heating and cooling. Simulations of such systems have shown promising results, and first-hand data from an existing installation in Italy illustrates the potential of integrated CO_2 systems in hotel buildings. Yet, it is necessary to gather information to evaluate the performance of integrated CO_2 hotel systems in other climates, where other factors for success may apply. It is well-established that elevated MT cooling and low-temperature glide in the gas cooler, e.g., operating conditions

that can occur in cooling or space heating mode, favor conventional working fluids over CO_2. Thus, as for CO_2 supermarket systems operating in warm climates, successful implementation of integrated CO_2 hotel systems is highly dependent on factors that can increase the overall performance. An example is applying cycle designs and components that can enhance energy savings in a sustainable manner, such as ejector technology and parallel compression. Another is to take advantage of simultaneous heating and cooling, which can be realized by applying thermal storage. The performance of integrated CO_2 heat pump systems is influenced by many factors, such as control strategy, operating pressure, return temperatures from secondary systems, and magnitudes of heating and cooling loads. Therefore, it is necessary to investigate the operation of integrated CO_2 heat pump systems and apply control strategies that enhance overall performance. The application and control of the thermal storage enable large flexibility in terms of operation, as demands can be "shifted" to other periods and allow more favorable operating conditions. Therefore, thermal storage is becoming an attractive choice in vapor compression systems to enhance efficiency, reduce peak electricity loads, minimize the size of installed components, and increase the lifetime of the system by limiting fluctuations. In hotels, the easiest and most effective way of achieving this is by implementing thermal storage in the form of DHW tanks, which stores water at a high temperature. The latest developments in regards to DHW thermal storage implementation and control strategies concerning CO_2 applications are discussed in the following section.

2.3.1 Control strategies for domestic hot water production and storage

Hot water storage is a well-established and efficient method of storing thermal energy. Commonly, DHW consumption follows a specific schedule depending on the occupancy and the daily activities, e.g., showering in the morning and the evening. This results in significant consumption peaks during particular hours of the day. Thus, hot water is produced and stored prior to utilization to avoid large power peaks in relation to DHW production and ensure sufficient hot water for the consumer. This is especially important in hotel buildings, which have many occupants and therefore immense DHW consumption peaks. Thermal stratification is often employed in DHW tanks to ensure high-quality thermal storage and high efficiency during production. This is an essential element when dealing with DHW production in CO_2 transcritical systems, as elevated DHW production temperatures can result in high temperatures prior to expansion, and thus low capacity and cycle efficiency.

The motivation of stratification is to minimize the mixing effect so that high-temperature water can be taken at the consumption end, thus maintaining high thermal efficiency at the demand side. The low-temperature water can be drawn from the cold end of the storage and directed towards reheat, thus maintaining

low supply temperature to the CO_2 gas cooler. Higher DHW storage temperatures entail larger heat storage capability and easier preservation of stratification. Typically, several DHW tanks are employed in series when a large volume of water is needed, as illustrated in Figure 2.6. As a result, stratification transpires across the entire storage with hot water tanks at the consumption end and cold tanks at the hot water production end. Minetto et al. [83] described the "charging" process in an investigation of CO_2 HPWH with several DHW tanks in series. During the DHW charging process, water is pumped from the cold end of the storage towards the CO_2 gas cooler. After heating until setpoint temperature, hot water is directed towards the storage. Hot water moves through the series of tanks during production until the storage is fully charged and the normally stratified storage reaches a high and uniform temperature.

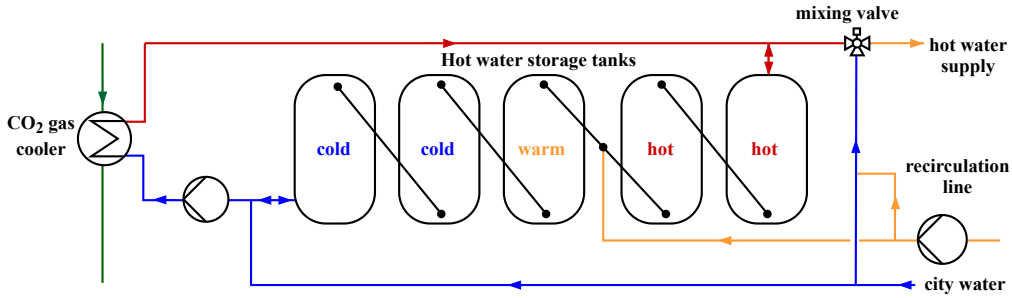

Figure 2.6: Illustration of hot water circuit and thermal storage tanks.

Cecchinato et al. [84] theoretically and experimentally studied an air-source CO_2 HPWH. The system was investigated when heating water from 15 to 45 °C and from 40 to 45 °C. These temperature spans represent hot water production during city water supply and reheat of mixed water, respectively. The results showed that the COP of the transcritical cycle decreased significantly in the case of mixing, by 35-55%, dependent on the season and the heat transfer area of heat exchangers. The authors concluded that the poor performance during mixing was due to higher temperature of the inlet water to the gas cooler, in addition to poor matched temperature profile between the fluids. To avoid this, stratification of water inside the tank must be preserved. Liu et al. [85] performed an investigation of a water-source CO_2 heat pump coupled with hot and cold thermal storage. The experimental results illustrated that higher heat loads lead to a shorter energy charging time and a higher overall COP of the heat pumping system. Moreover, low flow rates of hot and cold water resulted in good thermal stratification in the storage tanks, as mixing was avoided.

Cortella et al. [86] presented a numerical model of a CO_2 supermarket unit with heating, ventilation, and air-conditioning (HVAC) and DHW. Through simulations, they demonstrated how hot and cold thermal storage units can be applied to compensate for asynchronous demands and reduce peak loads. They investigated the implementation of water reservoirs to store the recovered heat from the supermarket and thereby cover the complete heating loads of the building. The motivation of applying the storage was to illustrate the extended heat recovery time throughout the day, thus shaving peaks and preventing the intervention of the auxiliary heating system. They found that implementation of thermal storage resulted in full heat coverage in months with moderate temperature when investigated at continental climate conditions. In addition, the amount of heat recovery increased by up to 30% during the coldest winter months. The authors suggested that energy flows in various plants should be fully understood before initiating the design process to achieve the heat recovery exploitation. Polzot et al. [87] developed a numerical model to evaluate the implementation of cold thermal storage in a CO_2 supermarket unit. The energy consumption of the CO_2 system was 9% lower than the baseline when applying a control strategy that utilized the thermal storage to reduce CO_2 gas cooler outlet temperature. Additionally, the authors concluded that the rejected heat could effectively be collected by applying hot thermal storage. Tammaro et al. [88] implemented an alternative control strategy in a numerical model of a CO_2 air-source heat pump for DHW production, where the frequency of compressors and pumps were reduced to maintain a constant temperature gradient inside the DHW tanks. The results revealed that the thermal storage enabled higher CO_2 operational flexibility and longer operational time for the heat pump.

These investigations have illustrated that the DHW charging strategy highly affects the overall performance of transcritical CO_2 systems. However, few studies have focused on implementing DHW charging strategies to enhance efficiency in large and complex systems dominated by heating and/or cooling demands. Moreover, the system design and balance between the thermal demands are also important considerations that influence energy efficiency.

2.4 Summary

The discussed challenges related to state-of-the-art CO_2 applications, integrated heat pump and refrigeration systems illustrate the necessity to further develop and investigate integrated CO_2 heat pump solutions. Integrated CO_2 systems have demonstrated great performance in Northern European supermarkets and could further be used as a sustainable solution in new sectors, especially where thermal demands are large. Therefore, this thesis investigates the potential of integrated CO_2 systems in hotels located in cold climates.

3 Methodology

This chapter explains the methodology applied to conduct the doctoral work. Firstly, data collection and analysis tools are presented. The second and final part describes the numerical simulation platform, models and boundary conditions applied in the transient investigations.

3.1 Data collection and analysis

Data collection is defined as the process of collecting, measuring, and analyzing targeted variables in an established system, enabling the opportunity to answer relevant questions and evaluate outcomes based on a systems behavior. Several data issues must be managed when collecting information from real-life thermal systems. For instance, recorded data are often incomplete due to missing measurements caused by system downtime or sensor fallout. The same problems may also cause an unrealistic response in the system, which must be identified and handled. The procedure of defining operational limits and identifying outliers for specific variables is often grounded in empirical knowledge and experience with the specific system. Moreover, sets of data can be incompatible due to differences in response and recording time. Variables may only be recorded at irregular intervals, which can vary from daily recordings to instantaneous values. After collecting and handling the data, analysis of the system can begin. However, data in thermal systems, especially in vapor compression systems, are often directly dependent. Thus, it can be difficult to identify data of importance for the overall system behavior. Some factors may not change much over time, making it challenging to detect their impact. In addition, certain variables, such as temperature and pressure, can vary simultaneously. Therefore, it is important to pinpoint which variable is responsible for particular system behavior.

3.1.1 Large-scale data analysis

A large investigation of the energy performance in a number of hotels was performed as part of the thesis work and is presented in Article I in the Appendix. Energy data from the hotels were collected via several web-monitoring services, such as the software *IWMAC* [89]. The resolution of the data varied from annual recordings to instantaneous values. In the case of the latter, the data were interpolated over the specific investigated time period. The energy data contained information about the specific energy use according to the thermal energy source in each hotel from 2015-2019. In addition, information regarding installed energy systems, energy consumption and guest nights were collected through surveys directed to the thermal system operator at each hotel. The initial number of hotels was limited to a sample group in Norway and Sweden. The following criteria were applied to increase the validity of the results:

- Energy data must be logged automatically through surveillance systems.
- Dependable data must be available for a minimum of three of the five years.
- Hotels must have replied to the survey.
- Information from the survey and logged data must be consistent.

Heating degree days (HDD) were applied to compare the energy consumption in the hotels, independent of variations in annual ambient temperature. The HDD values for the different zones were calculated with a standard threshold of 17 °C, as defined by Thom [90]. Figure 3.1 and Table 3.1 shows the different climate zones and lists the annual specific adjustment factor for heating, respectively. The adjustment factor was defined as the HDD for a particular year, divided by the HDD of a standard year. The values indicate the relative coldness for a particular year related to a normal year. The HDD data for Norway were obtained from Enova SF [91], while The Swedish Meteorological and Hydrological Institute provided the commercially available Swedish climate data. The annual heat energy consumption in the hotels was corrected according to their zone-specific adjustment factors, as shown in Equation 3.1.

$$E_{adjusted} = E_{recorded} \cdot \text{Adjustment factor} \tag{3.1}$$

$E_{recorded}$ and $E_{adjusted}$ is the annual thermal energy consumption in a specific hotel before and after correction, respectively. Heat supplied to the hotels was assumed to be dependent on ambient temperatures only.

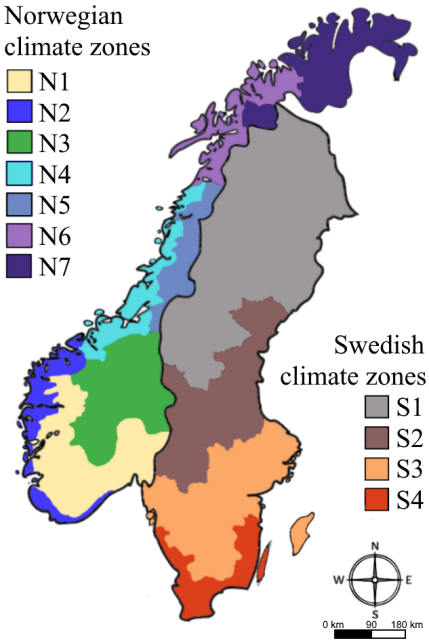

Figure 3.1: Hotel climate zones.

Table 3.1: Adjustment factor for climate zones in Norway and Sweden related to climate data from 1981-2010.

Zone	2015	2016	2017	2018	2019
N1	0.884	0.926	0.920	0.924	0.907
N2	0.885	0.928	0.913	0.931	0.911
N3	0.892	0.942	0.939	0.940	0.924
N4	0.873	0.939	0.930	0.950	0.944
N5	0.895	0.947	0.915	0.986	0.959
N6	0.868	0.926	0.953	0.962	0.985
N7	0.896	0.900	0.950	0.938	0.986
S1	0.892	0.950	0.971	0.968	0.981
S2	0.892	0.936	0.950	0.942	0.932
S3	0.885	0.937	0.927	0.916	0.896
S4	0.884	0.924	0.916	0.891	0.860

3.1.2 In-depth data analysis

An in-depth analysis of operational data from an integrated CO_2 hotel unit was performed as part of the doctoral work and is described in detail in Article II in the Appendix. The hotel thermal data were gathered and processed for the period from September 2018 to September 2019, and obtained through the real-time field measurement web-monitoring software *IWMAC*. The measurements were updated continuously. However, the data for a certain sensor were only logged if a change in the sensor value was detected. The recorded data points were therefore regarded as constant step values within the specific time interval until the next recorded value. All the recorded data were resampled and synchronized to the same time step, using the weighted average of the time intervals. The weighted average, $\overline{v}$, was calculated using Equation 3.2:

$$\overline{v} = \sum_{i=1}^{n} v_i \frac{t_i}{t} \tag{3.2}$$

where v_i is the value for the recorded duration of time, t_i. The duration of the weighted average value is defined by a selected time period, t.

Calculation of parameters

Due to the absence of an energy meter in the DHW supply line, the DHW heat energy consumption, $\dot{Q}_{DHW}$, was calculated using the energy balance equation on the DHW subsystem, as illustrated in Equation 3.3. The terms $\dot{Q}_{HX2}$, $\dot{Q}_{HX3}$ and $\dot{Q}_{HX4}$ defines the heat entering the subsystem by means of DHW preheat, reheat and back-up heating, respectively. The last expression in Equation 3.3 represents the change in internal energy in the thermal storage. Change of energy in the water storage at each time step, given by subscript i, is defined as the difference between the current time step, i, and the next, $i+1$.

$$\dot{Q}_{DHW_i} = \dot{Q}_{HX2_i} + \dot{Q}_{HX3_i} + \dot{Q}_{HX4_i} - \frac{\rho V C_p}{\Delta t_i} \sum_{j=1}^{10} (T_{j_{i+1}} - T_{j_i}) \tag{3.3}$$

A more detailed description of the calculation procedure is given in Article II.

Uncertainty

Several definitions of COP were applied to evaluate the performance of the integrated CO_2 unit and were defined as illustrated in Equation 3.4. The sum of useful thermal energy included in each evaluation, $\dot{Q}$, and the sum of work input in the form of electricity, $\dot{W}$, were calculated as shown in Equation 3.5.

$$COP = \frac{\dot{Q}}{\dot{W}} \tag{3.4}$$

$$\dot{Q} = \sum \dot{Q}_i; \qquad \dot{W} = \sum \dot{W}_i \tag{3.5}$$

The uncertainty of the thermal energies and the work input, $\sigma_{\dot{Q}}$ and $\sigma_{\dot{W}}$, were calculated according to the rules of propagating uncertainty, as illustrated in Equation 3.6:

$$\sigma_{\dot{Q}} = \sqrt{\sum (\sigma_{\dot{Q}_i})^2}; \qquad \sigma_{\dot{W}} = \sqrt{\sum (\sigma_{\dot{W}_i})^2} \tag{3.6}$$

Uncertainty for COP, σ_{COP}, was further calculated according to Equation 3.7:

$$\frac{\sigma_{COP}}{COP} = \sqrt{\left(\frac{\sigma_{\dot{Q}}}{\dot{Q}}\right)^2 + \left(\frac{\sigma_{\dot{W}}}{\dot{W}}\right)^2} \tag{3.7}$$

3.2 Numerical modeling and simulation

3.2.1 Principle of the Modelica language and Dymola platform

Modelica is a programming language developed to describe the behavior of technical systems [92]. The language is built on causal mathematical modeling, which requires the user to explain the cause-effect relationship among the different variables and concepts. Moreover, Modelica is object-oriented, thus revolving around the concepts of applying classes and objects to facilitate the reuse of dynamic system models in a standardized format.

A modeling and simulation platform is necessary to apply the Modelica language to solve physical problems. This platform, or environment, translates the defined set of equations so that the model can be efficiently simulated. The platform can conveniently convey information to the user through a visual interface, e.g., by graphical representations of variables. Dymola is an example of such a platform that is suitable for Modelica modeling and simulation of thermal systems [93]. It can efficiently translate large system models and be applied for real-time investigations. It supports hierarchical model construction and the application of external component libraries. TIL-Suite is a commercially available library developed by TLK-Thermo GmbH [94] for steady-state or transient simulations of thermodynamic systems, e.g., heat pumps, refrigeration, cooling and heating systems. Among the components that are included in the library are compressors, pumps, valves and heat exchangers that can be connected in Dymola to construct complex models. Each physical element in the diagram structure represents a real physical element in the system. When the component elements are connected in the model structure, the mathematical equations in all components constitute the behavior of the model. TIL-Suit includes the fluid properties library, TIL-Media, which is equipped with a range of refrigerants. External data for boundary conditions, e.g., ambient temperatures and heating loads, can be imported to the model environment with the software TIL-FileReader, enabling realistic representations of thermal systems. Thus, the TIL bundle supplies system components, refrigerant properties and interfaces to external data in the development of transient models of integrated CO_2 systems.

3.2.2 Transient model description

Several transient models were constructed and investigated as part of the doctoral work. The development of the models, definition of boundary conditions and component specifications are described in detail in Article III and Article IV in the Appendix. Table 3.2 lists the resolution and description of the six time-dependent variables applied in the construction of the simulation model in Article III, which will be presented in this section to describe the modeling process.

Table 3.2: Model input demands and temperatures.

Name	Variable	Unit	Intervals
$\dot{Q}_{VH}$	Ventilation heating load	W	20 minutes
$\dot{Q}_{RH}$	Radiators/floor heating load	W	20 minutes
$\dot{Q}_{AC}$	AC cooling load	W	20 minutes
$\dot{Q}_{DF}$	Evaporator defrost heating load	W	20 minutes
$\dot{m}_{DHW}$	DHW mass flow consumption	kg s^{-1}	20 minutes
T_a	Ambient temperature/ CO_2 evaporation temperature	°C	60 minutes

Logged thermal system data from a hotel equipped with an integrated CO_2 unit were collected and applied as inputs in the numerical model. Data for three different weeks of operation were selected based on ambient temperatures representative of the seasonal performance of the system, namely nominal (spring and fall), winter and summer. Figure 3.2 illustrates the transient model of the integrated CO_2 system. It includes the CO_2 heat pump loop (U), a hydronic circuit applied for defrosting evaporators (D), the DHW subsystem and thermal storage (W), and the medium and high-temperature circuits applied to transport heat to and from the hotel building (V).

Heat is supplied to the hydronic subsystems through two gas coolers in series, GC1 and GC2, at high (>60 °C) and medium (<50 °C) temperatures. The MT circuit provides heat primarily to ventilation batteries and a radiator/floor heating circuit, represented in the model by $\dot{Q}_{VH}$ and $\dot{Q}_{RH}$, respectively. The remaining heat is supplied to preheat DHW through heat exchanger HX2. During winter operations, HX1 in the MT circuit is applied to defrost evaporators through a brine circuit. The HT circuit mainly supplies heat for DHW reheat through HX3. The HT circuit also supplies extra heat through HX5 for the radiators during winter conditions. Four air evaporators serve as the primary heat source for the CO_2 unit. Alternatively, an interface to the chilled water circuit, HX6, can be employed for heat recovery if AC cooling is needed.

The DHW subsystem consists of 10 tanks in series. During DHW charging, water is drawn from tank no. 10 and is directed towards preheat and reheat in HX2 and HX3, receptively. Water is drawn from the top of each tank and directed towards the supply line, represented by the flow boundary, $\dot{m}_{DHW-S}$. Similarly, the interfaces to city water supply and circulated DHW are applied as the respective flow boundaries $\dot{m}_{CW}$ and $\dot{m}_{DHW-R}$. The thermal demands of the hotel building were implemented using thermal heat boundaries with the time-dependent input variables, thus limiting the numerical model to heat transport within the main branches of the system. The thermal boundaries include $\dot{Q}_{VH}$, $\dot{Q}_{RH}$, $\dot{Q}_{DF}$ and $\dot{Q}_{AC}$ described in Table 3.2, as well as EL1 and EL2, which represents heat from the electric boiler.

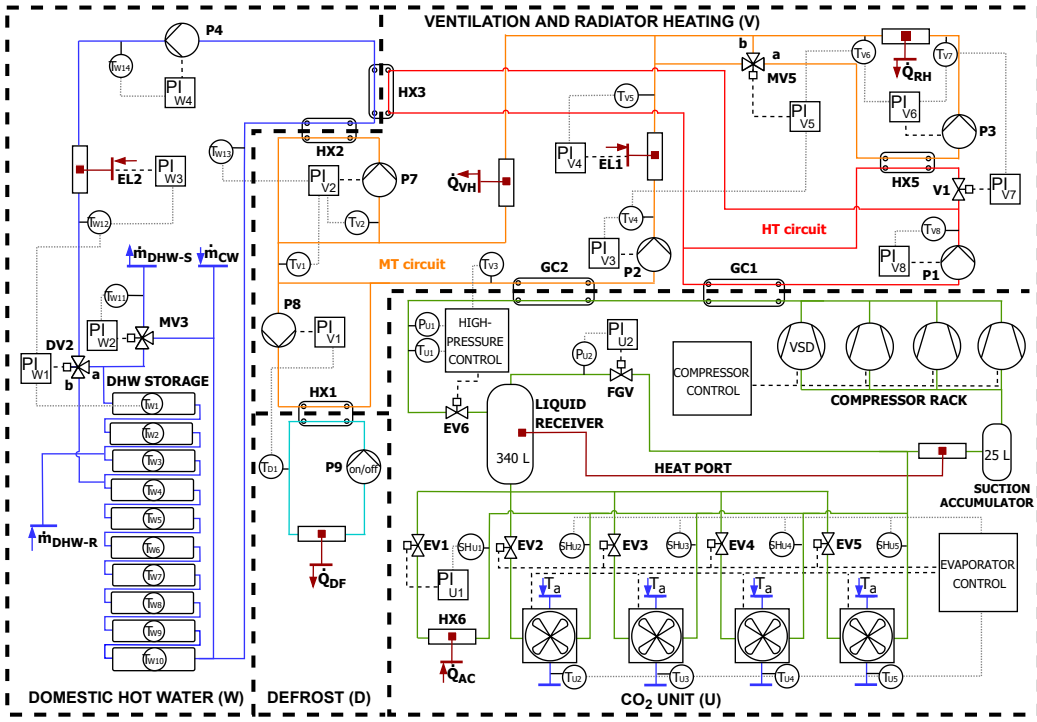

Figure 3.2: Illustration of a numerical model developed for the simulation of integrated CO_2 hotel unit.

The four air evaporator components share the same control logic, as illustrated by *evaporator control* in Figure 3.2. Initially, one evaporator is applied when the CO_2 unit is activated, and the compressors are turned on. The thermostatic expansion valve of the active evaporator, e.g., EV2, continuously modulates the opening degree of the valve to meet the setpoint for superheating at the exit of the evaporator. If more heat is required, additional evaporators are employed until the heat demand is satisfied. Similarly, active compressors are deactivated if the heat supplied by the CO_2 system is greater than the demand, which is represented by the thermal load boundaries. The fan unit controls the air volume flow rate to reach a specific temperature difference, ΔT, through the evaporator. ΔT is dependent on T_a, which is imported to the model through the air-flow boundaries.

The control scheme of the CO_2 unit and secondary systems were implemented according to specifications supplied by the system manufacturers. However, control of the high-pressure compressors and evaporators was approximated for simulation purposes. The requested heating load is calculated based on measured signals from the model system and is related to the maximum compressor capacity by the requested load ratio. The control scheme continuously ensures that the system set-

points, e.g., ventilation and radiator supply temperatures, are satisfied by adjusting the requested load accordingly. Control of individual components was achieved by applying proportional-integral (PI) -controllers. Setpoints, signals and control objectives for components in the model are listed in Table 3.3. The locations of the PI-controllers and sensors can be found in Figure 3.2 according to the subscript, which specifies the particular subsystem.

Table 3.3: Setpoints and control objectives for system components.

Name	Measured signal(s)	Control signal	Control objective
Domestic hot water subsystem (W)			
PI_{W1}	T_{W1}, T_{W12}	DV2	Hysteresis control with 5 min delay. Flow path *a* if $T_{W12} \geq T_{W1}$+2 K, flow path *b* if $T_{W12} \leq T_{W1}$+2 K.
PI_{W2}	T_{W11}	MV3	Mix water streams till T_{W11} = 55 °C.
PI_{W3}	T_{W12}	EL2	Backup heater. Activates if T_{W12} < 55 °C.
PI_{W4}	T_{W14}	P4	Controls pump speed to reach T_{W14} = 65 °C.
Ventilation and radiator heating (V)			
PI_{V1}	T_{D1}	P8	Activated when P9 is on. Controls pump speed to reach $T_{D1} \geq$ 20 °C.
PI_{V2}	T_{V1}, T_{V2}, T_{W13}	P7	Controls pump speed to reach T_{V1} = 23 °C. Turns off pump when $T_{W13} \geq T_{V2}$.
PI_{V3}	T_{V4}	P2	Controls pump speed to T_{V4} = Ventilation setpoint temperature.
PI_{V4}	T_{V5}	EL1	Backup heater. Activates if $T_{V5} \geq$ ventilation setpoint temperature.
PI_{V5}	T_{V4}, T_{V6}	MV5	Modulates flow through *b* to reach $T_{V6} = T_{V4}$ = ventilation setpoint temperature during winter operations.
PI_{V6}	T_{V6}, T_{V7}	P3	Controls pump speed to reach T_{V7} - T_{V6} = 15 K.
PI_{V7}	T_{V7}	V1	Closed if ventilation setpoint temperature $\geq$ radiators setpoint temperature. Controls opening to reach T_{V7} = radiators setpoint temperature.
PI_{V8}	T_{V8}	P1	Controls pump speed to reach min T_{V7} = 70 °C. Increases setpoint to 80 °C if radiators setpoint $\geq$ 70 °C.
CO_2 unit (U)			
PI_{U1}	SH_{U1}	EV1	Recovers cooling if heat pump is on and Q_{AC} is activated. Controlled to reach SH_{U1} = 5 K.
PI_{U2}	P_{U2}	FGV	Controls valve opening to hold P_{U2} = intermediate pressure setpoint (38-52 bar)

Additional information regarding the specification of components and heat transfer phenomena can be found in Article III.

3.2.3 Model validation process

The integrated CO_2 system model validation was achieved using measured data for several variables during three different scenarios. Equations 3.8 and 3.9 defines the coefficient of determination, R^2, and the relative root mean square error, RRMSE, which were applied to evaluate the accuracy of the modeled system. RRMSE indicated the average percentage error between measured and simulated values, while R^2 indicates (from 0 to 1) how well the model can predict the variability of the measured data. The measured and simulated values are denoted m and s, respectively.

$$R^2 = 1 - \frac{\sum_{i=1}^{n}(Y_{m,i} - Y_{s,i})^2}{\sum_{i=1}^{n}(Y_{m,i} - \overline{Y_m})^2} \tag{3.8}$$

$$RRMSE = \frac{\sqrt{\frac{1}{n}\sum_{i=1}^{n}(Y_{m,i} - Y_{s,i})^2}}{\sum_{i=1}^{n} Y_{m,i}} \cdot 100 \tag{3.9}$$

Hourly recorded measured and simulated values for a selected scenario are shown in Figure 3.3. The RRMSE and R^2 values is less than 10% and close to 1.000,

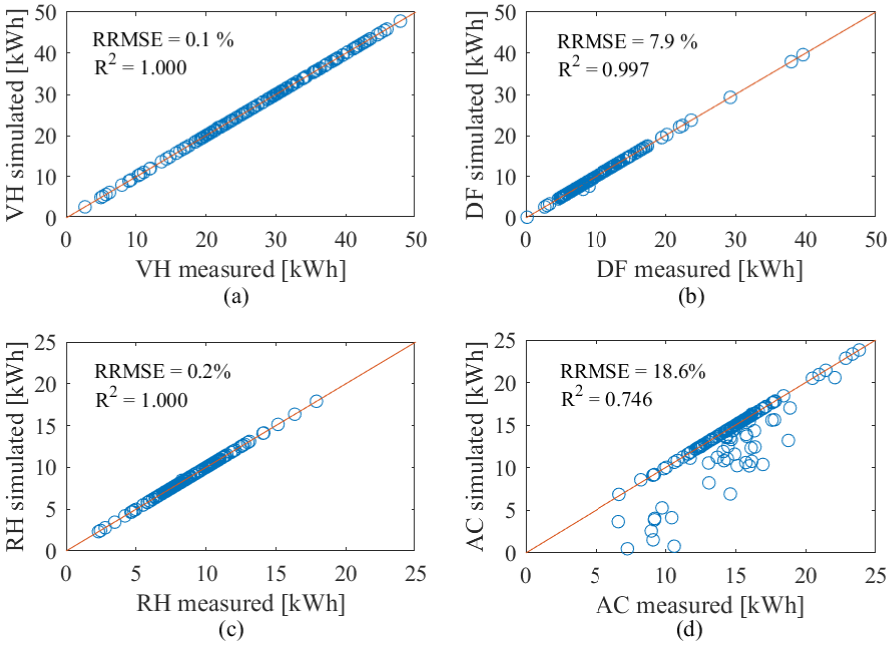

Figure 3.3: Measured and simulated values obtained for nominal week (October 18^{th}-25^{th} 2018) showing **(a)** ventilation heating energy (VH), **(b)** evaporator defrost heat energy (DF), **(c)** radiator/floor heating energy (RH) and **(d)** AC cooling energy (AC).

respectively, for the variables illustrates in (a), (b) and (c), which indicates that the model can represent heat energy values of ventilation (VH), defrost (DF) and radiators (RH), with high quality. A higher error is observed in Figure 3.3 (d) between simulated and measured AC cooling energy values, which demonstrate a relative error of 18.6%. The variation is reflected in the R^2-values for the same variable, which is above 0.743.

Figure 3.4 illustrates the variation between simulated and measured supplied DHW heat energy for a selected week. As illustrated in the figure, RRMSE is below 10% for the selected week. Moreover, the R^2 value of 0.993 indicates a high model accuracy.

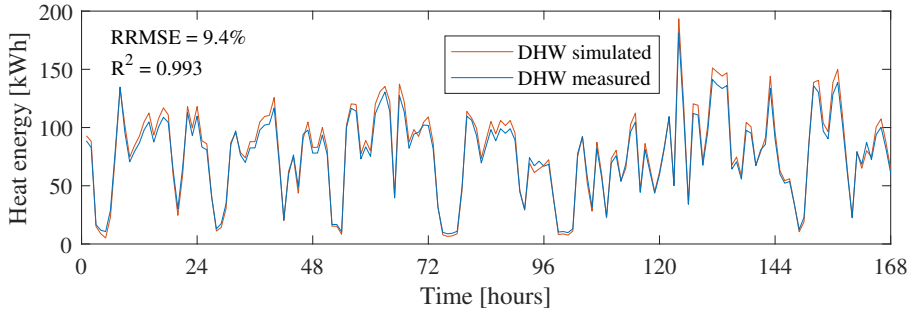

Figure 3.4: Measured and simulated DHW values for nominal week (October 18^{th}-25^{th} 2018).

Table 3.4 illustrates the seasonal COP (SCOP) for the particular week. Subscripts *h*, *HP* and *tot* indicates SCOP for heating, the entire heat pump unit and the complete thermal system of the hotel. Simulated $SCOP_h$ is lower than the counterpart measured values. A similar trend is observed for $SCOP_{HP}$. Thus, it can be concluded that the simulated performance is slightly lower when compared to the real system. All simulated SCOPs are comparable to the measured values and below a relative error of 10%. Thus, it can be concluded that the modeled system is sat-

Table 3.4: Comparison between monitored and simulated SCOPs for nominal week (October 18^{th}-25^{th} 2018).

Variable	Measured*	Simulated	Relative error [%]
$SCOP_h$	3.05 ± 0.17	2.81	7.87
$SCOP_{HP}$	3.23 ± 0.18	3.15	2.48
$SCOP_{tot}$	3.21 ± 0.34	3.12	2.80

* The range of uncertainty for the measured SCOP-values are described in Article II.

isfactory in characterizing the behavior of the real system for the nominal week of October. Similar investigations have been performed with data sets representative for summer and winter, which are described in Article III.

3.3 Summary

This chapter explains the methodology used to achieve the research objectives of the doctoral work. The analysis of collected data provided valuable information on the performance of thermal systems in hotels. In addition, the detailed evaluation of system performance and the influence of variables contributed to in-depth knowledge leading to measures that can enhance efficiency. The numerical investigations provided practical information regarding the performance of integrated CO_2 systems at diverse operating conditions.

4 Summary of research work

This chapter presents a summary of the doctoral work corresponding to the objectives of the thesis. The published articles are intended to accomplish the sub-objectives of the doctoral work in sequential order, in short, "investigate and quantify thermal energy demands within the hotel sector in cold climates", "evaluate the performance of an integrated CO_2 hotel system", "validate transient simulation models to evaluate charging strategies" and "evaluate concepts for integrated CO_2 systems with thermal storage for hotels". Each complete article is enclosed for an extensive introduction to the respective research topic.

4.1 Article I: Energy use and retrofitting potential of heat pumps in cold climate hotels

This article presents a study of the energy use of 140 hotels in Norway and Sweden over a five-year period. The energy use, available energy sources and thermal systems are investigated to identify successful and sustainable measures to reduce energy consumption and related emissions within the hotel sector. Information applied in the study was collected through web-monitoring services and surveys.

Figure 4.1(a) shows the available energy sources in the hotels from 2015 to 2019. The number of hotels with only electricity access has been halved over the five years. During the same period, the number of hotels connected to district heating and cooling networks increased by 18.0 and 10.9%, respectively. The total electricity consumption in the hotels was reduced by 8% from 2015 to 2019 in favor of district heating, which increased by 7% over the same period.

Figure 4.1(b) illustrates the primary and secondary thermal heating systems applied in the hotels. The results show that 70% of the hotels applied district heating as the main source of heating. The specific energy consumption for this group of hotels is 219.9 kWh/m2/year, which is larger when compared with hotels that use electricity or heat pump technology to generate heat. The 9% of the hotels that apply heat pumps as their main heating system have the lowest specific energy consumption of all the investigated thermal systems, with 175.4 kWh/m^2/year.

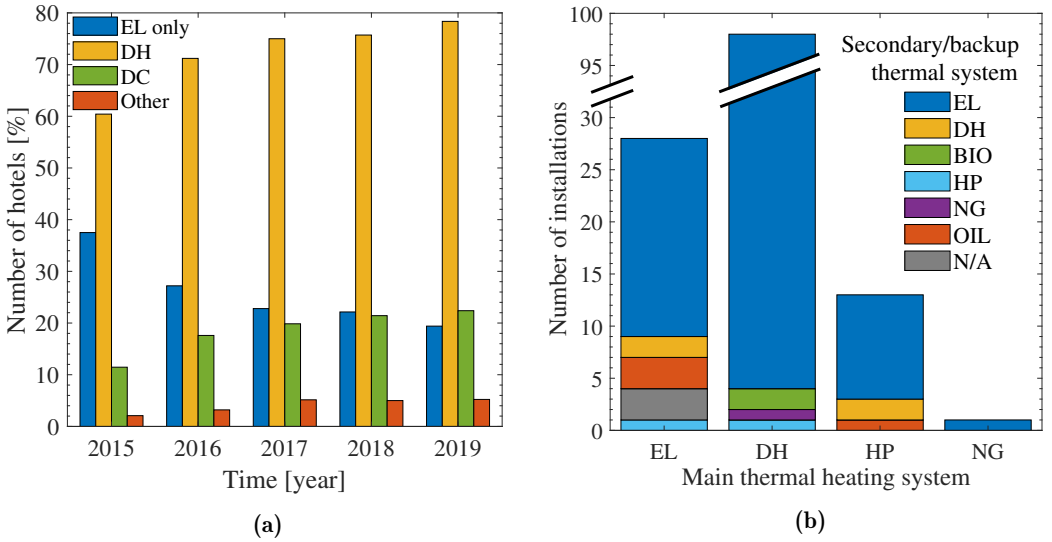

Figure 4.1: Results from energy study showing (a) available energy sources in the hotels and (b) an overview of primary and secondary thermal heating systems in all hotels in 2019. The evaluated energy sources include electricity (EL), district heating (DH) and cooling (DC), and *others*, i.e., biofuel (BIO), heat pumps (HP), natural gas (NG) and oil.

70% of the hotels have a mean annual energy consumption between 150 and 250 kWh/m^2/year, with the mean value for all hotels being 213 kWh/m^2/year. For the average hotel, the annual energy consumption is in the vicinity of 2 GWh. On average, large-sized hotels consume more than 4.5 GWh annually and have related annual emissions of close to 1,200 tonne CO_2-eq. Thus, there is a large potential to reduce energy consumption and emissions within the Nordic hotel sector.

Two of the investigated hotels have been equipped with integrated CO_2 heat pump systems and thermal storage, where a reduction in energy usage in the range of 73.2 to 88.6 kWh/m2/year was achieved. A heat energy consumption reduction of about 60% was observed in both cases, revealing the great potential of integrated CO_2 heat pump systems as a thermal solution for hotels.

4.2 Article II: Integrated CO_2 system with HVAC and hot water for hotels: Field measurements and performance evaluation

This article investigates the one-year performance of an integrated CO_2 unit in a Norwegian hotel, illustrated in Figure 4.2. The system consists of a single unit for heating, cooling and hot water production with a 6 m^3 integrated thermal storage.

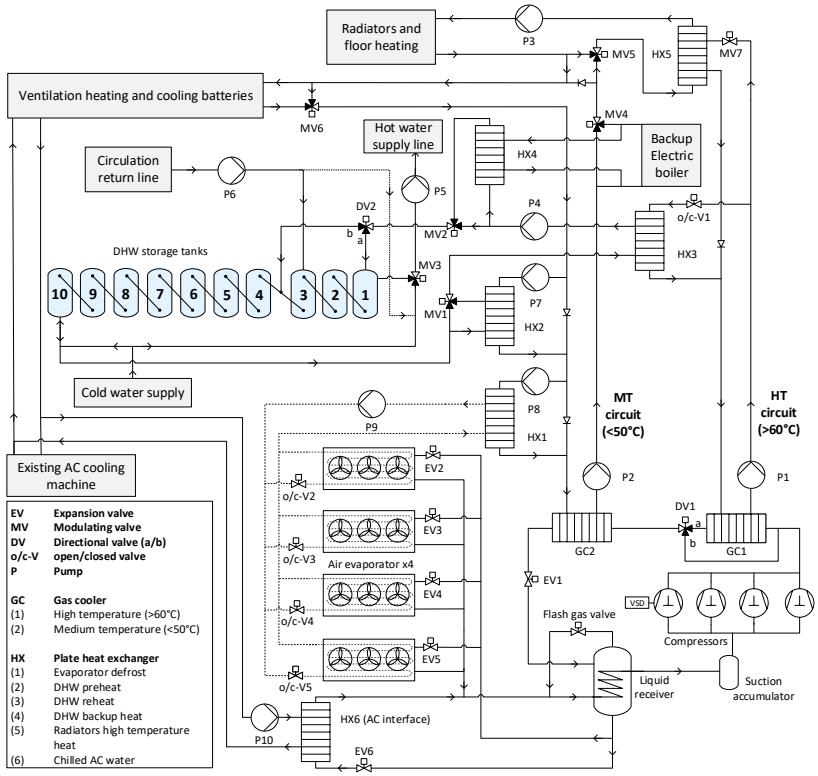

Figure 4.2: Schematic drawing of the integrated CO_2 hotel unit.

The analysis of field data shows that the DHW usage accounts for 52% of the annual heat load and that the thermal storage reduces hot water demands peak with more than 100 kW. The analysis of the integrated CO_2 system demonstrates an annual SCOP of 2.90 and thus an untapped system potential. The system performance is higher during the DHW charging process at ambient temperatures above 15 °C, due to limited space heating loads. The fluid return temperature from the building is elevated at high space heating loads, resulting in high gas cooler exit temperatures and reduced performance. System performance can be improved by charging the storage for longer periods of time at reduced capacities, limiting the number of CO_2 unit starts/stops and mixing in DHW tanks.

4.3 Article III: Performance improvement of integrated CO_2 systems with HVAC and hot water for hotels

This article presents the numerical investigation of an integrated CO_2 heating and cooling unit in the previous article. A transient numerical model of the hotel's thermal system was developed and validated for three seasonal representative weeks using recorded ambient temperatures, setpoints and thermal loads. All simulated SCOPs were within a relative error range of 8.5% and illustrated the same seasonal variations as the measured values. Thus, the modeled system was found to be satisfactory in characterizing the behavior of the real system.

A low load charging (LLC) strategy, which exploits the thermal storage flexibility, was evaluated as an approach to improve the overall system performance. The principle of the proposed control strategy is to reduce the return temperature from the secondary system by limiting supply temperatures to the building during DHW charging. In contrast to the current traditional baseline charging strategy, this entails constantly ensuring that setpoints are met and adjusting compressor load accordingly to minimize the heating load and peak power utilization.

Table 4.1 lists the main results obtained when applying the LLC strategy, which illustrates that the number of on/off cycles is reduced significantly. The active time, ON%, of CO_2 unit is increased, resulting in reduced application of the backup boiler. However, such a strategy increases the return temperature from the hotel during summer, as illustrated by T_R . Elevated T_R during summer operation is explained by an increased supply temperature when applying the LLC strategy. Yet, a significant increase was observed in COP_{tot} and energy savings in all investigated scenarios. Moreover, peak power usage in the thermal system was reduced by up to 32.5% when applying the LLC charging strategy.

Table 4.1: Performance indicators when applying the low load hot water storage charging (LLC) strategy in favor of the baseline control. Energy-saving and the performance of the entire hotel's thermal system, COP_{tot}, is evaluated relative to the measured data in the baseline scenario.

Case	Control strategy	ON/OFF cycles [-]	ON% [%]	T_R [°C]	Energy savings [%]	COP_{tot} increase [%]
Nominal	Baseline	33	92.4	33.5	-	-
	LLC	1	99.7	30.7	5.8	9.6
Winter	Baseline	0	100.0	28.4	-	-
	LLC	0	100.0	26.6	7.5	7.7
Summer	Baseline	86	72.1	33.9	-	-
	LLC	13	93.5	34.5	13.2	23.0

4.4 Article IV: Evaluation of integrated concepts with CO_2 for heating, cooling and hot water production

This article theoretically compares the energy consumption, environmental impact and cost of three different design concepts for integrated CO_2 units equipped with thermal storage. The main characteristics of the evaluated designs are single-stage compression (SC), parallel compression (PC) and ejector-supported parallel compression (EJ). Furthermore, two separate hot water charging strategies were implemented and investigated over a large span of ambient temperatures and loads, namely the *leveled* (LLC) and *aggressive* (traditional) charging strategies.

Figure 4.3 compares the COP of the investigated designs as a function of ambient temperature and charging strategy. The EJ system with the ejector arrangement outperforms both SC and PC, independent of charging strategy. Moreover, leveled charging generally increased COP compared with aggressive charging due to continuous DHW production during all operational hours.

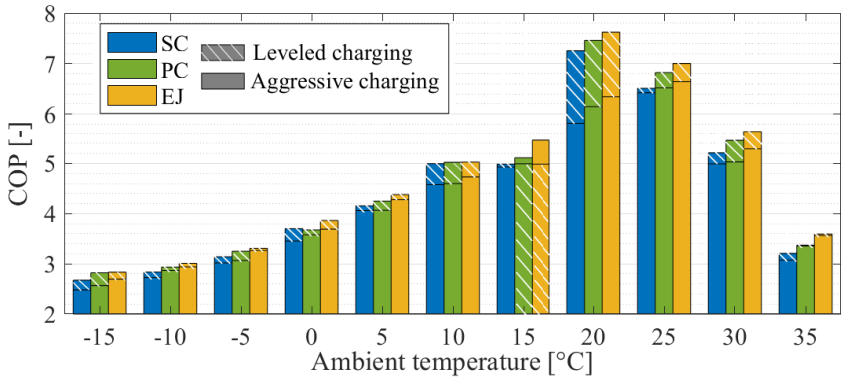

Figure 4.3: COP as a function of ambient temperature for the investigated designs when applying the aggressive DHW charging strategy.

The evaluations were carried out by considering eight different European locations, ranging from Scandinavia to the Mediterranean. The results revealed that the ejector-supported parallel compression design was superior in terms of annual COP, which was found to be in the range of 4.27 to 5.01 for the Scandinavian locations and 5.03 to 5.71 for the other European locations. When accounting for investment cost and electricity prices, the payback period at the Scandinavian locations was 6.3 to 7.7 years. Payback periods of 3 and 4.5 to 7.5 were obtained for hotels located in temperate and Mediterranean climates. The investigation also revealed that the hot water charging strategy, rather than the specific CO_2 heat pump design, is the least expensive measure to enhance performance.

All details and discussions regarding the results of the research work can be found in the enclosed articles in the Appendix.

5 Conclusions

The main objective of this work was to describe concepts and evaluate the performance of integrated CO_2 systems for hotels in cold climates. In order to complete this aim, investigations of the current energy status in hotels were performed to uncover the need and demand within the particular sector. Moreover, an in-depth comprehensive analysis of an integrated CO_2 hotel unit was performed and evaluated through numerical models. Finally, several concepts and control strategies for integrated CO_2 hotel systems were described and investigated through evaluations of the energy performance, environmental impact and economic viability. The following general conclusions can be summarized for the thesis work.

The investigation of hotels in Norway and Sweden revealed that the sector has a large potential to reduce energy consumption and related emissions. The group of medium and large-sized hotels demonstrated a mean annual energy consumption of 1.9 and 4.5 GWh, with accompanying emissions in the range of 500 to 1200 tonnes, respectively. Thus, the largest potential of energy reduction lies in these two specific groups of hotels.

A shift towards sustainable energy sources was observed over the five-year investigated period, which is in agreement with findings in the literature. The overall consumption of electricity was reduced by close to 8%, in favor of district heating. Access to district heating also increased substantially over the investigated period. As a consequence, hotels with only electricity access have been halved over the five years. Investigations of installed thermal energy systems illustrated that the majority (90%) of the hotels utilized either district heating or electric boilers as the primary heat source. Application of the latter represents the least efficient way to generate thermal energy. As a consequence, relatively high specific energy consumption is observed when this technology is applied. District heating was applied in all types of hotels, heavily related to network availability. Though considered

a green alternative, district heating does not necessarily contribute to reductions in operational costs. This is due to the fact that prices vary considerably depending on season and are generally high during the coldest months of the year when heating demand is at its peak. Thus, many hotels that apply district heating and electric boilers could benefit economically and in terms of emissions by applying more energy-efficient thermal systems.

Integrated CO_2 systems have been successfully established as a sustainable and efficient technology within the supermarket sector. As a natural refrigerant, CO_2 has a low global warming potential. The unique properties of CO_2, especially the large temperature glide in the transcritical region, is highly advantageous when heating domestic hot water. Hotels have relatively sizeable hot water demands, which makes CO_2 particularly applicable in this type of building. Moreover, CO_2 systems can be implemented with ease and high flexibility as a retrofit solution in existing hotels, where other natural refrigerants are limited due to safety restrictions on account of toxicity and flammability. An investigation was performed of the energy consumption in two hotels, newly equipped with integrated CO_2 systems and thermal storage. In both cases, heat energy consumption reductions of about 60% were observed, revealing the great potential of integrated CO_2 heat pump systems as a thermal solution for hotels.

An in-depth investigation of the operations of an integrated CO_2 unit revealed that the thermal energy demand of hot water heating represented more than half the annual heat requirement of the hotel. Significant consumption peaks were observed in the mornings and evenings, which were successfully reduced by more than 100 kW on account of the thermal buffer provided by the 6 m^3 hot water storage. It was found that a substantial thermal storage is essential for high performance of the integrated CO_2 hotel unit, as it enables more flexible operations and charging over longer periods of time. In the observed system, charging of the thermal storage took place over a period of 7-10 hours. With the current operating strategy at low ambient temperature, it was revealed that system performance, when charging did not occur, was generally higher when compared with charging mode. In general, during periods with high space heating demands, the COPs were about 1-5% lower during hot water charging at ambient temperatures below 10 °C, due to elevated fluid return temperatures from the hotel. This behavior was attributed to poor stratification caused by mixing in the storage tanks during hot water production. Moreover, the storage of the system was found to be inadequate, as it forced the CO_2 unit to operate under unfavorable conditions, i.e., high gas cooler pressures, to fulfill domestic hot water demands that were not covered by the storage. Thus, the flexibility that the storage provided was not fully utilized with the current hot water charging strategy.

A numerical transient model of the above-mentioned system demonstrated that the overall performance of the hotel's thermal system could be enhanced considerably when applying an alternative control scheme for charging the domestic hot water storage. The principle of the proposed low load control strategy was to charge the storage at longer periods of time and at reduced loads, thus utilizing the cold supply water to continuously cool down the CO_2 gas cooler outlet temperature and, by this, enhance performance. Applying this strategy resulted in an increase of energy savings of up to 13.2% depending on the season. The annual energy savings were estimated to be 8.4%. Other observed benefits from applying the strategy include reduction in peak power utilization and operational fluctuations, such as a high number of on/off cycles, which can shorten the system's lifetime.

Finally, three different design concepts for integrated CO_2 units were evaluated in terms of energy consumption, environmental impact and economic viability. The main characteristics of the evaluated designs were single-stage compression, parallel compression, and ejector-supported parallel compression. In addition, two hot water charging strategies were implemented and investigated, namely the low load strategy and the traditional approach. The investigations demonstrated that applying continuous charging at low loads enhanced the performance of the system over a wide range of ambient temperatures. It was also revealed that charging strategy, rather than specific cycle design, was a larger influence on COP and also the least expensive measure to enhance performance. Moreover, emissions reductions of up to 400 tonne CO_2-eq were achieved when applying integrated CO_2 solutions in place of a boiler and HFC-based chiller system. The payback periods for the different designs were comparable and varied from 3$\sim$8 years, depending on location.

Application of refrigerants with low global warming potential and known environmental effects is necessary to achieve the climate goals established in numerous international environmental protocols, regulations and agreements. The findings of the doctoral work demonstrate that integrated CO_2 systems are efficient in providing heating and cooling in hotels. Moreover, the performance of the system is enhanced with the application of a thermal storage, which enables the compensation of asynchronous thermal loads. This thermal management philosophy will be essential in the future to reduce energy and power consumption within the growing hotel sector. As demonstrated in this thesis, the charging strategy of the thermal storage is a crucial element in achieving high efficiency. This research can be applied to further climate goals, as it provides the theoretical basis for manufacturers and consumers to successfully introduce novel integrated CO_2 hotel solutions in cold climates.

6 Suggestions for further work

This doctoral work described concepts and evaluated the performance of integrated CO_2 systems for hotels in cold climates. Evaluation of field data and simulations revealed that the performance of the systems can be improved by applying a thermal storage charging strategy that aims to continuously produce hot water at low loads. However, more research is necessary to quantify and experimentally validate the findings in this thesis.

Future studies within the application of integrated CO_2 systems for hotels should focus on the following.

- This doctoral work revolved around the application of integrated CO_2 systems within medium-sized hotels. Due to the high level of individuality in terms of thermal demands within each specific building, the application of integrated CO_2 systems should be investigated for hotels of all sizes and functionalities, i.e., large conference hotels and small city hotels.
- Additional pilot installations of integrated CO_2 systems in hotels in cold climates should be established and thoroughly documented to quantify the findings of this research. Documented information regarding performance, energy savings, emissions reductions and achieved economic savings should be made available for potential customers in order for the technology to gain a higher degree of public confidence.
- Further research is necessary to evaluate the application of integrated CO_2 systems in other climates, such as temperate and Mediterranean locations. Experimental investigations applying typical demands for the specific regions should be performed. Moreover, detailed analysis of the recorded operational data, performance and economic viability should be performed to establish integrated CO_2 systems as an alternative to HFC-based thermal solutions.

In respect to the application of low load thermal storage charging in integrated CO_2 systems, the following suggestions are given for future research.

- Practical experimental investigations of the suggested charging strategy are necessary to validate the operating strategy in a real integrated CO_2 system. Such an investigation should take place over longer periods in order to validate the strategy for all possible operating conditions.
- Other measures that can enhance the performance and reduce operational cost during thermal storage charging should be evaluated in light of the proposed charging strategy. One such example that should be considered is accounting for fluctuation in electricity prices. Typically, electricity prices in Scandinavia are lower during nighttime when the overall public electricity consumption is low. Thus, integrated CO_2 systems, as well as other installations that apply a large thermal storage, could benefit from shifting the storage charging period to a time that enabled a reduction in operational costs.
- Finally, interesting results have been presented regarding the possibility of implementing prediction algorithms, e.g., machine learning, to predict demands within thermal systems. Such algorithms can be integrated with thermal system operational data, in addition to the planned guest load. A consequence of applying this technology is that hot water demands could be predicted and used as an input to the integrated CO_2 system. Thus, it would be possible to optimize control of the thermal system according to future demand, i.e., increase production in periods when high hot water demands are expected.

References

[1] European Commission (2016). *An EU Strategy on Heating and Cooling, COM 51 Final*. Brussels, Belgium, 2016: https://ec.europa.eu/energy/sites/ener/files/documents/1_EN_ACT_part1_v14.pdf. Accessed: 2020-10-08.

[2] Rousselot, M. (2018). *Energy efficiency trends in buildings*. ODYSSEE-MURE project Policy brief, June 2018. https://www.odyssee-mure.eu/publications/policy-brief/buildings-energy-efficiency-trends.pdf. Accessed: 2020-10-11.

[3] Eurostat (2017). *Final energy consumption by sector*. Accessed: 2020-11-11. URL: https://ec.europa.eu/eurostat/databrowser/view/ten00124/default/table?lang=en.

[4] Economidou, M., Atanasiu, B., Despret, C., Maio, J., Nolte, I., and Rapf, O. (2011). "Europe's buildings under the microscope. A country-by-country review of the energy performance of buildings". In: *Buildings Performance Institute Europe (BPIE)*, pp. 35–36.

[5] European Commission (EC) (2006). *Action Plan for Energy Efficiency: Realising the Potential, Communication from the Commission, COM (2006) 545 Final*. Accessed: 2020-11-11. URL: https://eur-lex.europa.eu/legal-content/EN/TXT/PDF/?uri=CELEX:52006DC0545&from=EN.

[6] PricewaterhouseCoopers (PwC) (2018). *Best placed to grow? European cities hotel forecast for 2018 and 2019*. April 2018.

[7] The World Tourism Organization (UNWTO) (2019). *UNWTO World Tourism Barometer and Statistical Annex*. Vol. 17(4). November 2019.

[8] Hotel Energy Solutions (2011). "Analysis on energy use by European hotels: Online survey and desk research". In: *Hotel Energy Solutions Project Publi-*

cation. Accessed: 2020-09-11. URL: https://www.e-unwto.org/doi/book/10.18111/9789284414970.

[9] Pérez-Lombard, L., Ortiz, J., and Pout, C. (2008). "A review on buildings energy consumption information". In: *Energy and buildings* 40.3, pp. 394–398.

[10] Langseth, B. (2015). *Analyse av energibruk i yrkesbygg (Analysis of energy consumption in commercial buildings)*. Tech. rep. NVE, pp. 1–48.

[11] Santamouris, M., Balaras, C., Dascalaki, E., Argiriou, A., and Gaglia, A. (1996). "Energy conservation and retrofitting potential in Hellenic hotels". In: *Energy and Buildings* 24.1, pp. 65–75.

[12] Norwegian Ministry of Environment (2008). *Norwegian climate policy - Summary in English: Report No. 34 (2006–2007) to the Storting)*. Tech. rep., pp. 29–31.

[13] Swedish Ministry of the Environment (2009). *A coherent climate and energy policy - climate. Government bill 2008/09:162)*. Tech. rep. Stockholm.

[14] Dalton, G., Lockington, D., and Baldock, T. (2008). "A survey of tourist attitudes to renewable energy supply in Australian hotel accommodation". In: *Renewable energy* 33.10, pp. 2174–2185.

[15] Bohdanowicz, P. (2006). "Environmental awareness and initiatives in the Swedish and Polish hotel industries—survey results". In: *International journal of hospitality management* 25.4, pp. 662–682.

[16] Stene, J. (2005). "Residential CO_2 heat pump system for combined space heating and hot water heating". In: *International Journal of Refrigeration* 28.8, pp. 1259–1265. DOI: 10.1016/j.ijrefrig.2005.07.006.

[17] Nekså, P. (2002). "CO_2 heat pump systems". In: *International journal of refrigeration* 25.4, pp. 421–427.

[18] Diaby, A. T., Byrne, P., and Maré, T. (2019a). "Simulation of heat pumps for simultaneous heating and cooling using CO_2". In: *International Journal of Refrigeration* 106, pp. 616–627.

[19] McNutt, M. K., Bradford, M., Drazen, J. M., Hanson, B., Howard, B., Jamieson, K. H., Kiermer, V., Marcus, E., Pope, B. K., Schekman, R., et al. (2018). "Transparency in authors' contributions and responsibilities to promote integrity in scientific publication". In: *Proceedings of the National Academy of Sciences* 115.11, pp. 2557–2560.

[20] Bodinus, W. S. (1999). "The rise and fall of carbon dioxide systems: The first century of air conditioning". In: *ASHRAE journal* 41.4, p. 37.

[21] Linde, C. (1894). *Zur Theorie der Kohlensäure-(Kaltdampf-) maschinen*. Springer.

[22] Velders, G. J., Andersen, S. O., Daniel, J. S., Fahey, D. W., and McFarland, M. (2007). "The importance of the Montreal Protocol in protecting climate". In: *Proceedings of the National Academy of Sciences* 104.12, pp. 4814–4819.

[23] Oberthür, S. and Ott, H. E. (1999). *The Kyoto Protocol: international climate policy for the 21st century*. Springer Science & Business Media.

[24] Lorentzen, G. (Jun. 12th, 1990). "Trans-critical vapour compression cycle device". Patent no. WO1990007683A1.

[25] Pettersen, J. (1994). "Operation of Trans-Critical CO_2 Vapour Compression Systems in Vehicle Air Conditioning". In: *Proceedings of the International Conference on New Applications of Natural Working Fluids in Refrigeration and Air Conditioning, Hannover, Germany (1994) May 10-13*.

[26] Kim, M.-H., Pettersen, J., and Bullard, C. W. (2004). "Fundamental process and system design issues in CO_2 vapor compression systems". In: *Progress in energy and combustion science* 30.2, pp. 119–174.

[27] Lorentzen, G. (1994). "Revival of carbon dioxide as a refrigerant". In: *International journal of refrigeration* 17.5, pp. 292–301.

[28] Lorentzen, G. (1995). "The use of natural refrigerants: a complete solution to the CFC/HCFC predicament". In: *International journal of refrigeration* 18.3, pp. 190–197.

[29] Lorentzen, G. and Pettersen, J. (1993). "A new, efficient and environmentally benign system for car air-conditioning". In: *International journal of refrigeration* 16.1, pp. 4–12.

[30] Nekså, P., Rekstad, H., Zakeri, G. R., and Schiefloe, P. A. (1998). "CO_2-heat pump water heater: characteristics, system design and experimental results". In: *International Journal of refrigeration* 21.3, pp. 172–179.

[31] Bredesen, A., Hafner, A., Pettersen, J., Neksa, P., and Aflekt, K. (1997). "Heat transfer and pressure drop for in-tube evaporation of CO_2". In: *Science et technique du froid*, pp. 35–49.

[32] Neksa, P., Girotto, S., Schiefloe, P., RIVET, P., and HALOZAN, M. (1998). "Commercial refrigeration using CO_2 as refrigerant: System design and experimental results. Discussion". In: *Science et technique du froid*, pp. 270–280.

[33] Girotto, S., Minetto, S., and Neksa, P. (2004). "Commercial refrigeration system using CO_2 as the refrigerant". In: *International journal of refrigeration* 27.7, pp. 717–723.

[34] Pearson, A. (2005). "Carbon dioxide—new uses for an old refrigerant". In: *international Journal of Refrigeration* 28.8, pp. 1140–1148.

[35] Calm, J. M. (2008). "The next generation of refrigerants–Historical review, considerations, and outlook". In: *international Journal of Refrigeration* 31.7, pp. 1123–1133.

[36] The European Parliament and the Council of the European Union (2006). "Directive 2006/40/EC of the European Parliament and of the Council of 17 May 2006 relating to emissions from air conditioning systems in motor vehicles and amending Council Directive 70/156/EEC". In: *Official Journal of the European Union*.

[37] Zhang, J.-F., Qin, Y., and Wang, C.-C. (2015). "Review on CO_2 heat pump water heater for residential use in Japan". In: *Renewable and Sustainable Energy Reviews* 50, pp. 1383–1391.

[38] Shecco (2020). *World Guide to Transcritical CO_2 Refrigeration (Part II)*. Tech. rep. Shecco Base, June 18th, 2020.

[39] Frank, T. (2021). *Impact of fluorinated refrigerants and their degradation products on the environment and health*. Tech. rep. Refolution Industrielkälte GmbH.

[40] Holland, R., Khan, M. A. H., Driscoll, I., Chhantyal-Pun, R., Derwent, R. G., Taatjes, C. A., Orr-Ewing, A. J., Percival, C. J., and Shallcross, D. E. (2021). "Investigation of the Production of Trifluoroacetic Acid from Two Halocarbons, HFC-134a and HFO-1234yf and Its Fates Using a Global Three-Dimensional Chemical Transport Model". In: *ACS Earth and Space Chemistry* 5.4, pp. 849–857.

[41] Campbell, J., Kable, S., and Hansen, C. (2021). *Photodissociation of CF3CHO provides a new source of CHF3 (HFC-23) in the atmosphere: implications for new refrigerants*. Preprint from Research Square doi:10.21203/rs.3.rs-199769/v1.

[42] Cecchinato, L., Chiarello, M., Corradi, M., Fornasieri, E., Minetto, S., Stringari, P., and Zilio, C. (2009). "Thermodynamic analysis of different two-stage transcritical carbon dioxide cycles". In: *International Journal of refrigeration* 32.5, pp. 1058–1067.

[43] Torrella, E., Sánchez, D., Llopis, R., and Cabello, R. (2011). "Energetic evaluation of an internal heat exchanger in a CO_2 transcritical refrigeration plant using experimental data". In: *International Journal of Refrigeration* 34.1, pp. 40–49.

[44] Matthiesen, O., Madsen, K., and Mikhailov, A. (2010). "Evolution of CO_2 systems design based on practical experiences from supermarket installations in Northern Europe". In: *9th IIR Gustav Lorentzen Conference, Sydney, Australia.*

[45] EU LIFE Project (2008). *Development and demonstration of a prototype transcritical CO_2 refrigeration system.* Tech. rep. European Commission.

[46] Ge, Y. and Tassou, S. (2011). "Thermodynamic analysis of transcritical CO_2 booster refrigeration systems in supermarket". In: *Energy Conversion and Management* 52.4, pp. 1868–1875.

[47] Sawalha, S., Karampour, M., and Rogstam, J. (2015). "Field measurements of supermarket refrigeration systems. Part I: Analysis of CO_2 trans-critical refrigeration systems". In: *Applied Thermal Engineering* 87, pp. 633–647.

[48] Gullo, P., Tsamos, K., Hafner, A., Ge, Y., and Tassou, S. A. (2017). "State-of-the-art technologies for transcritical R744 refrigeration systems–a theoretical assessment of energy advantages for European food retail industry". In: *Energy Procedia* 123, pp. 46–53.

[49] Javerschek, O., Craig, J., and Xiao, A. (2015). "CO_2 as a refrigerant – start right away!" In: *Proceedings of the 24th IIR International Congress of Refrigeration, Yokohama, Japan,* ID: 15.

[50] Wiedenmann, E., Schoenenberger, J., and Baertsch, M. (2014). "Efficiency analysis and comparison of innovative R744-refrigerating systems in commercial applications". In: *Proceedings of the 11th IIR Gustav Lorentzen Conference on Natural Refrigerants, Hangzhou, China*, pp. 406–412.

[51] Pardiñas, Á. Á., Hafner, A., and Banasiak, K. (2018). "Novel integrated CO_2 vapour compression racks for supermarkets. Thermodynamic analysis of possible system configurations and influence of operational conditions". In: *Applied Thermal Engineering* 131, pp. 1008–1025.

[52] Hafner, A. and Banasiak, K. (2016). "Full scale supermarket laboratory R744 ejector supported and AC integrated parallel compression unit". In: *Proceedings of the 12th IIR Gustav Lorentzen Conference on Natural Refrigerants, Edinburgh, UK*, pp. 21–24.

[53] Pardiñas, Á. Á., Contiero, L., Hafner, A., Banasiak, K., and Larsen, L. F. (2020). "Attaining a higher flexibility degree in CO_2 compressor racks". In: *Proceedings of the 14th IIR-Gustav Lorentzen Conference on Natural Refrigerants, Kyoto (online), Japan*. IIR.

[54] Elbel, S. and Lawrence, N. (2016). "Review of recent developments in advanced ejector technology". In: *International Journal of Refrigeration* 62, pp. 1–18.

[55] Hafner, A., Försterling, S., and Banasiak, K. (2014). "Multi-ejector concept for R-744 supermarket refrigeration". In: *International Journal of Refrigeration* 43, pp. 1–13.

[56] Gullo, P., Hafner, A., Banasiak, K., Minetto, S., and Kriezi, E. E. (2019). "Multi-ejector concept: A comprehensive review on its latest technological developments". In: *Energies* 12.3, p. 406.

[57] Hafner, A., Banasiak, K., Herdlitschka, T., Fredslund, K., Girotto, S., Haida, M., and Smolka, J. (2016). "R744 ejector system case: Italian supermarket, Spiazzo". In: *12th IIR Gustav Lorentzen Conference on Natural Refrigerants, Edinburgh, Scotland*.

[58] Tosato, G., Minetto, S., Rossetti, A., Hafner, A., Schlemminger, C., and Girotto, S. (2020a). "Field data of CO_2 integrated refrigeration, heating and cooling systems for supermarkets". In: *Proceedings of the 14th IIR-Gustav Lorentzen Conference on Natural Refrigerants, Kyoto (online), Japan*, pp. 363–368.

[59] Minetto, S., Marinetti, S., Saglia, P., Masson, N., and Rossetti, A. (2018). "Non-technological barriers to the diffusion of energy-efficient HVAC&R solutions in the food retail sector". In: *International Journal of Refrigeration* 86, pp. 422–434.

[60] Peters, T. (2018). "A Cool World: Defining the energy conundrum of cooling for all". In: *Technical Report. Birmingham Energy Institute, The Institute for Global Innovation*.

[61] Toby Peters (2019). "Doing cold better". In: *Proc. from ATMOsphere Europe 2019*.

[62] Abdin, N., Hafner, A., Girotto, S., Menten, F., Pruss, Y., and Savigliano, R. (2019). "CO_2 commercial refrigeration system in Jordan". In: *Proceedings of the 25th IIR International Congress of Refrigeration, August 24-30, Montreal, Canada*, pp. 3476–3483.

[63] Singh, S., Hafner, A., Maiya, M., Banasiak, K., and Neksa, P. (2021). "Multi-ejector CO_2 cooling system with evaporative gascooler for a supermarket application in tropical regions". In: *Applied Thermal Engineering* 190. ID: 116766.

[64] Singh, S., Hafner, A., Banasiak, K., Seshadri, S., Maiya, P., Smitt, S., and Gabrielii, C. H. (2020). "Heat pump/chiller system for centralized kitchens in India". In: *Proceedings of the 14th IIR-Gustav Lorentzen Conference on Natural Refrigerants, Kyoto (online), Japan*. IIR.

[65] Gullo, P., Hafner, A., and Banasiak, K. (2018). "Transcritical R744 refrigeration systems for supermarket applications: Current status and future perspectives". In: *International Journal of Refrigeration* 93, pp. 269–310.

[66] Rogstam, J. (2016). "Evolution of CO_2 as refrigerant in ice rink applications". In: *12th IIR Gustav Lorentzen Natural Working Fluids Conference, Edinburgh, UK*, pp. 21–24.

[67] Stensli, M. (2019). "Enter Norway largest CO_2 transcritical installation". In: *Proc. from ATMOsphere Europe 2019*.

[68] Jin, Z. (2017). "Investigation of CO_2 hybrid ground-coupled heat pumping system for warm climate". PhD thesis. Trondheim, Norway: Norwegian University of Science and Technology.

[69] Hafner, A. and Nekså, P. (2018). "Integrated CO_2 solutions for supermarkets". In: *13th IIR Gustav Lorentzen Conference, Valencia, Spain*.

[70] Karampour, M. and Sawalha, S. (2016). "Energy efficiency evaluation of integrated CO_2 trans-critical system in supermarkets: A field measurements and modelling analysis". In: *International journal of refrigeration* 82, pp. 470–486.

[71] Hafner, A., Claussen, I., Schmidt, F., Olsson, R., Fredslund, K., Eriksen, P., and Madsen, K. (2014). "Efficient and integrated energy systems for supermarkets". In: *11th IIR Gustav Lorentzen Conference on Natural refrigerants, IIR/IIF, Hangzhou, China*.

[72] Jorschick, H. (2014). "Measurement and evaluation of energy integrated supermarkets concept". PhD thesis. Master's thesis, Norwegian University of Science and Technology, Trondheim.

[73] Karampour, M. and Sawalha, S. (2015). "Theoretical analysis of CO_2 transcritical system with parallel compression for heat recovery and air conditioning in supermarkets". In: *24th IIR Refrigeration Congress of Refrigeration. IIF/IIR, Yokohama, Japan*. Vol. 304.

[74] Polzot, A., D'Agaro, P., and Cortella, G. (2016). "Energy analysis of a transcritical CO_2 supermarket refrigeration system with heat recovery". In: *8th International Conference on Sustainability in Energy and Buildings, Turin, Italy*.

[75] Karampour, M. and Sawalha, S. (2018). "State-of-the-art integrated CO_2 refrigeration system for supermarkets: A comparative analysis". In: *International journal of refrigeration* 86, pp. 239–257.

[76] Azzolin, M., Cattelan, G., Dugaria, S., Minetto, S., Calabrese, L., and Del Col, D. (2021). "Integrated CO_2 systems for supermarkets: Field measurements and assessment for alternative solutions in hot climate". In: *Applied Thermal Engineering* 187, p. 116560.

[77] Byrne, P., Miriel, J., and Lenat, Y. (2009). "Design and simulation of a heat pump for simultaneous heating and cooling using HFC or CO_2 as a working fluid". In: *International Journal of Refrigeration* 32.7, pp. 1711–1723. ISSN: 0140-7007. DOI: 10.1016/j.ijrefrig.2009.05.008.

[78] Minetto, S., Girotto, S., Rossetti, A., and Marinetti, S. (2015). "Experience with ejector work recovery and auxiliary compressors in CO_2 refrigeration systems. Technological aspects and application perspectives". In: *Proceedings of the Ammonia Refrigeration Technology International Conference, Ohrid, Macedonia*. Vol. 1618.

[79] Diaby, A. T., Byrne, P., and Maré, T. (2019b). "Simulation of heat pumps for simultaneous heating and cooling using CO_2". In: *International Journal of Refrigeration* 106, pp. 616–627. ISSN: 0140-7007. DOI: 10.1016/j.ijrefrig.2019.03.010.

[80] Tosato, G., Artuso, P., Minetto, S., Rossetti, A., Allouche, Y., and Banasiak, K. (2020b). "Experimental and numerical investigation of a transcritical CO_2 air/water reversible heat pump: analysis of domestic hot water production". In: *Proceedings of the 14th IIR-Gustav Lorentzen Conference on Natural Refrigerants*. IIR.

[81] Tosato, G., Girotto, S., Minetto, S., Rossetti, A., and Marinetti, S. (2019). "An integrated CO_2 unit for heating, cooling and DHW installed in a hotel. Data from the field." In: *37th UIT Heat Transfer Conference*.

[82] Hafner, A., Girotto, S., and Tosato, G. (2020). *CO_2 Heat Pump Water Chillers*. Eurammon Symposium/Webinar.

[83] Minetto, S. (2011). "Theoretical and experimental analysis of a CO_2 heat pump for domestic hot water". In: *International Journal of Refrigeration* 34.3, pp. 742–751.

[84] Cecchinato, L., Corradi, M., Fornasieri, E., and Zamboni, L. (2005). "Carbon dioxide as refrigerant for tap water heat pumps: a comparison with the traditional solution". In: *International Journal of Refrigeration* 28.8, pp. 1250–1258.

[85] Liu, F., Zhu, W., Cai, Y., Groll, E. A., Ren, J., and Lei, Y. (2017). "Experimental performance study on a dual-mode CO_2 heat pump system with thermal storage". In: *Applied Thermal Engineering* 115, pp. 393–405.

[86] Cortella, G., D'Agaro, P., Saro, O., and Polzot, A. (2014). "Modelling integrated HVAC and refrigeration systems in a supermarket". In: *Proc. 3rd IIR International Conference on Sustainability and the Cold Chain, Twickenham, London (UK)*.

[87] Polzot, A., D'Agaro, P., Gullo, P., and Cortella, G. (2016). "Modelling commercial refrigeration systems coupled with water storage to improve energy efficiency and perform heat recovery". In: *International Journal of Refrigeration* 69, pp. 313–323.

[88] Tammaro, M., Mauro, A., Montagud, C., Corberán, J., and Mastrullo, R. (2016). "Hot sanitary water production with CO_2 heat pumps: Effect of control strategy on system performance and stratification inside the storage tank". In: *Applied Thermal Engineering* 101, pp. 730–740.

[89] IWMAC (2019). *Centralized Operation and Surveillance by Use of WEB Technology*. Accessed: 2019-10-08. URL: `https://www.iwmac.com/`.

[90] Thom, H. C. S. (1954). "The rational relationship between heating degree days and temperature". In: *Monthly Weather Review* 82.1, pp. 1–6.

[91] Enova SF (2020). *Graddagstall 2019 (Heating Degree Days 2019)*. `https://www.enova.no/`. Accessed: 2020-08-08.

[92] Mattsson, S. E., Elmqvist, H., and Otter, M. (1998). "Physical system modeling with Modelica". In: *Control Engineering Practice* 6.4, pp. 501–510.

[93] Dassault Systems (2019). *DYMOLA Systems Engineering: Multi-Engineering Modeling and Simulation based on Modelica and FMI*.

[94] TLK-Thermo GmbH (2020). *TIL Suite – Simulates thermal systems*. URL: `https://www.tlk-thermo.com/index.php/en/software/til-suite`.

Appendix

Article I

S. Smitt, I. Tolstorebrov, P. Gullo, Á. Pardiñas, A. Hafner (2021). "Energy use and retrofitting potential of heat pumps in cold climate hotels." In: *Journal of Cleaner Production* 298, 2021, 126799. DOI: 10.1016/j.jclepro.2021.126799

Journal of Cleaner Production 298 (2021) 126799

Contents lists available at ScienceDirect

Journal of Cleaner Production

journal homepage: www.elsevier.com/locate/jclepro

Energy use and retrofitting potential of heat pumps in cold climate hotels

S. Smitt [a, *], I. Tolstorebrov [a], P. Gullo [b], A. Pardiñas [c], A. Hafner [a]

[a] Norwegian University of Science and Technology, Department of Energy and Process Engineering, Kolbjørn Hejes Vei 1D, 7491, Trondheim, Norway
[b] Technical University of Denmark, Department of Mechanical Engineering, Nils Koppels Allé 403, 2800, Kgs. Lyngby, Denmark
[c] SINTEF Energy Research, Kolbjørn Hejes Vei 1D, 7465, Trondheim, Norway

ARTICLE INFO

Article history:
Received 30 November 2020
Received in revised form
18 February 2021
Accepted 19 March 2021
Available online 24 March 2021

Handling editor: M.T. Moreira

Keywords:
Energy use
Hotels
Thermal energy systems
Cold climates

ABSTRACT

Tourism, and thereby hotels, play a crucial role in the European economy. The hotel sector features high energy consumption, which greatly contributes to the global warming effect. Thus, there is a need to investigate environmentally friendly technologies that have the potential to reduce energy usage within this sector. Information regarding the current status of the energy consumption in hotels is essential. Therefore, a study of 140 hotels in Norway and Sweden is presented in this paper to identify successful and sustainable measures to reduce energy consumption and related emissions.

The energy use, available energy sources and thermal systems in the hotels are studied over a five-year period to identify consumption trends. The results reveal that 70% of the hotels have a mean annual energy consumption between 150 and 250 kWh/m^2. A shift towards sustainable energy sources is observed in the hotels from 2015 to 2019, where application and overall consumption of district heating and cooling have increased, while electrical energy consumption has been reduced. District heating is the most prominent source of heating and is applied as the primary heat source in 70% of the hotels. The specific energy consumption for the group hotels that apply district heating is 218.9 kWh/m^2/year, which is nearly 25% higher than the specific energy consumption of the 9% of hotels that apply heat pump solutions as a primary heat source. Thus, there is a potential to reduce the specific energy consumption in hotels. Two integrated transcritical carbon dioxide (CO_2) heat pumps were investigated as a sustainable measure to reduce energy consumption. The results reveal that a reduction of thermal energy consumption of approximately 60% can be achieved.

1. Introduction

According to the EU strategic plan for heating and cooling in buildings, new and sustainable solutions for generating thermal energy must be applied to achieve the 2-degree goal of the Paris Agreement (EC, 2016). Presently, buildings account for more than 40% of the total end-use energy consumption in Europe (Rousselot, 2018). Approximately 1/3 of this energy consumption and related emissions is connected to the commercial sector (Eurostat, 2017). By implementing measures to increase efficiency and manage demands, it is estimated that energy saving of 30% can be achieved within the commercial sector (Economidou et al., 2011; EC, 2006).

Hotels are energy-intense buildings due to the nature of their operation and the behavior of the occupants (HES, 2011). The energy consumption in the hotel sector is high compared to other commercial sectors, such as the school and hospital sector (Pérez-Lombard et al., 2008). Many authors have tackled the challenge related to excessive energy consumption in hotels by applying alternative renewable energy sources and surveillance tools (Karagiorgas et al., 2006; Dalton et al., 2009; Aagreh and Al-Ghzawi, 2013). The largest contributor to excessive energy use within the hotel sector is hot water, space heating and cooling. In cold climates, it is estimated that approximately 61% of the total energy consumption in hotels is allocated to heating and cooling (Langseth, 2015). The application of conventional thermal energy sources in hotels is extensive, such as electric boilers in large inefficient central systems (Dalton et al., 2008b). A majority of hotels apply centralized heating stations, where thermal heat is generated and further transported throughout the building by a

* Corresponding author.
E-mail addresses: silje.smitt@ntnu.no (S. Smitt), ignat.tolstorebrov@ntnu.no (I. Tolstorebrov), parigul@mek.dtu.dk (P. Gullo), angel.a.pardinas@sintef.no (A. Pardiñas), armin.hafner@ntnu.no (A. Hafner).

https://doi.org/10.1016/j.jclepro.2021.126799

Nomenclature

AC	Air-Conditioning
BIO	Biofuel
COP	Coefficient of Performance
DC	District Cooling
DH	District Heating
EL	Electricity
GO	Guarantees of Origin
GWP	Global Warming Potential
HDD	Heating Degree Days
HFC	Hydrofluorocarbons
HP	Heat Pump
MAAT	Mean Annual Air Temperature [°C]
N	Norway
NG	Natural Gas
R	Hydrofluorocarbons
S	Sweden
T	Temperature [°C]

secondary hydronic circuit.

Heating in Nordic hotels has been highly dominated by electric panels or hydronic heating through electric boilers, as a result of relatively low electricity prices caused by the availability of renewable energy sources. Norway is nearly exclusively supplied with electricity from hydro- and wind power, which share of the national production totaled approximately 98% in 2017 (Scheben et al., 2020). In Sweden, about 58% of the electric energy was renewable in 2018, mainly supported by hydro- and nuclear power (SEA, 2020). However, due to the high amount of energy guarantees of origin (GO) exported to Europe from both Norway and Sweden, the end-use CO_2 emissions related to electricity is estimated to 396 and 339 g CO_2-eq/kWh for 2019, respectively (NVE, 2020; Ei, 2020).

Fossil fuel-fired boilers are still the most applied source of heating in Europe despite high emissions (EC, 2016). Boilers are combustion machines that burn fuel, such as oil and natural gas (NG), for heating purposes. The related emissions from boilers applying oil and NG are 268 and 205 g CO_2-eq/kWh, respectively (SDHA, 2018). To reduce the environmental footprint, legislation and favorable incentives have been introduced in Norway and Sweden to encourages building owners to adopt sustainable heating solutions (Di Lucia and Ericsson, 2014; Norwegian Ministry of Environment, 2008; Swedish Ministry of the Environment, 2009). An environmentally friendly alternative to traditional fossil fuels is biofuels, which have related emissions of 15 g CO_2-eq/kWh (Gustafsson et al., 2016).

District heating (DH) has become a well-established heat source within the Nordic countries. DH is a network of insulated pipes, where heat is distributed to customers that are connected to the grid through in-house heat exchangers. The heat is generated at a centralized location near industrial processes with surplus heat, such as waste disposal plants. 49 and 22% of the heat in the DH networks in Norway and Sweden were generated from waste disposal in 2019 (Swedenergy, 2020; SSB, 2020). The related emissions from DH heat consumption in Norway and Sweden are calculated based on the 2019 DH mix and footprint values established by SDHA (2018). DH related emissions for Norway and Sweden are calculated to 115 and 63 g CO_2-eq/kWh, respectively. For the production of district cooling (DC), cold water from lakes and the sea is normally used. Alternatively, DC can be produced with the cooling effect from heat pumps during DH heat generation. The emissions related to the use of DC is estimated to 60 g CO_2-eq/kWh (Dalin and Rubenhag, 2006).

In contrast with EL and DH, heat pumps upgrade heat from one temperature level to another. Thus, a considerably smaller amount of electricity is needed to generate thermal heat than for EL boilers. The performance indicator of a heat pump system, referred to as the coefficient of performance (COP), gives the amount of heat generated per unit of electricity. The COP of the heat pump is highly dependent on the supply and return temperatures in the heating system. The installation of thermal storage is an effective measure to improve the performance of heat pump systems. For hotels, thermal storage in the form of hot water tanks is applied to reduce peak loads (Tosato et al., 2019; Smitt et al., 2019).

The refrigerant, from which heat is transferred while undergoing the heat pump cycle, is selected based on characteristics like temperature, pressure, heat capacity, flammability and toxicity. The environmental impact of these fluids is referred to as global warming potential (GWP). Non-synthetic refrigerants that are naturally occurring, such as carbon dioxide (CO_2), ammonia and propane, have marginal GWPs (Lorentzen, 1995). Synthetic refrigerants, such as hydrofluorocarbons (HFCs), have high GWP and contribute significantly to global warming (Abas et al., 2018). Therefore, industrial and scientific efforts have been invested in improving heat pump systems with natural refrigerants and identifying new areas of applications, such as the hotel sector. Additionally, national legislation, governmental economical incentives and reduced operational costs are strengthening the position of efficient and environmentally friendly thermal systems (Norwegian Ministry of Environment, 2008; Swedish Ministry of the Environment, 2009). Moreover, the environmental aspect of tourism is becoming important for guests when selecting hotels (HES, 2011). Nearly 80% of potential guests believe that renewable energy is important for European tourist accommodations (Dalton et al., 2008a). Yet, reducing the operational cost is undeniably the biggest incentive among hotel owners to introduce environmentally-friendly initiatives (Bohdanowicz, 2006).

The European hotel sector has increased during the last decade with an annual market growth between 7 and 13% (PwC, 2018). Although heavily affected by the COVID-19 epidemic, it is expected that the European hotel sector will recover and that the number of international visitors will increase by 43 million a year until 2030 (UNWTO, 2020; UNWTO, 2019). In order to reduce the energy consumption of this growing sector, sustainable solutions for thermal energy production must be applied. Information regarding the current status of energy consumption and thermal heating in hotels is therefore essential. To the best of the authors' knowledge, no large-scale investigations of Nordic hotels have been conducted in the last decade. Furthermore, no analyses of thermal systems in hotels have been performed to differentiate energy consumption and emissions according to thermal heat source. This paper presents a study of 140 hotels in Norway and Sweden, where energy consumption, energy source and thermal systems are evaluated over a five-year period.

The scope of this paper is to evaluate key performance indicators related to energy consumption in Norwegian and Swedish hotels. The annual energy consumption per heated floor area (kWh/m^2/year) and energy consumption per guest-night (kWh/guest-night/year) are applied to evaluate the energy performance of the hotels. Energy usage based on different activities in the hotel buildings is beyond the scope of the research. The results are reviewed over a five-year period to reveal the energy-related trends and the long-term dynamics of the sample hotels. The focus of the study is the thermal heating systems, which are the main contributing source of excessive energy usage in cold-climate hotels. The environmental impact of different thermal solutions in hotels are evaluated by the use of the CO_2-equivalent carbon footprint values and the energy source-specific consumption in

each hotel. Two of the hotels in this study are among the first in Europe to implement thermal solutions with integrated CO_2 heat pumps, both heating and cooling. The energy performance and the sector-wide implementation potential of the systems are evaluated in terms of energy savings.

2. Methods and materials

2.1. Data collection

The sampled hotels presented in this analysis are located in Norway and Sweden. The sample group consists of 140 hotels. As a whole, the Norwegian and Swedish hotel sectors consist of nearly 3900 hotels (Horwath HTL, 2010). To increase the validity of the results, only hotels with automatic energy logging surveillance systems were included in this study. Energy data from the hotels have been collected via several web-monitoring services, such as the software *IWMAC* (IWMAC, 2019). The energy data contain information about the specific energy use according to the energy source in each hotel, e.g. DH and electricity. The data are presented on an annual basis. The performance of the hotels is considered over a five year period, from 2015 to 2019. Hotels with compromised energy data for specific years, due to e.g. energy system maintenance or facility closure, have been excluded from the analysis for that particular year. Information regarding installed energy systems, energy consumption and guest-nights have been collected through surveys. Further, the information has been compared and validated with logged data from each specific hotel.

2.2. Hotel classification

Fig. 1 illustrates the arrangement of the climate zones in Norway and Sweden according to their respective national standards. Norway (N) is divided into seven climate zones, primarily based on coastal, inland and highland climates, ranging from south to north (Tokle and Tønnesen, 1999).

The four Swedish (S) climate zones are established primarily based on latitude and are defined in the 2015 Swedish building code (Boverket, 2015). Climate zone characteristics, mean annual air temperature (MAAT) and the number of hotels in each zone are listed in Table 1 The number of hotels are equally distributed between Norway and Sweden, with 70 in each country. The location of the hotels, according to the different climate zones, is consistent with the population density of each country.

Approximately 10% of the Norwegian population and 6% of the Swedish population reside in the northern climate zones (SSB, 2014; SCB, 2020a). Consequently, a mere 12% of the sample hotels are located in the northern part of the countries (N6, N7 and S1). 60% of the sample hotels are located in the southern regions of Norway and Sweden, in zones N1, N2 and S3, due to the close proximity to major cities.

Heating degree days (HDD) are applied to compare energy consumption in buildings, independent of variations in annual ambient temperature and thus heating consumption. The HDD values for the different zones are calculated with a standard threshold of 17 °C, as defined by Thom (1954). Table 2 lists the annual specific adjustment factor [-] for heating, which is defined as the HDD for a particular year, divided by HDD of a standard year. The values indicate the relative coldness for a particular year related to a normal year. The HDD data for Norway have been obtained from Enova SF (2020), whilst the commercially available Swedish climate data have been provided by The Swedish Meteorological and Hydrological Institute. The heat energy consumption in the hotels has been corrected according to their zone-specific adjustment factors. As illustrated in Table 2, all zones have experienced elevated ambient temperatures during the five-year period, as the adjustment factor is below 1.00.

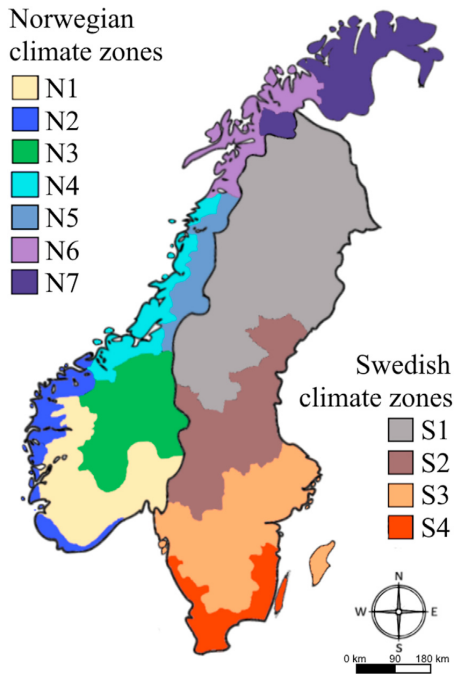

Fig. 1. Norwegian and Swedish climate zones.

Table 1
Description of climate zones and the location of the hotels.

Zone	Description	MAAT* [°C]	No. of hotels
N1	Southern Norway, coastal climate	5.1[a]	27
N2	Southern Norway, inland climate	7.1[a]	24
N3	Southern Norway, highland climate	2.3[a]	4
N4	Central Norway, coastal climate	5.4[a]	8
N5	Central Norway, inland climate	3.0[a]	0
N6	Northern Norway, coastal climate	3.8[a]	7
N7	Northern Norway, inland climate	0.7[a]	0
S1	Northern Sweden, inland climate	-2.0–0.0[b]	10
S2	Central Sweden, inland climate	2.0–4.0[b]	9
S3	Southern Sweden, inland climate	4.0–6.0[b]	34
S4	Southern Sweden, coastal climate	6.0–8.0[b]	17

* Mean annual air temperature.
[a] Tokle and Tønnesen (1999).
[b] Lundström et al. (2018).

All sample hotels have a heated floor area, henceforth referred to as floor area, in the range of 1446 to 38,000 m^2. The hotels have been arranged according to floor area to evaluate the energy performance of small, medium and large-sized hotels. As no standard for hotel classification exists in Norway and Sweden, a range of floor area has been selected for the classification, in preference to the number of rooms. This is done to best illustrate the energy consumption in a variety of hotels: small city hotels with many rooms to large spa hotels with a moderate number of rooms. However, the hotel sizes (small, medium and large) correlate to the number of hotel rooms in the range of 34–99, 100–299 and above 300. The number of hotels in each category is listed in Table 3.

Table 2
Adjustment factor for climate zones in Norway and Sweden related to climate data from 1981 to 2010.

Zone/Year	2015	2016	2017	2018	2019
N1	0.884	0.926	0.920	0.924	0.907
N2	0.885	0.928	0.913	0.931	0.911
N3	0.892	0.942	0.939	0.940	0.924
N4	0.873	0.939	0.930	0.950	0.944
N5	0.895	0.947	0.915	0.986	0.959
N6	0.868	0.926	0.953	0.962	0.985
N7	0.896	0.900	0.950	0.938	0.986
S1	0.892	0.950	0.971	0.968	0.981
S2	0.892	0.936	0.950	0.942	0.932
S3	0.885	0.937	0.927	0.916	0.896
S4	0.884	0.924	0.916	0.891	0.860

3. Results and discussion

3.1. Energy analysis

The energy data from the hotels have been analyzed and are presented in this section. Fig. 2 shows the five-year mean annual energy consumption per floor area for all the sample hotels (kWh/m^2/year). When observing the energy consumption for all the hotels, it can be seen that about 40% have an energy consumption in the range of 175–225 kWh/m^2. The majority of the hotels, approximately 70%, have an energy consumption between 150 and 250 kWh/m^2/year. The mean energy consumption for all hotels is calculated to 213 kWh/m^2/year, which is slightly low when compared with earlier findings in other large-scale investigations of Nordic hotels. A comprehensive study by Bohdanowicz et al. (2005) found that a sample of hotels located in Sweden had an annual specific energy consumption of approximately 280 kWh/m^2/year in 2003. SEA (2011) concluded that a mean energy consumption of 250 kWh/m^2/year applies for hotels in Sweden. At a later time, Langseth (2015) suggested that a mean energy consumption of 240 kWh/m^2/year is representative for Norwegian hotels. It is reasonable to assume that the energy consumption in Nordic hotels has decreased during the last decade, due to an increased focus on energy management, innovations in building technologies and legislative restrictions.

The energy consumption distribution profile for small and large-sized hotels are considerably shifted compared to the distribution for all the hotels. This is in agreement with the mean average consumption for the small, medium and large-sized hotels, which is calculated to 237, 209 and 192 kWh/m^2/year, respectively. Thus, the results indicate an inverse relationship between hotel size and specific energy consumption, which can be explained by the typical energy systems installed in different sized hotels. Smaller hotels are often located in city centers, where space, building mass and investment costs limit the economical advantages of replacing outdated thermal systems. Larger hotels consume considerable amounts of energy and therefore deal with high operational costs. The most efficient energy systems are therefore installed in this category of buildings, as the potential savings are substantial along with shorter payback time. When investigating the energy consumption of the hotels according to country, the Norwegian and Swedish hotels were found to have an annual specific energy consumption of 203 and 222 kWh/m^2/year, respectively. The difference can be attributed to the fact that 60% of small-sized hotels in this investigation are located in Sweden.

Table 3
Hotel classification.

Category	Size	No. of hotels
Small	floor area $\leq$ 5000 m^2	34
Medium	5000 m^2 < floor area $\leq$ 16,000 m^2	83
Large	floor area > 16,000 m^2	23

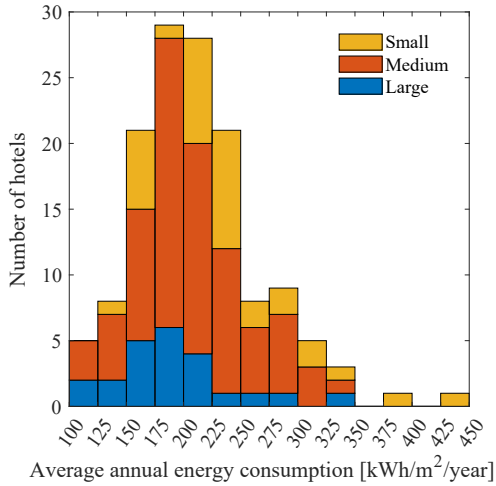

Fig. 2. Average annual energy consumption for the hotels per square meter floor area (2015–2019).

Fig. 3 shows the average annual energy consumption of the hotels per guest-night, where 55% of the hotels display a specific consumption in the range between 20 and 40 kWh/guest-night/year. The mean annual energy consumption for all the sample hotels is calculated to 37.8 kWh/guest-night/year.

Similar to Fig. 2, the distribution according to different hotel sizes is also illustrated in Fig. 3. The mean annual energy consumption is calculated to 29.2, 39.8 and 43.4 kWh/guest-night/year, for small, medium and large hotels, respectively. Thus, the opposite trend is observed when evaluating the specific energy consumption in terms of guest-nights and floor area. As can be observed in Fig. 3, the specific energy consumption per guest-night increases with hotel size, being that large hotels consume nearly 48% more than hotels that are categorized as small. Specialized hotels, such as spa and conference hotels, are generally of larger size and require more space and energy per guest due to the nature of the facilities.

Table 4 lists the mean annual energy consumption per guest-night, which is steady between 38 and 41 kWh/guest-night/year for the years 2015–2018. A small reduction in specific energy consumption per guest-night is observed in 2019, which can be attributed to the increase in the average number of guest-nights for that particular year.

The mean annual energy consumption (GWh/hotel), along with the related emissions (kg CO_2-eq/hotel), are included in Table 4. For the average hotel, the energy consumption is in the vicinity of 2 GWh/year. The energy consumption and the emissions related to hotel size is shown in Table 5. On average, large hotels consume more than 4.5 GWh/hotel/year, which is five times more than small-sized hotels. The same trend is observed for the total emissions, where small and large hotels emit, on average, 209,885 and 1,166,734 kg CO_2-eq/hotel/year, respectively. The mean annual emissions from energy consumption in the hotels vary with approximately 30,000 kg CO_2-eq/hotel during the five years, as

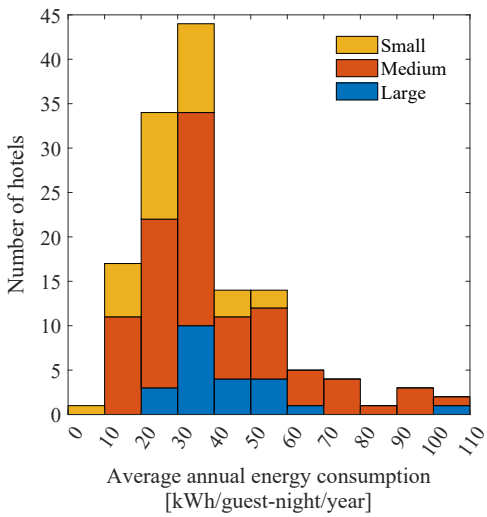

Fig. 3. Average annual energy consumption for the hotels per guest-night (2015–2019).

shown in Table 4.

The highest amount of emissions occurred in 2018, where more than 560,000 kg CO_2-eq on average were emitted from each hotel. Between 8.4 and 9.7 kg CO_2-eq is recorded per guest-night during the five-year period. The range of emissions related to the hotel sizes is shown in Table 5 and vary from 7.7 to 13.7 kg CO_2-eq/guest-night/year. The values presented in this study are higher than emissions reported for the Nordic hotel sector, which generally vary between 3.3 and 6.0 kg CO_2-eq/guest-night (Thompson, 2019; Larsson and Kamb, 2018). However, the contribution of energy GO export between nations was not accounted for in these studies, only each countries' standard calculated emissions per kWh consumed. This presents a challenge, as each country tend to calculate the energy-related emission with favorable values. Thus, some country standard values for emissions include the energy GO related emission and some do not. As explained in Section 1, GO related emissions are applied in this study to give a comparative account for the large-scale environmental impact from different energy sources and thereby the impact from different thermal systems in hotels.

The distribution of the energy consumption according to source is shown in Fig. 4, while the available energy sources in the hotels are illustrated in Fig. 5. The category *other* includes burners for oil, natural gas and biofuel. The energy consumption of this group is stable at around 1% for the whole period, as shown in Fig. 4. A slight

Table 5
Mean energy indicators for the hotels categorized by size based on data for all five years (2015–2019).

Value/Hotel size	Small	Medium	Large
Energy consumption			
GWh/hotel/year	0.8	1.9	4.5
Emissions			
kg CO_2-eq/hotel/year	209,885	508,232	1,166,734
kg CO_2-eq/guest-night/year	7.7	11.0	13.7

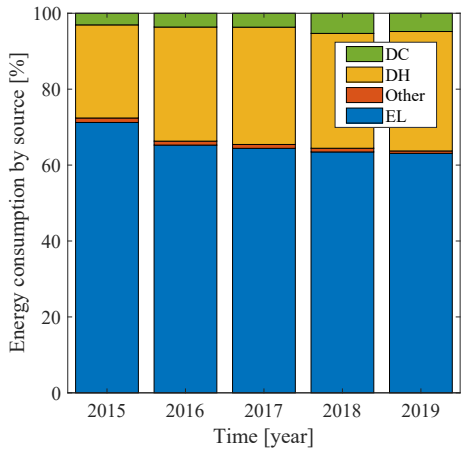

Fig. 4. Energy consumption by energy source in the hotels [%].

increase in the use of other energy sources is observed in Fig. 5, which is mainly

attributed to newly installed bio-fuel systems. EL in Fig. 4 constitutes the largest share of the energy consumption each year and includes the total electricity consumption in the hotels. All processes that require electricity within the buildings are included in this category. For certain hotels, this entails electricity for electric boilers, heating panels, heat pumps and air-conditioning (AC) units. Approximately 71% of the total energy consumption in 2015 was recorded as EL. However, an 8% decrease in the total share of EL energy consumption is observed over the five-year period. This is in agreement with the data presented in Fig. 5, which shows that the amount of hotels with EL-only access is almost halved, from 37.5% in 2015 to 19.4% in 2019. During the same period, the number of hotels connected to DH and DC networks has increased by 18.0 and 10.9%, respectively. This trend is reflected in the percentage DH consumption to the total energy usage in Fig. 4, which shows an increase of 7% over the five years, from 24.5 to 31.5%. Thus, many hotels have replaced electric thermal heating systems in favor of

Table 4
Mean annual energy indicators for the sample hotels.

Value/Year	2015	2016	2017	2018	2019
Hotels analyzed [-]	96	125	136	140	134
Guest-nights [guest-night/hotel]	54,772	58,178	59,472	60,382	64,377
Energy consumption [GWh/hotel]	1.8	2.1	2.0	2.1	2.0
Energy consumption per guest-night [kWh/guest-night]	38	39	38	41	36
Energy consumption per floor area [kWh/m^2]	195	214	214	218	211
Emissions from energy consumption [kg CO_2-eq/hotel]	529,739	567,132	548,069	560,371	538,116
Emissions per guest-night [kg CO_2-eq/guest-night]	9.7	9.7	9.2	9.3	8.4

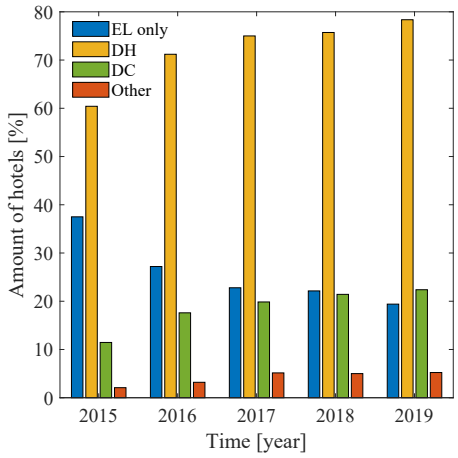

Fig. 5. Available energy sources in the hotels.

DH during this period. Likewise, DC energy consumption increased by about 2% from 2015 to 2019. Similar trends have been documented within the Swedish non-residential buildings sector, where the total share of DH consumption has increased by 7.6% from 2005 to 2016 (SEA, 2017).

Fig. 6 shows an overview of the primary and secondary thermal heating systems installed in the sample hotels. The four primary thermal heating systems that are applied in the hotels are DH, HP solutions, NG and EL, in which the latter includes both electric boilers and electric panels. DH represents the.

largest group of the primary thermal energy system, as 98 of the 140 hotels (70%) use DH as a primary heat source. DH is used as a secondary or back-up thermal energy system in four hotels. This corresponds to the data presented in Figs. 4 and 5, which illustrate high consumption levels of DH and a high degree of DH availability

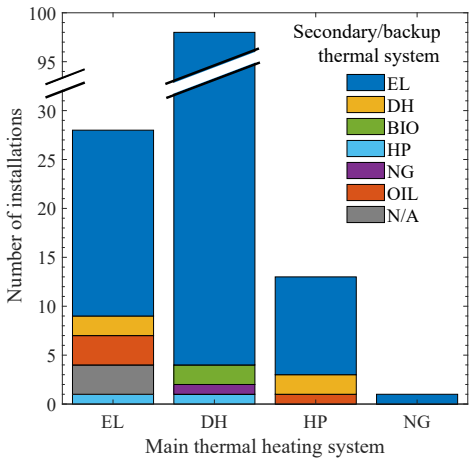

Fig. 6. Overview of primary and secondary thermal heating systems in all hotels (2019).

in the different hotels. The second most applied primary energy system is EL, with 28 hotels (20%). 9 of these hotels have an alternative backup heat source, with OIL and DH being the most prominent. Only three hotels lack information about secondary systems, denoted *N/A* in figure Fig. 6. Despite providing relatively low system efficiencies and a high carbon footprint, EL heating is reliable and easily implemented. EL is, therefore, favored as a secondary/peak heating source and applied as such in 124 hotels (88%). As shown in Figs. 6 and 13 hotels use HP systems as their primary heating system. This category includes stand-alone heat pump units, integrated heat pump and chiller units and large central heat pump units that supply heat to a collective of buildings. Only two of the hotels in this category apply natural working fluids, which have a minimal GWP compared to the HFC working fluids (Bolaji and Huan, 2013). Two additional heat pumps are applied as secondary system solutions, mainly for domestic hot water production.

Table 6 lists key energy indicators, such as energy use and emissions, with respect to the four primary thermal systems shown in Fig. 6.

The sole hotel that represents the NG primary systems has the largest area-specific energy consumption of the groups, at a value of 236.7 kWh/m^2/year. The DH primary thermal system group includes 70% of the hotels and is the most applied heating system in both countries. The mean specific energy consumption for this group is among the highest at a value of 218.9 kWh/m^2/year. However, the mean guest-specific energy consumption of DH systems is only 35.6 kWh/guest-night/year, which is lower than EL and NG based primary systems. The group of hotels that apply EL as their primary thermal heating system have the highest recorded guest-specific energy consumption at 43.1 kWh/guest-night/year, and area-specific energy consumption of 204.9 kWh/m^2/year. Thus, an inverse relationship exists between the specific energy consumption of the two groups, EL and DH, which can be explained by trends shown in Figs. 2 and 3. The group of hotels that apply EL as their primary thermal system are generally of medium-to-large size, whereas small-to-medium sized hotels are over-represented in the DH primary heat source category. As listed in Table 6, hotels that apply EL as their primary systems perform poorly in regards to energy-related emissions. The mean specific emissions from this group are 79.8 CO_2-eq/m^2 and 16.8 CO_2-eq/guest-night, which is considerably higher than for the alternative heating systems. The superior thermal solution, in terms of emissions, is DH primary systems. Both the area and guest-related emissions are considerably lower for the group of hotels with DH primary systems, at values of 48.7 CO_2-eq/m^2 and 8.3 CO_2-eq/guest-night. The low emissions of DH compared to the alternative systems are directly tied to the electricity GO export, which elevates the specific emissions of EL and HP primary systems.

The HP based system is the most efficient primary thermal system of the alternatives presented in Table 6. The hotels that are categorized within this group have a mean specific energy consumption of 175.4 kWh/m^2/year and 34.0 kWh/guest-night/year. Thus, the hotels equipped with HP as the primary systems consume

Table 6
Mean energy indicators with respect to primary thermal system (2015–2019).

Value/Main system	EL	DH	HP	NG
Energy consumption				
kWh/m^2	204.9	218.9	175.4	236.7
kWh/guest-night	43.1	35.6	34.0	36.3
Emissions				
kg CO_2-eq/m^2	79.8	48.7	62.8	64.4
kg CO_2-eq/guest-night	16.8	8.3	11.8	9.9

14.6% and 19.9% less kWh/m^2/year compared with EL and DH, respectively. The heat pumps that constitute the HP group are of different design and year of installation. The efficiencies of the heat pumps are not accounted for in this study. However, the recent development of heat pump technology affirms that heat pump solutions for hotels can achieve a considerably larger amount of energy savings when compared with EL and DH thermal systems. Bianco et al. (2017) illustrated how renewable technologies, such as heat pumps, could decrease the energy consumption and related emissions within the Italian hotel sector by 13% (1.6 TWh). Yet, not all working fluids are preferred for heat pumps in hotels, due to safety restrictions on account of toxicity and flammability (EN 378−1:2016). Additionally, many non-natural refrigerants, like HFC, are in the process of being phased out in the EU and Scandinavia (Heath, 2017). CO_2 is a natural and safe working fluid, which application in heat pumps is thoroughly accepted and documented (Rony et al., 2019; Zhang et al., 2015). If design properly, CO_2 heat pumps are efficient, safe, and sustainable solutions for thermal heating in hotels (Nekså, 2002; Smitt et al., 2020; Tosato et al., 2019; Smitt and Hafner, 2019). Section 3.2 presents the operational results of two hotels implemented with such thermal systems.

3.2. CO_2 heat pump solutions for hotels

Two different schematic designs of integrated transcritical CO_2 heat pump systems are shown in Fig. 7.

The system illustrated in Fig. 7(a) consists of four separate parallel units and has a total heating capacity of 800 kW. The system was installed in 2019 in hotel *A*, which is located in climate zone N2. The hotel was built in 1990 and has a floor area of 13,500 m^2. The CO_2 system collects heat from seawater through two titanium heat exchangers and lifts this to a temperature of approximately 80 °C. Through the secondary system, heat is supplied for space and water heating. The hot water system is equipped with 10 m^3 thermal storage and supplies hot water for guests in the main building and the hotel water park. Additionally, heat is exported from the hotel to a nearby gym. The space heating circuit supplies heat to both the hotel and the water park, as well as heating of the swimming pool. An 8 m^3 thermal storage is included in this circuit as a heat buffer to reduce the return temperature from the hotel to the CO_2 heat pump. This is imperative in transcritical CO_2 systems to achieve high efficiency and is described thoroughly in the literature (Minetto et al., 2016; Tammaro et al., 2016). Fig. 7(b) illustrates the integrated CO_2 system that was installed in hotel *B* in 2018, which is located in zone N4. The hotel is 9000 m^2 and the thermal system consists of a single CO_2 unit that supplies heat to space heating and the 6 m^3 hot water storage. The heating and AC cooling capacity of the system is 280 and 75 kW, respectively. A detailed description and analysis of the system installed in hotel *B* is given by Smitt et al. (2020). Though different in design, a key feature in both transcritical CO_2 systems is the thermal storage, which acts as a buffer that allows for flexible operation of the thermal system. Thus, peak power demands are reduced by accumulating heat over time, rather than supplying peak-heating to meet the instantaneous demands.

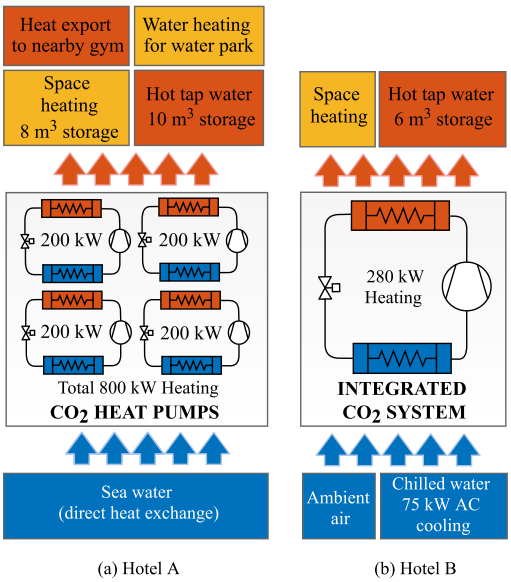

Fig. 7. Schematic of thermal systems installed in (a) hotel *A* and (b) hotel *B*.

Fig. 8 shows the specific energy consumption of hotel *A* for the last five years. Hotel *A* was equipped with an electric boiler before the CO_2 heat pump was installed in November 2019. For the year 2019, hotel *A* achieved a reduction in the overall energy consumption in the hotel of 26.3%, which corresponds to a reduction of 1.2 GWh/year or 88.6 kWh/m^2/year.

In order to indicate the performance of the CO_2 system after the commissioning period, the energy consumption and guest-nights for selected months in 2020 are shown in Fig. 9. The mean monthly energy consumption and guest-nights from 2015 to 2019 are given as a reference. Months of operation that were influenced by the COVID-19 outbreak are not included in Fig. 9. All selected months in 2020 demonstrate a reduction in the specific energy consumption compared to the mean values (2015−2019), despite the increase in guest load over this period. The largest change in specific energy consumption is observed during the month of September when a 51.3% reduction in energy consumption is achieved. July represents the month with the lowest reduction in total specific energy consumption, at -31.6% compared to the mean value. It should, however, be noted that hotel *A* experienced a 32.9%

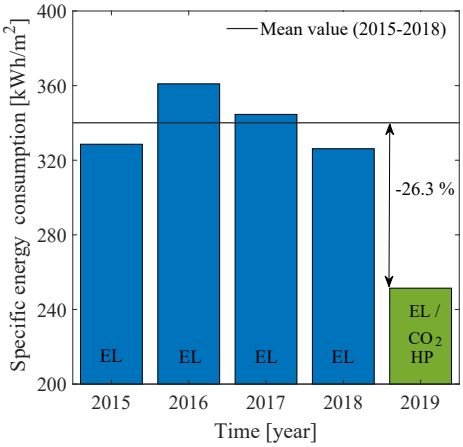

Fig. 8. Energy consumption of hotel *A* for the years 2015−2019. The reduction in energy usage after retrofit in 2019 is related to the mean of the four previous year.

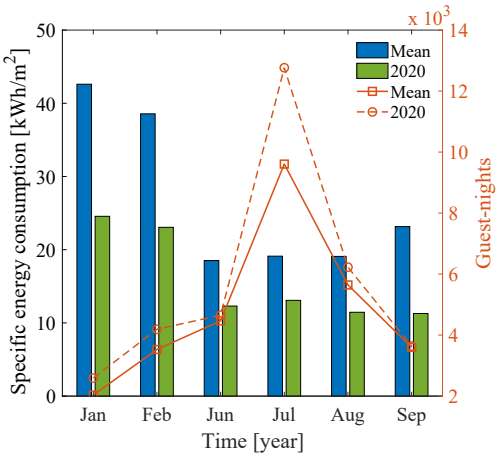

Fig. 9. Specific energy consumption and guest-nights for hotel *A* for selected months in 2020. Mean values for energy consumption and guest-nights for the period 2015–2019 are used as reference.

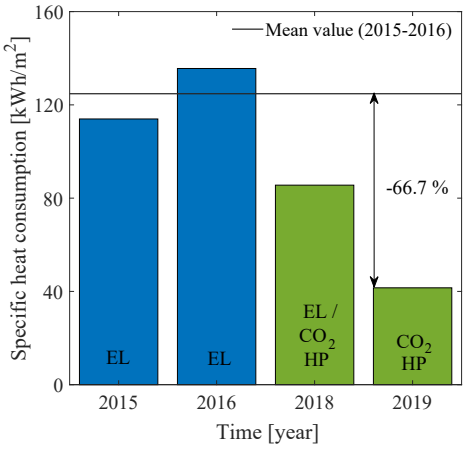

Fig. 10. Heat energy consumption of hotel *B* for specific years. The reduction in energy usage after retrofit is related to the mean heat energy consumption from 2015 to 2016, as the data from 2017 is insufficient.

increase in the guest-load during July 2020. The average monthly savings based on the selected months in Fig. 9 is calculated to 39.8%. If the monthly reduction in specific energy consumption is extrapolated to the annual performance of the thermal system, more than 1.8 GWh of energy could be saved each year. This is a considerable improvement in the efficiency of the thermal system and would correspond to a 60% reduction in the hotel's area-specific heat consumption.

The specific heat consumption of hotel *B* in relation to the reference years 2015 and 2016 is shown in Fig. 10. Operational data from 2017 is not included. The system was installed in June 2018 and, similar to hotel *A*, demonstrated a meager improvement in thermal system efficiency during the first year of operation. However, a reduction of 66.7% in specific heat energy consumption was achieved in 2019, which corresponds to an overall reduction of 73.2 kWh/m^2/year or 600 MWh/year in the hotel.

The operation data from hotel *A* and *B* demonstrate that CO_2 heat pump systems can achieve a reduction in heat consumption of approximately 60% when compared with EL and DH. However, optimal design of main and secondary systems is essential for a successful implementation of CO_2 heat pumps. The integrated CO_2 unit in hotel *B* illustrates a sustainable approach to heating and cooling in hotels, as thermal energy is recovered within the building itself and stored for later use. This thermal management philosophy will be essential in the future to reduce energy and power consumption within the hotel sector. The integration of CO_2 technology for heating and cooling in hotels is in its infancy, and the technology must be improved to be acknowledged as a worthy competitor to the traditional HFC systems (Diaby et al., 2019; Byrne et al., 2009). CO_2 refrigeration systems for supermarkets faced similar challenges when the first units were installed in the early 2000s. At present, CO_2 refrigeration is the benchmark solution within the European supermarket sector, where more than 29,000 units are installed (Shecco, 2020). Heat pump and refrigeration systems with low GWP refrigerants are unarguably necessary to reduce global warming and to reach the 2-degree goal of the Paris Agreement (Rogelj et al., 2016). Thus, new areas of application for natural refrigerants must be identified, such as integrated CO_2 heat pumps solution in hotels.

4. Conclusions

The energy consumption in cold-climate hotels has been studied for the period 2015–2019 by using field measurements. The following conclusions can be made based on the investigation of 140 hotels in Norway and Sweden.

- 70% of the hotels have a mean annual energy consumption between 150 and 250 kWh/m^2/year, with the mean value for all hotels being 213 kWh/m^2/year. Thus, there is a potential to further reduce the energy consumption in the hotels.
- A shift towards sustainable energy sources is observed in the sample hotels from 2015 to 2019. Electricity is the most applied energy source in hotels and accounted for more than 70% of the total energy use in 2015. However, the overall electricity consumption was reduced by 8% from 2015 to 2019 in favor of district heating, which increased by 7% over the same period. The access to district heating and cooling increased by 18.0 and 10.9% from 2015 to 2019. The number of hotels with only electricity access has been halved over the five-year period.
- The evaluation of primary and secondary thermal heating systems revealed that 70% of the hotels apply district heating as the main source of heating in 2019. The specific energy consumption for this group of hotels is 219.9 kWh/m^2/year, which is larger when compared with hotels that use electricity or heat pump technology to generate heat. The 9% of the hotels that apply heat pumps as their main heating system have the lowest specific energy consumption of all the investigated thermal systems, with 175.4 kWh/m^2/year.
- Two of the investigated hotels have been equipped with integrated CO_2 heat pump systems and thermal storage, where a reduction in energy usage in the range of 73.2–88.6 kWh/m^2/year was achieved. In both cases, a heat energy consumption reduction of about 60% is observed, revealing the great potential of integrated CO_2 heat pump systems as a thermal solution for hotels.

It can be concluded that heat pump systems, especially the ones relying on CO_2 as the sole working fluid, represent the most

sustainable solution for cold climate hotels, regardless of their size. Therefore, it is thought that highly energy-efficient hotels involving reversible transcritical CO_2 heat pump units and renewable energy technologies will become standard in cold climates in the next few years.

Declaration of competing interest

The authors declare that they have no known competing financial interests or personal relationships

Acknowledgments

The authors would like to thank The Swedish Meteorological and Hydrological Institute for access to their data. The authors would like to acknowledge the Norwegian Research Council for funding this project.

References

Aagreh, Y., Al-Ghzawi, A., 2013. Feasibility of utilizing renewable energy systems for a small hotel in Ajloun city, Jordan. Appl. Energy 103, 25–31.
Abas, N., Kalair, A.R., Khan, N., Haider, A., Saleem, Z., Saleem, M.S., 2018. Natural and synthetic refrigerants, global warming: a review. Renew. Sustain. Energy Rev. 90, 557–569.
Bianco, V., Righi, D., Scarpa, F., Tagliafico, L.A., 2017. Modeling energy consumption and efficiency measures in the Italian hotel sector. Energy Build. 149, 329–338.
Bohdanowicz, P., 2006. Environmental awareness and initiatives in the Swedish and polish hotel industriessurvey results. Int. J. Hospit. Manag. 25, 662–682.
Bohdanowicz, P., Simanic, B., Martinac, I., 2005. Environmental training and measures at scandic hotels, Sweden. Tourism Rev. Int. 9, 7–19.
Bolaji, B., Huan, Z., 2013. Ozone depletion and global warming: case for the use of natural refrigerant–a review. Renew. Sustain. Energy Rev. 18, 49–54.
Boverket, 2015. Konsekvensutredning BBR, Ndring Av Boverkets Byggregler [BBR] Avsnitt 9 Energihushllning (Impact Assessment BBR, Amendment of the National Board of Housing, Building and Planning's Building Rules Section 9 Energy Management). Karlskrona, Sweden, 2015.
Byrne, P., Miriel, J., Lenat, Y., 2009. Design and simulation of a heat pump for simultaneous heating and cooling using HFC or CO_2 as a working fluid. Int. J. Refrig. 32, 1711–1723.
Dalin, P., Rubenhag, A., 2006. Possibilities with more district cooling in Europe. Ecoheatcool, Work package 5.
Dalton, G., Lockington, D., Baldock, T., 2008a. A survey of tourist attitudes to renewable energy supply in Australian hotel accommodation. Renew. Energy 33, 2174–2185.
Dalton, G., Lockington, D., Baldock, T., 2008b. Feasibility analysis of stand-alone renewable energy supply options for a large hotel. Renew. Energy 33, 1475–1490.
Dalton, G., Lockington, D., Baldock, T., 2009. Feasibility analysis of renewable energy supply options for a grid-connected large hotel. Renew. Energy 34, 955–964.
Di Lucia, L., Ericsson, K., 2014. Low-carbon district heating in Sweden - examining a successful energy transition. Energy Research & Social Science 4, 10–20.
Diaby, A.T., Byrne, P., Maré, T., 2019. Simulation of heat pumps for simultaneous heating and cooling using CO_2. Int. J. Refrig. 106, 616–627.
Economidou, M., Atanasiu, B., Despret, C., Maio, J., Nolte, I., Rapf, O., 2011. Europe's Buildings under the Microscope. A Country-By-Country Review of the Energy Performance of Buildings. Buildings Performance Institute Europe (BPIE), pp. 35–36.
Swedish Energy Markets Inspectorate (Ei), 2020. Ursprungsmrkning Av El 2019 (Origin Marking of Electricity 2019). Accessed: 2020-08-08, Ω. https://ei.se/sv/for-energiforetag/el/ursprungsmarkning-av-el/.
Enova, S.F., 2020. Graddagstall 2019 (Heating Degree Days 2019). Accessed: 2020-08-08. https://www.enova.no/.
European Commission (EC), 2006. Action plan for energy efficiency: realising the potential, communication from the commission, COM, 545, Accessed: 2020-11-11. https://eur-lex.europa.eu/legal-content/EN/TXT/PDF/?uri=CELEX:52006DC0545&from=EN.
European Commission (EC), 2016. An EU Strategy on Heating and Cooling, COM 51 Final. Brussels, Belgium. Accessed: 2020-10-08. https://ec.europa.eu/energy/sites/ener/files/documents/1_EN_ACT_part1_v14.pdf.
European Committee for Standardization, 2016. EN 378-1:2016 Refrigerating Systems and Heat Pumps - Safety and Environmental Requirements - Part 1: Basic Requirements, Definitions, Classification and Selection Criteria.
Eurostat, 2017. Final energy consumption by sector. Accessed: 2020-11-11. https://ec.europa.eu/eurostat/databrowser/view/ten00124/default/table?lang=en.
Gustafsson, M., Rönnelid, M., Trygg, L., Karlsson, B., 2016. CO_2 emission evaluation of energy conserving measures in buildings connected to a district heating system–Case study of a multi-dwelling building in Sweden. Energy 111, 341–350.
Heath, E.A., 2017. Amendment to the Montreal protocol on substances that deplete the ozone layer (Kigali Amendment). Int. Leg. Mater. 56, 193–205.
Hotel Energy Solutions (HES), 2011. Analysis on Energy Use by European Hotels: Online Survey and Desk Research. Hotel Energy Solutions Project Publication URL: https://www.e-unwto.org/doi/book/10.18111/9789284414970. Accessed: 2020-09-11.
Horwath, H.T.L., 2010. European Chains and Hotels Report 2019. Accessed: 2020-10-08. https://horwathhtl.com/publication/european-chains-hotels-report-2019/.
IWMAC, 2019. Centralized operation and surveillance by use of WEB technology. Accessed: 2019-10-08. https://www.iwmac.com/.
Karagiorgas, M., Tsoutsos, T., Drosou, V., Pouffary, S., Pagano, T., Lara, G.L., Mendes, J.M.M., 2006. HOTRES: renewable energies in the hotels. An extensive technical tool for the hotel industry. Renew. Sustain. Energy Rev. 10, 198–224.
Langseth, B., 2015. Analyse Av Energibruk I Yrkesbygg (Analysis of Energy Consumption in Commercial Buildings) (Technical Report. NVE).
Larsson, J., Kamb, A., 2018. Semestern Och Klimatet (Vacation and the Climate). Metodrapport. Version 1.
Lorentzen, G., 1995. The use of natural refrigerants: a complete solution to the CFC/HCFC predicament. Int. J. Refrig. 18, 190–197.
Lundström, K., Dehlbom, B., Löfroth, H., Vesterberg, B., 2018. Klimatlasters Effter På Naturlig Mark Och Geokonstruktioner: Geotekniska Aspekter På Klimatförändringen (Climate Change Effects on Natural Soil and Geoconstructions: Geotechnical Aspects of Climate Change).
Minetto, S., Cecchinato, L., Brignoli, R., Marinetti, S., Rossetti, A., 2016. Water-side reversible CO_2 heat pump for residential application. Int. J. Refrig. 63, 237–250.
Nekså, P., 2002. Co_2 heat pump systems. Int. J. Refrig. 25, 421–427.
Norwegian Ministry of Environment, 2008. Norwegian Climate Policy - Summary in English: Report No. 34 (20062007) to the Storting) (Technical Report).
Norwegian Energy Regulatory Authority (NVE), 2020. Electricity disclosure 2019. Accessed: 2020-08-08, Ω. https://www.nve.no/energy-supply/electricity-disclosure/.
Pérez-Lombard, L., Ortiz, J., Pout, C., 2008. A review on buildings energy consumption information. Energy Build. 40, 394–398.
PricewaterhouseCoopers (PwC), 2018. Best Placed to Grow? European Cities Hotel Forecast for 2018 and 2019. April 2018.
Rogelj, J., Den Elzen, M., Höhne, N., Fransen, T., Fekete, H., Winkler, H., Schaeffer, R., Sha, F., Riahi, K., Meinshausen, M., 2016. Paris Agreement climate proposals need a boost to keep warming well below 2 C. Nature 534, 631–639.
Rony, R.U., Yang, H., Krishnan, S., Song, J., 2019. Recent advances in transcritical CO_2 (R744) heat pump system: a review. Energies 12, 457.
Rousselot, M., 2018. Energy Efficiency Trends in Buildings. ODYSSEE-MURE Project Policy Brief. Accessed: 2020-10-11. https://www.odyssee-mure.eu/publications/policy-brief/buildings-energy-efficiency-trends.pdf.
Statistics Sweden (SCB), 2020a. Population in the Country, Counties and Municipalities on 30 June, 2020. Accessed: 2020-01-10. https://www.scb.se/en/.
Scheben, H., Klempp, N., Hufendiek, K., 2020. Impact of long-term water inflow uncertainty on wholesale electricity prices in markets with high shares of renewable energies and storages. Energies 13, 2347.
Swedish District Heating Association (SDSA), 2018. Överenskommelse I Värmemarknadskommittén 2018 (Agreement in the Swedish Heating Committee 2018). Energiföretagen Sverige, Stockholm, Sweden. Accessed: 2020-08-08.
Swedish Energy Agency (SEA), 2011. Energianvändning I Hotell, Restauranger Och Samlingslokaler, ER 2011:11 (Energy Use in Hotels, Restaurants and Meeting Points, ER 2011:11) (Technical Report).
Swedish Energy Agency (SEA), 2017. Energy Statistics for Non-residential Premises 2016. Accessed: 2020-09-10. https://energimyndigheten.a-w2m.se/.
Swedish Energy Agency (SEA), 2020. Energy in Sweden 2018: an Overview. Accessed: 2020-08-08. https://energimyndigheten.a-w2m.se/.
Shecco, 2020. World Guide to Transcritical CO_2 Refrigeration (Part II). Technical Report. Shecco Base. June 18th, p. 2020.
Smitt, S., Hafner, A., 2019. Numerical Performance Investigation of a CO_2 Heat Pump and Refrigeration System for a Nordic Hotel, in: Proceedings of the 25th IIR International Congress of Refrigeration. Montréal, Canada. August 24-30, 2019, International Institute of Refrigeration.
Smitt, S., Hafner, A., Hoksrød, E., 2019. Presentation of the First Combined CO^2 Heat Pump, Air Conditioning and Hot Tap Water System for a Hotel in Scandinavia, in: Proceedings of the 8th Conference on Ammonia and CO_2 Refrigeration Technologies, pp. 11–13. April 2019. Ohrid, Republic of Macedonia.
Smitt, S., Tolstorebrov, I., Hafner, A., 2020. Integrated CO_2 system with HVAC and hot water for hotels: field measurements and performance evaluation. Int. J. Refrig. 116, 59–69.
Statistics Norway (SSB), 2014. Norwegian Geographical Population Statistics. Accessed: 2020-01-10. https://www.ssb.no/.
Statistics Norway (SSB), 2020. Statistics: District Heating and District Cooling. Accessed: 2020-08-08. https://www.ssb.no/.
Swedenergy, 2020. Fjrrvrmestatistik (District Heating Statistics). Accessed: 2020-08-08. https://www.energiforetagen.se/.
Swedish Ministry of the Environment, 2009. A Coherent Climate and Energy Policy - Climate. Government bill 2008/09:162). Technical Report. Stockholm.
Tammaro, M., Mauro, A., Montagud, C., Corberán, J., Mastrullo, R., 2016. Hot sanitary water production with CO_2 heat pumps: effect of control strategy on system performance and stratification inside the storage tank. Appl. Therm. Eng. 101, 730–740.
Thom, H., 1954. The rational relationship between heating degree days and

temperature. Mon. Weather Rev. 82, 1–6.
Thompson, S., 2019. Klimagassutslipp Knyttet Til Norsk Reiseliv (Greenhouse Gas Emission Related to Tourism in Norway). NHO Reiseliv. Technical Report.
Tokle, T., Tønnesen, J., 1999. Inndeling Av Norge I Klimasoner (Division of Norway into Climate Zones). SINTEF Energi AS.
Tosato, G., Girotto, S., Minetto, S., Rossetti, A., Marinetti, S., 2019. An Integrated CO_2 Unit for Heating, Cooling and DHW Installed in a Hotel. Data from the field., in: 37th UIT Heat Transfer Conference.
The World Tourism Organization (UNWTO), 2019. UNWTO World Tourism Barometer and Statistical Annex, vol. 17 (4). November 2019.
The World Tourism Organization (UNWTO), 2020. New Data Shows Impact of COVID-19 on Tourism as UNWTO Calls for Responsible Restart of the Sector. June 22th, Madrid, p. 2020.
Zhang, J.F., Qin, Y., Wang, C.C., 2015. Review on CO_2 heat pump water heater for residential use in Japan. Renew. Sustain. Energy Rev. 50, 1383–1391.

Article II

S. Smitt, I. Tolstorebrov, A. Hafner (2020). "Integrated CO_2 system with HVAC and hot water for hotels: Field measurements and performance evaluation." In: *International Journal of Refrigeration* 116, pp. 59-69. DOI: 10.1016/j.ijrefrig.2020.03.021.

International Journal of Refrigeration 116 (2020) 59–69

Contents lists available at ScienceDirect

International Journal of Refrigeration

journal homepage: www.elsevier.com/locate/ijrefrig

Integrated CO_2 system with HVAC and hot water for hotels: Field measurements and performance evaluation

S. Smitt*, I. Tolstorebrov, A. Hafner

Norwegian University of Science and Technology, Kolbjørn Hejes vei 1D, Trondheim 7491, Norway

ARTICLE INFO

Article history:
Received 13 December 2019
Revised 20 March 2020
Accepted 23 March 2020
Available online 8 April 2020

Keywords:
R744
Heat pump
HVAC
Hot water
Thermal storage
Hotel energy systems

ABSTRACT

This study investigates the performance of an integrated CO_2 (R744) heat pump and chiller unit in a Norwegian hotel. The system consists of a single unit for heating, cooling and hot water with an integrated thermal storage. The thermal system of the hotel is described and data from the first year of operation are analyzed. Using the field measurements, hot water loads and COPs are calculated and averaged to 20-minute intervals. The heating and cooling capacities supplied by the R744 unit are studied on a weekly and monthly basis to evaluate the seasonal behavior of the system. The hot water storage holds an energy capacity of 350 kWh at fully charged conditions and demonstrates peak demand reductions of more than 100 kW during a 2-day period. The results show that the hot water usage accounts for 52% of the annual heat load of the hotel. Energy efficiency analysis of the integrated R744 system reveals an annual system SCOP of 2.90, and thus an untapped system potential that can be exploited by increasing the AC load delivered by the R744 unit. Other factors that greatly influence the efficiency of the system are variations in the ambient temperature and high gas cooler exit temperatures. The latter is often a result of high temperatures in the water returning from the subsystems of the hotel. This can be improved by reducing the number of starts and stops of the R744 unit and by insuring stratification in hot water tanks.

Système de CVC et de production d'eau chaude intégré au CO_2 pour les hôtels : mesures sur le terrain et évaluation des performances

Mots-clés: R744; Pompe à chaleur ; CVC; Eau chaude; Stockage de chaleur; Systèmes énergétiques dans l'hôtellerie

1. Introduction

In order to secure a sustainable future, it is necessary to adopt more efficient means of converting, storing and using thermal energy. Buildings are directly responsible for more than 40% of end-use energy consumption and CO_2 emissions in the EU (EC, 2010). Non-residential buildings, which are largely represented by the commercial sector, account for 35% of the energy use and related emissions (Eurostat, 2017). The potential energy savings within the commercial sector is estimated to 30%, which can be achieved by implementing measures to manage demand and increase energy efficiency (Economidou et al., 2011; EC, 2006). Hotels are categorized as high energy demanding buildings, due to their operational characteristics and the behavior of occupants (HES, 2011). The application of conventional thermal energy sources in hotels is extensive, such as fossil fuels and electric boilers for heating in large inefficient central systems (Dalton et al., 2008). Excessive use of electrical power by peak heating and the use of low-efficiency air-conditioning (AC) units aggravate the electricity problems society is facing. Existing hotels exhibit the most severe problems of excessively high energy demand rates, inevitably requiring renovations along with retrofitting of thermal systems (Santamouris et al., 1996).

Vapor compression systems are among the most energy-efficient methods of providing heating and cooling in buildings (Liu et al., 2017). An increased focus on environmentally friendly

* Corresponding author.
E-mail addresses: silje.smitt@ntnu.no (S. Smitt), ignat.tolstorebrov@ntnu.no (I. Tolstorebrov), armin.hafner@ntnu.no (A. Hafner).

https://doi.org/10.1016/j.ijrefrig.2020.03.021

Nomenclature

COP	Coefficient of Performance
DHW	Domestic Hot Water
SH	Space heating
T	Temperature [°C]
V	volume [l]
C_p	specific heat capacity [kWh kg^{-1} K^{-1}]
ref	reference
i	time step index
set	setpoint
E	Energy [kWh]
AC	Air Conditioning
F.S.	Full Scale
$\dot{Q}$	cooling or heating load [kW]
$\dot{m}$	mass flow rate [kg s^{-1}]
$\dot{W}$	power [kW]
P	Pressure [bar]
HPWH	Heat Pump Water Heater
comp	compressors
fans	evaporator fans
pumps	all system pumps
aux, el	auxiliary electrical systems
evap	evaporation
w	supply water
exit	exit
gc	gas cooler
a	ambient
avg	average
SH	space heating
DHW	Domestic Hot Water
AC	Air conditioning
sys	system
min	minimum
max	maximum
ch	DHW charging
nch	No DHW charging
HVAC	Heating, Ventilation, and Air-Conditioning
usage	consumption by end users
supply	supply by heat pump
HFC	Hydrofluorocarbon

Greek symbols

Δ	change
ρ	density [kg m^{-3}]

solutions together with a global effort to reduce the application of fluorinated gases is strengthening the position of natural refrigerants (UNEP, 2016; EP and EC, 2014). Carbon dioxide (R744) is a natural refrigerant with negligible environmental impact and favorable thermodynamic properties (Lorentzen, 1994; Gullo et al., 2019; Ciconkov, 2018). It is inexpensive, readily available and is neither flammable nor toxic. These qualities make R744 suitable in applications where other natural refrigerants, such as ammonia and propane, are challenging due to safety concerns (Bolaji and Huan, 2013). R744 is firmly established in both heating and refrigeration applications and is accepted as a viable alternative in several sectors, e.g. supermarket, transportation, domestic hot water (DHW) heat pumps and industrial processes (Gullo et al., 2018; Hafner, 2015; Neksa et al., 2010). The distinctive temperature glide of R744 in the gas cooler during transcritical operations allows for efficient heating of water (Neksa, 2002; Neksa et al., 1998), even up to temperatures of 90 °C (Bamigbetan et al., 2017). In the Japanese market alone, more than 5 million R744 heat pump water heaters (HPWHs) are installed (Shecco, 2016). However, as illustrated by Cecchinato et al. (2005), a suitable R744 heat pump design is imperative to ensure a high efficiency when compared with hydrofluorocarbon (HFC) installations, such as R134a. In their later work, Cecchinato et al. (2010) identified compressor capacity rate and secondary fluid temperatures as key influencing factors on optimum R744 high pressure, and thus cycle efficiency. Minetto (2011) presented experimental results from the development of an R744 air/water HPWH for residential buildings, and also concluded that optimum operating high-pressure conditions are highly dependent on both inlet temperature and production setpoint temperature for hot water. Several other works have tackled the high-pressure control problem to achieve maximum cycle coefficient of performance (COP) (Yang et al., 2015; Hu et al., 2015; Wang et al., 2013; Cecchinato et al., 2012). The design and operation of the secondary system, especially the DHW storage, is equally important to ensure high efficiency in R744 HPWH installations. It is firmly established that reducing the return temperature from the secondary system to the gas cooler will limit the R744 gas cooler outlet temperature, and thus enhance cycle COP (Lorentzen, 1994). Thermal stratification of the DHW storage should therefore be employed to reduce mixing and ensure the return of cold water to the gas cooler (Fernandez et al., 2010). The impact of the return temperature of water on cycle efficiency, with respect to ambient air and city water temperatures, was illustrated by Yokoyama et al. (2007). They concluded that the R744 HPWH efficiency does not always increase with ambient temperature, as the storage efficiency decreases with the increase of city water temperatures. Besides DHW, another application of the transcritical R744 heat pump is a combined heat supply system for space heating (SH) and DHW by the means of several gas coolers in series (Stene, 2005; Heinz et al., 2010).

R744 systems have a long tradition in refrigeration processes. In the European supermarket sector alone, more than 16,000 stores are relying on R744, where 14% of the installations are operating in the transcritical region (Skačanová and De Oña, 2019). Transcritical R744 systems with integrated heating and cooling applications are traditionally found within this sector, where excess heat is recovered as a byproduct of the refrigeration process (Pardiñas et al., 2018; Hafner, 2017; Girotto, 2016). Combined operations with heat recovery highly enhance the performance of the R744 refrigeration system (Karampour and Sawalha, 2017), and can be especially beneficial in warm climate applications, as demonstrated by Gullo (2019). However, the control strategy during these operations of heating and cooling can highly influence the efficiency (Sarkar et al., 2004; Sarkar et al., 2006). Water storage units can be applied to compensate for asynchronous heating and cooling demands, and reduce peak load operation (D'Agaro et al., 2019; Polzot et al., 2016). Integrated heating, ventilation, air-conditioning (HVAC) and DHW systems for buildings are widely applied (Fabrizio et al., 2014; Chua et al., 2010; Omer, 2008). However, applications of R744 integrated HVAC and DHW systems outside the supermarket sector are not well-established nor sufficiently documented. The current status of R744 systems proves the potential benefits of implementing integrated R744 in buildings with large DHW demands, such as hotels. Byrne et al. (2009) conducted a theoretical comparison between an integrated R744 unit for HVAC and DHW with a state-of-the-art R407A system, and found the energy performances comparable. Minetto et al. (2016) presented a water-side reversible R744 HVAC and DHW unit that operated highly efficient during DHW production. However, COP was significantly reduced during the SH heating mode, due to high return temperatures from the heating system. Tosato et al. (2019) presented a layout of an integrated HVAC and DHW R744 unit for a hotel located in Northern Italy, where ground-water was utilized as a heat source. Results from a charging cycle of the 1.5 m^3 DHW storage revealed a COP of 4.1 during the process. As of yet, no studies have been con-

duction of long term operations of R744 systems in hotels. At the same time, there is a need to evaluate these systems with respect to DHW storage capacities during different operational modes, e.g. charging and discharging. This paper presents the evaluation of long-term logged data from an integrated R744 unit installed in a hotel in Norway. A 6 m^3 DHW storage is included in the thermal system for peak load shaving, the operation of which is presented and discussed.

2. System description

The R744 system analyzed in this work is part of the existing heating system for a medium-size hotel in Værnes, Norway. The system provides HVAC and DHW for a floor area of approximately 9000 m^2, which includes 157 guest rooms. The hotel was built in 1987, with an annual heat energy demand of approximately 1.2 GWh prior to the refurbishment of the thermal system in June 2018. The annual heat demand was reduced to approximately 1 GWh following the refurbishment. The location of the hotel is characterized by cold climate conditions with a normalized average annual temperature of 5.3 °C and 4276 heating degree days (HDD) (average from 1961 to 1990). HDD for the location of the hotel is calculated as described in Thom (1954) with Scandinavian standard values (Skaugen et al., 2002). The annual average temperature for the first year of operation was recorded to be 6.8 °C with 3860 HDD over the period from September 2018 to September 2019.

2.1. R744 heat pump and chiller unit

The previous thermal system of the hotel, consisting of an electric- and oil boiler, has been replaced with the R744 heat pump and chiller system. The first 6 months of operation revealed a monthly energy-saving potential of 59–69% (Smitt et al., 2019). The installed heating and AC cooling capacity is 280 kW and 75 kW, respectively. In this paper, *AC* is defined as the ventilation cooling load. Fig. 1 illustrates the configuration of the R744 heat pump and chiller unit and secondary distribution systems. The R744 unit is an adapted single-stage supermarket refrigeration unit with heat recovery towards two separate hydronic circuits. The compressor rack consists of four parallel compressors (displacement range from 17.8 to 21.2 $m^{-3}h^{-1}$ at 50 Hz). One compressor is equipped with a variable speed drive (VSD), while the three other compressors are controlled by ON/OFF. The compressors are activated based on the requested capacity. The VSD compressor is always active to meet the capacity setpoint between the constant capacity steps provided by the other compressors.

The main function of the R744 system is to provide heating and DHW for the hotel, which is achieved with the same strategy as for heat recovery in transcritical R744 supermarket units (Danfoss, 2015; Danfoss, 2012), with the exception that the heating load, rather than the cooling load, is the controlling parameter. The capacity control of the R744 unit is based on feedback signals from the hotel, such as from the DHW, ventilation- and radiator circuits. The building side supplies a heat demand signal to the R744 controller, which adjusts the setpoints for the compressor capacity and the high pressure. If an increase in capacity is requested, the setpoint for the evaporation temperature is temporarily reduced to activate another compressor in the rack. This somewhat unconventional control is due to the conversion of the R744 unit from a supermarket refrigeration rig. The high pressure P_{gc} is regulated based on the gas cooler outlet temperature $T_{gc,exit}$. The control principle of the gas cooler pressure is described in Gullo et al. (2016). The high pressure control valve (EV1) expands the fluid directly to the liquid separator at an intermediate pressure of 38–55 bar. Four air evaporators (50 kW at −15 °C) are fed from the liquid receiver. Thermostatic expansion valves (EV2–EV5) regulate the superheat at the exit of each evaporator. The number of active evaporators is dependent on the heating load. The gas returning from the evaporators is mixed with flash gas and is directed in a passage through the liquid receiver for heat exchange before compression. Also, a heat exchanger (HX) interface (75 kW at 12/7 °C) to the chilled water circuit (HX6) can be employed to recover heat if AC is needed. The chilled water produced by the R744 system is used to supplement the existing AC chiller unit, and is thus only applied as an auxiliary function during heat generation.

2.2. Subsystems and hot water storage

The system is designed to supply heat for ventilation heating, DHW and SH. Heat is supplied to the hydronic subsystems through two gas coolers in series, GC1 and GC2 as shown in Fig. 1, at high (> 60 °C) and medium (< 50 °C) temperatures. The medium temperature (MT) circuit provides heat primarily to ventilation batteries and a radiator/floor heating circuit. Remaining heat is used to preheat DHW through HX2 from approximately 8 to 30 °C. During winter operations, HX1 in the MT circuit is applied for defrosting of the evaporators through a brine circuit.

The high temperature (HT) circuit mainly supplies heat for DHW reheat through HX3. During operational conditions with negligible SH demand, the entirety of the DHW production can be covered with HX3. HX2 is then bypassed with valve MV1. Similarly, GC1 can be bypassed through the directional valve, DV1, if the DHW storage is fully charged and there is no demand for HT heat. The R744 unit will in these instances operate at a subcritical high-pressure level. The HT circuit also supplies extra heat thought HX5 for the radiators and floor heating during winter conditions. This is typically done when the setpoint temperature of the radiators exceeds the setpoint of the MT circuit. When the return temperature is higher than the setpoint temperature of the MT circuit, MV5 closes off the passage between MT and the radiators. A shunt circuit is then established exclusively between the radiators and HX5, to prevent an increase in water temperature to GC2.

The DHW subsystem consists of several tanks in series with a combined volume of 6 m^3. The subsystem is supplied with heat from the R744 unit through HX2 and HX3, or from the backup electric boiler through HX4. The system control is characterized by two distinctive modes of operation depending on the state of the DHW storage and whether active charging is needed. When active charging of the storage is unnecessary, the majority of the heating load is allocated to the MT circuit to cover the moderate temperature demands, e.g. radiators, floor and ventilation heating. Excess heat is allocated to the DHW subsystem, usually at a low load to meet the required DHW temperature.

The second mode of operation occurs during active charging of the DHW storage and is activated when the temperatures in tanks 1 or 3 fall below a threshold. A few steps are initiated to start the charging process. First, the setpoint of Pump P4 is changed to provide a higher flow rate. Then, the heat demand from the building is then given an offset signal to induce charging. The increase in demand triggers an increase in compressor load, which is maintained by temperature insurance of the HT and MT circuit supply temperatures. During the charging process, excess hot water is stored and moves through the series of tanks as the buffer is gradually charged from tank no. 1 to no. 10. Water is drawn from tank no. 10 and is sent through the heating process, in the same manner as described by Minetto (2011). The thermal storage is fully charged when the normally stratified storage reaches a high and uniform temperature. During discharge, water is drawn from tank no. 1 and is mixed in MV3 with cold water to a temperature of 55 °C before entering the supply line. The setpoint for DHW production is 66 °C. Once a week, the setpoint temperature is boosted to 86 °C, during which all tanks must meet the setpoint temperature for at

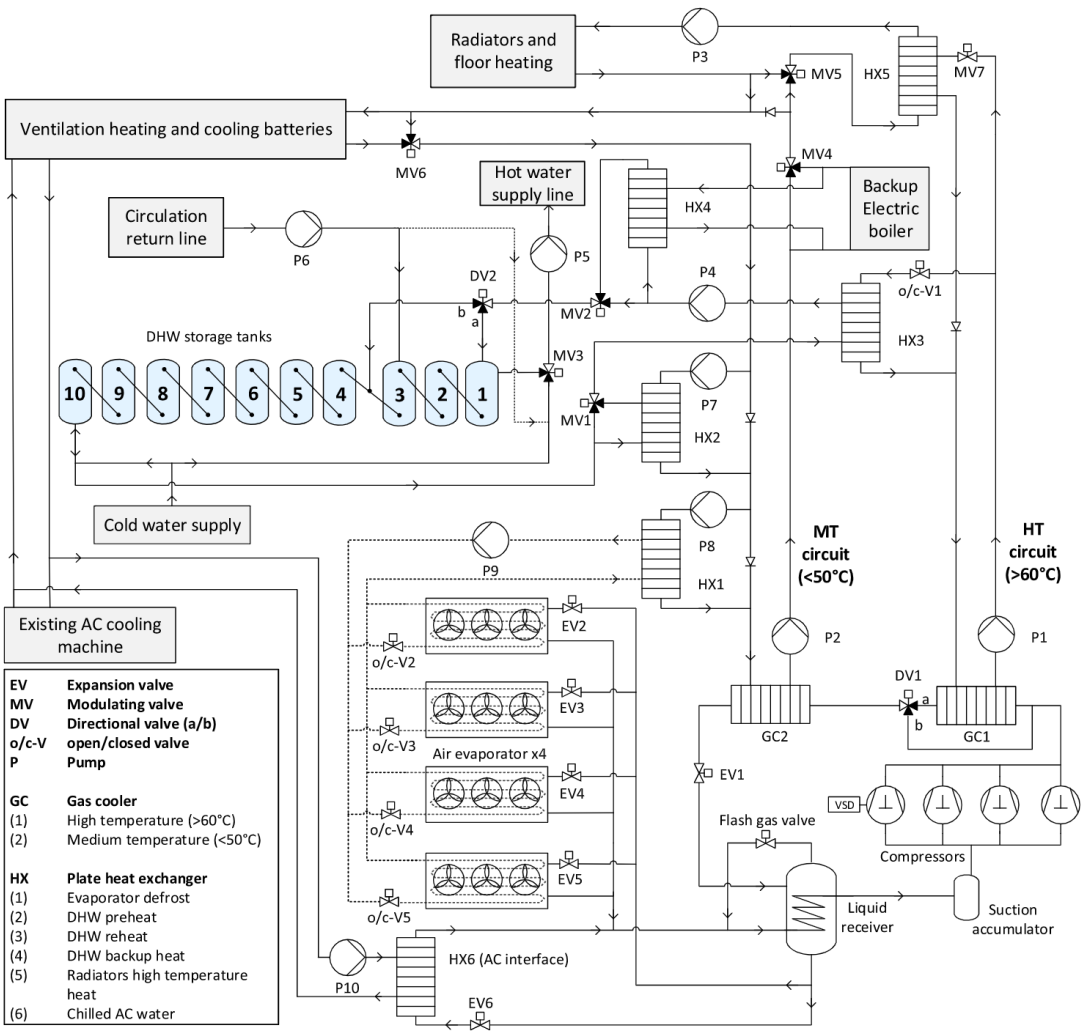

Fig. 1. Schematic drawing of the R744 heat pump and chiller unit with thermal storage and secondary system.

least one hour to prevent legionella growth. The start signal for the timer is reset if the temperature level has been reached. As additional insurance, heating elements are installed in each tank for temperature boosting purposes.

3. Data collection and evaluation methods

The secondary hydronic system is instrumented with temperature sensors (NTC10 thermistors, ± 0.2 K) and mass flow meters (oscillator mass flow sensor, class 2) in every fluid branch. Temperature sensors in the DHW tanks and secondary systems have been validated to operate within a range of ± 0.1 K. Heat flow meters for secondary fluids are installed at every HX (PT500 temperature sensors, oscillator mass flow sensor, class 2). Pressure sensors (± 0.3% at full scale), temperature sensors (PT500 temperature sensors, ± 0.15 + 0.002T) and electrical power supply monitors (energy analyzer in control unit, ± 2%) are installed in the R744 unit. The real-time field measurements of the hotel have been obtained via the web-monitoring software *IWMAC* (IWMAC, 2019). The measurements are updated continuously, but the data at a certain time is only logged by the measurement system if it differs from the value in the previous time step. The recorded data points are therefore regarded as constant step values within the specific time interval until the next recorded value. All the recorded data have been resampled and synchronized to the same time step, using the weighted average of the time intervals. The data used in this analysis were collected and processed for the period from September 2018 to September 2019.

3.1. Domestic hot water (DHW) loads

Due to the absence of an energy meter in the DHW supply line, the consumption load and mass flow rate are calculated using the energy balance equation on the DHW subsystem. The reference temperature, T_{ref}, represents the temperature of the cold supply water, which is fairly stable throughout the year. The water temperature is therefore assumed to keep a constant temperature of 8 °C. The energy stored in the tanks, E_{tanks} [kWh], at each time

step, i, is calculated by Eq. (1).

$$E_{tanks_i} = \rho V C_p \sum_{j=1}^{10} (T_{j_i} - T_{ref}) \quad (1)$$

where T_j is temperature measured in tank j, which holds a water volume, V, of 600 l. The temperature in the storage tanks normally varies between T_{ref} and 66 °C, and are measured in the middle of each tank, which gives a good overview of the temperature gradient across the storage. space Water density, ρ [kg m^{-3}], and specific heat capacity, C_p [kWh kg^{-1} K^{-1}], at the mean operation temperature of 30 °C are used in the calculations. Applying the energy balance on the DHW subsystem yields the following equation:

$$\frac{\Delta E_{tanks_i}}{dt_i} = \dot{Q}_{HX2_i} + \dot{Q}_{HX3_i} + \dot{Q}_{HX4_i} - \dot{Q}_{DHW_i} \quad (2)$$

where

$$\Delta E_{tanks_i} = E_{tanks_{i+1}} - E_{tanks_i} \quad (3)$$

$\dot{Q}_{DHW_i}$ [kW] in Eq. (2) is the heat load accompanying DHW usage. Other parameters are explained in Sections 2.1 and 2.2. Change of energy in the water storage at each time step, ΔE_{tanks_i} [kWh] (Eq. (3)), is defined as the difference between the current time step, i, and the next, $i+1$. The DHW heat load, (Eq. (4)), is derived from Eqs. (1) to (3). The heat losses from the storage tanks are accounted for in $\dot{Q}_{DHW_i}$. The average value of calculated measurement uncertainty [%] is presented in the equation.

$$\dot{Q}_{DHW_i} = \dot{Q}_{HX2_i} + \dot{Q}_{HX3_i} + \dot{Q}_{HX4_i} - \frac{\rho V C_p}{dt_i} \sum_{j=1}^{10} (T_{j_{i+1}} - T_{j_i}) \pm 4.5\% \quad (4)$$

The DHW consumption mass flow rate, $\dot{m}_{DHW_i}$ [kg s^{-1}], is then calculated as

$$\dot{m}_{DHW_i} = \frac{\dot{Q}_{DHW_i}}{(T_{set} - T_{ref}) C_p} \quad (5)$$

where T_{set} is the DHW supply setpoint temperature (55 °C).

3.2. Coefficients of performance (COPs)

Collected measurements for heating capacities, AC capacities and power consumption are used to calculated the COPs of the integrated thermal system. The total system COP [-], referred to as COP_{sys}, is defined as the ratio of useful thermal load to the total electricity consumption, using Eq. (6):

$$COP_{sys} = \frac{\dot{Q}_{GC1} + \dot{Q}_{GC2} + \dot{Q}_{AC}}{\dot{W}_{comp} + \dot{W}_{fans} + \dot{W}_{pumps} + \dot{W}_{aux,el}} \pm 6.2\% \quad (6)$$

where $\dot{W}_{comp}$, $\dot{W}_{fans}$ and $\dot{W}_{pumps}$ [kW] represent the combined electricity consumption for all compressors, evaporation fans and pumps, respectively. $\dot{W}_{aux,el}$ [kW] is the electricity consumption for auxiliary systems, such as control systems. $\dot{Q}_{AC}$ is the AC load that is supplied through HX6.

The heat pump COP, COP_h [-], is the ratio of the total heat load to the electricity necessary to provide the heating functions. This includes electricity consumption of the compressors and the fans in the evaporators, as shown in Eq. (7).

$$COP_h = \frac{\dot{Q}_{GC1} + \dot{Q}_{GC2}}{\dot{W}_{comp} + \dot{W}_{fans}} \pm 5.7\% \quad (7)$$

The COP of the AC chiller system is not evaluated as a singular parameter since cooling is not a controlling parameter in the R744 unit, but rather a byproduct of the heating operation.

The seasonal coefficient of performance (SCOP) for the entire heat pump system with/without boiler, $SCOP_{sys+el}$ [-] and $SCOP_{sys}$ [-], and SCOP for heating, $SCOP_h$ [-], are calculated as the ratio between supplied heating and/or AC cooling energy [kWh] to the work of compressors and auxiliary devices [kWh], as shown in Eqs. (8) and (9).

$$SCOP_{sys} = \frac{\sum(\int \dot{Q}_{GC1} + \int \dot{Q}_{GC2} + \int \dot{Q}_{AC})}{\sum(\int \dot{W}_{comp} + \int \dot{W}_{fans} + \int \dot{W}_{pumps} + \int \dot{W}_{aux,el})} \pm 6.2\% \quad (8)$$

$$SCOP_{sys+el} = \frac{\sum(\int \dot{Q}_{GC1} + \int \dot{Q}_{GC2} + \int \dot{Q}_{AC} + \int \dot{Q}_{EL})}{\sum(\int \dot{W}_{comp} + \int \dot{W}_{fans} + \int \dot{W}_{pumps} + \int \dot{W}_{aux,el} + \int \dot{W}_{EL})} \pm 10.5\% \quad (9)$$

$$SCOP_h = \frac{\sum(\int \dot{Q}_{GC1} + \int \dot{Q}_{GC2})}{\sum(\int \dot{W}_{comp} + \int \dot{W}_{fans})} \pm 5.7\% \quad (10)$$

where $\dot{Q}_{EL}$ and $\dot{W}_{EL}$ is the heat and power associated with the operation of the electric boiler, respectively.

4. System performance analysis

4.1. Analysis of key operating parameters

In order to assess the system performance during different operational conditions with variations in heating, DHW and AC loads, key operating parameters of the system are evaluated and discussed in this section. Specific periods are categorized based on weather conditions that demonstrate different seasonal performance of the system: summer (June through August), winter (November through March), and nominal for operating conditions representing fall and spring (September through October, April through May).

4.1.1. Key system operational parameters

Key R744 cycle parameters and high-side temperatures are analyzed. The studied parameters include ambient air temperature T_a [°C], R744 evaporation temperature T_{evap} [°C], as well as MT and HT supply water temperatures, represented by $T_{w,MT}$ and $T_{w,HT}$ [°C], respectively. The high pressure, P_{gc} [bar], and gas cooler outlet temperature, $T_{gc,exit}$ [°C] are included in the analysis. The performance of the system under four weeks of winter operation is shown in Fig. 2. The period is characterized by low ambient temperature and marginal AC loads.

As can be observed in Fig. 2, P_{gc} operates in the transcritical pressure region with a maximum working pressure of 100 bar. Relatively large fluctuations in pressure occur during this period, as a result of variations in $T_{gc,exit}$. Low fluid return temperature from the secondary thermal systems will consequently limit $T_{gc,exit}$ and thus also P_{gc}. However, some situations will cause unwanted high return temperatures from the MT circuit to the second gas cooler: (a) transitions between different modes of operation, (b) low load operations with many starts and stops, and (c) mixing in DHW tanks, which result in high return temperature during charging. The negative impact of high return temperature can be reduced by increasing the gas cooler pressure.

Heat is supplied to the secondary thermal system at the two different temperature levels $T_{w,MT}$ and $T_{w,HT}$. The MT and HT circuit setpoint temperatures are regulated based on outdoor temperature compensation curves, which varies from 25 to 50 °C and 60 to 70 °C, respectively. Fig. 2 shows that $T_{w,HT}$ generally operates between 65 and 70 °C.

The mass flows through the four air evaporators are controlled according to the superheat at the exit of each evaporator. Hence,

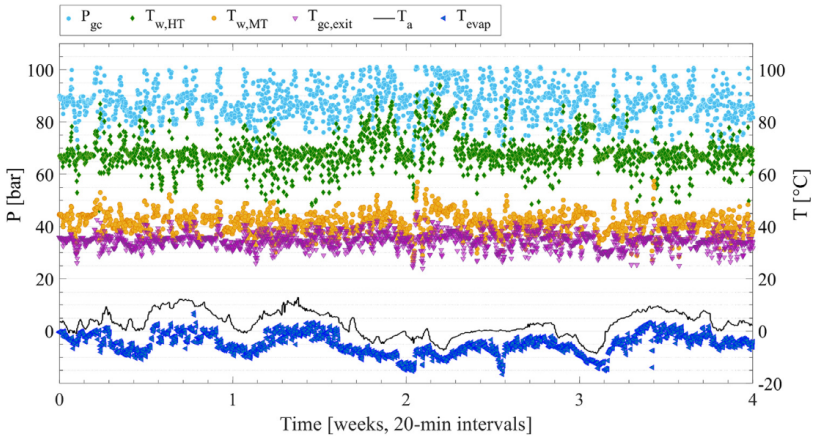

Fig. 2. Key operating parameters for winter operations (November 6th to December 4th 2018).

T_{evap} generally follows the pattern of T_a with a temperature difference determined by the superheat control. The setpoint for superheat is periodically changed according to temperature level of T_a. For the interval displayed in Fig. 2, the superheat setpoint is fixed to a minimum of 4 K. The sudden drop of T_{evap} is illustrated halfway through week 2. This behavior occurs when the heat load is increased, e.g. during heat pump start-up, capacity increase or during activation of additional evaporators. Hence, the setpoint of the evaporation, T_{evap}, is reduced to boost the discharge temperature and to increase the capacity. The reduction of T_{evap} is extra work for the compressors and cause excessive superheat that reduces COP considerably.

4.1.2. Domestic hot water (DHW) accumulation

The consumption of hot water typically follows a certain pattern dependent on the behavior of the residents and the operation of the hotel facilities. The major consumers of hot water in hotels are primarily guests, kitchens, laundry services and spa or pool facilities (Bohdanowicz, 2006; Lawson, 2001). Generally, the hot water consumption in hotel buildings is characterized by large consumption peaks for a few hours during the mornings and evenings (Ndoye and Sarr, 2008; Rankin and Rousseau, 2006; Deng and Burnett, 2002). In circumstances where no DHW storage buffer is installed, the high consumption peaks will be directly reflected in the hotel's power consumption. Fig. 3 shows the hot water average daily consumption profile, DHW_{usage} [kWh], and the profile of energy supplied by the heat pump to the storage, DHW_{supply} [kWh], over a period of one year. The average DHW daily usage during this period is 1104 kWh/day. However, significant variations in daily consumption were recorded with maximum and minimum values of 2480 and 480 kWh/day. On average, 2.3% of the DHW_{usage} is covered by the electric boiler.

As seen in Fig. 3, most of the DHW consumption occurs between hour 8 and midnight. The DHW usage during this time period accounts for 87% of the daily consumption. The activity level in the hotel is low between hours 0 and 6, hence the DHW usage is lower during this time. DHW_{usage} peaks occur during the hours 9 and 23 at values around 70 kWh. However, DHW_{supply} does not exceed 58 kWh due to the buffer effect granted by the storage, and demonstrates how the system handles power peaks on an average basis. The impact of the storage is the difference between DHW_{usage} and DHW_{supply}, which reaches a peak of 22 kWh during hour 8. The charging of the storage begins at hour 0 and declines to a minimum around hour 6, as the storage is fully charged. When

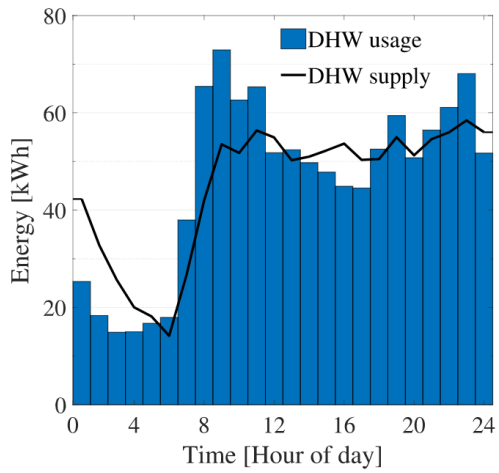

Fig. 3. Hourly-average DHW consumption and supply profiles over a one-year period.

DHW_{usage} increases to a peak of 73 kWh at hour 9, the storage is empty and active charging begins, holding a value between 50 and 55 kWh through the day.

The control strategy of the stratified heat storage in an R744 system is essential for successful operation, as described by Tammaro et al. (2016). Detailed operating parameters of the DHW storage are shown with a 20-minute resolution over a 2-day period in Fig. 4. Fig. 4A shows the temperature stratification across the storage, which is illustrated by the temperatures in tanks 1, 3, 5, 7 and 10, as labeled in Fig. 1. The storage load and the corresponding energy in the storage over the period are shown in Fig. 4B and C, respectively. The water temperature of the storage fluctuates between 8 and 78 °C during the period. The state of the storage can be determined by studying the temperatures *Tank*1 and *Tank*10. As the last tank in the series, *Tank*10 is sensitive to change in DHW mass flow rates entering and exiting the DHW subsystem. Supply water at 8 °C enters tank 10 during discharge and is gradually pushed through the storage as hot water is drawn from *Tank*1 and supplied to the hotel. The sudden drop in all temperatures in Fig. 4A illustrates the discharge of the storage

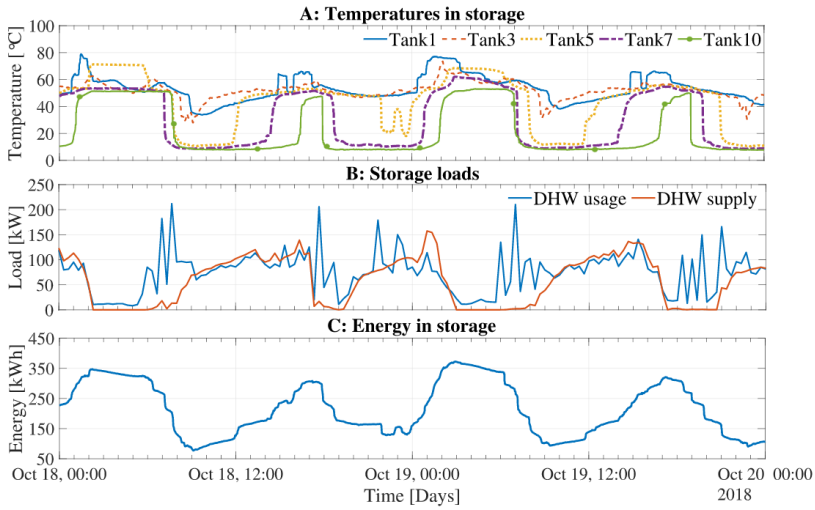

Fig. 4. Operation of the DHW subsystem over a 2-day period showing (a) storage temperature, (b) DHW usage and supply and (c) energy in the storage.

and corresponds to peaks in the *DHWusage*, as can be observed in Fig. 4B. The energy potential of the storage is fully exploited when *Tank*1 reaches its minimum water temperature. The charging of the storage is illustrated by the increase in the temperatures across the buffer. Hot water is supplied to the storage via tank 1 and is circulated through the buffer. The temperature boundary between hot and cold moves through the storage, as tank temperatures are lifted. As a consequence, the temperatures in the middle of the storage (tanks 3–7) can occasionally be higher than the temperature of tank 1 if the hot water supply temperature fluctuates during the charging process. This behavior is illustrated by *Tank5*, which sometimes is higher than *Tank1*. Simultaneously, cold water is drawn from tank 10 for heating, as explained in Section 2.2. The storage is charged when *Tank*10 reaches its peak temperature. As seen from Figs. 4A, there is a 24-hour pattern to the behavior of the DHW storage temperatures. The DHW storage energy is fully exerted and is recharged twice a day, which is in agreement with the findings in Fig. 3. Fig. 4B shows that the storage is typically charged for 7–10 h. The sudden drop in storage temperature can be seen in reference to the behavior of *DHWusage*. As shown in Fig. 4A and B, large *DHWusage* peaks in the range of 200 kW cause a rapid decrease in the storage temperatures. It can be observed from Fig. 4C that it takes approximately 2 hours to discharge the entire storage during these periods. There is still a high demand for DHW at hour 9 each day when the storage reaches its minimum energy potential. The hot water generated by the R744 unit is then supplied directly to the hotel to compensate for large demands. This system behavior indicates that the storage volume of 6 m^3 is not quite sufficient to meet the peak DHW demands of the hotel. This is especially evident in the mornings, as *Tank*1 drops below its setpoint of 55 °C. At fully charged conditions, the storage reaches an energy potential of approximately 350 kWh. A possible solution for the insufficient energy reserve in the storage is to store the water at higher temperatures. By increasing the water temperature in all tanks to 70 °C, one could increase the energy storage capacity with about 25%. Nevertheless, the storage buffer still provides a beneficial reduction of peak loads. This is represented by the difference between *DHWusage* and *DHWsupply*, which is more than 100 kW during peak hours. Another benefit of the large storage volume is higher flexibility in DHW production, which allows for low-intensity DHW generation over longer time intervals.

4.2. Evaluation of energy performance

The energy efficiency of the system including the provided heating, AC loads and COPs are evaluated in the following subsections.

4.2.1. Heating and AC cooling loads

Seasonal hourly-averaged heating and AC loads, $\dot{Q}$, of the integrated R744 system, together with hourly-averaged ambient temperatures, $T_{a,\,avg}$, and recorded maximum and minimum temperatures, $T_{a,max}$ and $T_{a,min}$, are shown in Fig. 5A–C. The specific load for DHW, SH and AC are indicated by subscripts. Heating loads are shown as positive values and the AC loads are shown as negative values. Error bars for the loads indicate the range of values recorded for that particular hour. The hourly-averaged loads are investigated over 24-hours during summer, winter and nominal periods of the year, which definitions are explained in Sections 4.1. Fig. 5D shows the annual heating and AC cooling energy supplied by the R744 system, E, and ambient temperatures on a monthly basis. The hourly-averaged loads and the monthly total energy consumption are used to evaluate the performance of the system for the full range of operation from September 2018 to September 2019. The trends for the different loads are discussed individually in the following paragraphs. It should also be stated that the Y-axis temperature scale for the seasonal cases are different.

- $\dot{Q}_{SH}$: The SH load is dependent on $T_{a,\,avg}$ and varies in a range of 5–100 kW for the different seasonal scenarios displayed in Fig. 5A–C. The lowest recorded values are observed in the summer case, where $\dot{Q}_{SH}$ decreases significantly when $T_{a,\,avg}$ exceeds 15 °C. In this case, the entirety of $\dot{Q}_{SH}$ is supplied to the batteries in the ventilation units. Naturally, the highest recorded hourly-averaged values are observed in the winter scenario in Fig. 5B. Approximately 80% of $\dot{Q}_{SH}$ is then supplied to the ventilation units, due to the relatively large capacity of these units. Thus, only a small portion of the heat load is used to cover direct SH, e.g. for floor heating and radiators.

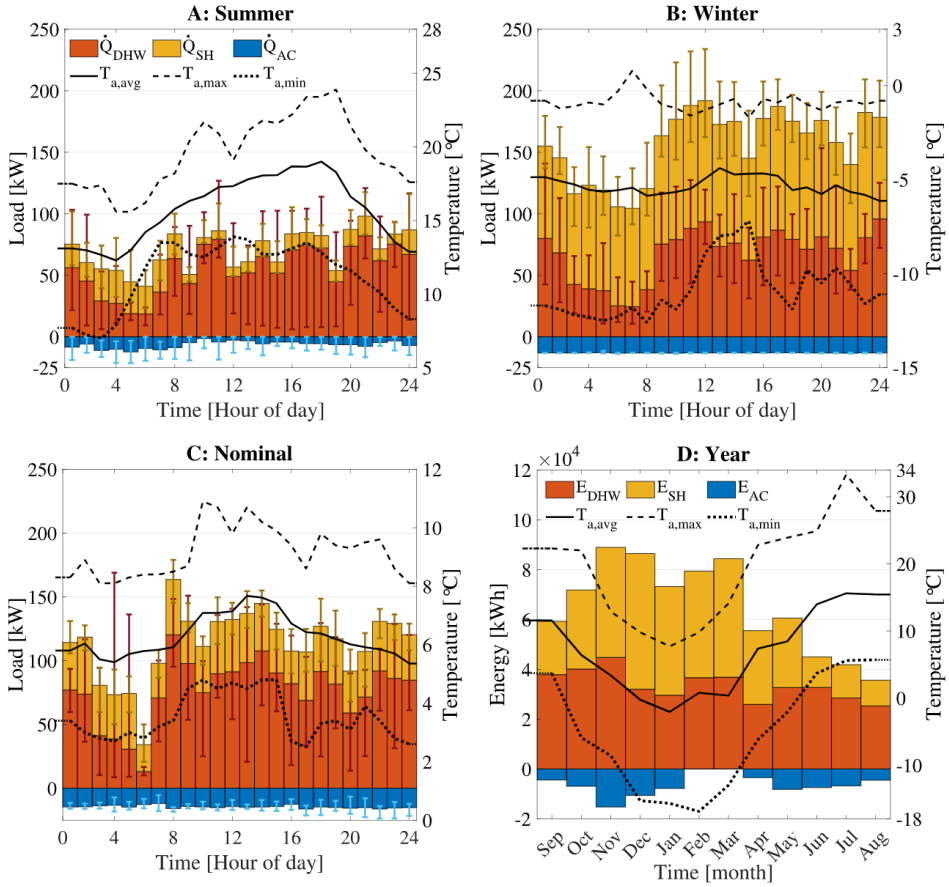

Fig. 5. Hourly-averaged heating and AC loads for (A) summer (May 18th–25th 2019), (B) winter (January 15th to 22nd 2019) and (C) nominal (October 18th–25th 2018). Total annual energy supplied by the R744 unit on (D) monthly basis (Sep. 2018 to Sep. 2019).

- $\dot{Q}_{DHW}$: The DHW loads in Fig. 5A to 5 C drop to the minimum value of 20 to 30 kW at hour 6, followed by a rapid increase in $\dot{Q}_{DHW}$ between 60 to 80 kW, which stay present throughout the day. A noticeable difference in the magnitude of $\dot{Q}_{DHW}$ is shown in the various seasonal scenarios. These inconsistencies are due to variations in guest load and are independent of seasonal operational load and $T_{a,\,avg}$.
- $\dot{Q}_{AC}$: The AC refrigeration capacity varies in a limited range of 0 to 24 kW in all seasonal cases. The load is independent of the hour-of-day and $T_{a,\,avg}$. However, the AC load provided by the R744 is not independent of $T_{a,\,avg}$. This unusual behavior in supplied AC load from the R744 unit is caused by the fact that it is an auxiliary system to the pre-installed separate cooling unit. It should be noted that AC cooling provided by the primary stand-alone chiller is not included in Fig. 5A–D. The separate AC chiller unit is operating at full load during the summer scenario in Fig. 5A, though hardly any AC is supplied by the R744 unit during this time due to the low-side pressure control. As shown in Fig. 1, the air evaporators and HX6 in the R744 unit operate at the same pressure level, controlled solely by the air evaporators. The R744 unit therefore only supplies extra AC when the evaporation temperature is below the 7 °C setpoint for AC chilled water. The largest $\dot{Q}_{AC}$ capacities are observed in the winter and nominal scenarios in Fig. 5B and C, respectively. In these scenarios, moderate $T_{a,\,avg}$ enables operation of the chilled water HX within the acceptable evaporation-temperature range.
- E_{SH}: E_{SH} varies in a range of approximately 10,000 to 55,000 kWh, in close connection to $T_{a,\,avg}$. As shown in Fig. 5D, the heating demand is still present during the summer months, due to the relatively cold climate at the hotel's location. The largest recorded values of E_{SH} is observed during the winter months when $T_{a,\,avg}$ is below 5 °C. E_{SH} is then in a range of 42,000–55,000 kWh monthly, which is up to 5 times the SH usage for the summer months. The total amount of E_{SH} over the year is 380,000 kWh.
- E_{DHW}: The monthly energy for DHW shown in Fig. 5D is stable throughout the year in a range of 30,000 to 40,000 kWh per month, with an average value of 33,600 kWh. The annual energy supplied for DHW over the year is 403,000 kWh. Thus, 52% of the annual heating energy to the hotel is allocated to DHW heating. The relative consumption of DHW to total heating in hotels is typically between 40 and 70%,

Table 1
COPs for selected intervals in the period from Sep. 2018 to Sep. 2019.

Season	Period	$SCOP_{sys}$[-]	$SCOP_{sys+el}$[-]	$SCOP_h$[-]	$T_{a,\,avg}$[°C]
Winter	November–April	2.78 ± 0.17	2.57 ± 0.27	2.69 ± 0.15	0.4
	January 15th to 22nd	2.63 ± 0.16	2.37 ± 0.25	2.49 ± 0.14	−5.3
Summer	June–September	3.20 ± 0.20	2.75 ± 0.29	3.09 ± 0.18	15.0
	May 18th–25th	3.34 ± 0.21	2.97 ± 0.31	3.30 ± 0.19	15.8
Nominal	September–November, April–June	2.99 ± 0.19	2.73 ± 0.29	2.90 ± 0.17	8.4
	October 18th–25th	3.23 ± 0.20	3.21 ± 0.34	3.05 ± 0.17	6.3
Annual	September–September	2.90 ± 0.18	2.64 ± 0.28	2.80 ± 0.16	6.8

Seasonal intervals are from the 1*st* to the 1*st* in the stated months.

and is dependent on the location, building envelope and use of facilities (Su, 2012; Deng and Burnett, 2000).

- E_{AC}: As previously explained, E_{AC} is larger during the nominal months of operation. AC is primarily used for climate control and temperature adjustments in common areas and guest rooms. The AC cooling capacity is therefore larger during periods with high guest loads and large heating demands. For the entire year, only 75,500 kWh of AC cooling energy was recovered through the chilled water HX.

4.2.2. Coefficient of performance (COPs)

The SCOPs for the scenarios depicted in Fig. 5, together with seasonal and annual values are listed in Table 1. The average ambient temperature, $T_{a,\,avg}$, for the specified intervals are included in the table. Predictably, $SCOP_{sys}$ is higher than $SCOP_h$ for the investigated scenarios. However, the annual $SCOP_{sys}$ is only 0.1 or 3.6% higher than the $SCOP_h$. Byrne et al. (2009) estimated numerically a SCOP of 3.57 for a heat pump and chiller system for hotels using R407a. They also investigated an R744 system with similar operational conditions and found a SCOP of 3.24. However, secondary systems and real operating conditions were not accounted for in this study. The conventional thermal systems found in the Nordic hotel market normally utilize electric boilers/district heating stations in combination with separate HFC-units for AC. Typically, a $SCOP_{sys}$ in the vicinity of 1 is achieved for these systems, due to the relatively large magnitude of heating load to AC load. The somewhat low value of annual $SCOP_{sys}$ for the integrated system is partially due to the limited recovery of cold energy to the AC cooling circuit. This is also the case for the long-term seasonal periods, e.g. winter, summer and nominal. On an annual basis, approximately 5% of the total heat to the hotel is supplied by the electric boiler. As a result, $SCOP_{sys+el}$ is reduced by 9% when compared to $SCOP_{sys}$. It is expected that the boiler is applied during the winter season to cover peak heating. However, the low value of $SCOP_{sys+el}$ during the summer season indicates excessive use of the boiler for DHW heating. This is explained by the high return temperature of water to GC2. A temperature above 45 °C triggers a signal to reduce the compressor capacity, due to compromised efficiency. Consequently, DHW production by the heat pump is reduced and the required load is then compensated by the boiler.

All SCOPs are highly dependent on $T_{a,\,avg}$ and increase with approximately 0.4 from the winter to the summer season. A larger difference between the specific SCOPs is observed when comparing the summer and winter week scenarios (Fig. 5A and B), which can be attributed to the change in $T_{a,\,avg}$. The nominal week of October 18th–25th reveals uncharacteristically high values of $SCOP_{sys}$ when related to the nominal season. Moreover, $T_{a,\,avg}$ for this week is 2.1 °C below the average temperature for the particular season. The high value of $SCOP_{sys}$ during this week can be explained by the relatively large utilization of AC, as displayed in Fig. 5C. The gain from $\dot{Q}_{AC}$ is therefore larger than the contribution from $\dot{W}_{fan}$ and $\dot{W}_{aux,el}$ in the calculation of $SCOP_{sys}$, as defined in Eq. (8).

The mean COP_{sys} and COP_h for transcritical operations (> 73.9 bar), according to specific temperature intervals, are listed in Table 2. The COPs are categorized by whether or not DHW charging is taking place. The subscript *nch* includes circumstances when the heat supply to the hotel is controlled by SH demands, and no active charging of the DHW storage is taking place. Situations when the DHW storage is being actively charged, and the system is controlled according to both SH and DHW loads are identified by the subscript *ch*. The analysis of variance (ANOVA: single factor) was applied to analyze the efficiency of the system under different modes of operations. The difference is considered significant at $p < 0.05$.

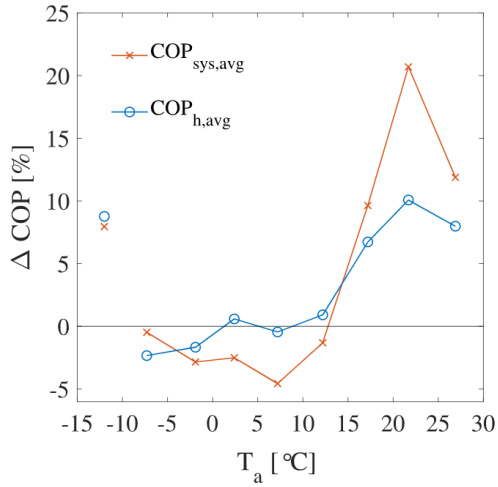

Fig. 6. Difference between the DHW charging and no charging COPs.

Table 2 shows a significant difference between charging and no charging values of $COP_{h,\,avg}$ at temperatures below 0 °C and above 15 °C. $COP_{sys,\,avg}$ exhibit significant difference between all intervals, with the exception of −10 to −5 °C and 10 to 15 °C. Fig. 6 depicts the relative change in COP, ΔCOP [%], from no charging (COP_{nch}) to charging (COP_{ch}). The COPs during no DHW charging are generally higher than charging mode at low temperatures, which results in a decrease of ΔCOP. However, both $COP_{sys,\,avg}$ and $COP_{h,\,avg}$ increase considerably at T_a above 15 °C. This unusual relationship between the two modes of operation can be explained by the magnitude of the SH load and the temperature of the water returning to the second gas cooler. The temperature of the fluid returning from the secondary system is generally higher at high values of SH, as the setpoints of SH and thus the return temperatures are elevated at low values of T_a. Additionally, DHW charging provides a temperature lift in the return circuit when the stratification in the DHW storage is not fully intact, as discussed in Sections 4.1.2. This behavior was also illustrated by Tosato et al. (2019). They noted a reduction in COP of 18% during the final part of the DHW charging process, which was caused by high return temperatures from the

Table 2
System and heating COPs during DHW charging and no charging at different temperature intervals.

T_a [°C]	[−15,−10)	[−10,−5)	[−5,0)	[0,5)	[5,10)	[10,15)	[15,20)	[20,25)	[25,30)
$COP_{sys\,ch,\,avg}$ [−]	2.59 (0.50)	2.40[a] (0.22)	2.53 (0.34)	2.82 (0.44)	3.17 (0.50)	3.38[a] (0.58)	3.37 (0.61)	3.38 (0.62)	3.28 (0.50)
$COP_{sys\,nch,\,avg}$ [−]	2.40 (0.70)	2.41[a] (0.33)	2.61 (0.56)	2.89 (0.66)	3.32 (0.68)	3.43[a] (0.92)	3.07 (0.92)	2.80 (0.83)	2.93 (0.85)
$COP_{h\,ch,\,avg}$ [−]	2.47 (0.46)	2.32 (0.23)	2.53 (0.34)	2.77[a] (0.45)	3.03[a] (0.47)	3.11[a] (0.50)	3.19 (0.54)	3.23 (0.57)	3.24[a] (0.53)
$COP_{h\,nch,\,avg}$ [−]	2.27 (0.70)	2.38 (0.31)	2.58 (0.49)	2.76[a] (0.57)	3.04[a] (0.53)	3.08[a] (0.80)	2.99 (0.87)	2.93 (0.87)	3.00[a] (0.85)
$T_{a\,ch,\,avg}$ [°C]	−12.0 (1.3)	−7.2 (1.4)	−2.0 (1.4)	2.4 (1.5)	7.4 (1.4)	12.3 (1.4)	17.3 (1.5)	21.9 (1.3)	26.9 (1.4)
$T_{a\,nch,\,avg}$ [°C]	−12.1 (1.3)	−7.5 (1.4)	−1.8 (1.4)	2.3 (1.4)	7.1 (1.5)	12.0 (1.4)	17.0 (1.5)	21.6 (1.3)	26.8 (1.4)

[a] No significant statistical difference ($p > 0.05$) between corresponding DHW charging and no charging values. Standard deviation is shown in the brackets. Values for calculated measurement uncertainties are not included.

storage. Hence, during seasons with low T_a, high SH and thus generally high return fluid temperature, the heating load of the CO_2 unit is limited due to high $T_{gc,exit}$. This problem diminishes when the SH load is limited, as can be observed in Fig. 6 at T_a above 15 °C. The COPs during DHW charging are generally higher than the no charging mode at high ambient temperatures, which is in agreement with the findings in Tosato et al. (2019). Thus, the DHW charging strategy of the system should be regarded as a key influencing factor to achieve high efficiency.

5. Conclusions

This work investigated key operating parameters for an R744 heating and AC cooling unit installed in a Norwegian hotel. The system is integrated with HVAC, DHW and a 6 m^3 thermal storage. Field measurements from the hotel were analyzed for a one-year period and essential parameters to evaluate the system performance were discussed, including heating and AC loads, temperatures, pressures and mass flow rates. DHW consumption loads and COPs were calculated using the collected data. The DHW consumption was estimated by the energy balance due to the peculiarities of the instrumentation installed by the supplier. Consequently, the heat loss from the storage tanks were included in the DHW consumption rate and thus not evaluated in this study. The same applies to the existing AC cooling machine, as this unit is not integrated in the measurement and control system.

The heating and AC loads supplied by the R744 unit were studied on a weekly and monthly basis to assess the seasonal behavior of the system. The results reveal that the DHW load is fairly stable throughout the year and is independent of seasonal ambient temperatures. The DHW load accounts for 52% of the annual heat load supplied to the hotel and follows a particular 24-h pattern, with low consumption between midnight and hour 6. The peak DHW load occurs around hour 9 and reaches an hourly-averaged value of 73 kWh. The DHW storage holds an energy capacity of 350 kWh at fully charged conditions and demonstrates peak demand compensation of more than 100 kW during October 18th–20th 2018. Periodical decrease in storage temperatures to values below the set-point indicates that the storage is not fully equipped to handle the peak DHW loads of the hotel. This can be solved by installing more tanks in series or by increasing the water storage temperature.

The COPs during DHW charging mode are higher when compared with no charging at ambient temperatures above 15 °C, due to limited SH demands. The SH is highly dependent on ambient temperatures and varies noticeably in the different seasonal scenarios. The monthly supply of SH energy increases significantly at average ambient temperatures below 5 °C. The AC capacity delivered by the R744 unit is limited and not fully exploited, which is reflected in the moderate annual $SCOP_{sys}$ of 2.90. Additionally, about 5% of the total heat to the hotel is supplied by the electric boiler, which decreases overall $SCOP_{sys}$ by 9%. The latter is often a result of high return temperatures from the building, which is aggravated by increased number of R744 unit starts and stops and mixing in DHW tanks. Other factors that greatly influence the efficiency of the system are variations in the ambient temperatures and high temperatures at the gas cooler exit.

Observations from this work can be used as a good starting point for modeling and optimization of the existing and similar systems. Future work should focus on increasing the system performance by charging the storage during longer periods at reduced capacities. The optimal storage volume for this type of system is an important issue that should be prioritized.

Declaration of Competing Interest

The authors declare that they have no known competing financial interests or personal relationships that could have appeared to influence the work reported in this paper.

Acknowledgments

The authors would like to acknowledge the Norwegian Research Council for funding this project. We would also like to thank Kelvin AS for in-depth system details and Scandic Hotel Hell for access to their system data. Also, we would like to acknowledge Yannick Pruss for his contribution to this research work.

Supplementary material

Supplementary material associated with this article can be found, in the online version, at doi:10.1016/j.ijrefrig.2020.03.021.

References

Bamigbetan, O., Eikevik, T.M., Nekså, P., Bantle, M., 2017. Review of vapour compression heat pumps for high temperature heating using natural working fluids. Int. J. Refrig. 80, 197–211.
Bohdanowicz, P., 2006. Responsible Resource Management in Hotels: Attitudes, Indicators, Tools and Strategies. KTH.
Bolaji, B., Huan, Z., 2013. Ozone depletion and global warming: case for the use of natural refrigerant–a review. Renew. Sustain. Energy Rev. 18, 49–54.
Byrne, P., Miriel, J., Lenat, Y., 2009. Design and simulation of a heat pump for simultaneous heating and cooling using HFC or CO_2 as a working fluid. Int. J. Refrig. 32 (7), 1711–1723.
Cecchinato, L., Corradi, M., Cosi, G., Minetto, S., Rampazzo, M., 2012. A real-time algorithm for the determination of R744 systems optimal high pressure. Int. J. Refrig. 35 (4), 817–826.
Cecchinato, L., Corradi, M., Fornasieri, E., Zamboni, L., 2005. Carbon dioxide as refrigerant for tap water heat pumps: a comparison with the traditional solution. Int. J. Refrig. 28 (8), 1250–1258.
Cecchinato, L., Corradi, M., Minetto, S., 2010. A critical approach to the determination of optimal heat rejection pressure in transcritical systems. Appl. Therm. Eng. 30 (13), 1812–1823.
Chua, K.J., Chou, S.K., Yang, W., 2010. Advances in heat pump systems: a review. Appl. Energy 87 (12), 3611–3624.
Ciconkov, R., 2018. Refrigerants: there is still no vision for sustainable solutions. Int. J. Refrig. 86, 441–448.
Council of the European Commission and others (EC), 2010. Directive 2010/31/EU of the European Parliament and of the council of 19 May 2010 on the energy performance of buildings. Off. J. Eur. Union L 153, 13–35.
D'Agaro, P., Coppola, M., Cortella, G., 2019. Field tests, model validation and performance of a CO_2 commercial refrigeration plant integrated with HVAC system. Int. J. Refrig. 100, 380–391.
Dalton, G., Lockington, D., Baldock, T., 2008. Feasibility analysis of stand-alone renewable energy supply options for a large hotel. Renew. Energy 33 (7), 1475–1490.

Danfoss, 2012. Application guide: 1 and 2 stage Transcritical CO_2 systems – how to control the system. Application guide RA8AA302 http://files.danfoss.com/TechnicalInfo/Dila/01/RA8AA302.pdf.

Danfoss, 2015. Application guide: heat reclaim in transcritical CO_2systems. Application guide DKRCE.PA.R1.F1.22 https://assets.danfoss.com/documents/DOC167786419094/DOC167786419094.pdf.

Deng, S.-M., Burnett, J., 2000. A study of energy performance of hotel buildings in Hong Kong. Energy Build. 31 (1), 7–12.

Deng, S.-M., Burnett, J., 2002. Water use in hotels in Hong Kong. Int. J. Hosp. Manag. 21 (1), 57–66.

Economidou, M., Atanasiu, B., Despret, C., Maio, J., Nolte, I., Rapf, O., 2011. Europe's Buildings Under the Microscope. aCountry-by-Country Review of the Energy Performance of Buildings. Buildings Performance Institute Europe (BPIE), pp. 35–36.

European Commission (EC), 2006. Action Plan for Energy Efficiency: realising the potential, communication from the commission, COM (2006) 545 Final. https://eur-lex.europa.eu/legal-content/EN/TXT/PDF/?uri=CELEX:52006DC0545&from=EN

European Parliament and Council of the European Union (EP and EC), 2014. Eu regulation no 517/2014 of the european parliament and of the council of 16 april 2014 on fluorinated greenhouse gases and repealing regulation (EC) no 842/2006. Official J. Eur. Union 57, 195–230.

Eurostat, 2017. Final energy consumption by sector. Accessed: 2019-11-11 https://ec.europa.eu/eurostat/databrowser/view/ten00124/default/table?lang=en.

Fabrizio, E., Seguro, F., Filippi, M., 2014. Integrated HVAC and DHW production systems for Zero Energy Buildings. Renew. Sustain. Energy Rev. 40, 515–541.

Fernandez, N., Hwang, Y., Radermacher, R., 2010. Comparison of CO_2 heat pump water heater performance with baseline cycle and two high COP cycles. Int. J. Refrig. 33 (3), 635–644.

Girotto, S., 2016. Direct Space Heating and Cooling with CO_2Refrigerant. ATMOsphere Europe.

Gullo, P., 2019. Innovative fully integrated transcritical R744 refrigeration systems for a HFC-free future of supermarkets in warm and hot climates. Int. J. Refrig. 108, 283–310.

Gullo, P., Elmegaard, B., Cortella, G., 2016. Advanced energy analysis of a R744 booster refrigeration system with parallel compression. Energy 107, 562–571.

Gullo, P., Hafner, A., Banasiak, K., 2018. Transcritical R744 refrigeration systems for supermarket applications: current status and future perspectives. Int. J. Refrig. 93, 269–310.

Gullo, P., Hafner, A., Banasiak, K., 2019. Thermodynamic performance investigation of commercial R744 booster refrigeration plants based on advanced exergy analysis. Energies 12 (3), 354.

Hafner, A., 2015. 2020 perspectives CO_2 refrigeration and heat pump systems. In: Proceedings of the 6th IIR Ammonia and CO_2 Refrigeration Technologies Conference, Ohrid, Macedonia, pp. 16–18.

Hafner, A., 2017. Integrated CO_2 system refrigeration, air conditioning and sanitary hot water. In: Proceedings of the 7th IIR Ammonia and CO_2 Refrigeration Technologies Conference, Ohrid, Macedonia, pp. 11–13.

Heinz, A., Martin, K., Rieberer, R., Kotenko, O., 2010. Experimental analysis and simulation of an integrated CO_2 heat pump for low-heating-energy buildings. In: 9th IIR Gustav Lorentzen Conference 2010. ..

Hotel Energy Solutions (HES), 2011. Analysis on energy use by European hotels: Online survey and desk research. http://hes.unwto.org/sites/all/files/docpdf/analysisonenergyusebyeuropeanhotelsonlinesurveyanddeskresearch2382011-1.pdf

Hu, B., Li, Y., Cao, F., Xing, Z., 2015. Extremum seeking control of COP optimization for air-source transcritical CO_2 heat pump water heater system. Appl. Energy 147, 361–372.

IWMAC, 2019. Centralized operation and surveillance by use of WEB technology. https://www.iwmac.com/

Karampour, M., Sawalha, S., 2017. Energy efficiency evaluation of integrated CO_2 trans-critical system in supermarkets: a field measurements and modelling analysis. Int. J. Refrig. 82, 470–486.

Lawson F., 2001. Hotels and Resorts – Planning, Design and Refurbishment Architectural Press; London, UK (2001).

Liu, S., Li, Z., Dai, B., 2017. Energy, economic and environmental analyses of the CO_2heat pump system compared with boiler heating system in China. Energy Procedia 105, 3895–3902.

Lorentzen, G., 1994. Revival of carbon dioxide as a refrigerant. Int. J. Refrig. 17 (5), 292–301.

Minetto, S., 2011. Theoretical and experimental analysis of a CO_2 heat pump for domestic hot water. Int. J. Refrig. 34 (3), 742–751.

Minetto, S., Cecchinato, L., Brignoli, R., Marinetti, S., Rossetti, A., 2016. Water-side reversible CO_2 heat pump for residential application. Int. J. Refrig. 63, 237–250.

Ndoye, B., Sarr, M., 2008. Analysis of domestic hot water energy consumption in large buildings under standard conditions in Senegal. Build. Environ. 43 (7), 1216–1224.

Nekså, P., 2002. CO_2 heat pump systems. Int. J. Refrig. 25 (4), 421–427.

Nekså, P., Rekstad, H., Zakeri, G.R., Schiefloe, P.A., 1998. CO_2-heat pump water heater: characteristics, system design and experimental results. Int. J. Refrig. 21 (3), 172–179.

Nekså, P., Walnum, H.T., Hafner, A., 2010. CO_2– a refrigerant from the past with prospects of being one of the main refrigerants in the future. In: 9th IIR Gustav Lorentzen Conference. Citeseer, pp. 2–14.

Omer, A.M., 2008. Ground-source heat pumps systems and applications. Renew. Sustain. Energy Rev. 12 (2), 344–371.

Pardiñas, Á.Á., Hafner, A., Banasiak, K., 2018. Novel integrated CO_2 vapour compression racks for supermarkets. thermodynamic analysis of possible system configurations and influence of operational conditions. Appl. Therm. Eng. 131, 1008–1025.

Polzot, A., D'Agaro, P., Gullo, P., Cortella, G., 2016. Modelling commercial refrigeration systems coupled with water storage to improve energy efficiency and perform heat recovery. Int. J. Refrig. 69, 313–323.

Rankin, R., Rousseau, P., 2006. Sanitary hot water consumption patterns in commercial and industrial sectors in South Africa: impact on heating system design. Energy Convers. Manag. 47 (6), 687–701.

Santamouris, M., Balaras, C., Dascalaki, E., Argiriou, A., Gaglia, A., 1996. Energy conservation and retrofitting potential in Hellenic hotels. Energy Build. 24 (1), 65–75.

Sarkar, J., Bhattacharyya, S., Gopal, M.R., 2004. Optimization of a transcritical CO_2 heat pump cycle for simultaneous cooling and heating applications. Int. J. Refrig. 27 (8), 830–838.

Sarkar, J., Bhattacharyya, S., Gopal, M.R., 2006. Simulation of a transcritical CO_2 heat pump cycle for simultaneous cooling and heating applications. Int. J. Refrig. 29 (5), 735–743.

Shecco, 2016. Guide 2016: Guide to Natural Refrigerants in Japan -State of the Industry. Brussel, Belgium.

Skačanová, K.Z., De Oña, A., 2019. Market and technology trends for CO_2 and Ammonia in commercial and industrial refrigeration. In: Proceedings of the 8th IIR Ammonia and CO_2 Refrigeration Technologies Conference, Ohrid, Macedonia, pp. 334–338.

Skaugen, T., Tveito, O., Førland, E., 2002. Heating Degree-Days – Present Conditions and Scenario for the Period 2021–2050. DNMI report.

Smitt, S., Hafner, A., Hoksrød, E., 2019. Presentation of the first combined CO_2 heat pump, air conditioning and hot tap water system for a hotel in Scandinavia. In: Proceedings of the 8th Conference on Ammonia and CO_2 Refrigeration Technologies. 11-13 April 2019. Ohrid, Republic of Macedonia

Stene, J., 2005. Residential CO_2 heat pump system for combined space heating and hot water heating. Int. J. Refrig. 28 (8), 1259–1265.

Su, B., 2012. Hotel design and energy consumption. World Acad. Sci. Eng. Technol. 72, 1655–1660.

Tammaro, M., Mauro, A., Montagud, C., Corberán, J., Mastrullo, R., 2016. Hot sanitary water production with CO_2 heat pumps: effect of control strategy on system performance and stratification inside the storage tank. Appl. Therm. Eng. 101, 730–740.

Thom, H., 1954. The rational relationship between heating degree days and temperature. Mon. Weather Rev. 82 (1), 1–6.

Tosato, G., Girotto, S., Minetto, S., Rossetti, A., Marinetti, S., 2019. An integrated CO_2 unit for heating, cooling and DHW installed in a hotel. Data from the field.. In: 37th UIT Heat Transfer Conference.

United Nations Environment Programme (UNEP), 2016. Decision XXVIII/Further Amendment of the Montreal Protocol. Twenty-Eighth Meeting of the Parties to the Montreal Protocol on Substances That Deplete the Ozone Layer. UNEP/OzL.Pro.28/CRP/10, United Nations Environment Programme, Nairobi, Kenya, 14 October.

Wang, S., Tuo, H., Cao, F., Xing, Z., 2013. Experimental investigation on air-source transcritical CO_2 heat pump water heater system at a fixed water inlet temperature. Int. J. Refrig. 36 (3), 701–716.

Yang, L., Li, H., Cai, S.-W., Shao, L.-L., Zhang, C.-L., 2015. Minimizing COP loss from optimal high pressure correlation for transcritical CO_2 cycle. Appl. Therm. Eng. 89, 656–662.

Yokoyama, R., Shimizu, T., Ito, K., Takemura, K., 2007. Influence of ambient temperatures on performance of a CO_2 heat pump water heating system. Energy 32 (4), 388–398.

Article III

S. Smitt, I. Tolstorebrov, A. Hafner (2021). "Performance improvement of integrated CO_2 systems with HVAC and hot water for hotels." In: *Thermal Science and Engineering Progress* 23, 1 June 2021, 100869. DOI: 10.1016/j.tsep.2021.100869

New Journal and we have not received input yet 23 (2021) 100869

Contents lists available at ScienceDirect

Thermal Science and Engineering Progress

journal homepage: www.sciencedirect.com/journal/thermal-science-and-engineering-progress

Performance improvement of integrated CO_2 systems with HVAC and hot water for hotels

S. Smitt *, I. Tolstorebrov, A. Hafner

Norwegian University of Science and Technology, Kolbjørn Hejes vei 1D, 7491 Trondheim, Norway

ARTICLE INFO

Keywords:
R744 heat pump and chiller system
HVAC and DHW integration
Thermal storage
Hotel thermal energy systems
Modeling
Control strategy

ABSTRACT

Carbon dioxide (R744) systems have emerged as a sustainable and viable alternative to hydrofluorocarbon (HFC) applications within refrigeration. During the past decade, advancements in R744 technology and system architecture have paved the way for new areas of application. Integrated R744 systems for heating and cooling in hotels have demonstrated promising results within a sector characterized by high thermal demands and a large carbon footprint. However, further research is necessary to establish integrated R744 systems as a competitive alternative to traditional HFC systems in hotels. This paper presents the numerical model of an R744 heating and cooling unit installed in Northern Europe. The system is integrated with HVAC and a 6 m^3 thermal storage for domestic hot water. A dynamic model of the hotel's thermal system was created and validated for three seasonal representative weeks using recorded ambient temperatures, heating, and cooling loads. A low load charging strategy, which exploits the thermal storage flexibility, was evaluated as an approach to improve the overall system performance. Simulations demonstrated that charging the thermal storage for longer periods at low compressor loads enhanced the overall efficiency of the system. Energy savings in the range of 5.8–13.2% were achieved based on the different seasonal scenarios. Additionally, peak power usage, operational fluctuations, and ON/OFF cycles were considerably reduced with the low load charging strategy. The proposed strategy can be implemented in similar applications to enhance overall system performance.

1. Introduction

Increasing environmental awareness and strict regulations are strengthening the position of natural refrigerants within heat pump and chiller applications [18]. This is mainly due to their low global warming potential when compared with hydrofluorocarbon (HFC) refrigerants. The hotel sector features high thermal demands, which are often realized through processes that contribute to the global warming effect [11]. The energy consumption within the hotel sector is high compared to other commercial sectors, due to the number and the behavior of occupants [29]. The largest contributor to excessive energy use within the hotel sector is domestic hot water (DHW), space heating, and cooling. In cold climates, it is estimated that approximately 61% of the total energy consumption in hotels is allocated to heating and cooling [21]. The application of conventional thermal energy sources in hotels is extensive, such as electric boilers in large inefficient central systems [7]. However, national legislation, governmental economic incentives, and reduced operational costs are promoting efficient and environmentally friendly thermal systems [26].

The application of natural and environmentally friendly refrigerants, such as air, water, hydrocarbons, ammonia, and carbon dioxide (R744), has gained much attention as an approach to reduce greenhouse gas emissions from refrigeration, air-conditioning (AC), and heat pump systems [4]. R744 has a negligible global warming potential (GWP = 1), is inexpensive, readily available, and non-flammable [22]. Despite being non-toxic, leakage detection in the machine room is necessary as R744 can displace oxygen in air at high concentrations. R744 systems operate at significantly higher pressures than conventional vapor compression systems, especially at operations above the critical point. Thus, high-pressure rated components are required, and special care must be taken when handling the system.

In the past decade, R744 refrigeration systems have become the benchmark solution in the European supermarket sector [33]. Integrated R744 systems, with heating, ventilation, and air-conditioning (HVAC), and DHW are spreading within this sector [17]. The heat for HVAC and DHW is recovered as a byproduct from the refrigeration process in integrated R744 supermarket units [15]. The cooling load, rather than the heating load, is the controlling parameter for these systems. Integrated HVAC and DHW systems for heat pump applications

* Corresponding author.
E-mail addresses: silje.smitt@ntnu.no (S. Smitt), ignat.tolstorebrov@ntnu.no (I. Tolstorebrov), armin.hafner@ntnu.no (A. Hafner).

https://doi.org/10.1016/j.tsep.2021.100869

Available online 15 February 2021

Nomenclature

Nomenclature

$\dot{m}$	Mass flow rate [kg s^{-1}]
P	Pressure [bar]
$\dot{Q}$	Cooling or heating load [kW]
T	Temperature [°C]
V	Volume [l]
$\dot{W}$	Power [kW]

Abbrevations

AC	Air-Conditioning
Avg	Average
COP	Coefficient Of Performance
DHW	Domestic Hot Water
fans	Evaporator fans
GC	Gas Cooler
GWP	Global Warming Potential
HFC	Hydrofluorocarbon
HT	High Temperature
HTA	Heat Transfer Area
HVAC	Heating, Ventilation, and Air-Conditioning
HX	Heat Exchanger
LLC	Low Load Charging
MT	Medium Temperature
PI	Proportional Integral
RRMSE	Relative Root Mean Square Error
SCOP	Seasonal Coefficient of Performance
SD	Standard Deviation
VSD	Variable Speed Drive

Subscripts

a	Ambient
AC	Air-Conditioning
aux,el	Auxiliary electrical systems
comp	Compressors
CW	City Water
DF	Evaporator defrost heat
DHW	Domestic Hot Water
EL	Electric boiler
fans	Evaporator fans
GC	Gas Cooler
h	Heating
HP	Heat Pump
i	Index
max	Maximum
min	Minimum
pumps	All system pumps
R	Return
RH	Radiators/floor Heating
S	Supply

Setpoint

tot	Total
VH	Ventilation Heating
Δ	Change
ρ	Density [kg m^{-3}]

outside the supermarket sector are dominated by synthetic refrigerant systems [13].

The integrated R744 heat pump system is a promising technology for HVAC and high-temperature DHW production [37]. In these systems, the heat rejection process occurs in the transcritical region at high working pressures and gliding temperatures. The cooling of transcritical R744 gas provides a considerably higher temperature difference between the inlet and outlet of the gas cooler when compared with traditional condensers. Thus, R744 is superior in heating processes that require a high-temperature lift, such as DHW production [25]. However, the efficiency of the transcritical R744 systems can be compromised if the gas cooler outlet temperature becomes too high [1]. Therefore, a low fluid (water) inlet temperature is essential in counter-current R744 gas coolers to reduce the temperature before expansion, thereby ensuring a high coefficient of performance (COP) [20].

The potential benefits of applying integrated R744 systems in hotels are considerable due to the characteristically substantial DHW demand [10]. R744 systems can be implemented with ease and high flexibility as a retrofit solution in existing hotels, where other natural refrigerants are limited due to safety restrictions on account of toxicity and flammability [12]. Consequently, the hotel sector is recognized as a promising area of application for integrated R744 heating and cooling systems [34]. The first R744 heat pump and chiller unit installed in a Nordic hotel was presented by [35]. The system consists of a single unit for heating, cooling, and DHW with an integrated 6 m^3 thermal storage. Key operating parameters were evaluated, and system capacities were analyzed for a one-year period. The first-year seasonal coefficient of performance (SCOP) for the R744 system was found to be 2.90. The DHW usage was identified as the largest contributor to the overall thermal energy use in the hotel, accounting for 52% of the annual heat load. The DHW consumption follows a particular 24-h pattern with high consumption peaks during morning and evening hours, enabling operational freedom in terms of the thermal storage charging strategy. The main influencing parameter on efficiency was identified as high fluid return temperatures from secondary systems, resulting in elevated R744 temperatures before expansion.

Numerous authors have investigated control strategies to enhance the performance of transcritical R744 systems [44,28,45]. The performance of these systems is influenced by many factors, such as control strategy, operating pressure, return temperatures from secondary systems, and asynchronous heating and cooling loads. Few studies have focused on improving the control strategy by utilizing thermal storage to increase the performance of transcritical R744 systems. Cortella et al. [5] presented a numerical model of an R744 supermarket unit equipped with HVAC and DHW. Through simulations, they demonstrated how hot and cold thermal storage units can be applied to compensate for asynchronous demands and reduce peak loads. Polzot et al. [30] developed a numerical model to evaluate the implementation of cold thermal storage in an R744 supermarket unit. The energy consumption of the R744 system was 9% lower than the baseline when applying a control strategy that utilized the storage to reduce R744 gas cooler outlet temperature. Additionally, the authors concluded that the rejected heat could effectively be collected by the use of hot thermal storage. Tammaro et al. [38] implemented an alternative control strategy in a numerical model of an R744 air-source heat pump for DHW production, where the frequency of compressors and pumps were reduced to maintain a constant temperature inside the hot thermal storage tanks. The results revealed that the thermal storage enabled higher R744 operational flexibility and longer operational time for the heat pump. Field data presented by Tosato et al. [42] illustrated how the operating strategy during DHW charging influences the efficiency of an integrated R744 heat pump unit in an Italian hotel, which features both HVAC and DHW production. The authors highlighted that the compressor control strategy during charging should be evaluated to enhance the performance of the system. Thus, there is a need to investigate alternative control strategies to improve integrated R744 heat pump units for HVAC and DHW heating.

The charging strategy is a key influencing factor to achieve a high overall system performance in R744 heat pumps. As illustrated by recent studies, thermal storage provides a buffer that enables a high degree of flexibility with regard to operating strategy. The control strategy for integrated R744 heat pumps with simultaneous HVAC and DHW production is, to the best of the authors' knowledge, not yet investigated. For the first time in the literature, an alternative charging strategy is presented to increase the efficiency of integrated R744 heat pump systems with combined HVAC and DHW production. The principle of the strategy is to utilize the storage capacity to charge the DHW storage for longer periods of time at a reduced load. Charging at reduced loads has the potential to limit return temperatures from the secondary systems and by this, enhance system performance. The influence of the charging strategy is evaluated through a dynamic simulation model for different representative seasonal scenarios. The current research contributes to improving the performance of integrated R744 systems with HVAC and DHW production, thereby benefiting current and future installations.

2. System description and operation

The R744 integrated unit analyzed in this work is part of an existing heating system for a hotel in Trondheim, Norway (63.44 °N, 10.40 °E). The hotel's location is characterized as a cold coastal climate with a normalized average annual temperature of 5.3 °C [41]. The R744 system provides HVAC and DHW for a floor area of approximately 9000 m^2, including 157 guest rooms. The installed heating and cooling capacity is 280 kW and 75 kW, respectively. Fig 1 presents the entire thermal system and the secondary distribution circuits. Heat is supplied to the hydronic subsystems through two gas coolers in series, GC1 and GC2, at high (>60 °C) and medium (<50 °C) temperatures. The medium temperature (MT) circuit provides heat primarily to the ventilation heating (VH) batteries and a radiator/floor heating (RH) circuit. The remaining heat is used to preheat DHW through the heat exchanger (HX) HX2. The high temperature (HT) circuit mainly supplies heat for DHW reheat through HX3. During winter operations, HX1 in the MT circuit is applied to supply heat for the defrosting of evaporators through a brine circuit. The HT circuit supplies extra heat through HX5 during winter conditions when the setpoint temperature of the radiator/floor heating circuit is

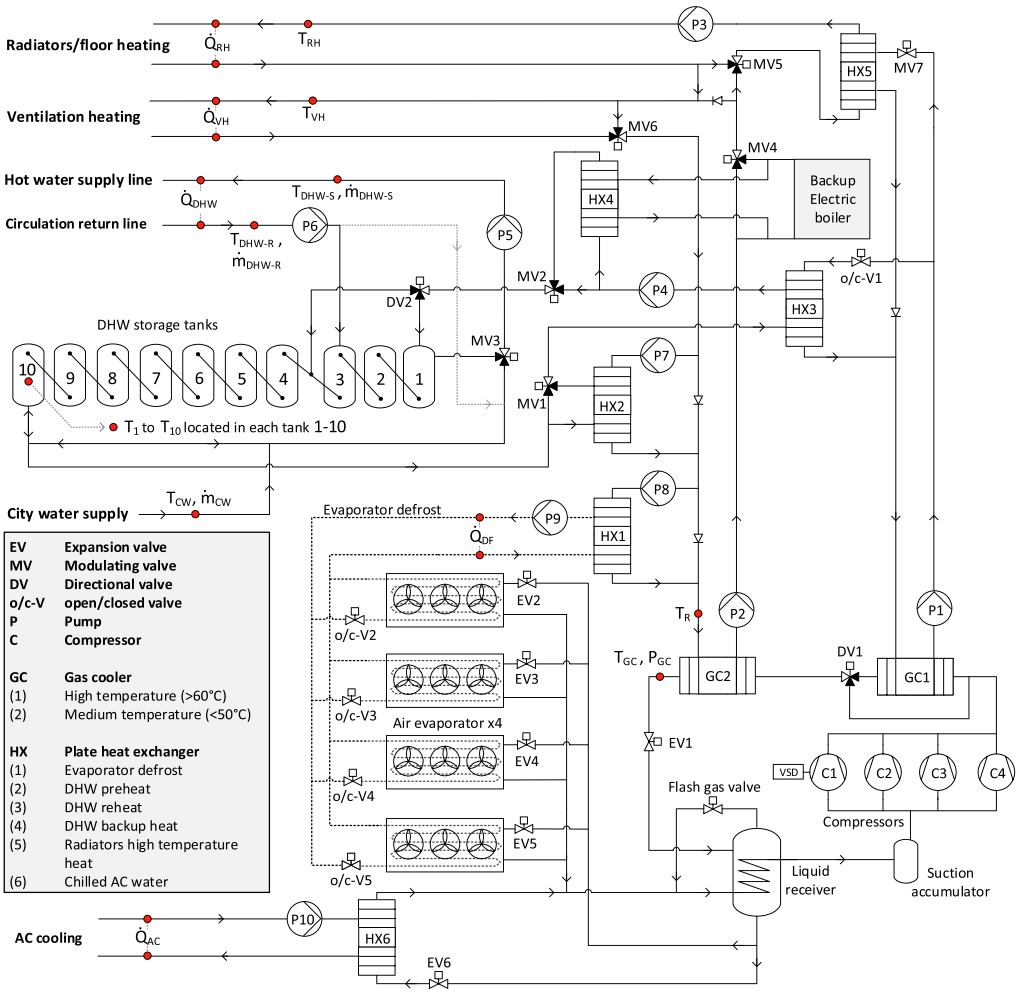

Fig. 1. Schematic drawing of the R744 heat pump and chiller unit including thermal storage and secondary system with control points for simulations.

elevated. MV5 is, in these instances, closed towards the MT circuit to prevent elevated return temperatures towards GC2. An additional modulating valve (not included in Fig 1) recirculates flow to reduce the supply temperature to floor heating. Four air evaporators (50 kW at −15 °C) serve as the main heat source for the R744 unit. Alternatively, a HX interface to the chilled water circuit (HX6) can be employed for heat recovery if AC is needed. The chilled water supplied through HX6 is used to supplement the existing AC chiller unit, and is thus only applied as an auxiliary function during heat generation.

The DHW subsystem consists of several tanks in series with a combined volume of 6 m^3. The DHW system control is characterized by two distinctive modes of operation: *DHW charging* and *non-charging mode*. During non-charging mode, the majority of the heating load is allocated to the MT circuit to cover the moderate temperature demands, e.g. radiators, floor, and ventilation heating. Excess heat is supplied to the DHW subsystem. During DHW charging, water is drawn from tank No. 10 and passes through the preheat and reheat section. Hot water is stored and moves through the series of tanks as the buffer is gradually charged from tank No. 1 to No. 10, with the same strategy as described by Minetto [24]. The thermal storage is fully charged when the normally stratified storage reaches a high and uniform temperature. During discharge, water is drawn from tank No. 1 and is mixed in the modulating valve, MV3, with cold water to a temperature of 55 °C before entering the hot water supply line.

3. Methodology

The research strategy consisted of four primary steps:

1. Collecting thermal energy demand profiles from the hotel, which includes profiles for DHW, ventilation heat, heat for radiators, and AC cooling loads. Recorded ambient temperatures and evaporator defrost load (DF) profiles were also included in the analysis.
2. Developing a dynamic simulation model of the hotel's thermal system in Dymola, including the R744 unit and all secondary hydronic systems.
3. Simulating various seasonal scenarios to validate the model according to variations in load, setpoint temperatures, and modes of operation.
4. Implementing a low load charging strategy and investigating potential benefits through simulations.

These steps are described in detail in the following sections.

3.1. Data management

Climate and operational data were collected and used as input in the numerical model. Ambient temperatures, T_a, were obtained from the Norwegian Meteorology Institute Database and applied to the model. The annual average temperature for the first year of operation was recorded to be 6.8 °C. Field data from the hotel have been obtained via the web-monitoring software *IWMAC* [19]. The measurements are not logged at specific time intervals, but rather when a change in a sensor value is registered. Therefore, the recorded data points are regarded as constant step values within the specified time interval until the next recorded value. The hydronic system is instrumented with temperature sensors and mass flow meters in every fluid branch. Moreover, heat flow meters for secondary fluids are installed at every heat exchanger. Due to the absence of an energy meter in the DHW supply line, the consumption load and mass flow rate were calculated using the energy balance equation on the DHW subsystem, as described in Smitt et al. [35]. Heat losses from the storage tanks were accounted for in the DHW demand profile.

All input variables have been resampled and the weighted averaged value over 20 min were applied to the model. The weighted average, $\bar{v}$, was calculated using Eq. 1:

$$\bar{v} = \sum_{i=1}^{n} v_i \frac{t_i}{t} \tag{1}$$

where v_i is the value of the variable, v, over the time interval t_i. The length of the time interval was selected as a trade-off between accuracy and model computational time. All model inputs were interpolated using Steffen Interpolation, such that the monotonicity is preserved and the first derivative is continuous [36].

3.1.1. Performance indicators

Key performance indicators were defined to validate the model and to evaluate the DHW charging strategy for different seasonal scenarios. The R744 unit heating SCOP, $SCOP_h$ [–], is defined as the sum ratio of the total heat load to the electricity necessary to provide the heating functions, as shown in Eq. 2:

$$SCOP_h = \frac{\sum\left(\int \dot{Q}_{GC1} + \int \dot{Q}_{GC2}\right)}{\sum\left(\int \dot{W}_{comp} + \int \dot{W}_{fans}\right)} \tag{2}$$

where $\dot{W}_{comp}$ and $\dot{W}_{fans}$ [kW] represent the combined electricity consumption for all compressors and evaporation fans, respectively.

The R744 unit heating and cooling SCOP, $SCOP_{HP}$ [–], is defined as the ratio of useful thermal load to the total electricity consumption necessary to supply the thermal load, using Eq. 3:

$$SCOP_{HP} = \frac{\sum\left(\int \dot{Q}_{GC1} + \int \dot{Q}_{GC2} + \int \dot{Q}_{AC}\right)}{\sum\left(\int \dot{W}_{comp} + \int \dot{W}_{fans} + \int \dot{W}_{pumps} + \int \dot{W}_{aux,el}\right)} \tag{3}$$

$\dot{W}_{pumps}$ and $\dot{Q}_{AC}$ [kW] represent the total pump work in secondary systems and the AC cooling load, respectively. $\dot{W}_{aux,el}$ [kW] represents the electricity consumption for auxiliary systems, such as control systems, which were not included in the simulation SCOP evaluation.

$SCOP_{tot}$ [–] is defined as the SCOP for the entire integrated thermal system, including the R744 unit, secondary systems, and the electric boiler. $SCOP_{tot}$ is the ratio between supplied thermal load and total work [kW] over a specific period of time, as shown in Eq. 4.

$$SCOP_{tot} = \frac{\sum\left(\int \dot{Q}_{GC1} + \int \dot{Q}_{GC2} + \int \dot{Q}_{AC} + \int \dot{Q}_{EL}\right)}{\sum\left(\int \dot{W}_{comp} + \int \dot{W}_{fans} + \int \dot{W}_{pumps} + \int \dot{W}_{aux,el} + \int \dot{W}_{EL}\right)} \tag{4}$$

$\dot{Q}_{EL}$ and $\dot{W}_{EL}$ [kW] represent the heat and power associated with the operation of the electric boiler, respectively.

3.2. Numerical model

A detailed model of the entire thermal system was created in the Modelica object-oriented programming language. The programming environment, Dymola 2017, was used to simulate the model. The standard solver, DASSL, was applied for this investigation [8]. Construction of the model was achieved by using components from the commercially available thermodynamic library TIL-Suite 3.5, developed by TLK-Thermo GmbH [39]. TIL-Media 3.5 library was applied for the simulation of the fluids used in the model, which includes refrigerant R744, water, glycol, and dry air [40]. The TIL extensions are advanced libraries for transient simulations of fluid systems and are especially applicable for heat transfer modeling purposes, i.e. heat pumps, refrigeration, cooling, and heating systems. Among the components that are included in the library are compressors, pumps, valves, and heat exchangers. The components are connected in the oriented physical modeling interface, Dymola, to construct complex models. External data for boundary conditions, heating, and cooling loads were imported to the model, as illustrated in Fig. 2.

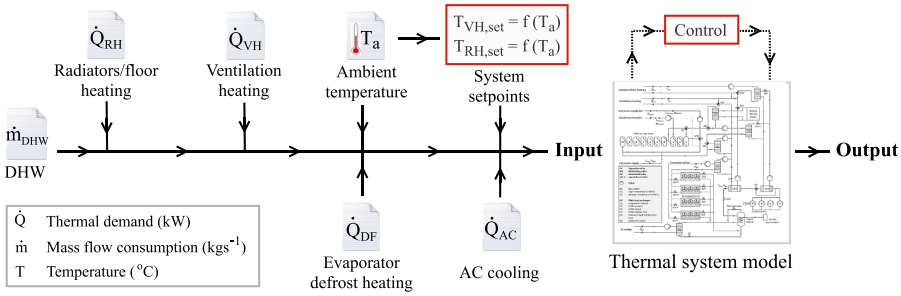

Fig. 2. Outline of numerical model with external inputs.

3.2.1. Components

The R744 unit consists of four parallel compressors that are connected to the 25 L suction accumulator. One compressor is equipped with variable speed drive (VSD) while the rest is controlled by on/off power supply. All compressors were modeled by their swept volumes, as well as correlations for circulated mass flow rate and electric power consumption based on the data published by the manufacturer. Correlations for each compressor were implemented in the model as a function of suction and discharge conditions, in addition to the rotational speed of the frequency converter (for the VSD compressor) [27]. The operation of the oil return system and the influence of oil in the refrigerant were neglected.

Table 1 lists thermal system components and specification, which were applied in the simulation. The components are labeled in reference to Fig. 1.

The R744 high-pressure valve, EV1 in Fig. 1, was modeled using an orifice-valve, where the Bernoulli equation was applied to calculate the mass flow rate as a function of pressure difference. An ideal separator with a volume of 340 L was applied to model the liquid receiver. Each evaporator was modeled as fin-and-tube cross-flow heat exchangers, as specified by technical data provided by the manufacturer. Constant fin efficiency was assumed and the heat transfer coefficient on the refrigerant side was estimated to 2500 W m^2 K^{-1}. The fan power was formulated as a function of air volume flow through each evaporator.

The gas coolers and the heat exchangers in the hydronic circuits were implemented using plate heat exchanger models from the TIL library. The pressure drop in each heat exchanger was approximated using quadratic correlations formulated based on nominal pressure loss at nominal volume flow rate [43]. The heat transfer coefficient for the refrigerant in the gas cooler was estimated to 3000 W m^2 K^{-1}, while the VDI Heat Atlas correlation for chevron plate heat exchangers was applied to calculate the coefficient of heat transfer for the single-phase fluids [23]. The gas coolers (GC1 and GC2) were modeled as brazed plate heat exchangers for extreme high-pressure requirements, while the single-phase heat exchangers (HX1-HX5 in Fig. 1) were modeled as standard brazed plate heat exchangers. Each heat exchanger was specified according to the number of plates, thickness, length, and width.

External demands were implemented using thermal heat boundaries with specified time-dependent input variables, as discussed in Section 3.1. A closed brine circuit was implemented to simulate the heat transport from the MT circuit (HX1 in Fig. 1) to the evaporators during defrosting. Consequently, the specific mechanisms related to frost formation in the evaporators were not evaluated. The electric boiler was modeled as a heat boundary, in which the amount of load supplied through the boundary was determined based on specified setpoints.

The DHW subsystem was included in the model as a water circuit with 10 hot water tanks in series. Each tank was modeled as a tube element of approximately 600 liters (I.D. × H = 0.325 m × 1.8 m). Five stratified temperature layers were included in each tank to approximate the water stratification from top to bottom. The inlet of each tank is located at the top, which is connected via the bottom of the next tank in the series. Water enters the top of each tank element during charging and the stratified water layers are pushed towards the last tank in the series (tank nr. 10). Water is drawn from the top of each tank and directed towards the supply line, $\dot{m}_{DHW-S}$, during discharging of the storage. $\dot{m}_{DHW-S}$ is displaced with +0.2 kg s^{-1} as an approximation for the circulation in the hot water line. The hot water, which is circulated back to the subsystem from the hotel ($\dot{m}_{DHW-R}$), was assumed to have a temperature of T_{DHW-S} − 5 K and a mass flow rate of 0.2 kg s^{-1}, on the bases of analysis of the system during periods with negligible hot water demands. A mass flow boundary ($\dot{m}_{CW}$) supplies cold city water to the subsystem. The city water is assumed to maintain a temperature of 8 °C. All pumps, standard valves, and three-port valves were implemented using standard components from the TIL library and are controlled with proportional integral (PI) controllers.

3.2.2. Control

The control scheme of the R744 unit and secondary systems have been implemented according to specifications supplied by the system manufacturers. However, control of the high pressure, compressors, and evaporators have been approximated for simulation purposes. The high

Table 1
Thermal system components and specifications.

Component	Label	Model/type	Specification
Compressors	C1, C2	4FTC-30 K (C1 with VSD)	Swept volume: 17.8 m^{3}h^{-1} at 50 Hz
	C3, C4	4DTC-25 K	Swept volume: 21.2 m^{3}h^{-1} at 50 Hz
Heat exchangers	GC1, GC2	High-pressure rated brazed plate	HTA: 7.6–16.6 m^2
	HX1 - HX6	Standard brazed plate	HTA: 2.8–11.0 m^2
Evaporators		CXGHN	HTA: 561.9 m^2, tube volume: 0.157 m^3
Pumps	P1 - P10	In-line centrifugal pumps (VSD)	Capacity: 4.5–21.9 m/h at 50 Hz
Temperature sensors	T_x	NTC10/TP500	Accuracy: ± 0.2 K/ ± 0.15 + 0.002 T
Pressure sensors	P_x	Pressure transmitter	Accuracy: ± 0.3% at full scale
Mass flow meters	$\dot{m}_x$	Oscillator mass flow meter	Accuracy: Class 2
Energy meters	$\dot{Q}_x$	Oscillator mass flow meter, TP500	Accuracy: Class 2

HTA: Heat Transfer Area.

pressure controller regulates P_{GC} in Fig. 1, where a temperature approach of 2 °C between T_{GC} and T_R is applied. The maximum and minimum gas cooler running pressure is 100 and 60 bar, respectively. The operating pressure is divided into operating zones, according to the principles described by Gullo et al. [16].

The model is equipped with four air evaporator components that share the same control logic. Initially, one evaporator is applied when the R744 unit is activated and the compressors are turned on. The thermostatic expansion valve of the active evaporator, e.g. EV2 in Fig. 1, continuously modulates the opening degree to meet the setpoint for superheating at the exit of the evaporator. The air volume flow rate is controlled by the fan unit to reach a specific temperature difference, ΔT, through the evaporator. ΔT is dependent on T_a and is regulated in a range from 3 to 5 K. The number of active evaporators is determined based on fan capacity. Initially, one evaporator is activated during start-up conditions. An additional evaporator is applied if the fan capacity (0 to 100%) of the current evaporator(s) exceeds 80% for more than 5 min. If the fan capacity for the active evaporator(s) is below 20% for more than 5 min, one evaporator is deactivated. The is also the case during defrosting operations. All evaporators are deactivated at the same time when the heat pump is inactive.

The control of the compressor rack consists of two separate schemes to manage (1) the requested heat load and (2) the operation of the compressors. The modeled controllers are based on the specification published by the manufacturer. The requested load ratio is used as the controlling parameter for the activation of the different compressors. The compressors are employed according to the combination of active compressors that satisfies the requested load. The control logic to determine the requested heat load ratio from the building is shown in Fig. 3.

The requested heat load is calculated based on measured signals from the modeled system. The control scheme continuously ensures that the system setpoints, e.g. ventilation and radiators supply temperatures (T_{VH} and T_{RH} in Fig. 1), are satisfied by adjusting the requested load accordingly. When the thermal storage requires charging, the requested heat load ratio is increased and adjusted further if the conditions in Fig. 3 are not satisfied. The heat load during charging is determined based on the temperature difference across the storage. The requested compressor load ratio is boosted if the temperatures in the storage tanks, T_1 to T_{10}, do not increase towards the setpoint. This is illustrated in Fig. 3 by the sub-process during the DWH charging mode.

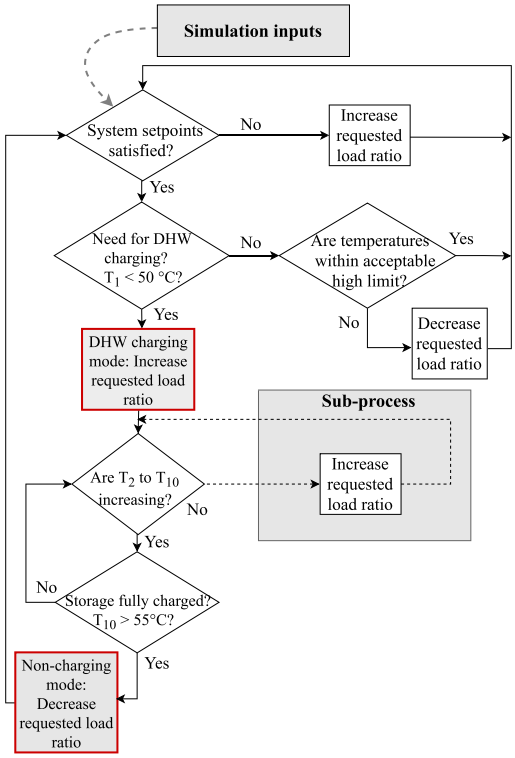

Fig. 3. Simplified decision tree control logic to determine requested compressor load ratio. Safety regulations are not included.

3.3. Simulations

Three different weeks of operation were selected to validate the model based on weather conditions that demonstrate the different seasonal performance of the system: nominal (spring and fall), winter, and summer. The heating and cooling demands for the different weeks are shown in Fig. 4. It should be noted that the demands applied to the model are equal to the loads in the real system. The operational characteristics of the different representative seasonal scenarios are listed below and discussed in detail by Smitt et al. [35]. Only supplied cooling energy from the R744 system have been included in this analysis, as cooling energy from the auxiliary chiller unit is not logged. Information regarding minimum, maximum, and average demands along with ambient temperatures are listed in Table 2.

- Nominal week (October 18^{th}-25^{th} 2018): Moderate and fluctuating space heating demands. High AC cooling load due to indoor setpoint temperature adjustments. This week represents seasonal operations from September through October, and April through May.
- Winter week (January 15^{th}-22^{nd} 2019): High heating demands corresponding to low ambient temperature. The operation characteristics for the week are representative of system operations from November through March.
- Summer week (May 18–25th 2019): Characterized by low heating demands and moderate AC cooling demands. Relative low AC cooling loads when compared with nominal and winter weeks, as a result of high evaporation temperatures. Due to high ambient temperatures, summer week is representative for the period of June through August.

The model has been validated with the collected operational data from the specific periods, which characteristics are listed in Table 2.

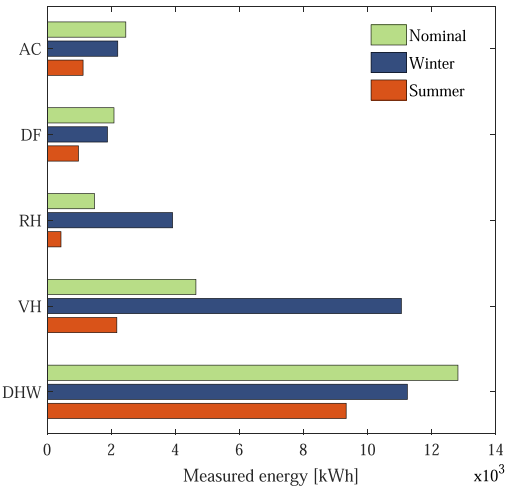

Fig. 4. Measured energy demands for the representative seasonal weeks.

Table 2
Demands and temperature characteristics for representative seasonal scenarios.

Case name/variable		Nominal			Winter			Summer		
		Max	Min	Avg	Max	Min	Avg	Max	Min	Avg
$\dot{Q}_{VH}$	[kW]	66.8	1.0	27.6	119.7	2.4	65.8	85.5	1.0	5.3
$\dot{Q}_{RH}$	[kW]	23.5	1.0	8.7	45.4	1.9	23.3	47.8	1.0	1.7
$\dot{Q}_{AC}$	[kW]	25.6	1.0	14.6	15.0	9.0	13.1	25.1	1.0	6.4
$\dot{Q}_{DF}$	[kW]	88.0	1.0	12.4	72.6	1.0	10.9	107.6	1.0	12.8
$\dot{Q}_{DHW}$	[kW]	229.6	6.4	76.3	207.6	8.1	66.9	251.8	4.5	55.6
T_a	[°C]	10.9	2.5	6.3	0.8	-12.6	-5.3	23.9	7.0	15.8

A minimum requested load limit of 1 kW is applied to all inputs for computational purposes.

4. Results and discussion

4.1. Model validation

Transient simulations were conducted for the three representative weeks that reflect the seasonal variations in operating conditions to illustrate the model validity. Table 3 lists the measured demands (weekly integrated) and error related to the simulated supplied loads. The R^2-values and relative root mean square error (RRMSE) values for hourly results are also listed in the table and have been calculated as described by Despotovic et al. [9]. The simulated relative error for weekly supplied energy is below 8% for all loads in all scenarios. This is acceptable according to D˙Agaro et al. [6], which found that a relative weekly error below 10% for supplied energy is sufficient to validate a transient model for an integrated R744 system with storage.

The simulated supplied heat energy shows high accuracy in terms of hourly RRMSE-values of less than 10% [2]. All R^2-values are above 0.743, which is in same range as other validations of transient thermal systems [31,32]. However, deviations occur between the measured and simulated values for the cooling energy, AC in Table 3. The variations are reflected in the hourly RRMSE-values for this variable, which have a range of 17–18% for the summer and nominal scenarios. The reduced accuracy for the simulated AC energy is explained by the on/off activation of the heat pump, which is controlled by the heating demand, as explained in Section 2. The setpoints are not always met in the real system, and thus activation of the heat pump does not always trigger according to the constraints specified by the manufacturers, as discussed by Smitt et al. [35]. In the modeled system, control of the heat pump is limited by the model constraints and responds directly to these. Thus, a larger portion of the AC cooling energy is recovered during the winter simulation, as the total heat load provided by the simulated system is larger for this scenario.

Table 3
Comparison between monitored and simulated energy values.

Case	Variable	Measured weekly [kWh]	Relative weekly error [%]	RRMSE hourly [%]	R^2 hourly [–]
Nominal	VH	4640	−0.005	0.101	1.000
	DF	1472	−0.012	0.184	1.000
	AC	2451	−6.101	18.674	0.746
	DF	2082	−0.014	7.916	0.997
	DHW	12823	−3.829	9.387	0.993
Winter	VH	11054	−0.007	0.133	1.000
	RH	3911	−0.001	0.026	1.000
	AC	2200	0.008	0.115	0.996
	DF	1878	−0.002	0.173	0.999
	DHW	11214	−0.360	8.088	0.990
Summer	VH	2171	−0.064	1.010	1.000
	RH	427	−0.662	6.296	0.999
	AC	1116	−7.981	17.044	0.950
	DF	973	−0.025	4.252	0.991
	DHW	9332	4.827	4.825	1.000

The total delivered heat energy from the heat pump on a daily basis is shown in Fig. 5, in which the R^2-value for measured and simulated values is 0.958. Fig. 5 illustrates a slight overestimation of supplied heat from the thermal system, despite the low deviations displayed in Table 3. This behavior is reflected in the simulated SCOPs for the hotels' entire thermal system in Table 4, $SCOP_{tot}$, which is underestimated for both the nominal and the summer scenario. Hence, a larger portion of the heat supplied to the hotel is covered by the electric boiler in these simulations. The opposite is true for the winter scenario, where the values in Fig. 5 are slightly underestimated. Thus, the $SCOP_{tot}$ is higher than the measured value for the winter simulation.

All simulated SCOPs for heating, $SCOP_h$, are lower than their counterpart measured values. A similar trend is observed in the SCOPs for the entire R744 unit, $SCOP_{HP}$, for the nominal and winter scenarios. Thus, it can be concluded that the simulated performance is slightly lower when compared to the real system. However, when accounting for the uncertainties, a majority of the simulated SCOPs are within the measurement range of error. All simulated SCOPs are comparable to the measured values and within a relative error range of 8.5%. In addition, the simulated SCOPs illustrate the same seasonal variations as the measured values. Thus, it can be concluded that the modeled system is satisfactory in characterizing the behavior of the real system.

4.2. Low load domestic hot water charging strategy

The DHW charging strategy is a key influencing factor on the overall system performance, as discussed in Section 1. On an annual basis, more

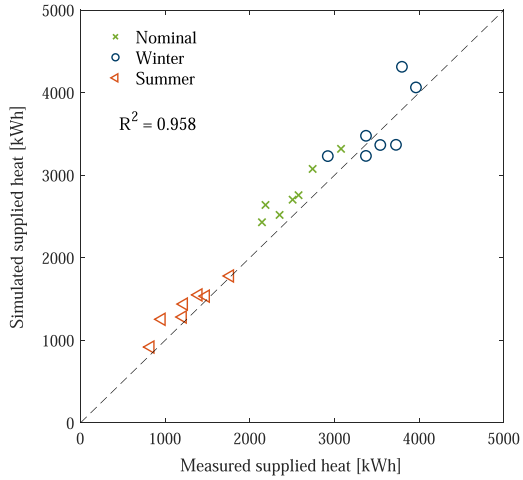

Fig. 5. Measured and simulated total heat energy supplied to the hotel per day for different seasons.

Table 4
Comparison between monitored and simulated SCOPs for the selected seasonal scenarios.

Case name/Variable	Nominal			Winter			Summer		
	Measured*	Simulated	Relative error [%]	Measured*	Simulated	Relative error [%]	Measured*	Simulated	Relative error [%]
$SCOP_h$	3.05 ± 0.17	2.81	7.87	2.45 ± 0.14	2.39	4.02	3.30 ± 0.19	3.24	1.82
$SCOP_{HP}$	3.23 ± 0.18	3.15	2.48	2.63 ± 0.16	2.60	1.14	3.34 ± 0.21	3.57	6.89
$SCOP_{tot}$	3.21 ± 0.34	3.12	2.80	2.37 ± 0.25	2.49	5.06	2.97 ± 0.31	2.72	8.42

* The range of uncertainty for the measured SCOP-values are described by Smitt et al. [35].

than 52% of the heat energy in the hotel is allocated to DHW heating [35]. Thus, improving the DHW strategy can have a significant influence on the overall system performance. With the current charging strategy, illustrated in Fig. 3, it was discovered that the DHW storage capacity of 6 m^3 occasionally is insufficient. The heat supplied to DHW is in these instances compensated by the boiler. Also, DHW charging mode can negatively impact the overall performance of the thermal system, especially during operations with low T_a and high loads, resulting in high return temperature, T_R, from the secondary system. Implementing a strategy that supplies heat for longer periods of time at low loads can reduce fluctuations and high return temperatures from secondary systems during DHW charging mode. Thus, improving the operating strategy could have a positive influence on the overall system performance.

A low load charging (LLC) strategy was established and incorporated in the model to investigate its influence on the overall system efficiency. A simplified decision tree describing the outline of the control strategy algorithm is shown in Fig. 6. The principle of the proposed control strategy is to reduce the return temperature from the secondary system by limiting supply temperatures to the building during DHW charging. In contrast to the current charging strategy, this entails constantly insuring that setpoints are met, and to adjust compressor load accordingly to minimize the heating load and peak power utilization. This achieved by establishing a high limit for the different temperature supply sensors, such as T_{RH} and T_{VH}. When the temperature exceeds this limit, the requested heat load ratio is reduced if all other conditions are within acceptable limits.

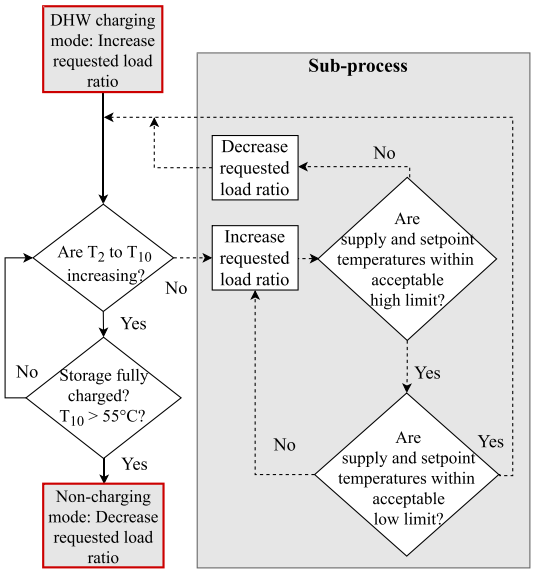

Fig. 6. Simplified decision tree control logic to determine requested compressor load ratio for the low load charging strategy.

4.2.1. Results obtained when applying the low load charging strategy

Simulations have been conducted for the three specified seasonal representative weeks, in which the LLC strategy has been implemented to evaluate the influence on the overall system performance during different operating conditions. The inputs used in the LLC simulations were identical to the baseline cases, which were described in Table 2 and Fig. 4. All results obtained with the LLC strategy are related to the results obtained with seasonal baseline scenarios presented in Section 4.1.

The SCOPs and energy savings obtained with the LLC strategy are shown in Fig. 7. It can be observed that there is an increase in $SCOP_h$ [%] during the nominal and the winter scenarios by 6.6 and 4.5%, respectively. When evaluating $SCOP_h$ for the summer case, the impact of the LLC strategy is distinctively negative. Similar results were obtained for $SCOP_{HP}$ for all seasonal cases.

The SCOP for the entire thermal system, $SCOP_{tot}$ in Fig. 7, demonstrates the beneficial effects of applying the LLC strategy. The largest improvement in overall performance is achieved for the summer case, in which a 23% increase in $SCOP_{tot}$ is achieved. When comparing the values of $SCOP_{HP}$ and $SCOP_{tot}$ in Table 4, it can be concluded that the electric boiler covers a large part of the heat during the baseline summer case. This is due to operational restrictions that require the R744 unit to reduce the compressor load at high gas cooler outlet temperatures (>45 °C), due to compromised efficiency. Consequently, DHW production by the heat pump is significantly reduced in the baseline case, as the heat pump operates at temperatures above the threshold.

Table 5 shows the share of active operation, ON%, of the R744 unit for different cases. For the summer cases, the active operational time is increased from 72.1 to 93.5% when applying the LLC strategy. Thus, the heat pump can cover a larger portion of the heating demand during summer than the baseline. The strain on the system is also reduced as the

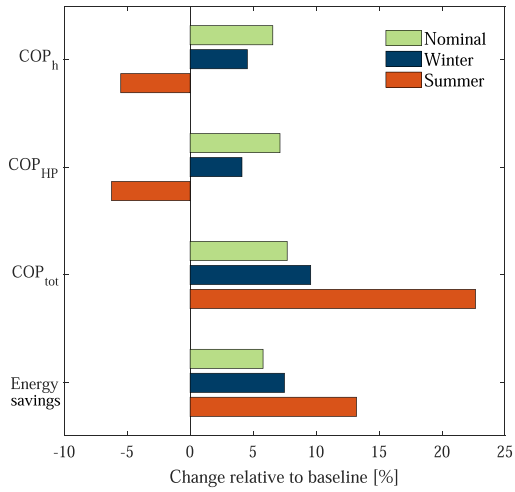

Fig. 7. Simulation results showing relative $SCOP_h$, $SCOP_{HP}$, $SCOP_{tot}$ and energy savings in relation to seasonal baseline for nominal, winter and summer operations.

Table 5
Results for the control logic comparison of baseline cases and low load charging strategy implementation.

Case	Control strategy	ON/OFF cycles [–]	ON% [%]	T_R[°C]
Nominal	Baseline	33	92.4	33.5
Nominal	LLC	1	99.7	30.7
Winter	Baseline	0	100.0	28.4
Winter	LLC	0	100.0	26.6
Summer	Baseline	86	72.1	33.9
Summer	LLC	13	93.5	34.5

number of ON/OFF cycles is decreased from 86 to 13 in the summer case. However, such a strategy results in an increase of the return temperature from the hotel, as illustrated by T_R in Table 5. The elevated return temperature during summer operation is explained by an increased supply temperature when applying the LLC strategy. During the baseline case, return temperatures exceed the established limit for T_R. The response of the thermal system is to rely solely on boiler heat, supplied at lower temperatures. Thus, an increase in T_R is observed during the LLC summer case. However, the range of operation of the R744 system is increased when applying the LLC strategy. As a result, $SCOP_h$ and $SCOP_{HP}$ are reduced for the summer case when applying LLC strategy. Thus, a trade-off occurs between high R744 system performance and overall system performance. The LLC strategy improved the $SCOP_{tot}$ during the nominal and winter week with 9.6 and 7.7%, respectively. This result can be significant for R744 heat pump applications in cold climates, as these two scenarios represent the largest period of annual operations, from September through May.

The energy savings obtained with the LLC strategy in Fig. 7 exhibit the same trends as $SCOP_{tot}$. A 13.2% increase in savings is observed during the summer week when applying the LLC strategy in comparison to the baseline scenario. The nominal and winter scenarios demonstrate energy savings of 5.8 and 7.5%, respectively. If the results are extrapolated to annual operation, a 8.4% increase in energy saving is achieved when applying the LLC strategy. Thus, a significant increase in energy savings of integrated R744 heat pump systems can be realized by reducing the load and stabilizing the system operations.

The peak power utilization is analyzed to illustrate how the LLC strategy can benefit R744 heat pump operations beyond an increase in SCOP and energy savings. Fig. 8 demonstrates how the daily power peak

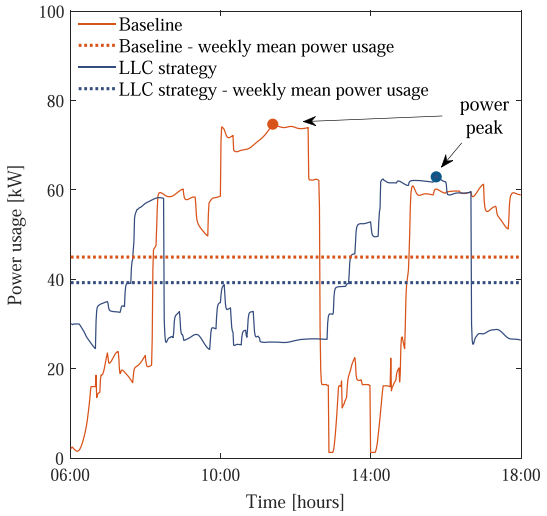

Fig. 8. Demonstration of mean and peak power results for baseline and low load charging strategy for the nominal case (20^{th} October).

is reduced relative to the baseline scenario. The maximum peak recorded for that specific day is reduced by approximately 12 kW with the LLC strategy. The weekly mean power usage for the nominal case is reduced from 45.0 to 39.3 kW.

The results for power and total R744 electricity usage for all seasonal cases are listed in Table 6. The smallest reduction of mean power usage occurs in winter case, due to the magnitude of the heating demand. However, the application of the LLC strategy for the summer case results in a mean power reduction of 14 kW or 5% of the installed heating capacity. Similar reductions are obtained in the standard deviation (SD) of power usage, which illustrates the R744 system operational fluctuations. The SD for power usage is reduced significantly for both the nominal and summer cases. Additionally, a reduction in total electricity usage can be observed in all cases.

The electricity usage at high loads are listed in Table 6 and is defined as the amount of supplied electric energy [kWh] at values above the mean weekly power usage [kW] for that specific week. A noticeable reduction in electricity usage at high loads can be observed in comparison to the respective baseline scenarios. Thus, the benefits of the LLC strategy are considerable in terms of stabilizing the operation of the thermal system. To evaluate the reduction in peak power usage, the maximum power peak every 24-h was recovered and averaged for all cases, as illustrated by Fig. 8. The largest peak power reduction is achieved during summer operations, where a 32.5% reduction is gained. For the nominal and winter cases, peak power reductions of 14.3 and 21.2% were achieved. Based on the results in Table 5 and Table 6, it can be concluded that operational fluctuations are decreased when applying the LLC strategy, as a result of reduced peak power utilization and on/off cycles. Excessive power usage represents a significant operational expense due to peak power tariffs established by the power companies, as reported by Chua et al. [3]. Implementing an LLC strategy that aims to reduce peak power usage will have positive consequences beyond increased energy savings. Meeting the increasing power demand is a large challenge for power networks and suppliers. It is necessary to apply demand-side management of power utilization to ensure successful implementation of smart grids technology [14]. A heat pump system with thermal storage offers a high degree of operational freedom, which can reduce electricity peak usage and decoupling electricity consumption from heat demand. Applying an LLC strategy that aims to reduce power usage, therefore, offers benefits beyond reduced operational costs.

5. Conclusions

Heat pump and refrigeration systems with low global warming potential refrigerants are unarguably necessary to reduce global warming and to reach the 2-degree goal of the Paris Agreement. Thus, new areas of application for natural refrigerants must be identified, such as integrated R744 systems in hotels. The findings in this paper can be applied to improve system performance in current and future installations of R744 integrated systems in hotel buildings.

The thermal storage enables a high degree of operational freedom for heating and cooling systems. Utilizing the buffer capability that the storage provides, by applying a low load thermal storage charging strategy, can highly influence overall system performance. The following conclusions can be made based on the numerical investigations of the charging strategy.

- Low load charging of the DHW storage for longer periods of time has a positive influence on heat pump SCOP at low ambient temperatures, eg. spring, fall, and winter. However, the heat pump SCOP, $SCOP_{HP}$, is reduced in the summer case due to high return temperatures from secondary systems. Thus, the low load charging strategy is more applicable in cold-climate conditions in terms of $SCOP_{HP}$. Yet, the total thermal system performance, $SCOP_{tot}$, is improved for all representative scenarios. The largest improvement of $SCOP_{tot}$ is

Table 6
Comparison of electricity and power usage of R744 unit with the LLC strategy.

Case name/Variable		Nominal		Winter		Summer	
		Baseline	LLC strategy	Baseline	LLC strategy	Baseline	LLC strategy
Mean power usage	[kW]	45.0	39.3	68.9	63.7	39.0	24.8
SD power usage	[kW]	22.3	12.7	25.8	16.9	23.6	11.4
Total electrical usage	[kWh]	6982	6577	11573	10706	4726	3890
Electricity usage at high loads	[kWh]	1665	906	1825	1191	1742	804
Peak power*	[kW]	79.0	67.7	118.3	90.9	75.3	50.8
Peak power reduction	[%]	-	14.3	-	23.2	-	32.5

* Maximum peak power is recorded over 24 h and averaged over one week.

achieved in the summer case, where a 22.6% increase is gained when applying the low load charging strategy.

- Energy savings in the range of 5.8–13.2% are achieved when applying the low load charging strategy to the different seasonal scenarios. The application of the back-up boiler is reduced as the R744 system is operating for longer periods of time. An annual energy savings of 8.4% can be obtained by applying the low load charging strategy.
- Peak power usage is reduced within the range of 14.3–32.5% in the different scenarios when applying the new charging strategy. Though not evaluated in this paper, the decrease in peak power usage represents a considerable reduction in operational costs. System fluctuations are reduced with the new charging strategy due to limited ON/OFF cycles and high loads operations of the R744 unit. Thus, the benefits of charging at low loads are considerable in terms of stabilizing the operation of the thermal system.

CRediT authorship contribution statement

S. Smitt: Conceptualization, Investigation, Software, Writing - original draft, Writing - review & editing, Visualization. **I. Tolstorebrov:** Conceptualization, Writing - review & editing, Supervision. **A. Hafner:** Conceptualization, Supervision.

Declaration of Competing Interest

The authors declare that they have no known competing financial interests or personal relationships that could have appeared to influence the work reported in this paper.

Acknowledgments

The authors would like to acknowledge the Norwegian Research Council for funding this project. We would also like to thank Scandic Hotel Hell for access to their system data.

References

[1] L. Cecchinato, M. Corradi, E. Fornasieri, L. Zamboni, Carbon dioxide as refrigerant for tap water heat pumps: a comparison with the traditional solution, Int. J. Refrig. 28 (2005) 1250–1258.
[2] T. Chai, R.R. Draxler, Root mean square error (RMSE) or mean absolute error (MAE)?–arguments against avoiding RMSE in the literature, Geosci. Model Dev. 7 (2014) 1247–1250.
[3] K.H. Chua, Y.S. Lim, S. Morris, Energy storage system for peak shaving, Int. J. Energy Sect. Manage. (2016).
[4] R. Ciconkov, Refrigerants: there is still no vision for sustainable solutions, Int. J. Refrig. 86 (2018) 441–448.
[5] G. Cortella, P. D'Agaro, O. Saro, A. Polzot, Modelling integrated HVAC and refrigeration systems in a supermarket, in: Proc. 3rd IIR International Conference on Sustainability and the Cold Chain, Twickenham, London, UK, 2014.
[6] P. D'Agaro, M. Coppola, G. Cortella, Field tests, model validation and performance of a CO_2 commercial refrigeration plant integrated with HVAC system, Int. J. Refrig. 100 (2019) 380–391.
[7] G. Dalton, D. Lockington, T. Baldock, Feasibility analysis of stand-alone renewable energy supply options for a large hotel, Renew. Energy 33 (2008) 1475–1490.
[8] Dassault Systems, 2019. DYMOLA Systems Engineering: Multi-Engineering Modeling and Simulation based on Modelica and FMI. URL:https://www.3ds.com/products-services/catia/products/dymola/.
[9] M. Despotovic, V. Nedic, D. Despotovic, S. Cvetanovic, Evaluation of empirical models for predicting monthly mean horizontal diffuse solar radiation, Renew. Sustain. Energy Rev. 56 (2016) 246–260.
[10] A.T. Diaby, P. Byrne, T. Maré, Simulation of heat pumps for simultaneous heating and cooling using co_2, Int. J. Refrig. 106 (2019) 616–627.
[11] European Commission (EC), 2016. An EU Strategy on Heating and Cooling, COM 51 Final. Brussels, Belgium, 2016: URL:https://ec.europa.eu/energy/sites/ener/files/documents/1_EN_ACT_part1_v14.pdf.
[12] European Committee for Standardization, 2016. EN 378-1:2016 Refrigerating systems and heat pumps – safety and environmental requirements – Part 1: basic requirements, definitions, classification and selection criteria.
[13] E. Fabrizio, F. Seguro, M. Filippi, Integrated HVAC and DHW production systems for Zero Energy Buildings, Renew. Sustain. Energy Rev. 40 (2014) 515–541.
[14] X. Fang, S. Misra, G. Xue, D. Yang, Smart grid–the new and improved power grid: a survey, IEEE Commun. Surveys Tutor. 14 (2011) 944–980.
[15] S. Girotto, G. Tosato, Improvements on water & brine chiller for air conditioning & process cooling, Testing on water chiller within the Multipack project., in: Proceedings ATMOsphere/Danish Technological Institute Online Conference: The Future of Air Conditioning. 23–24 June, Online platform, 2020.
[16] P. Gullo, B. Elmegaard, G. Cortella, Advanced exergy analysis of a R744 booster refrigeration system with parallel compression, Energy 107 (2016) 562–571.
[17] P. Gullo, A. Hafner, K. Banasiak, Transcritical R744 refrigeration systems for supermarket applications: Current status and future perspectives, Int. J. Refrig. 93 (2018) 269–310.
[18] E.A. Heath, Amendment to the Montreal protocol on substances that deplete the ozone layer (Kigali amendment), Int. Legal Mater. 56 (2017) 193–205.
[19] IWMAC, 2019. Centralized Operation and Surveillance by Use of WEB Technology. URL:https://www.iwmac.com/.
[20] M.H. Kim, J. Pettersen, C.W. Bullard, Fundamental process and system design issues in CO_2 vapor compression systems, Prog. Energy Combust. Sci. 30 (2004) 119–174.
[21] B. Langseth, Analysis of energy consumption in commercial buildings (Analyse av energibruk i yrkesbygg). Technical Report. NVE, 2015.
[22] G. Lorentzen, The use of natural refrigerants: a complete solution to the CFC/HCFC predicament, Int. J. Refrig. 18 (1995) 190–197.
[23] H. Martin, N6 pressure drop and heat transfer in plate heat exchangers, in: VDI Heat Atlas, 2010.
[24] S. Minetto, Theoretical and experimental analysis of a CO_2 heat pump for domestic hot water, Int. J. Refrig. 34 (2011) 742–751.
[25] P. Nekså, CO_2 heat pump systems, Int. J. Refrig. 25 (2002) 421–427.
[26] Norwegian Ministry of Environment, 2008. Norwegian climate policy – Summary in English: Report No. 34 (2006–2007) to the Storting). Technical Report.
[27] Á.Á. Pardiñas, A. Hafner, K. Banasiak, Novel integrated CO_2 vapour compression racks for supermarkets. Thermodynamic analysis of possible system configurations and influence of operational conditions, Appl. Therm. Eng. 131 (2018) 1008–1025.
[28] I. Peñarrocha, R. Llopis, L. Tárrega, D. Sánchez, R. Cabello, A new approach to optimize the energy efficiency of CO_2 transcritical refrigeration plants, Appl. Therm. Eng. 67 (2014) 137–146.
[29] L. Pérez-Lombard, J. Ortiz, C. Pout, A review on buildings energy consumption information, Energy Build. 40 (2008) 394–398.
[30] A. Polzot, P. D'Agaro, P. Gullo, G. Cortella, Modelling commercial refrigeration systems coupled with water storage to improve energy efficiency and perform heat recovery, Int. J. Refrig. 69 (2016) 313–323.
[31] D. Rohde, T. Andresen, N. Nord, Analysis of an integrated heating and cooling system for a building complex with focus on long–term thermal storage, Appl. Therm. Eng. 145 (2018) 791–803.
[32] A.A. Safa, A.S. Fung, R. Kumar, Performance of two-stage variable capacity air source heat pump: field performance results and trnsys simulation, Energy Build. 94 (2015) 80–90.
[33] Shecco, 2020. World Guide to Transcritical CO_2 Refrigeration (Part II). Technical Report. Shecco Base, June 18th, 2020.
[34] S. Smitt, A. Hafner, E. Hoksrød, Presentation of the first combined CO_2 heat pump, air conditioning and hot tap water system for a hotel in Scandinavia, in: Proceedings of the 8th Conference on Ammonia and CO_2 Refrigeration Technologies, 11–13 April 2019. Ohrid, Republic of Macedonia, 2019.

[35] S. Smitt, I. Tolstorebrov, A. Hafner, Integrated CO_2 system with HVAC and hot water for hotels: field measurements and performance evaluation, Int. J. Refrig. 116 (2020) 59–69.
[36] M. Steffen, A simple method for monotonic interpolation in one dimension, Astron. Astrophys. 239 (1990) 443.
[37] J. Stene, Residential CO_2 heat pump system for combined space heating and hot water heating, Int. J. Refrig. 28 (2005) 1259–1265.
[38] M. Tammaro, A. Mauro, C. Montagud, J. Corberán, R. Mastrullo, Hot sanitary water production with CO_2 heat pumps: Effect of control strategy on system performance and stratification inside the storage tank, Appl. Therm. Eng. 101 (2016) 730–740.
[39] TLK-Thermo GmbH, 2020a. TIL Suite – Simulates thermal systems. URL:https://www.tlk-thermo.com/index.php/en/software/til-suite.
[40] TLK-Thermo GmbH, 2020b. TILMedia Suite – Software package for calculating the properties of thermophysical substances. URL:https://www.tlk-thermo.com/index.php/en/software/tilmedia-suite.
[41] T. Tokle, J. Tønnesen, Inndeling av Norge i klimasoner (Division of Norway into climate zones), SINTEF Energi AS (1999).
[42] G. Tosato, S. Girotto, S. Minetto, A. Rossetti, S. Marinetti, An integrated CO_2 unit for heating, cooling and DHW installed in a hotel. Data from the field, in: 37th UIT Heat Transfer Conference.
[43] W. Wagner, Strömung und Druckverlust, Vogel, 2008.
[44] L. Yang, H. Li, S.W. Cai, L.L. Shao, C.L. Zhang, Minimizing COP loss from optimal high pressure correlation for transcritical CO_2 cycle, Appl. Therm. Eng. 89 (2015) 656–662.
[45] W.J. Zhang, C.L. Zhang, A correlation-free on-line optimal control method of heat rejection pressures in CO_2 transcritical systems, Int. J. Refrig. 34 (2011) 844–850.

Article IV

S. Smitt, Á. Pardiñas, A. Hafner (2021). "Evaluation of integrated concepts with CO_2 for heating, cooling and hot water production." In: *Energies* 14 (14), 4103. DOI: https://doi.org/10.3390/en14144103

energies

MDPI

Article

Evaluation of Integrated Concepts with CO_2 for Heating, Cooling and Hot Water Production

Silje Smitt [1,*], Ángel Pardiñas [2] and Armin Hafner [1]

[1] Department of Energy and Process Engineering, Norwegian University of Science and Technology, Kolbjørn Hejes vei 1D, 7491 Trondheim, Norway; armin.hafner@ntnu.no
[2] SINTEF Energy Research, Kolbjørn Hejes vei 1D, 7465 Trondheim, Norway; angel.a.pardinas@sintef.no
* Correspondence: silje.smitt@ntnu.no

Abstract: The hotel sector is characterized by high thermal demands and a large carbon footprint, which greatly contributes to the global warming effect. Consequently, there is a need to investigate solutions that can reduce energy usage within this sector by means of environmentally friendly and sustainable technologies. Integrated CO_2 heat pump systems for heating, cooling, and hot water production in hotels have demonstrated promising results. This paper theoretically compares the energy consumption, environmental impact, and cost of three different design concepts for integrated CO_2 units equipped with thermal storage. The main characteristics of the evaluated designs are single-stage compression, parallel compression, and ejector-supported parallel compression. Furthermore, two separate hot water charging strategies were implemented and investigated over a large span of ambient temperatures and loads. The evaluations were carried out by considering eight different European locations, ranging from Scandinavia to the Mediterranean. The results revealed that the ejector-supported parallel compression design was superior in terms of annual COP, which was found to be in the range of 4.27 to 5.01 for the Scandinavian locations and 5.03 to 5.71 for the other European locations. When accounting for investment cost and electricity prices, the payback period at the Scandinavian locations was 6.3 to 7.7 years. Payback periods of 3 and 4.5 to 7.5 were obtained for hotels located in the temperate and Mediterranean climates, respectively. The investigation also revealed that the hot water charging strategy, rather than the specific CO_2 heat pump design, is the least expensive measure to enhance performance.

Keywords: heat pump; system design; heating and cooling; hotels; CO_2; thermal storage; numerical modeling; concept evaluation

Citation: Smitt, S.; Pardiñas, A.; Hafner, A. Evaluation of Integrated Concepts with CO_2 for Heating, Cooling and Hot Water Production. *Energies* **2021**, *14*, 4103. https://doi.org/10.3390/en14144103

Academic Editor: Dimitris Katsaprakakis

Received: 11 June 2021
Accepted: 30 June 2021
Published: 7 July 2021

1. Introduction

Different actors are involved in a global and intersectoral effort to achieve the 2-degree goal of the Paris Agreement by limiting CO_2 emissions through efficiency and reduction of energy demands [1]. Energy use in buildings involves approximately 18% of greenhouse gas emissions globally. A staggering one-third of these emissions are linked to commercial buildings, such as hotels [2]. Similar numbers are given for Europe, with the commercial sector being responsible for one-third of the total energy consumption and related emissions in buildings [3]. Thus, measures to increase efficiency by improved technology, management, and integration of demands in the hotel sector will significantly contribute towards realizing the goals of the Paris Agreement. Estimations indicate a potential in energy saving within the commercial sector of approximately 30% [4,5]. This is particularly important as the tourism sector is estimated to increase by 3.8% annually until 2030 [6].

The dominant thermal demands in hotels include domestic hot water (DHW) production, space heating (SH), and cooling, with the share between them depending on hotel location or quality of construction (level of insulation), among other factors. For SH and

DHW, Nordic hotels have been utilizing conventional thermal energy sources, e.g., electric boilers with inefficient central systems [7], justified by relatively low electricity prices. Within Europe in general, fossil fuel-fired boilers still represent the most applied heating source [5]. In the past decade, district heating and cooling networks have gained solid footing and are becoming important in Scandinavia [8,9]. Yet, separate chillers, i.e., vapor compression units, are generally utilized to fulfill the cooling demands in hotels, even if access to the district cooling network exists at the location. Heat pumps appear as a suitable alternative to meet all the different demands with a single unit while boosting energy efficiency and reducing operational costs. This is achieved through their principle of operation of upgrading heat from one temperature level to another with a considerably low input of work, namely, electricity. Furthermore, a recent five-year study of hotels in Nordic countries has shown that the specific energy consumption in hotels with heat pumps as the primary heat source is lowest compared to those using alternative systems, such as electric boilers or district heating [10].

Heat pumps are vapor compression systems that transfer heat from a heat source at relatively low temperature, e.g., air, water, ground, or chilling water loop, to a heat sink at a higher temperature, such as a SH circuit or hot water tanks. Heat is transferred through a fluid, i.e., refrigerant, which is circulated and adapted to the required temperature levels by means of work input to a compressor. Refrigerant selection has been a hot topic in the last decades, mainly as the historically favored synthetic refrigerants are, or have been, responsible for significant environmental consequences, either destruction of the ozone layer by CFCs (chlorofluorocarbons) and HCFCs (hydrochlorofluorocarbons) or global warming by HFCs (hydrofluorocrbons). Natural refrigerants, such as ammonia, CO_2, and hydrocarbons, are widely utilized in different applications and have the potential to replace synthetic refrigerants in heat pumps and chillers. The natural refrigerants were among the first utilized in vapor compression systems and have negligible impact on the environment, but can introduce challenges in terms of toxicity, operation at high pressure, or flammability [11]. Natural refrigerants are competing for the niche of heat pumps with the newly developed HFOs (hydrofluoroolefins), which fulfill the requirements of low global warming potential (GWP) dictated by several national or international regulations, e.g., F-gas in Europe. However, recent studies and reports have raised concerns regarding the HFO's decomposition product trifluoroacetic acid (TFA). Widespread and long-term application of HFOs can result in TFA accumulating in drinking water, which can have severe effects on human health and the environment [12]. In addition, a newly published report demonstrates that one of the most applied HFOs (HFO-1234ze) in current use ultimately decomposes partially into the refrigerant R23; one of the most potent greenhouse gases known (100-year GWP of 14,800) [13]. Although a recent study predicts that HFOs, HFCs and their mixtures will still have a significant market share as far as 2030 [14], it could be agreed that natural refrigerants are the long-term solution, and among them CO_2 (GWP = 1) appears as a safe and sustainable choice for commercial heat pumps, e.g., for hotels. CO_2 has had a success story in commercial refrigeration (centralized units, condensing units, and plugins). Now, CO_2 is becoming a competing alternative in other sectors, such as industrial refrigeration, due to factors like increased efficiency and component size, reductions in operational costs (economy of scale), and legislation [15].

Due to its low critical temperature (31 °C), CO_2 applications were initially limited to operations where heat rejection (condenser) would happen well below the critical point, such as freezing in cascade refrigeration units. The implementation of CO_2 in heat pumps and commercial refrigeration, which can operate with heat rejection or production above CO_2's critical temperature, was realized thanks to the investigations of Gustav Lorentzen and his team. Lorentzen (1994) [16] presented the basic layout of a transcritical CO_2 heat pump, based on a system with suction accumulator, high-pressure control through the valve feeding the evaporator, and the application of a gas cooler in place of the condenser. At the time, this unit was suggested as an efficient and environmentally friendly replacement of R12 in mobile air conditioning (AC) [17]. Nekså et al. (1998) [18] stated that transcritical

CO_2 heat pumps are suitable to produce DHW, as the temperature glide in the refrigerant side of the gas cooler follows nearly perfectly the relatively large temperature difference in the waterside, reaching up to 90 °C. Additionally, Nekså (2002) [19] mentioned other applications for CO_2 heat pumps that, with the course of years, were realized, e.g., SH and residential heat pumps and heat pump dryers. Stene (2005) [20] investigated the efficient integration of SH and DHW to maximize the use of the gliding heat rejection of CO_2 heat pumps. The concept is based on splitting the gas cooler into three parts connected in series: the warmest and coldest parts to reheat and preheat DHW, and the intermediate part to produce SH. Thus, it is possible to minimize CO_2 temperature downstream of the gas cooler, reducing expansion losses and improving the performance. Tosato et al. (2020) [21] performed an experimental and numerical investigation of a newly developed CO_2 air/water reversible heat pump, intended for household applications. The system was evaluated at a range of ambient temperatures (−2.0 to 11.2 °C), and at DHW setpoint temperatures ranging from 60 to 80 °C. The results illustrated that the highest COP was achieved at DHW setpoint temperature of 60 °C, due to an increase in DHW mass flow rate through the gas cooler. However, charging time was significantly reduced in comparison to when setpoints of 70 and 80 °C were applied. Dai et al. (2019) [22] suggested using mechanical subcooling in CO_2 transcritical heat pump cycle to reduce the gas cooler outlet temperature. They found that the primary energy consumption was reduced compared to a conventional transcritical single-stage CO_2 heat pump, which resulted in additional reductions in emissions of around 16%. Emissions were reduced by approximately 18–33% and 62–69% compared to a coal-fired boiler and direct electric heating, respectively.

Another measure to increase the system efficiency of CO_2 heat pumps is simultaneous production of DHW and cooling. Byrne et al. (2009) [23] investigated a CO_2 heat pump layout for simultaneous production of heating and cooling aimed at hotels, luxury dwellings, or smaller office buildings. The system design is based on a division of the gas cooler into three parts: a DHW heat exchanger, a SH heat exchanger, and a subcooler that heats water to defrost a backup air evaporator. This air evaporator is necessary to balance the system when the space cooling demand is an insufficient heat source to achieve the heating demand. The authors performed a numerical study to compare this heat pump architecture operating with CO_2 and with R407C, and observed that CO_2 can outperform the HFC in terms of environmental impact. Diaby et al. (2019) [24] is a continuation of the previous work, as the authors present heat pump models for either simultaneous cooling, SH, and DHW or desalination. The numerical results in both cases are satisfactory, and the authors conclude that CO_2 is an exceptionally suited refrigerant for multipurpose heat pumps compared to "standard" refrigerants. This statement is supported by the conclusions in the study from Liu et al. (2016) [25], where the purpose of the heat pumps would be cooling and heating processes in food processing industries. An experimental study of combined AC and DHW production with a CO_2 heat pump is introduced in Adriansyah (2004) [26]. The results revealed a combined (heating and cooling) coefficient of performance (COP) as high as 8 when all the heat available in the gas cooler can be recovered. Farsi et al. (2016) [27] delved into the use of heat pumps for combined cooling and desalination, and the authors indicate the potential of CO_2 to improve desalination. Moreover, energy savings are maximized and the total annual cost is reduced when compared to separate systems (CO_2 refrigeration system and a desalination unit using steam from a boiler run with methane). Singh et al. (2020) [28] presented numerical simulations of a planned installations of a 140 kW transcritical CO_2 heat pump for a centralized kitchen in Bangalore, India. The heat pump will preheat hot water to 90 °C for steam production while supplying AC cooling for the entire building and utilizing thermal storage to compensate for asynchronous thermal demands. Simulations illustrated that the system can achieve a COP above 6 when operating in combined heating and cooling mode. The total energy consumption is expected to be reduced by 33% compared to the current solution, which will reduce yearly $CO_{2\text{-eq}}$ emissions by about 300 tonnes.

CO_2 heat pumps are increasing their presence in the portfolio of different manufacturers in Europe, in some cases adapting existing compressor packs for commercial refrigeration. An example of this is shown in Smitt et al. (2020) [29], with a performance analysis based on field measurements of a CO_2 heat pump for integrated production of heating and cooling with a 6 m^3 thermal storage. The study evaluates how different demands change during the specific year and how they affect the different performance indicators. One of the main conclusions of this study is that COPs improve with DHW charging (compared to SH only), meaning that DHW charging strategy is crucial to boost efficiency. A later numerical study of the same system demonstrated how the energy savings could be reduced with 5.8–13.2% for different seasonal scenarios when charging the DHW storage at low loads [30]. Additional perks of applying the low load charging strategy were reduced peak power usage, operational fluctuations, and ON/OFF cycles.

A dedicated and more complex CO_2 heat pump architecture is introduced in Tosato et al. (2020) [31], including two-stage evaporation supported by ejector (heat source or AC production, depending on operation mode). Results from a limited period in winter are presented, indicating a good efficiency with DHW production and the benefit of developing control strategies to minimize start and stops. The potential of evaporation in two stages was not fully evaluated with the available data in Tosato et al. (2020) [31]. The first results in summer mode for the aforementioned CO_2 heat pump were presented in Hafner et al. (2020) [32], showing COPs around 5 when producing chilled water at 7 °C (from 11 °C) and DHW at 60 °C (from 30 °C). The authors concluded that the potential of two-stage evaporation with an ejector could not be fully utilized unless higher waterside temperature differences are allowed in the evaporators.

In contrast to most of the previous articles and references, which analyzed or introduced rather simple layouts for CO_2 heat pumps, this work presents sophisticated architectures applicable for hotels, which are evaluated numerically with transient models. These systems include ejectors, parallel compression, and combined air-to-CO_2 evaporators/gas coolers, which can be applied as either heat source or sink. Load profiles are established based on previous analysis of a medium-sized hotel, and the performance is determined for each heat pump architecture and according to the climate of different cities in Scandinavia. Additional locations in Central Europe and the Mediterranean are included to evaluate the feasibility of such installations in warmer climates. Two separate DHW charging strategies are implemented to evaluate the influence of charging strategy in comparison to design with respect to performance. The sustainability of each design is investigated in terms of annual global warming contribution at each location. An economic evaluation is included to discuss whether these CO_2 heat pumps are cost-efficient compared to more conventional approaches, including electric boilers and separate chillers for AC cooling applications.

2. System Description

The approach of the integrated solution with CO_2 is to use a single unit with a flexible design to supply SH, DHW, and AC within the building. The simplified schematic of an integrated CO_2 unit with a standard single-stage compression (SC) is shown in Figure 1. The main system components are four compressors, a gas cooler section for heat production, AC evaporators, an intermediate temperature (INT) liquid receiver, and four air evaporators that can be employed as gas coolers for heat rejection when surplus heat is produced. The integrated unit is dimensioned to operate in the Scandinavian ambient-temperature range, from −15 to 35 °C. In addition to SC integrated system design, which is described in Section 2.1, two alternative system configurations are presented in Section 2.2 to investigate measures that can enhance efficiency. Note that ambient air has been selected as the main heat source for all configurations. Superior heat sources, such as seawater and boreholes, could be applied in place of ambient air. However, alternative heat sources are highly dependent on the building's specific location and would not be applicable everywhere. As a result, air heat exchangers are applied in all system configurations.

2.1. Design and Operation

Figure 1 illustrates the SC integrated CO_2 unit. The evaporation level consists of four ambient air fin-and-tube evaporators and two glycol AC heat exchangers, which function to supply the heating and cooling load, respectively. Simultaneous operation with both air and glycol evaporators is limited, as SH and AC cooling loads are rarely concurrent. The cooling demand of the building is realized by employing the plate evaporators, $EVAP_{AC,1}$ and $EVAP_{AC,2}$ in Figure 1, which supply chilled glycol to the AC units in the building. Each evaporator's thermostatic expansion valve controls the mass flow of CO_2 according to the superheat at the exit of the respective unit. The mass flow of glycol is controlled to achieve the AC setpoint temperature.

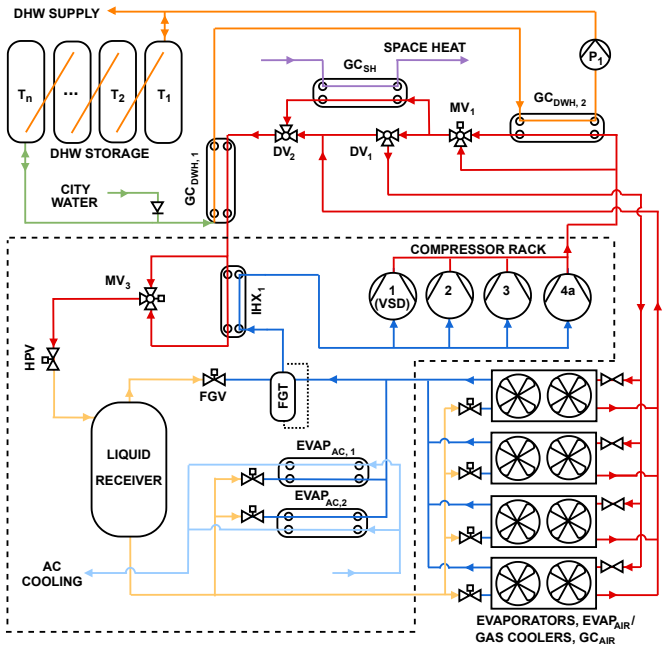

Figure 1. Simplified representation of the standard integrated CO_2 concept, equipped with single-stage compression (SC). High-pressure lines are indicated in red, intermediate pressure lines in yellow, and low-pressure lines in dark blue.

The fin-and-tube heat exchangers are exclusively connected to either the high-pressure side (red line) for gas coolers operation or the low-pressure line (dark blue) for evaporation at low temperature (LT). The distribution lines through the heat exchangers are switched between the different pressure levels, dependent on the mode of operation. Traditionally, a design selection with separate evaporators and gas coolers is preferred for simplicity and heat transfer considerations. However, due to advances within heat exchanger development and operation, several suppliers offer combined units to reduce the investment cost. The air heat exchangers are employed according to the heating demand of the building when operating in evaporator mode. Airflow through the evaporators is controlled by fans equipped with high-efficiency brushless DC motors. The CO_2 evaporation pressure is controlled by the thermostatic expansion valves, which secure a superheat at the exit of each evaporation unit. The superheat is fixed to a minimum, such that enhanced heat transfer is achieved in the heat exchangers. The suction accumulator and the internal heat exchanger, FGT and IHX_1 in Figure 1, respectively, ensure no liquid carryover to the compressors.

The CO_2 compressors remove vapor from the evaporator pressure level and discharge it to the gas coolers at high pressure. The compressor rack consists of four parallel piston compressors, in which compressor 1 in Figure 1 is equipped with a variable speed drive (VSD). Compressors 2 to 4 operate at a fixed speed and are controlled by ON/OFF, while the VSD compressor continuously adjusts the compressor section capacity according to demand. Thus, a broad range of capacities can be achieved by employing the VSD compressor alongside various combinations of the fixed compressors. The number of active compressors is determined based on the magnitude and combination of thermal demands; typically, high SH and DHW demands at low ambient temperatures and high AC cooling demands at high ambient temperatures.

The CO_2 gas cooler section is applied for heat recovery to SH and DHW, heat rejection to the ambient, or as a combination of the aforementioned. When heat rejection to the ambient is required, the directional valve, DV_1, directs the flow towards the air-cooled gas coolers, GC_{air}. The gas cooler section producing SH, GC_{SH}, are in these instances bypassed. The number of gas cooler units employed is determined based on the AC cooling and the DHW demand.

The main CO_2 gas cooler section consists of three plate heat exchangers that supply heat for DHW and SH. The temperature span of each heat exchanger is arranged according to the transcritical temperature glide of CO_2 [20]. Preheating of the DHW takes place at the lower end of the CO_2 temperature glide, in $GC_{DHW,1}$, as cold city water enters the heat exchanger. The DHW is further reheated to its setpoint temperature in $GC_{DHW,2}$. The modulating valve, MV_1, continuously controls the flow of CO_2 through $GC_{DHW,2}$ to reach the DHW setpoint temperature. Thus, the load distribution between $GC_{DHW,1}$ and $GC_{DHW,2}$ automatically adjust according to the load and temperature profile of the mid heat exchanger, GC_{SH}. For instance, the majority of the DHW load is rejected through $GC_{DHW,1}$ when the SH demand and setpoint temperature are high. During operations with low SH demand, most of the DHW load is rejected through $GC_{DHW,2}$. This configuration enables continuous low load production of DHW, which in turn reduces gas cooler outlet temperature and enhances overall system COP [30]. The requested DHW heating load is determined based on the energy reserve in the DHW storage, constituted by the temperature and volume in the storage tanks.

The storage, which is shown in Figure 1, has a water volume of 6 m^3 and is comprised of hot water tanks connected in series. The energy reserve is calculated based on the temperature boundary across the storage. At times when the temperature in the storage is low, a signal is sent to the DHW pump, P_1, to increase the mass flow and thus DHW charging load. DHW enters the first tank in the series, T_1, and the hot water boundary gradually moves across the storage from right to left during charging. Cold water is supplied from city water or drawn from the last tank, T_n, and is directed towards preheating. The storage is fully charged when the last tank in the series, T_n, reaches a high and uniform temperature.

The control of the high pressure is achieved with the high-pressure valve (HPV) in Figure 1. The integrated unit typically operates in the transcritical region (above 73.8 bar) to ensure the DHW setpoint temperature is reached. The maximum operating pressure of the system is 105 bar. After expansion, liquid enters the receiver, which holds a pressure between 36 to 50 bar. The receiver pressure is controlled by the flash gas valve, FGV, and is regulated according to evaporating pressure. During operations with low ambient temperature and high heating loads, receiver pressure is reduced to limit the vapor fraction at the inlet of the evaporators.

2.2. Alternative System Configurations

Two alternative system designs are presented in Figure 2. Both configurations, (a) parallel compression (PC) and (b) ejector-supported parallel compression (EJ), introduce compression from the liquid receiver at INT pressure level. Compressors 2 and 3 are equipped with pivoting suction ports, which directions are controlled by DV_3 and DV_4,

respectively. The pivoting suction port of the particular compressor refers to the possibility of selecting the suction manifold connection and integrating it in either the LT section or the INT parallel section. Thus, flexibility is significantly enhanced as the integrated system can swiftly adapt the number of compressors assigned to a particular suction group [33]. Both pivoting compressors work in support of the LT base compressor at low ambient temperature and high SH loads. During operational conditions with high ambient temperatures and dominant AC cooling loads, the pivoting compressors are employed at the INT level. Thus, the number of compressors employed at each pressure level is adjusted to meet both heating and cooling loads without the need for additional compressors.

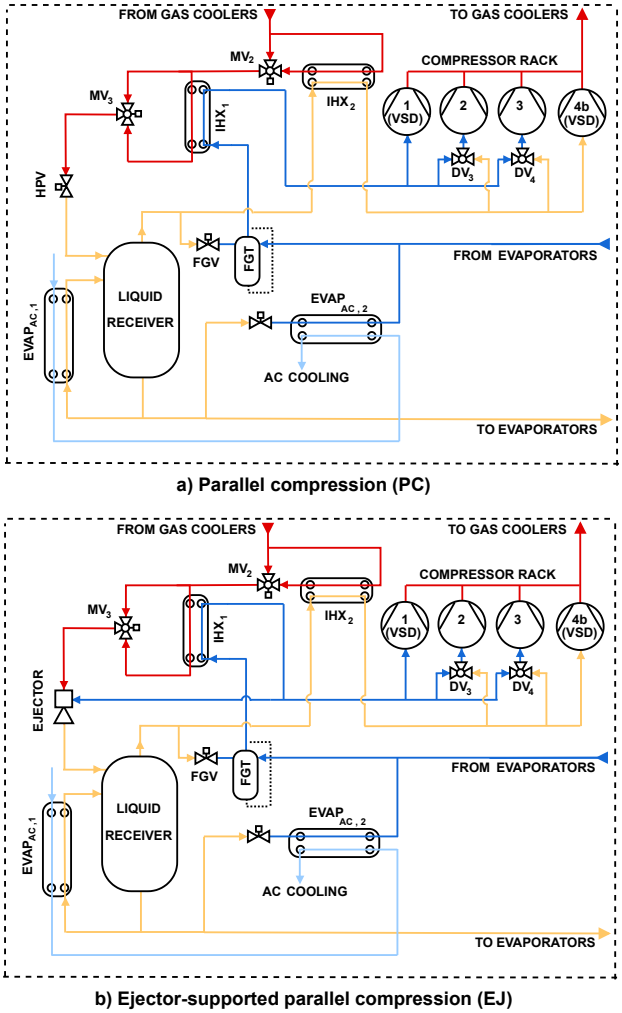

Figure 2. Alternative design of CO_2 integrated system with (**a**) parallel compression (PC), and (**b**) ejector-supported parallel compression (EJ).

Both configurations presented in Figure 2 are equipped with two AC evaporators, which are applied to provide cooling in series at different pressure levels. $EVAP_{AC,1}$ is installed at the INT pressure level and relies on gravity self-circulation from the liquid receiver. The evaporator is installed below the liquid receiver and is fed through a liquid column from the bottom of the receiver, creating a static pressure difference. The cooling load is determined based on the chilled water mass flow rate and the INT pressure level.

The parallel compressor section controls the latter in order to meet the total cooling demand from the building. $EVAP_{AC,2}$ is installed at the LT evaporation level and ensures cooling of the chilled water to setpoint conditions.

The HPV in Figure 2a is replaced by a ejector block in Figure 2b. The ejector is connected to the high-pressure side and recovers the expansion work in the high-pressure stream to lift the pressure of refrigerant from the LT pressure level. The vapor ejector operates in parallel to the LT compressors and is installed downstream of IHX_1, and so provides a dual benefit. First, it ensures a high value of superheat at the suction port of both the ejector and the compressor, which allows the evaporators to operate with a low superheat. Second, additional cooling downstream of the gas cooler is provided to reduce expansion losses. Typically, applications of ejectors demonstrate the largest benefits when the gas cooler outlet temperature is elevated. Such a scenario transpires in both winter and summer when either SH or AC cooling loads are high and DHW demands are low.

2.3. Operational Modes

The system designs have been established to provide flexibility and a high degree of operational freedom independent of the specific mode of operation, e.g., summer and winter.

2.3.1. Winter Mode

The air evaporators shown in Figure 1, $EVAP_{air}$, are employed based on SH demand. Vapor is sucked from $EVAP_{air}$ through IHX_1 by the LT base compressors. The compressor capacity is mainly controlled by the SH demand, as additional heat for DHW is continuously recovered as a byproduct if needed. Neither of the AC cooling evaporators is active during winter mode. For the the system solutions shown in Figure 2, parallel compressors are employed to remove flash gas from the system and control the pressure of the liquid receiver. The number of compressors employed at LT and INT pressure levels is determined based on heating demand. Vapor from the liquid receiver is superheated in IHX_2 before compression. The ejector in Figure 2b introduces expansion work recovery from the high pressure level. Thus, a portion of the required compressor capacity is moved from the LT section to the INT section, reducing the total work of the system.

2.3.2. Summer Mode

The base compressor capacity is controlled by the cooling load, as the LT pressure is regulated to meet the requested AC cooling demand of the building. The mass flow rate of chilled water is controlled to meet the setpoint at the outlet of the AC evaporators. For the AC-chiller arrangements presented in Figure 2, two separate pressure levels are used to chill down the liquid. After the first stage of cooling, chilled water from $EVAP_{AC,1}$ is directed to the second AC evaporator, $EVAP_{AC,2}$, for further cooling until the setpoint is reached. $EVAP_{AC,2}$ is installed in parallel to the air evaporators, which are generally not employed during summer mode. The pressure of $EVAP_{AC,2}$ is controlled by the LT base compression block, which during cooling mode operates 4 to 6 bar below the INT level. The parallel compressor(s) will increase capacity and thus reduce INT pressure if additional cooling is needed. Simultaneously, the AC chilled water pumps will increase the mass flow rate through the heat exchangers. In the case of the ejector-supported system displayed in Figure 2b, a large portion of the CO_2 is lifted from LT to the INT pressure level.

The DHW storage functions as the only useful heat sink to the system during summer mode, as SH demand is lacking during high ambient temperature operations. If removal of excess heat is needed, DV_1 directs the flow towards GC_{air} for rejection towards the ambient air.

3. Methodology

3.1. Numerical Model

Detailed models of the thermal systems were created in the object-oriented programming language Modelica. The programming environment Dymola 2018 was applied to

simulate the models. The standard solver, DASSL, was used for the investigations [34]. Construction of the models was achieved by using components from the commercially available thermodynamic library TIL-Suite 3.9, developed by TLK-Thermo GmbH [35]. The TIL-Media 3.9 library was applied for the simulation of the fluids used in the models, which includes CO_2, water, propylene glycol (30% mass fraction), and air with an assumed relative humidity of 60% [36]. The TIL extensions are advanced libraries for transient simulations of fluid systems and are especially applicable for heat transfer modeling purposes, i.e., heat pumps, refrigeration, cooling, and heating systems. Among the components that are included in the library are compressors, pumps, valves, and heat exchangers. The components are connected in the oriented physical modeling interface, Dymola, to construct complex models. Data for boundary conditions, such as ambient temperatures and thermal demands, were externally imported to the model.

All investigated cases are equipped with four compressors, which were modeled by their swept volumes. Correlations for circulated mass flow rate and electric power consumption were implemented based on the data published by the manufacturer. The compressor sizes were selected based on which combination of active compressors satisfied all operating criteria in the investigated cases. Compressors 1 to 4a were defined based on compressor model 4FTE-30K, with a swept volume of 17.5 m^3h^{-1} at 50 Hz. Compressor 4b was modeled after type 4JTE-15K, with a swept volume of 9.3 m^3h^{-1} at 50 Hz, and was implemented in the alternative system designs, i.e., PC and EJ. Correlations for each compressor were implemented in the model as a function of suction and discharge conditions, in addition to the rotational speed of the frequency converter (for the VSD compressors) [33].

All expansion valves were modeled using orifice valves, where the Bernoulli equation was applied to calculate the mass flow rate as a function of pressure difference. Modulating and directional valves (MV and DV) were modeled using three-way linear directional control valves, in which inlet mass flow is split into two flows, depending on the value of the switching position. The opening of the valves is regulated by proportional-integral (PI) controllers to reach their respective setpoints temperature. MV_1 controls the flow of CO_2 through $GC_{DHW,2}$ to reach a DHW temperature of 70 °C. MV_2 and MV_3 are controlled to ensure a superheat of 10 K at the suction line of the parallel and base compression stack, respectively. The mass flow rate of each branch is calculated using a linear pressure drop relation, which is formulated based on nominal pressure loss at nominal volume flow rate [37]. Table 1 lists the characteristics and heat transfer area for the heat exchangers applied in the models.

Table 1. Heat exchangers characteristics based on commercial available components.

Label	Heat Exchanger	Type	Secondary Fluid	Heat Transfer Area [m^2]
GC_{SH}	Gas cooler	Plate	Water	16.87
$GC_{DHW,1}$	Gas cooler	Plate	Water	5.07
$GC_{DHW,2}$	Gas cooler	Plate	Water	2.73
GC_{AIR}	Gas cooler	Fin and tube	Air	4 × 297.60 *
$EVAP_{AC,1}$	Evaporator	Plate	Glycol	9.61
$EVAP_{AC,2}$	Evaporator	Plate	Glycol	7.67
$EVAP_{AIR}$	Evaporator	Fin and tube	Air	4 × 297.60 *
IHX_1	Internal heat exchanger	Plate	CO_2	0.85
IHX_2	Internal heat exchanger	Plate	CO_2	1.75

* Air-side heat transfer area, tube volume of 51.2 L.

The four air heat exchanger units, which can be applied as both evaporators and gas coolers, are modeled in the same manner independent of operation. Each unit was modeled as a fin-and-tube cross-flow heat exchanger. Haaf's correlation [38] was applied to calculate the air-side heat transfer coefficient. The heat transfer coefficient on the refrigerant side

was estimated to 2500 W m^{-2} K^{-1}. The fin efficiency of each unit was modeled after the correlation by Schmidt [39]. In evaporation mode, the setpoint of the airflow through each heat exchanger is controlled to maintain an evaporating temperature 4 K below ambient temperature. Similarly, airflow is controlled to cool the temperature of CO_2 down to 4 K above ambient temperature in gas cooler mode.

The gas coolers for SH and DHW production, AC evaporators, and internal heat exchangers were implemented using plate heat exchanger models from the TIL library. The pressure drop in each heat exchanger was approximated using quadratic correlations formulated based on nominal pressure loss at nominal volume flow rate [37]. The correlation for chevron plates developed by Huang et al. [40] was applied to calculate the coefficient of heat transfer for the single-phase fluids in the gas coolers. This correlation was also applied to calculate the heat transfer coefficient on the glycol side in each of the two AC evaporators. An ideal separator with a volume of 300 L was applied to model the liquid receiver.

The gas cooler pressure is regulated with the high pressure valve, HPV, in the system configurations presented in Figures 1 and 2a. A PI-controller continuously regulates the valve opening area to meet the setpoint for the high pressure, which is defined based on operating zones, according to the principles described by Gullo et al. [41]. Additional constraints, such as supply temperature for SH and DHW, are applied to ensure that setpoints of the system are satisfied. The minimum and maximum gas cooler running pressure is 60 and 105 bar, respectively. In the system configuration presented in Figure 2b, the ejector is applied to control the gas cooler pressure. The ejector is modeled as a Multi-ejector block based on type HP 2875, which consists of fixed-geometry ejectors of different sizes, arranged in parallel within a block and which can be enabled or disabled according to the operating conditions. The nozzle flow was modeled using correlations by Brennen [42] and continuous control of the ejector opening degree was assumed. The ejector efficiency, η, was defined according to the relations presented in Elbel and Hrnjak [43]. Furthermore, the ejector efficiency was modeled by the use of the correlations given in Equations (1) and (2), which were developed based on operational performance data made publicly available from the manufacturer. The correlations are applicable for an ejector pressure-lift range of 4 to 6 bar.

$$\eta = a + bP_m + cT_m + dP_m^2 + eP_mT_m + fT_m^2 + gP_m^2T_m + hP_mT_m^2 + iT_m^3 - \eta_{corr}(6 - P_{lift}) \quad (1)$$

where T_m [°C] and P_m [bar] represents the motive temperature and pressure, respectively. The pressure lift, P_{lift} [bar], is introduced and corrected for, within the limits of the pressure-lift range, by the means of η_{corr} given in Equation (2). Values for the correlation coefficients applied in the equations are listed in Table 2.

$$\eta_{corr} = a + bP_m + cT_m + dP_m^2 + eP_mT_m + fT_m^2 + gP_m^3 + hP_m^2T_m + iP_mT_m^2 \quad (2)$$

Table 2. Values of correlation coefficients for Equations (1) and (2), which were applied to simulate the multi-ejector efficiency (developed for the range 4–6 bar).

η (Equation (1))	η_{corr} (Equation (2))
$a = 4.258$	$a = -6.839 \times 10^{-1}$
$b = -7.943 \times 10^{-2}$	$b = 4.743 \times 10^{-2}$
$c = -1.718 \times 10^{-1}$	$c = -9.552 \times 10^{-2}$
$d = 3.902 \times 10^{-4}$	$d = -7.155 \times 10^{-4}$
$e = 0.378 \times 10^{-2}$	$e = 1.688 \times 10^{-3}$
$f = -1.348 \times 10^{-4}$	$f = 6.161 \times 10^{-4}$
$g = -2.334 \times 10^{-5}$	$g = 2.996 \times 10^{-6}$
$h = 1.780 \times 10^{-5}$	$h = -6.288 \times 10^{-6}$
$i = -2.459 \times 10^{-5}$	$i = -7.867 \times 10^{-6}$

3.2. DHW Charging Strategy

The DHW charging strategy is a key influencing factor to achieve a high overall system performance in CO_2 heat pumps [29]. The thermal storage of 6 m^3 provides a buffer that enables a high degree of flexibility with regard to operating strategy. Two different charging strategies, *leveled* and *aggressive* charging, are investigated to evaluate the influence of thermal storage operation in light of design and overall performance.

3.2.1. Leveled Charging

Charging at reduced loads has the potential to limit return temperatures from the secondary systems and, by this, enhance system performance. A control scheme that aims to reduce DHW charging load and increase charging time has been formulated based on the storage volume and the temperature span across the storage. The simplified decision tree describing the outline of the leveled control strategy algorithm to determine the DHW charging load at time i, L_i, is shown in Figure 3.

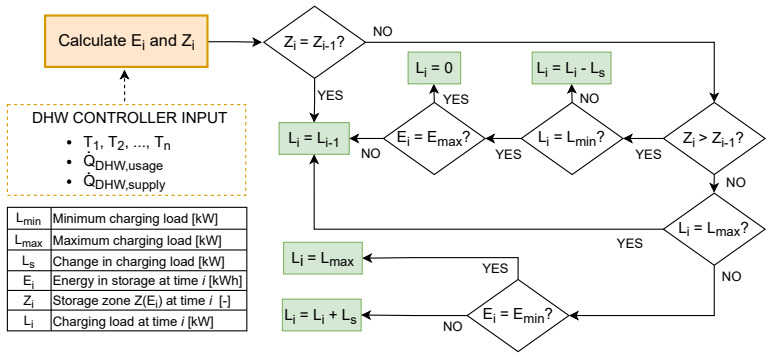

Figure 3. Simplified decision tree control logic to determine DHW charging load with the leveled charging strategy.

The DHW storage is divided into six separate zones, Z, which are formulated based on the maximum available energy reservoir of the storage,E_{max}. For instance, zone 1 applies when the DHW storage has a low temperature and, thus, no useful energy reserve. Zone 6 is reached when all tanks attain a temperature of 70 °C. The energy in storage at time i,E_i, is calculated based on DHW controller input variables, which include the temperatures across the storage, $T_1 - T_n$, the rate of energy entering, $\dot{Q}_{DHW,supply}$, and exiting the storage, $\dot{Q}_{DHW,usage}$. These values are attained directly in the simulations but could easily be calculated in a real-life system as a function of measured mass flow rates and temperatures of water entering and exiting the DHW storage tanks. The zone at time i,Z_i, is further calculated to determine L_i. The minimum and maximum loads in which the heat pump can actively produce hot water, L_{min} andL_{max}, are defined as 50 kW and 110 kW, based on the load profile and the size of the heat exchangers. The step value in which the charging load increases or decreases, L_s, is fixed to 10 kW.

3.2.2. Aggressive Charging

The aggressive charging strategy represents a common practice in regards to the operation of DHW thermal storage's [29,30]. The aim of the strategy is to charge the DHW storage tanks periodically from low to high temperature, which results in charging over several periods during the day, usually at high loads and intervals of 8 to 12 h. Typically, the aggressive charging strategy is applied when DHW is produced through heat recovery, e.g., from a supermarket, as the heat source is more available for particular hours of the day [44]. In addition, heat pump operations with under-dimensioned thermal storage or

excessive DHW demands will inevitably result in aggressive charging to meet demands. The control logic for the aggressive charging strategy is shown in Figure 4.

Similar to the leveled charging strategy illustrated in Figure 3, six separate zones, Z, are applied. Also, L_{min} and L_{max} are defined as 50 kW and 110 kW, respectively. The starting point of the algorithm for the aggressive charging strategy is when the energy in the storage, E_i, reaches its minimum, E_{min}. The charging load, L_i, is set to zero when the energy in the storage reaches its maximum, E_{max}.

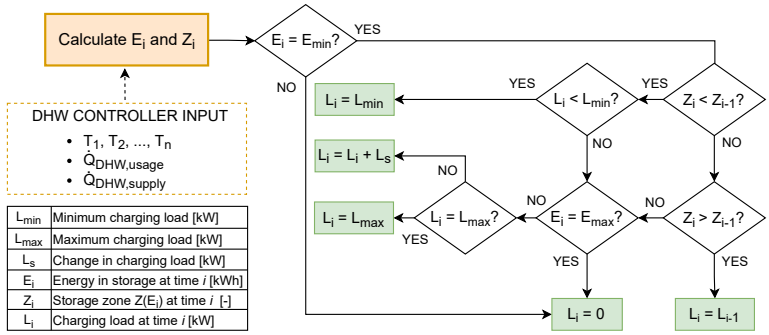

Figure 4. Simplified decision tree control logic to determine DHW charging load with the aggressive charging strategy.

3.3. Operating Range

The integrated CO_2 heat pumps have been designed with the aim of achieving high performance through system flexibility. An ambient temperature span from −15 to 35 °C has been selected to demonstrate different operating modes in a typical Scandinavian climate. The assumed SH and AC cooling loads supplied by the heat pump at different ambient temperatures are listed in Table 3. The loads have been established based on thermal demands of a medium-sized Norwegian hotel [29]. The setpoint curve for the SH water temperature is dependent on ambient conditions and is shown in Figure 5. The dimensioning supply and return temperature of chilled water are 7 and 12 °C, respectively. The values have been defined as per the industry rule-of-thumb for AC cooling in Scandinavia [45].

Table 3. Ambient temperature dependent space heating and AC cooling loads supplied by the integrated system.

Ambient temperature [°C]	−15	−10	−5	0	5	10	15	20	25	30	35
Space heating load [kW]	180	180	140	100	80	60	40	0	0	0	0
AC cooling load [kW]	0	0	0	0	0	0	0	40	80	150	220

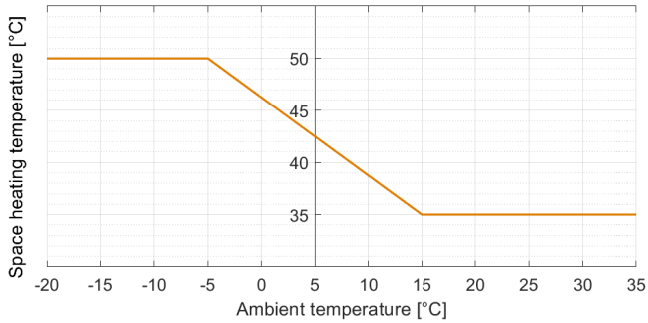

Figure 5. Set point curve for hydronic circuit for space heating depending on ambient temperature.

Four Scandinavian cities have been selected for comparisons, covering a broadest range of temperature profiles. Included in the analysis are four cities located in Central and Southern Europe to evaluate the warm climate performance potential of the designs. The climate data were obtained with the software MeteoNorm 7.1 and is based on recorded data from the period 1991–2010 [46]. The occurrences of ambient temperatures across a standard year are shown in Figure 6. A temperature bin of ±2.5 °C for given ambient temperatures has been applied.

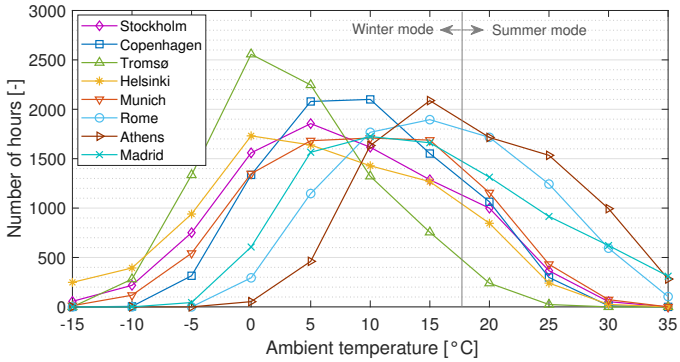

Figure 6. Number of hours per year at different ambient temperatures for the selected locations.

An hourly-dependent DHW demand profile is applied to the models to demonstrate the DHW thermal storage charging and discharging. Figure 7 depicts the DHW demand profile, which is repeated every 24 h. As for the thermal demands established for SH and AC cooling, the DHW demand profile is based on recorded operational data presented by Smitt et al. [29]. The city water temperature and DHW setpoint temperature are assumed independent of ambient conditions and have been applied to the models as constant values of 10 and 70 °C, respectively.

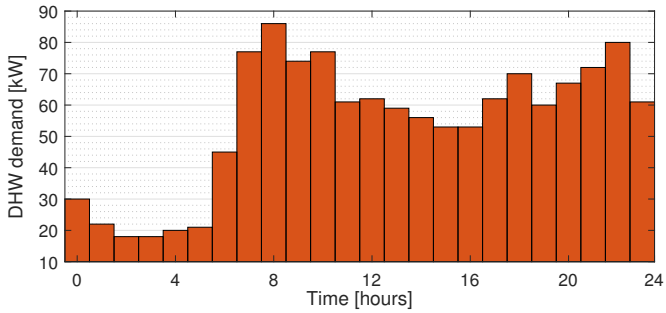

Figure 7. Domestic hot water consumption curve for the hotel, which is applied to the models.

3.4. Performance Evaluation

The overall COP of the system, hereafter referred to as COP, is applied to evaluate the performance of the system designs, and is defined in Equation (3):

$$COP = \frac{\dot{Q}_{SH} + \dot{Q}_{DHW} + \dot{Q}_{AC}}{\dot{W}} \quad (3)$$

where $\dot{Q}_{SH}$, $\dot{Q}_{DHW}$ and $\dot{Q}_{AC}$ represent SH, DHW, and AC loads, respectively, and $\dot{W}$ the electricity consumption of the compressor(s). Which terms are included at the span of ambient temperatures is given by Table 3. For instance, only the heating loads for DHW

and SH are considered during winter mode. While operating in summer mode, only DHW heating and AC cooling loads are included in the COP calculation.

3.5. Environmental Impact Evaluation

The total equivalent warming impact (TEWI) assesses both the direct and indirect emissions of greenhouse gases related to the system. Direct emissions are due to refrigerant leaks and is a function of refrigerant GWP [kg $CO_{2\text{-eq}}\cdot kg^{-1}$] and leakage rate, L [kg]. Indirect emissions are a product of annual electric energy consumption at each location, E_e, and the CO_2 emissions associated with the process of electricity generation at each location, β [g $CO_{2\text{-eq}}\cdot kWh^{-1}$]. The annual TEWI, $TEWI_{annual}$, is defined in Equation (4).

$$TEWI_{annual} = TEWI_{direct} + TEWI_{indirect} \quad (4)$$

$$TEWI_{direct} = GWP \cdot L \quad (5)$$

$$TEWI_{indirect} = E_e \cdot \beta \quad (6)$$

The following values were applied in the analysis:

- GWP of CO_2 = 1. GWP of existing R134a AC system = 1430 [47].
- Annual leakage rate is assumed 15% of refrigerant charge for all systems [48].
- The charge of the CO_2 systems is assumed to be 300 kg. The charge of the R134a system is assumed to be 2 $kg_{134a}\cdot kW_{AC,max}{}^{-1}$ [48].
- Emissions associated with electricity generation at each location is given according to country values (2019) as $\beta_{Stockholm}$ = 12, $\beta_{Copenhagen}$ = 112, $\beta_{Tromsø}$ = 19, $\beta_{Helsinki}$ = 89, β_{Munich} = 350, β_{Rome} = 233, β_{Athens} = 606 and β_{Madrid} = 210 [49].

3.6. Economic Evaluation

In evaluating the proposed designs' economic viability as retrofit solutions, both initial capital cost and operational costs are considered. Cost functions were applied for all major system components, i.e., compressors, heat exchangers and valves. Equipment costs were collected from the manufacturer catalogs for specialized components, such as the ejector and the combined air evaporator/gas cooler. Table 4 lists the capital cost functions applied in the economic analysis, which are applied for full load conditions.

Table 4. Cost functions of various components [50–52].

Component	Capital Cost Function
Compressors with electrical motor	$10{,}167.5 \times \dot{W}^{0.46}$ [a]
Plate HX	$1397 \times A^{0.89}$ [a]
Fin-and-tube HXs	119,500 [b,*]
Valves	$114.5 \times \dot{m}$ [a]
Receiver	1000 [b]
Ejector	9000 [b,*]

[a] Function given in $, [b] Function given in €, * From manufacturer catalog.

Investment costs related to the secondary systems have not been considered, as the necessary components would already be in place during a retrofit. The cost of installation and additional equipment, such as the control system and piping, is assumed to be equal to 15% of the total capital cost of the system [53].

The Chemical Engineering Plant Cost Index is applied to adjust the original cost to the cost at reference year [54]. The annual average cost index (607.5) of 2019 is used as a reference. The cost of the components is adjusted according to the cost index as given by Equation (7) [55].

$$\text{Cost at reference year} = \text{original cost} \times \frac{\text{Index value for reference year}}{\text{Index value for original year}} \quad (7)$$

The economic viability of the designs is evaluated by means of the net present value (NPV) and discounted payback period (DPP), defined in Equations (8) and (10), respectively. NPV is a method to represent the discounted cash flow, which is defined as the sum of net cash flows over the plant economic life, N, calculated as

$$NPV = C_i + \sum_{t=0}^{N} \frac{C_e(1+r_e)^t}{(1+r_d)^t} \quad (8)$$

where r_d is the average annual effective discount rate (cost of money), and r_e is the general inflation rate of electricity prices. The net cash flow is represented by the initial investment cost, C_i, and the sum of all operational incomes over the system's lifetime, which in this analysis amount to the saved electricity expenses, C_e. The latter is defined in Equation (9).

$$C_e = p\left(\frac{E_{SH}+E_{DHW}}{\eta_{el}} + \frac{E_{AC}}{COP_{AC,al}} - \frac{E_{SH}+E_{DHW}+E_{AC}}{COP}\right) \quad (9)$$

An existing reference system (capital cost = 0), consisting of an electric boiler and an alternative standard AC cooling unit, is applied for the analysis. It is assumed that all SH and DHW energy requirements, E_{SH} and E_{DHW}, are covered by the electric boiler, while all cooling energy, E_{DHW}, is covered by the alternative AC chiller.

The DPP, defined in Equation (10), determines the time from investment to return of the invested capital. DDP is calculated by identifying the year, Y_n, in which the proceeding cumulative net cash flow (NCF), $\sum_{t=0}^{n} NCF_n$, turns positive. The exact time of return is found by accounting for the discounted value of the cash flow of the next period, NCF_{n+1}.

$$DPP = Y_n + \frac{abs(\sum_{t=0}^{n} NCF_n)}{NCF_{n+1}} \quad (10)$$

Data applied in the economic analysis are listed below.

- The general inflation rate is r_e = 2.5% [53].
- The average annual effective discount rate is r_d = 10% [53].
- The plant economic life is N = 15 years [52,53].
- The electric boiler efficiency is η_{el} = 95% [56].
- The European seasonal energy efficiency ratio (ESEER) of the alternative R134a AC cooling system is ESEER = $COP_{AC,al}$ = 2.52 (from manufacturer catalog).
- Costs related to system maintenance and operation have been neglected [52,53].

4. Results and Discussion

4.1. System Performance and Operation

Transient simulations were conducted for the purposed CO_2 systems with the boundary conditions and control schemes described in Section 3. Figure 8 compares the COP of the investigated designs as a function of ambient temperature and charging strategy. Naturally, the COP for all designs increases with ambient temperature as the pressure ratio of the compressors diminishes. At 20 °C, the COP of all designs increases considerably to values in the range of 7.3 to 7.6 and 5.8 to 6.3 for leveled and aggressive charging, respectively. This is explained by the presence AC cooling demand during high ambient temperatures, which enables combined heat pump and chiller operations. The COP of all designs are gradually reduced from 25 °C, due to the increase in AC cooling loads relative to the DHW production load.

Figure 8 clearly illustrates that the system with the ejector arrangement, EJ, outperforms both SC and PC, independent of charging strategy. A more significant benefit is achieved from the ejector at ambient temperatures above 15 °C, where the performance is enhanced by up to 20% and 14% compared with SC and PC, respectively. Moreover, leveled charging results typically increased COP compared with aggressive charging due to continuous DHW charging during all operational hours. In contrast, DHW production

transpires in about 60% of the operation when aggressive charging. The most considerable difference in performance in terms of charging strategy occurs at 20 °C, in which leveled charging enhances COP considerably. As observed in the figure, an increase in COP of more than 20% is achieved for all investigated designs. DHW is continuously produced when applying the leveled charging strategy, and thus, there is no need to dump heat to the ambient. In contrast, DHW is periodically produced at high loads when applying aggressive charging, resulting in heat rejection to the ambient and reduced COP compared with leveled charging.

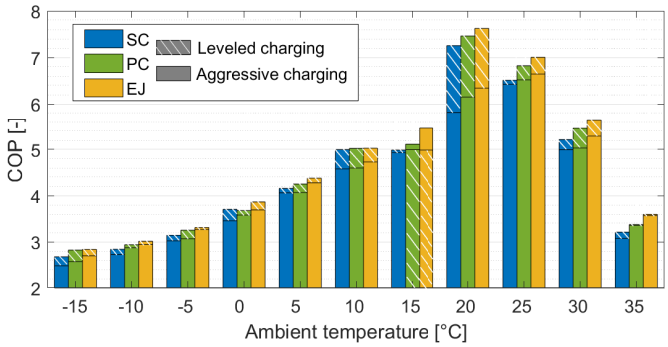

Figure 8. COP as a function of ambient temperature for the investigated designs when applying the aggressive DHW charging strategy.

The power consumption of the compressors is illustrated in Figure 9; also included in the figure is the arrangement of the pivoting compressors for the PC and EJ designs. The data shown in Figure 9 demonstrate the behavior of the system when the leveled charging strategy is applied. Generally, the SC design attains higher power consumption due to a slight increase in compressor pressure ratio compared to PC and EJ, which are both equipped with optional pivoting parallel compressors. However, the power consumption of all investigated designs are nearly equal in the temperature range from 10 to 15 °C. This is explained by the relatively large DHW demand, which results in a reduced CO_2 gas cooler outlet temperature, and thus less vapor formation after expansion to the liquid receiver. Consequently, solely base compressor 1 is employed to cover the heating demand in all investigated designs.

Both PC and EJ designs rely heavily on the base compressors during low ambient temperature operations from −15 to 5 °C. Compressor 2 is in both designs employed as a base compressor. The opposite trend is observed at ambient temperatures of 20 °C and above, as the pivoting compressors (2 and 3) are integrated in the parallel compressors section. Thus, the pivoting compressors enable flexible and efficient operation of integrated CO_2 systems over a wide range of ambient temperatures. In addition, a smaller total compressor capacity is needed when applying the pivoting option, as illustrated by the reduced swept volume of compressor 4 (b) in PC and EJ, the value of which is given in Section 3.1. Thus, pivoting compressors have the potential to reduce both investment and operational costs when compared with a single-stage compression system, especially for installations of considerable size [57].

Figure 10 presents the ejector efficiency and entrainment ratio for the EJ system design when applying both the leveled and aggressive charging strategy. The average ejector efficiency is recorded in the range of 0.0 to 0.34 when leveled charging is applied. The low values of efficiency occur at 10 and 15 °C, as the efficiency function (Equation (1)) advances towards zero when the CO_2 temperature before expansion is low. In the case of aggressive charging, the ejector operates in an average efficiency range of 0.17 to 0.28. Moreover, it can be observed that more liquid is entertained when applying the aggressive charging strategy. Thus, the overall benefit of the ejector is more significant when applying the aggressive

charging strategy, explained by the elevated gas cooler outlet temperature during this mode of operations.

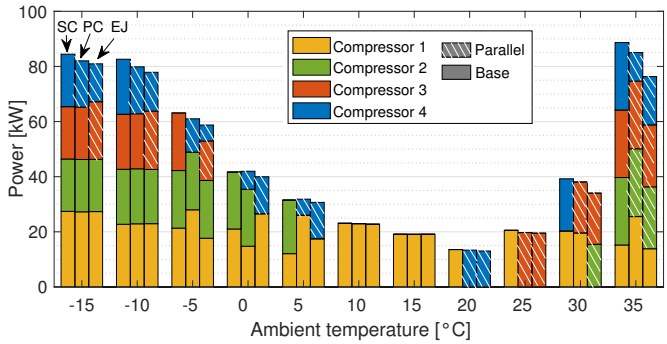

Figure 9. Electric power consumption and arrangement of the compressors when applying the leveled charging strategy. The three different bars at each temperature interval represents the designs of SC, PC, and EJ.

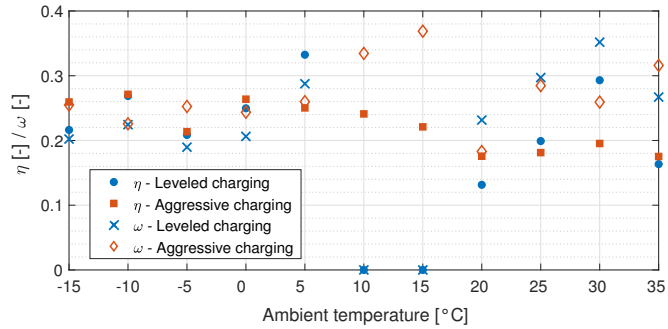

Figure 10. Ejector efficiency (η) and entrainment ratio (ω) for the EJ design when applying the leveled and aggressive charging strategy.

As illustrated in Figure 7, a constant DHW demand pattern was selected for this investigation. However, fluctuations will occur in real-life systems due to variation in hotel guest load, which will highly influence the magnitude of DHW demand peaks. Thus, it is likely that the CO_2 system is occasionally forced to operate with aggressive charging to fulfill excessive DHW demands. An alternative scenario is heat pump operations during periods when the guest load is low. In these instances, a surplus of stored DHW will result in periods of operation without DHW production, and as a consequence, elevated gas cooler outlet temperatures. Therefore, the advantages of the ejector are likely more prominent than what was achieved in this investigation. This may speak for applying ejector technology in CO_2 heat pump and chiller systems for hotels, despite the fact that the benefits and influence on COP are limited when applying the leveled charging strategy.

4.2. Annual Energy Consumption and Environmental Impact

The annual COP and energy consumption of the investigated solutions for different locations are listed in Table 5. The EJ design demonstrated superior performance, followed by PC and SC for all locations independent of charging strategy. The COP at the locations were improved by 3.1% (Copenhagen) to 4.1% (Athens) when comparing EJ to SC (leveled charging strategy). Similar results were obtained with the aggressive charging strategy, in which the COP at each location increased by 4.7% (Stockholm) to 6.9% (Athens) with the EJ design.

Table 5. Annual COP, energy usage, and emissions (TEWI) of the investigated systems at the selected locations when applying the leveled charging strategy.

Strategy	Variable/Location	Annual COP [-]			Annual Energy Usage [MWh· y^{-1}]			Annual Emissions [Tonne $CO_{2\text{-eq}}$· y^{-1}]		
		SC	PC	EJ	SC	PC	EJ	SC	PC	EJ
Leveled charging	Stockholm	4.68	4.75	4.85	278.65	277.19	268.32	3.39	3.37	3.26
	Copenhagen	4.86	4.92	5.01	240.64	240.90	233.61	27.00	27.02	26.21
	Tromsø	4.12	4.16	4.27	333.56	331.32	319.54	6.38	6.34	6.11
	Helsinki	4.48	4.55	4.64	311.25	308.52	298.82	27.74	27.50	26.64
	Munich	4.86	4.93	5.03	253.35	252.57	244.84	88.72	88.44	85.73
	Rome	5.49	5.61	5.71	206.74	205.60	199.60	48.21	47.95	46.55
	Athens	5.62	5.76	5.85	213.01	210.34	203.40	129.18	127.51	123.30
	Madrid	5.19	5.30	5.40	237.44	235.76	227.15	49.91	49.55	47.75
Aggressive charging	Stockholm	4.43	4.45	4.64	293.56	290.39	276.11	3.57	3.53	3.36
	Copenhagen	4.50	4.61	4.80	254.05	252.64	240.35	28.50	28.34	26.96
	Tromsø	3.88	3.96	4.14	349.94	345.25	328.18	6.69	6.61	6.28
	Helsinki	4.17	4.28	4.46	327.84	323.07	307.26	29.22	28.80	27.39
	Munich	4.51	4.65	4.82	267.18	264.57	251.45	93.56	92.64	88.05
	Rome	5.03	5.20	5.40	218.57	217.10	206.23	50.97	92.64	88.05
	Athens	5.19	5.34	5.55	224.95	221.68	209.86	136.36	134.38	127.22
	Madrid	4.82	4.94	5.15	250.07	247.09	234.02	52.56	51.94	49.19

The results in Table 5 illustrate that the ambient temperatures at each location highly influence annual energy consumption. The lowest annual energy consumption was achieved in the warmest city, Rome, where the range of consumption was recorded from 199.60 to 218.57 MWh· y^{-1} for all investigated cases. In the coldest city, Tromsø, the annual energy consumption was found to approximately 60% higher, in the range of 319.54 to 349.94 MWh· y^{-1}. When comparing results obtained with the two different charging strategies, it can be concluded that the highest annual COPs were achieved when applying the leveled charging strategy. Furthermore, results from aggressive charging with the best design in terms of COP, EJ, are comparable to the COPs obtained with SC when applying leveled charging. For instance, Munich achieved an annual COP of 4.86 with SC (leveled charging) and 4.82 with EJ (aggressive charging). Thus, DHW control strategy rather than system design appears to be the largest influence factor on COP and energy consumption at each investigated location.

The annual global warming impact from each system, in terms ton $CO_{2\text{-eq}}$ emission, is included in Table 5. A large variation in emission is observed at the different locations, in which Stockholm displays the lowest emission values of approximately 3 tons $CO_{2\text{-eq}}$ per year. This amounts to approximately 2.5% of the related emissions in Athens, which are between 123 to 129 tonne per year, dependent on system design. Energy savings and emission reductions associated with installing the SC design in place of the existing solution (boiler + separate AC chiller) are shown in Figure 11. The largest reduction of emissions is achieved in Athens and Rome, where between 310 to 380 tonnes $CO_{2\text{-eq}}$ can be prevented on an annual basis. In terms of energy utilization, the largest savings were achieved in the Scandinavian locations, ranging from 850 to 1000 MWh·y^{-1}. Information related to energy savings and emission reduction for PC and EJ can be found in Appendix Table A1.

4.3. Economical Analysis

The total capital cost of the considered designs is listed in Table 6. As can be observed from the table, the investment cost related to compressors and heat exchanger represent the majority of the capital cost in all cases. When considering all designs, the total capital cost for each of the suggested designs is within a range of ±2.5%.

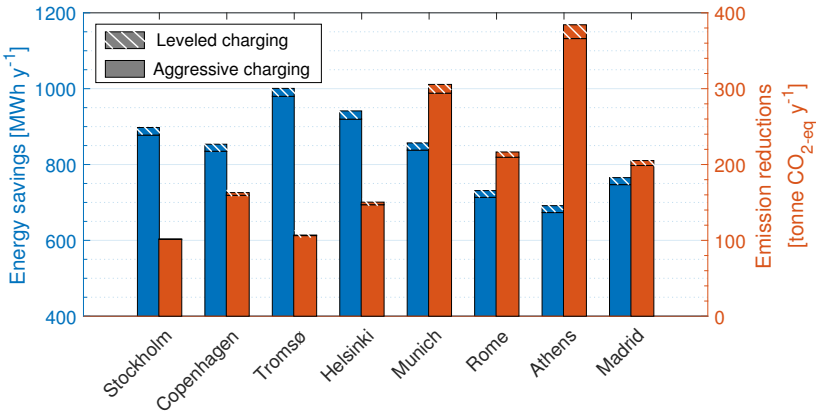

Figure 11. Annual energy savings and reduction in related emissions (TEWI) of SC design in relation to the reference thermal system. The eight selected locations are investigated when applying both the leveled and aggressive charging strategy.

Table 6. Total equipment investment cost of the CO_2 designs with single-stage compression (SC), parallel compression (PC), and ejector-supported parallel compression (EJ).

Investment	**Capital Cost [k€]**		
	SC	**PC**	**EJ**
Compressors	174.6	169.2	169.2
Heat exchangers	171.7	174.2	174.2
Valves/receiver/ejector	2.3	2.4	11.2
Installation and additional equipment (15%)	50.6	51.9	53.2
Total	**399.2**	**397.7**	**407.8**

The DPP and NPV for the SC design at different electricity prices are shown in Figures 12 and 13. The results for the eight locations have been divided into two separate plots for each economic comparison. Moreover, the influence of both the leveled and the aggressive charging strategies is included in the figures.

As seen from Figure 12, aggressive charging prolongs the DPP for all locations with approximately 0.7 to 1.5 years at 0.06 €·kWh^{-1}. As the electricity price increases, the benefit of the charging strategy on DPP is reduced to a few months at 0.20 €·kWh^{-1}. However, the economic benefit at high electricity prices for each location is more evident when evaluating NPV. As shown in Figure 13, the difference in NPV for leveled and aggressive charging varies between 0.07 and 0.1 M€ at an electricity price 0.20 €·kWh^{-1} for all evaluated locations. Thus, it is possible to save up to 25% of the initial investment cost by applying the leveled charging strategy.

The DPP for the locations drops significantly from a range of 9 to 16 to around 3 years as the electricity price increases from 0.06 to 0.20 €·kWh^{-1}. Similarly, the NPV for the locations varies between 0 and 0.02 M€ and 0.8 and 1.4 M€ at the selected range of electricity prices (Figure 13). Locations with low ambient temperatures and low annual COP display the shortest DPP and highest NPV, which is in contrast to COP values listed in Table 5. This is explained by the large savings in SH energy achieved at locations characterized by low ambient temperatures, such as Tromsø and Helsinki, where the alternative would be application of an electric boiler. The best performing location in the operational analysis, Athens, has the longest DPP with a break-even point between 3.3 and 16+ years. The NPVs for Athens, Rome, and Madrid are close to and below zero at an electricity price of 0.06 €·kWh^{-1}, and thus not economically viable investments. However, the actual electricity price at the locations must be considered to give a more accurate evaluation. Generally, the electricity price for commercial actors in Scandinavia is in the

range of 0.06 to 0.08 €·kWh^{-1}, while the equivalent electricity price in Germany (Munich), Italy (Rome), and Athens (Greece) is typically at values of 0.18, 0.15, and 0.10 €·kWh^{-1}, respectively [58]. If only considering results in which leveled charging is applied, DPPs of approximately 3 (Munich), 4.5 (Rome), and 7.5 years (Athens) and NPVs in the range of 0.25 to 0.95 M€ were achieved when considering typical electricity prices at the locations. Thus, integrated heating and cooling systems with CO_2 can be efficient, cost-effective and environmentally friendly when applied in warmer European climates.

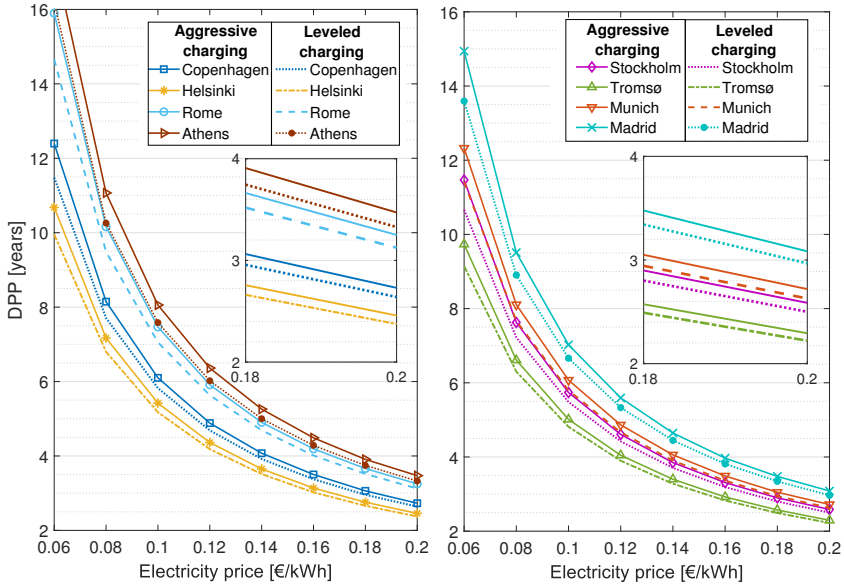

Figure 12. Discounted payback period for selected cities with the SC design at different electricity prices when applying the leveled and aggressive charging strategy.

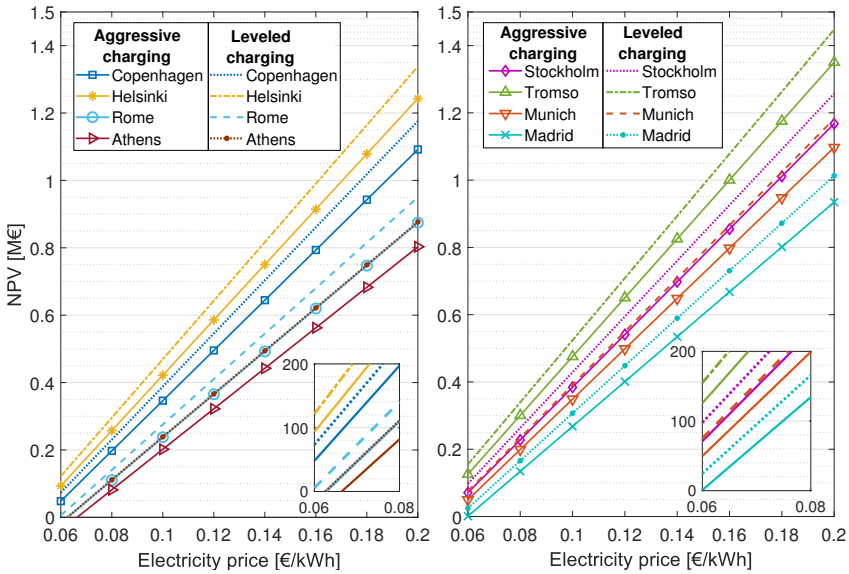

Figure 13. Net present value for selected cities with the SC design at different electricity prices when applying the leveled and aggressive charging strategy.

The DPP for the Scandinavian locations is 9 to 12.5 years at 0.06 €·kWh^{-1}. At an electricity price of 0.08 €·kWh^{-1}, DPP and NPV for the Scandinavian locations are between 6.3 to 7.7 years. This is considered high when related to the rule-of-thumb for heat pump investments within Scandinavia, which generally points to a payback time of 5 years or less. However, the NPV for this investment for the Scandinavian locations is between 0.23 to 0.34 M€. Thus, profits of approximately 50–85% of the initial investment can be gained over the systems' economic lifetime. Integrated CO_2 heat pumps and chillers are, therefore, cost-efficient compared to more conventional approaches, including electric boilers or district heat in combination with separate chillers for AC. Nevertheless, when compared to HFO systems for hotels, CO_2 integrated systems still face a challenge in terms of the high investment cost. Throughout history, new and supposedly safe refrigerants have been introduced (CFC, HCFC and HFC) as an alternative to natural refrigerants. All of them have eventually been phased out as their impact on human health and the environment is revealed. In later years, research suggests that the decomposition products from HFO refrigerants are harmful. Moreover, the research community is investing significant efforts to uncover all unknown side effects of applying HFOs [12,13]. Thus, when factoring in environmental concerns, and the fact that future regulations regarding HFOs are unknown and thus pose an economic risk for the hotel owner, one can argue that the somewhat high investment costs related to integrated CO_2 systems in Scandinavia are justified.

Tables 7 and 8 list the NPV and DPP at the selected locations when the PC and EJ system designs are applied, respectively. Results for the entire range of electricity prices can be found in Tables A3 and A2. Both PC and EJ display comparable results to SC (Figures 12 and 13). However, the economic data obtained with PC illustrate a slightly better NPV and DPP at all locations when applying the leveled charging strategy.

In contrast to the results presented in Section 4.2, in which EJ was found to be the superior solution in terms of annual COP and energy consumption, the economical analysis reveals that PC is better when considering overall system cost. However, results from both the operational and the economic evaluation show that improving the DHW charging strategy is the least expensive and most efficient measure to enhance the performance of integrated CO_2 systems.

Table 7. Net present value (NPV) and discounted payback period (DPP) for selected cities with the PC design at different electricity prices when applying the leveled and aggressive charging strategy.

Strategy	Variable/Location	NPV at Selected Electricity Prices [M€]			DPP at Selected Electricity Prices [years]		
		0.06	**0.14**	**0.20**	**0.06**	**0.14**	**0.20**
Leveled charging	Stockholm	0.10	0.77	1.27	10.5	3.7	2.5
	Copenhagen	0.08	0.71	1.18	11.4	3.9	2.6
	Tromsø	0.16	0.90	1.46	9.0	3.2	2.2
	Helsinki	0.13	0.83	1.35	9.8	3.5	2.3
	Munich	0.08	0.71	1.19	11.3	3.9	2.6
	Rome	0.01	0.55	0.96	14.4	4.6	3.1
	Athens	<0	0.50	0.89	15<	4.9	3.3
	Madrid	0.03	0.60	1.02	13.4	4.4	2.9
Aggressive charging	Stockholm	0.08	0.71	1.18	11.3	3.8	2.6
	Copenhagen	0.05	0.65	1.10	12.2	4.0	2.7
	Tromsø	0.13	0.84	1.37	9.6	3.4	2.3
	Helsinki	0.10	0.76	1.26	10.5	3.6	2.4
	Munich	0.05	0.66	1.11	12.1	4.0	2.7
	Rome	<0	0.50	0.89	15<	4.8	3.2
	Athens	<0	0.45	0.82	15<	5.2	3.4
	Madrid	0.01	0.54	0.95	14.6	4.6	3.0

Table 8. Net present value (NPV) and discounted payback period (DPP) for selected cities with the EJ design at different electricity prices when applying the leveled and aggressive charging strategy.

Strategy	Variable/Location	NPV at Selected Electricity Prices [k€]			DPP at Selected Electricity Prices [years]		
		0.06	**0.14**	**0.20**	**0.06**	**0.14**	**0.20**
Leveled charging	Stockholm	0.10	0.77	1.27	10.8	3.7	2.5
	Copenhagen	0.07	0.71	1.18	11.7	4.0	2.7
	Tromsø	0.15	0.90	1.46	9.2	3.3	2.2
	Helsinki	0.12	0.82	1.35	10.1	3.5	2.4
	Munich	0.07	0.71	1.19	11.6	3.9	2.7
	Rome	0.00	0.55	0.96	14.9	4.7	3.2
	Athens	<0	0.50	0.89	15.0	5.0	3.4
	Madrid	0.02	0.59	1.02	13.8	4.5	3.0
Aggressive charging	Stockholm	0.07	0.71	1.19	11.5	3.9	2.6
	Copenhagen	0.05	0.65	1.11	12.5	4.1	2.7
	Tromsø	0.13	0.84	1.38	9.7	3.4	2.3
	Helsinki	0.10	0.77	1.27	10.7	3.6	2.5
	Munich	0.05	0.66	1.12	12.4	4.1	2.7
	Rome	<0	0.50	0.89	15.0	4.9	3.3
	Athens	<0	0.45	0.82	15.0	5.3	3.5
	Madrid	0.00	0.55	0.96	14.9	4.6	3.1

5. Conclusions

In this paper, three different designs of integrated CO_2 systems with thermal storage for hotels were evaluated through an energetic and economic analysis. The investigated designs were standard single-stage compression (SC), parallel compression (PC), and ejector-supported parallel compression (EJ). The performance of the systems was numerically investigated by implementing two separate DHW charging strategies: aggressive and leveled charging. In addition, variations in loads, ambient temperatures, and setpoints were applied to each numerical model. Evaluations of the annual efficiency, emissions, energy performance, net present value, and discounted payback period were carried out at eight different locations, ranging from Scandinavia to the Mediterranean.

The main conclusions drawn from this investigation are as follows.

- The EJ design demonstrated enhanced annual performance, followed by PC and SC, at all locations independent of charging strategy. Annual COPs of 4.27 to 5.03 were achieved at the location in central Europe and Scandinavia. In the Mediterranean locations, Annual COPs in the range of 5.40 to 5.70 were obtained. Considerable reductions in both related emissions and energy consumption were achieved at all locations.
- The highest annual COPs were achieved when applying the leveled charging strategy, independent of design. An increase in COPs of up to 7.3% was attained compared to the aggressive charging strategy. Thus, control of the DHW charging is a larger influencing factor on performance than system designs.
- DPP and NPV for the Scandinavian locations were found to be between 6.3 to 7.7 years and 0.23 to 0.34 M€ at typical Scandinavian electricity prices. Hotels in temperate and Mediterranean climates obtained DPPs of approximately 3 and 4.5 to 7.5 years, respectively, and NPVs in the range of 0.25 to 0.95 M€. Thus, integrated heating and cooling systems with CO_2 can be an efficient, cost-effective and environmentally friendly solution for hotels located in temperate and Mediterranean locations.

Integrated CO_2 systems have proven to be efficient and sustainable alternatives for hotel applications. However, high investment cost decelerates the rate of installation for these type of solutions. History has shown that potential harmful refrigerants are eventually heavily regulated and even banned. As a result, HFO alternatives may pose an economic risk for hotel owners. Thus, the somewhat high investment costs of integrated CO_2 systems can be justified. Further research is necessary to establish integrated CO_2

systems as a competitive alternative to traditional synthetic refrigeration systems. From this study, it can be concluded that improving the DHW charging strategy is the least expensive and most efficient measure to enhance the performance of integrated CO_2 systems.

Author Contributions: Conceptualization, S.S., Á.P. and A.H.; methodology, S.S. and Á.P.; software, S.S.; investigation, S.S.; writing—original draft preparation, S.S. and Á.P.; writing—review and editing, S.S., Á.P. and A.H.; visualization, S.S.; supervision, Á.P. and A.H. All authors have read and agreed to the published version of the manuscript.

Funding: This research received no external funding.

Institutional Review Board Statement: Not applicable.

Informed Consent Statement: Not applicable.

Conflicts of Interest: The authors declare no conflicts of interest.

Nomenclature

Symbols

β	CO_2 emission factors [g $CO_{2\text{-eq}}$·kWh^{-1}]
η	efficiency [-]
C	cost [€]
E	energy [kWh]
L	leakage rate [%]
N	plant economic life [years]
P	pressure [bar]
p	electricity price [€·kWh^{-1}]
$\dot{Q}$	heat [kW]
r	rate [%]
T	temperature [°C]

Subscript

AC	air-conditioning
al	alternative
corr	corrected
d	discount
DHW	domestic hot water
e	electricity
el	electric boiler
eq	equivalent
i	investment
lift	pressure lift
m	motive
SH	space heating

Abbreviations

AC	air-conditioning
CFC	chlorofluorocarbons
CO_2	carbon dioxide
COP	coefficient of performance
DHW	domestic hot water
DPP	discounted payback period
DV	directional valve
EJ	ejector-supported parallel compression
ESEER	European seasonal energy efficiency ratio
EVAP	Evaporator
FGT	flash gas tank
GC	gas cooler
GWP	global warming potential
HCFC	hydrochlorofluorocarbons

HFC	hydrofluorocarbons
HFO	hydrofluoroolefins
HX	heat exchanger
IHX	internal heat exchanger
INT	intermediate temperature
LT	low temperature
MV	modulating valve
NCF	net cash flow
NPV	net present value
PC	parallel compression
PI	proportional–integral
SC	single-stage compression
SH	space heating
TEWI	total equivalent warming impact
TFA	trifluoroacetic acid
VSD	variable speed drive

Appendix A

Table A1. Annual energy savings and emission reductions (TEWI) of the investigated systems in relation to the reference thermal system. The eight selected locations are listed when applying both the leveled and aggressive charging strategy.

Strategy	Variable/Location	Annual Energy Savings [MWh· y^{-1}]		Annual Emission Reduction [Tonne $CO_{2\text{-eq}}$· y^{-1}]	
		PC	EJ	PC	EJ
Leveled charging	Stockholm	901.97	908.64	101.83	102.02
	Copenhagen	856.32	861.78	163.26	164.69
	Tromsø	1005.47	1014.84	107.14	107.55
	Helsinki	947.00	954.30	151.16	152.67
	Munich	860.54	866.28	307.12	311.84
	Rome	735.52	739.52	217.81	220.14
	Athens	697.00	701.46	389.25	396.15
	Madrid	770.38	776.34	206.61	209.66
Aggressive charging	Stockholm	884.03	896.07	101.46	101.77
	Copenhagen	839.85	850.18	160.10	162.64
	Tromsø	987.30	1002.01	106.53	107.14
	Helsinki	927.71	941.19	148.15	150.76
	Munich	843.74	854.70	297.05	305.47
	Rome	718.33	727.00	211.12	215.68
	Athens	679.56	688.63	371.81	384.47
	Madrid	753.48	763.76	200.68	205.58

Table A2. Net present value (NPV) and discounted payback period (DPP) for selected cities with the EJ design at different electricity prices when applying the leveled and aggressive charging strategy.

Strategy	Variabl/Locatione	NPV at Selected Electricity Prices [M€]								DPP at Selected Electricity Prices [years]							
		0.06	**0.08**	**0.10**	**0.12**	**0.14**	**0.16**	**0.18**	**0.20**	**0.06**	**0.08**	**0.10**	**0.12**	**0.14**	**0.16**	**0.18**	**0.20**
Leveled charging	Stockholm	0.10	0.26	0.43	0.60	0.77	0.93	1.10	1.27	10.8	7.3	5.5	4.5	3.7	3.2	2.8	2.5
	Copenhagen	0.07	0.23	0.39	0.55	0.71	0.86	1.02	1.18	11.7	7.8	5.9	4.8	4.0	3.4	3.0	2.7
	Tromsø	0.15	0.34	0.53	0.72	0.90	1.09	1.28	1.46	9.2	6.4	4.9	3.9	3.3	2.9	2.5	2.2
	Helsinki	0.12	0.30	0.47	0.65	0.82	1.00	1.18	1.35	10.1	6.9	5.2	4.2	3.5	3.0	2.7	2.4
	Munich	0.07	0.23	0.39	0.55	0.71	0.87	1.03	1.19	11.6	7.8	5.9	4.7	3.9	3.4	3.0	2.7
	Rome	0.00	0.14	0.27	0.41	0.55	0.68	0.82	0.96	14.9	9.6	7.1	5.7	4.7	4.1	3.6	3.2
	Athens	<0	0.11	0.24	0.37	0.50	0.63	0.76	0.89	15<	10.4	7.7	6.1	5.0	4.3	3.8	3.4
	Madrid	0.02	0.17	0.31	0.45	0.59	0.74	0.88	1.02	13.8	9.0	6.7	5.4	4.5	3.8	3.4	3.0
Aggressive charging	Stockholm	0.07	0.23	0.39	0.55	0.71	0.87	1.03	1.19	11.50	7.6	5.7	4.6	3.9	3.3	2.9	2.6
	Copenhagen	0.05	0.20	0.35	0.50	0.65	0.81	0.96	1.11	12.50	8.2	6.1	4.9	4.1	3.5	3.1	2.7
	Tromsø	0.13	0.31	0.49	0.67	0.84	1.02	1.20	1.38	9.70	6.6	5.0	4.0	3.4	2.9	2.6	2.3
	Helsinki	0.10	0.26	0.43	0.60	0.77	0.94	1.10	1.27	10.70	7.2	5.4	4.4	3.6	3.1	2.8	2.5
	Munich	0.05	0.20	0.36	0.51	0.66	0.81	0.97	1.12	12.40	8.1	6.1	4.9	4.1	3.5	3.1	2.7
	Rome	<0	0.11	0.24	0.37	0.50	0.63	0.76	0.89	15<	10.2	7.5	5.9	4.9	4.2	3.7	3.3
	Athens	<0	0.08	0.21	0.33	0.45	0.58	0.70	0.82	15<	11.1	8.0	6.4	5.3	4.5	3.9	3.5
	Madrid	0.00	0.14	0.27	0.41	0.55	0.68	0.82	0.96	14.90	9.5	7.0	5.6	4.6	4.0	3.5	3.1

Table A3. Net present value (NPV) and discounted payback period (DPP) for selected cities with the PC design at different electricity prices when applying the leveled and aggressive charging strategy.

Strategy	Variable/Location	NPV at Selected Electricity Prices [M€]								DPP at Selected Electricity Prices [years]							
		0.06	**0.08**	**0.10**	**0.12**	**0.14**	**0.16**	**0.18**	**0.20**	**0.06**	**0.08**	**0.10**	**0.12**	**0.14**	**0.16**	**0.18**	**0.20**
Leveled charging	Stockholm	0.10	0.27	0.43	0.60	0.77	0.93	1.10	1.27	10.5	7.1	5.4	4.4	3.7	3.2	2.8	2.5
	Copenhagen	0.08	0.23	0.39	0.55	0.71	0.87	1.02	1.18	11.4	7.6	5.8	4.6	3.9	3.3	2.9	2.6
	Tromsø	0.16	0.34	0.53	0.72	0.90	1.09	1.27	1.46	9.0	6.2	4.8	3.9	3.2	2.8	2.5	2.2
	Helsinki	0.13	0.30	0.48	0.65	0.83	1.00	1.18	1.35	9.8	6.7	5.1	4.1	3.5	3.0	2.6	2.3
	Munich	0.08	0.24	0.40	0.56	0.71	0.87	1.03	1.19	11.3	7.6	5.7	4.6	3.9	3.3	2.9	2.6
	Rome	0.01	0.15	0.28	0.42	0.55	0.67	0.82	0.96	14.4	9.4	7.0	5.6	4.6	4.0	3.5	3.1
	Athens	<0	0.12	0.25	0.37	0.50	0.63	0.76	0.89	15<	10.1	7.5	5.9	4.9	4.2	3.7	3.3
	Madrid	0.03	0.17	0.31	0.46	0.60	0.74	0.88	1.02	13.4	8.8	6.6	5.3	4.4	3.8	3.3	2.9
Aggressive charging	Stockholm	0.08	0.23	0.39	0.55	0.71	0.87	1.02	1.18	11.3	7.5	5.7	4.5	3.8	3.3	2.9	2.6
	Copenhagen	0.05	0.20	0.35	0.50	0.65	0.80	0.95	1.10	12.2	8.0	6.0	4.8	4.0	3.5	3.0	2.7
	Tromsø	0.13	0.31	0.48	0.66	0.84	1.01	1.19	1.37	9.6	6.5	4.9	4.0	3.4	2.9	2.5	2.3
	Helsinki	0.10	0.26	0.43	0.60	0.76	0.93	1.09	1.26	10.5	7.0	5.3	4.3	3.6	3.1	2.7	2.4
	Munich	0.05	0.21	0.36	0.51	0.66	0.81	0.96	1.12	12.1	8.0	6.0	4.8	4.0	3.4	3.0	2.7
	Rome	<0	0.12	0.24	0.37	0.50	0.63	0.76	0.89	15<	10.0	7.4	5.8	4.8	4.1	3.6	3.2
	Athens	<0	0.09	0.21	0.33	0.45	0.57	0.70	0.82	15<	10.9	7.9	6.3	5.2	4.4	3.9	3.4
	Madrid	0.01	0.14	0.28	0.41	0.54	0.69	0.81	0.95	14.6	9.3	6.9	5.5	4.6	3.9	3.4	3.0

References

1. UNFCCC. The Paris Agreement, 2021 United Nations Framework Convention on Climate Change. Available online: https://unfccc.int/process-and-meetings/the-paris-agreement/the-paris-agreement (accessed on 23 June 2021).
2. Ritchie, H. *Sector by Sector: Where Do Global Greenhouse Gas Emissions Come from?* Our World in Data: Oxford, UK, 2020. Available online: https://ourworldindata.org/ghg-emissions-by-sector#licence (accessed on 23 June 2021).
3. Eurostat. Final Energy Consumption by Sector. 2017. Available online: https://ec.europa.eu/eurostat/databrowser/view/ten00124/default/table?lang=en (accessed on 20 June 2021).
4. Economidou, M.; Atanasiu, B.; Despret, C.; Maio, J.; Nolte, I.; Rapf, O. *Europe's Buildings under the Microscope. A Country-by-Country Review of the Energy Performance of Buildings*; Buildings Performance Institute Europe (BPIE): Brussels, Belgium, 2011; pp. 35–36.
5. European Commission (EC). Action Plan for Energy Efficiency: Realising the Potential, Communication from the Commission, COM (2006) 545 Final. 2006. Available online: https://eur-lex.europa.eu/legal-content/EN/TXT/PDF/?uri=CELEX:52006DC0545&from=EN (accessed on 23 June 2021).
6. UNWTO. *Baseline Report on the Integration of Sustainable Consumption and Production Patterns into Tourism Policie*s; Technical Report; United Nations World Tourism Organization: Madrid, Spain, 2019. Available online: https://www.e-unwto.org/ (accessed on 24 June 2021).
7. Dalton, G.; Lockington, D.; Baldock, T. Feasibility analysis of stand-alone renewable energy supply options for a large hotel. *Renew. Energy* **2008**, *33*, 1475–1490, doi:10.1016/j.renene.2007.09.014.
8. Werner, S. District heating and cooling in Sweden. *Energy* **2017**, *126*, 419–429, doi:10.1016/j.energy.2017.03.052.
9. Lund, H.; Möller, B.; Mathiesen, B.V.; Dyrelund, A. The role of district heating in future renewable energy systems. *Energy* **2010**, *35*, 1381–1390, doi:10.1016/j.energy.2009.11.023.
10. Smitt, S.; Tolstorebrov, I.; Gullo, P.; Pardiñas, A.; Hafner, A. Energy use and retrofitting potential of heat pumps in cold climate hotels. *J. Clean. Prod.* **2021**, *298*, 126799, doi:10.1016/j.jclepro.2021.126799.
11. Bolaji, B.; Huan, Z. Ozone depletion and global warming: Case for the use of natural refrigerant—A review. *Renew. Sustain. Energy Rev.* **2013**, *18*, 49–54, doi:10.1016/j.rser.2012.10.008.
12. Frank, T. *Impact of Fluorinated Refrigerants and Their Degradation Products on the Environment and Health*; Technical Report; Refolution Industrielkälte GmbH: Karlsruhe, Germany, 2021.
13. Koronen, C.; Tedesco, R. *One Step Forward, Two Steps Back—A Deep Dive into the Climate Impact of Modern Fluorinated Refrigerants*; Technical report; Environmental Coalition on Standards (ECOS): Brussels, Belgium, 2021.
14. Mota-Babiloni, A.; Makhnatch, P. Predictions of European refrigerants place on the market following F-gas regulation restrictions. *Int. J. Refrig.* **2021**, *127*, 101–110, doi:10.1016/j.ijrefrig.2021.03.005.
15. Zolcer Skačanová, K.; Battesti, M. Global market and policy trends for CO_2 in refrigeration. *Int. J. Refrig.* **2019**, *107*, 98–104, doi:10.1016/j.ijrefrig.2019.08.010.
16. Lorentzen, G. Revival of carbon dioxide as a refrigerant. *Int. J. Refrig.* **1994**, *17*, 292–301, doi:10.1016/0140-7007(94)90059-0.
17. Lorentzen, G.; Pettersen, J. A new, efficient and environmentally benign system for car air-conditioning. *Int. J. Refrig.* **1993**, *16*, 4–12, doi:10.1016/0140-7007(93)90014-Y.
18. Nekså, P.; Rekstad, H.; Zakeri, G.; Schiefloe, P.A. CO_2-heat pump water heater: Characteristics, system design and experimental results. *Int. J. Refrig.* **1998**, *21*, 172–179, doi:10.1016/S0140-7007(98)00017-6.
19. Nekså, P. CO_2 heat pump systems. *Int. J. Refrig.* **2002**, *25*, 421–427, doi:10.1016/S0140-7007(01)00033-0.
20. Stene, J. Residential CO_2 heat pump system for combined space heating and hot water heating. *Int. J. Refrig.* **2005**, *28*, 1259–1265, doi:10.1016/j.ijrefrig.2005.07.006.
21. Tosato, G.; Artuso, P.; Minetto, S.; Rossetti, A.; Allouche, Y.; Banasiak, K. Experimental and numerical investigation of a transcritical CO_2 air/water reversible heat pump: Analysis of domestic hot water production. In Proceedings of the 14th IIR-Gustav Lorentzen Conference on Natural Refrigerants, Kyoto, Japan, 6–9 December 2020; IIR: Paris, France, 2020.
22. Dai, B.; Qi, H.; Liu, S.; Zhong, Z.; Li, H.; Song, M.; Ma, M.; Sun, Z. Environmental and economical analyses of transcritical CO_2 heat pump combined with direct dedicated mechanical subcooling (DMS) for space heating in China. *Energy Convers. Manag.* **2019**, *198*, 111317, doi:10.1016/j.enconman.2019.01.119.
23. Byrne, P.; Miriel, J.; Lenat, Y. Design and simulation of a heat pump for simultaneous heating and cooling using HFC or CO_2 as a working fluid. *Int. J. Refrig.* **2009**, *32*, 1711–1723, doi:10.1016/j.ijrefrig.2009.05.008.
24. Diaby, A.T.; Byrne, P.; Maré, T. Simulation of heat pumps for simultaneous heating and cooling using CO_2. *Int. J. Refrig.* **2019**, *106*, 616–627, doi:10.1016/j.ijrefrig.2019.03.010.
25. Liu, Y.; Groll, E.A.; Yazawa, K.; Kurtulus, O. Theoretical analysis of energy-saving performance and economics of CO_2 and NH_3 heat pumps with simultaneous cooling and heating applications in food processing. *Int. J. Refrig.* **2016**, *65*, 129–141, doi:10.1016/j.ijrefrig.2016.01.020.
26. Adriansyah, W. Combined air conditioning and tap water heating plant using CO_2 as refrigerant. *Energy Build.* **2004**, *36*, 690–695, doi:10.1016/j.enbuild.2004.01.014.
27. Farsi, A.; Mohammadi, S.; Ameri, M. An efficient combination of transcritical CO_2 refrigeration and multi-effect desalination: Energy and economic analysis. *Energy Convers. Manag.* **2016**, *127*, 561–575, doi:10.1016/j.enconman.2016.09.038.

28. Singh, S.; Hafner, A.; Banasiak, K.; Seshadri, S.; Maiya, P.; Smitt, S.; Gabrielii, C.H. Heat pump/chiller system for centralized kitchens in India. In Proceedings of the 14th IIR-Gustav Lorentzen Conference on Natural Refrigerants, Kyoto, Japan, 7–9 December 2020; IIR: Paris, France, 2020.
29. Smitt, S.; Tolstorebrov, I.; Hafner, A. Integrated CO_2 system with HVAC and hot water for hotels: Field measurements and performance evaluation. *Int. J. Refrig.* **2020**, *116*, 59–69, doi:10.1016/j.ijrefrig.2020.03.021.
30. Smitt, S.; Tolstorebrov, I.; Hafner, A. Performance improvement of integrated CO_2 systems with HVAC and hot water for hotels. *Therm. Sci. Eng. Prog.* **2021**, *23*, 100869, doi:doi.org/10.1016/j.tsep.2021.100869.
31. Tosato, G.; Girotto, S.; Minetto, S.; Rossetti, A.; Marinetti, S. An integrated CO_2 unit for heating, cooling and DHW installed in a hotel. Data from the field. *J. Phys. Conf. Ser.* **2020**, *1599*, 012058.
32. Hafner, A.; Girotto, S.; Tosato, G. *CO_2 Heat Pump Water Chillers*; Eurammon Symposium/Webinar: Frankfurt, Germany, 2020.
33. Pardiñas, Á.Á.; Hafner, A.; Banasiak, K. Novel integrated CO_2 vapour compression racks for supermarkets. Thermodynamic analysis of possible system configurations and influence of operational conditions. *Appl. Therm. Eng.* **2018**, *131*, 1008–1025, doi:10.1016/j.applthermaleng.2017.12.015.
34. Dassault Systems. DYMOLA Systems Engineering: Multi-Engineering Modeling and Simulation based on Modelica and FMI. 2019. Available online: https://www.3ds.com/products-services/catia/products/dymola/ (accessed on 1 May 2021).
35. TLK-Thermo GmbH. TIL Suite—Simulates Thermal Systems. 2020. Available online: https://www.tlk-thermo.com/index.php/en/software/til-suite (accessed on 1 May 2021).
36. TLK-Thermo GmbH. TILMedia Suite—Software Package for Calculating the Properties of Thermophysical Substances. 2020. Available online: https://www.tlk-thermo.com/index.php/en/software/tilmedia-suite (accessed on 1 May 2021).
37. Wagner, W. *Strömung und Druckverlust (Flow and Pressure Drop)*; Vogel: Höchberg, Germany, 2008; p. 67.
38. Haaf, S. Wärmeübertragung in luftkühlern (Heat transfer in air coolers). In *Wärmeaustauscher (Heat Exchangers)*; Springer: Berlin/Heidelberg, Germany, 1988; pp. 435–491.
39. Schmidt, T.E. Heat transfer calculations for extended surfaces. *Refrig. Eng.* **1949**, *57*, 351–357.
40. Huang, D.; Wu, Z.; Sunden, B. Pressure drop and convective heat transfer of Al2O3/water and MWCNT/water nanofluids in a chevron plate heat exchanger. *Int. J. Heat Mass Transf.* **2015**, *89*, 620–626, doi:10.1016/j.ijheatmasstransfer.2015.05.082.
41. Gullo, P.; Elmegaard, B.; Cortella, G. Advanced exergy analysis of a R744 booster refrigeration system with parallel compression. *Energy* **2016**, *107*, 562–571, doi:10.1016/j.energy.2016.04.043.
42. Brennen, C.E. *Fundamentals of Multiphase Flow*; Cambridge University Press: Cambridge, UK, 2005; doi:10.1017/CBO9780511807169..
43. Elbel, S.; Hrnjak, P. Experimental validation of a prototype ejector designed to reduce throttling losses encountered in transcritical R744 system operation. *Int. J. Refrig.* **2008**, *31*, 411–422, doi:10.1016/j.ijrefrig.2007.07.013.
44. Gullo, P.; Hafner, A.; Banasiak, K. Transcritical R744 refrigeration systems for supermarket applications: Current status and future perspectives. *Int. J. Refrig.* **2018**, *93*, 269–310, doi:10.1016/j.ijrefrig.2018.07.001.
45. Norwegian Standard (NS). NS-EN 14825:2018 (English Translation). *Air Conditioners, Liquid Chilling Packages and Heat Pumps, with Electrically Driven Compressors, for Space Heating and Cooling: Testing and Rating at Part Load Conditions and Calculation of Seasonal Performance*; Norwegian Council for Building Standardization: Oslo, Norway, 2018.
46. Meteotest AG. Meteonorm Software—Worldwide Irradiation Data. 2021. Available online: https://meteonorm.meteotest.ch/en/ (accessed on 1 May 2021).
47. United States Environmental Protection Agency. Refrigerant Transition & Environmental Impacts. 2020. Available online: https://www.epa.gov/mvac/refrigerant-transition-environmental-impacts (accessed on 23 June 2021).
48. EMERSON Climate Technologies. Refrigerant Choices for Commercial Refrigeration—Finding the Right Balance. Technical report No.: TGE124-091/E. 2010. Available online: https://climate.emerson.com/ (accessed on 18 June 2021).
49. European Environment Agency. Greenhouse Gas Emission Intensity of Electricity Generation. 2020. Available online: https://www.eea.europa.eu/data-and-maps/indicators/overview-of-the-electricity-production-3/assessment-1 (accessed on 23 June 2021).
50. Rezayan, O.; Behbahaninia, A. Thermoeconomic optimization and exergy analysis of CO_2/NH_3 cascade refrigeration systems. *Energy* **2011**, *36*, 888–895, doi:10.1016/j.energy.2010.12.022.
51. Sanaye, S.; Shirazi, A. Thermo-economic optimization of an ice thermal energy storage system for air-conditioning applications. *Energy Build.* **2013**, *60*, 100–109, doi:10.1016/j.enbuild.2012.12.040.
52. Gullo, P.; Elmegaard, B.; Cortella, G. Energetic, exergetic and exergoeconomic analysis of CO_2 refrigeration systems operating in hot climates. In Proceedings of the 28th International Conference on Efficiency, Cost, Optimization, Simulation and Environmental Impact of Energy Systems, Pau, France, 30 June–3 July 2015.
53. Fazelpour, F.; Morosuk, T. Exergoeconomic analysis of carbon dioxide transcritical refrigeration machines. *Int. J. Refrig.* **2014**, *38*, 128–139, doi:10.1016/j.ijrefrig.2013.09.016.
54. Garrett, D.E. *Chemical Engineering Economics*; Springer Science & Business Media: Berlin/Heidelberg, Germany,2012.
55. Wang, Y.; Ye, Z.; Song, Y.; Yin, X.; Cao, F. Energy, exergy, economic and environmental analysis of refrigerant charge in air source transcritical carbon dioxide heat pump water heater. *Energy Convers. Manag.* **2020**, *223*, 113209, doi:10.1016/j.enconman.2020.113209.
56. Blarke, M.B. Towards an intermittency-friendly energy system: Comparing electric boilers and heat pumps in distributed cogeneration. *Appl. Energy* **2012**, *91*, 349–365, doi:10.1016/j.apenergy.2011.09.038.

57. Pardiñas, Á.Á.; Contiero, L.; Hafner, A.; Banasiak, K.; Larsen, L.F. Attaining a higher flexibility degree in CO_2 compressor racks. In Proceedings of the 14th IIR-Gustav Lorentzen Conference on Natural Refrigerants, Kyoto, Japan, 6–9 December 2020; IIR: Paris, France, 2020.
58. Eurostat. Electricity Prices for Non-Household Consumers. 2020. Available online: https://ec.europa.eu/eurostat/statistics-explained/index.php?title=Electricity_price_statistics (accessed on 1 June 2021).

Paper I

S. Smitt, A. Hafner (2018). "Integrated energy concepts for high performance hotel buildings." In: *Proceedings of the 13th IIR Gustav Lorentzen Conference on Natural Refrigerants*, València, Spain.

10.18462/iir.gl.2018.1113

INTEGRATED ENERGY CONCEPTS FOR HIGH PERFORMANCE HOTEL BUILDINGS

Silje Marie Smitt, Armin Hafner
Norwegian University of Science and Technology,
Kolbjørn Hejes vei 1D, 7491 Trondheim, Norway,
silje.smitt@ntnu.no, armin.hafner@ntnu.no

ABSTRACT

Integrated energy concepts with heat recovery are not widely applied for hotels, i.e. there is a huge potential to further reduce the specific primary energy demand in this kind of buildings. The development and implementation of such concepts would reduce the cost of ownership and the environmental footprints in the sector, significantly.

A combined heat pump and refrigeration system applying carbon dioxide (CO_2) and propane is presented for the main and backup system, respectively. Grey Water (GW) usage and thermal energy storage are included in the energy system. A model of the system has been developed and several simulations were carried out in order to investigate the energy demand of a hotel building in several scenarios and ambient temperatures.

The integrated energy system can efficiently provide heating, Air Conditioning (AC), Domestic Hot Water (DHW) and refrigeration capacities at various temperature levels. The implementation of thermal storage resulted in both reduction and delay of peak loads.

Keywords: CO_2 heat pump and refrigeration, hot and cold thermal energy storage, integrated energy systems

1. INTRODUCTION

The EU fluorinated greenhouse gas regulation aims for a major phase out of hydrofluorocarbons (HFCs) by the year 2030, which grants natural working fluids a strong position in regards to implementation in new systems (Heath, 2017). CO_2 and propane are both natural working fluids widely used in both heat pumps and chiller units. Due to heat rejection at gliding temperatures in the transcritical region, CO_2 is exceptional for DHW heating. Propane, on the other hand, is suitable for both low and medium temperature applications. If combined in an integrated system, excessive heating and cooling loads can be efficiently covered. By introducing an energy system that employs natural working fluids to cover all thermal demands, one is able to induce both economic and environmental benefits.

This paper aims to investigate the energy related potential of a combined heat pump and refrigeration system intended for hotels in cold climates, where the combined demands for DHW, space heating and cooling are substantial. The main motivation behind the system design is to utilize excess heat for useful purposes, which otherwise would be disregarded. By recovering heat from freezing rooms, refrigerated rooms and the AC circuit to provide space heating and to produce DHW, one is able to provide multiple services simultaneously.

Optimizing features, such as heat recovery from additional heat sources, like GW and thermal energy storage, have been included in order to balance the daily thermal demands. These elements will function as thermal buffers that provide peak load reduction and allow, to a greater extent, optimum operational conditions for both the CO_2 and propane heat pumps. Combined heating and cooling systems using CO_2 are mainly found within the supermarket industry, where excess heat is integrated into space heating, DHW and even district heating (Polzot et. al, 2017; Hafner and Banasiak, 2016; Selvnes, 2017). Stene (2004) described the use of a tripartite CO_2 gas cooler for domestic hot water and space heating supply in different operational modes. However, few investigations have been carried out regarding combined CO_2 systems for large scale building with complex heating and cooling demand, such as hotels.

2. INTEGRATED SYSTEM SOLUTION AND SIMULATION MODEL

2.1 Building modeling and load estimations

A building model of a hotel had to be made in order to estimate the annual demand for DHW, space heating and cooling. A model, based on the building design of *Britannia Hotel Trondheim,* was created in the software *Simien*[1]. The building occupies 4 floors and has a combined floor area of 8400 m^2, including 247 guest rooms. The building body is modeled as a single temperature zone with 24-hour operation of the heating and cooling systems. The building construction is assumed to meet minimum standards in accordance to the *Norwegian Building Regulations (TEK10).* Climate data for Trondheim were used in the simulation. Additional demand curves for conference rooms, refrigerated rooms and freezers were constructed using *CoolPack*[2]. As infiltration losses due to high activity are sporadic, it is assumed that the load from refrigeration rooms and freezers are constant. The cooling demand for refrigeration rooms and freezers were assumed to be 5 kW and 10 kW, respectively. The DHW consumption for the hotel has been estimated based on *Standard Norway* SN/TS 3031:2016 and has an average demand of 30 kW and a peak of 70 kW. To simplify the energy flow tool, a constant operational load per hour is assumed. Figure 1 displays the annual accumulated load-duration curve for the hotel. Thermal loads for one week were picked for each season to serve as input data in the *Dymola*[3] energy simulation model.

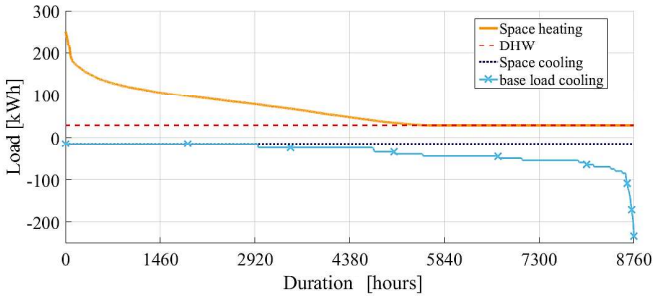

Figure 1: Annual load-duration curve for the hotel including space heating and AC, DHW and the base load cooling from refrigeration and freezing rooms

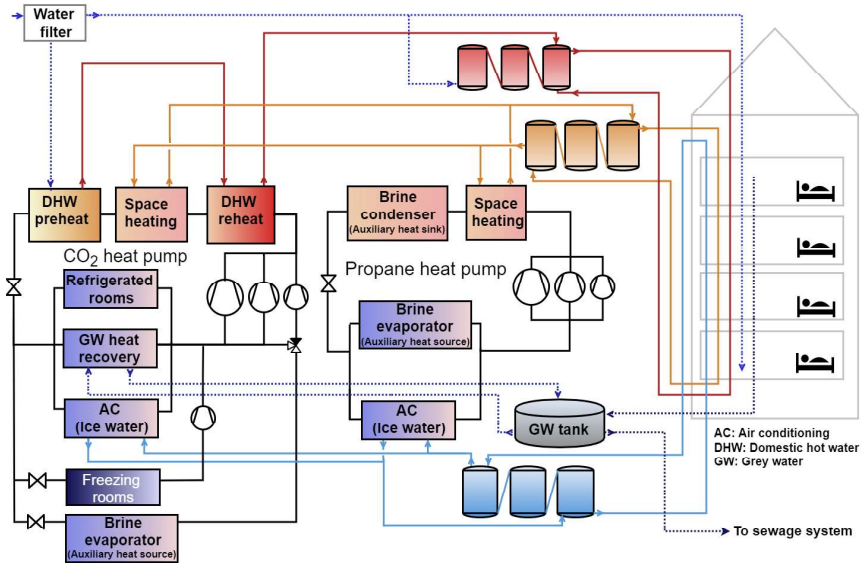

Figure 2: Conceptual sketch of integrated energy system

[1] Building energy simulation software by *ProgramByggerne, http://www.programbyggerne.no/.*
[2] Refrigeration system modeler by *IPU*, http://www.en.ipu.dk/Indhold/refrigeration-and-energy-technology/coolpack.aspx.
[3] Dynamic modeling software by *Dassault Systèmes*, https://www.3ds.com/products-services/catia/products/dymola/.

2.2 Integrated energy system concept

The main energy system concept is to provide flexibility according to the demand for DHW, space heating and AC. The combined system for the hotel consists of two separate heat pumps working in parallel, as presented in Figure 2. The primary system utilizes CO_2 as a working fluid to mainly produce DHW from continues sources, such as refrigerated rooms and freezers. A propane heat pump can be employed in parallel to the primary system for redundancy or in case additional heating or AC is needed. The propane heat pump thus functions as a backup system that is activated if the demand is larger than the load provided by the CO_2 system. The solution grants the possibility of only using the CO_2 cycle during parts of the year when space heating and AC demands are sufficiently low, for instance during late spring.

The heat pumps are provided with interfaces to indirect hydronic subsystems for distribution and collection of heat. Only the refrigerated and freezing rooms are implemented with direct cooling by CO_2 evaporators. The DHW subsystem is equipped with buffer storage tanks of a combined size of 10 m^2, as it necessary to meet instantaneous demand. Filtered water is preheated and reheated at gliding temperatures in the CO_2 gas cooler. After reaching the desired temperature of 70°C, water is supplied to tanks for storage and circulated within the hotel building. As the thermal buffer for heating purposes is charged, fluid is distributed in parallel lines to both heat pumps. The propane cycle can be operated purely as a heat pump, refrigeration unit or as a combination unit, depending on the application of the different heat exchangers.

Rather than having a direct heat exchange with ambient air, a secondary loop circuit is implemented between both heat pumps and the ambient. The circuit provides an indirect interface to the ambient, as heat can be absorbed or rejected via an air-to-brine heat exchanger, not shown in Figure 2. Dependent on necessity, the circuit can function both as heat source and heat sink within a single loop.

The low-temperature hydronic space heating system utilizes the middle section of the CO_2 temperature glide to generate water at around 35°C, which is supplied to buffer storage tanks or directly distributed for heating purposes. After heat has been rejected across the building, the fluid enters the return line and is recirculated to the tanks or to the CO_2 heat pump for reheating. Ice water is utilized as a primary heat source in the CO_2 cycle, where the brine is cooled to 7°C before storage and/or distribution. For the space heating and AC subsystems, the purpose of the thermal storage is to shift peak demands and grant a higher degree of continuous operation of the combined heating and cooling system (Fleischer, 2015). It is desirable to maximize the storing potential of the thermal energy tanks, which can be achieved by utilizing phase changing materials (PCMs). The phase change takes place at an almost constant temperature, resulting in a stable thermal environment around the elements. The PCM module tanks can be installed for both hot and cold storage. Figure 3 displays a hydronic tank equipped with PCM modules, similar to the 11,200 kWh cold storage units installed at Bergen University College (Stavset and Kauko, 2015).

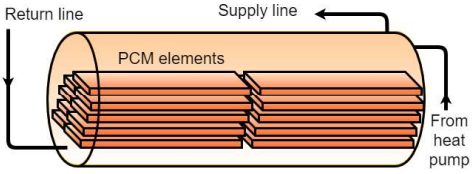

Figure 3: PCM tank for hot and cold thermal storage

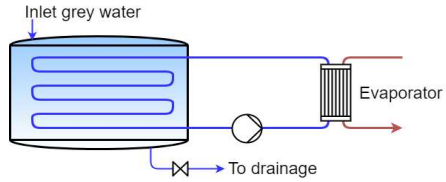

Figure 4: GW heat recovery with secondary fluid circulation to evaporator

The hotel energy system model was equipped with both a space heating and cooling energy reservoir of approximately 500 kWh and 440 kWh, respectively. This corresponds to a 10 m^3 tank with PCM elements of the same capacity as the aforementioned installation for both heating and cooling. Compared to sensible hydronic energy storage of equal sizes, this is a 473- 481 % increase in capacity. This type of energy storage was used in the model with a temperature difference of 10 K and 5 K for heating and cooling, respectively.

Optimizing measures related to thermal energy production involves covering demands by utilizing available and easily accessible heat sources. For buildings with large DHW demand, GW is a potential heat source that will remain fairly constant throughout the year. GW is in this paper defined as drainage water from showers, bathtubs, sinks, dishwashers and washing machines, which generally has a high temperature before entering the sewage system. The potential energy to be recovered from the fluid is dependent on the supply temperature of the GW and the temperature approach in the heat exchanger, where the amount of available heat is tied to the DHW consumption. By assuming that GW has a temperature difference of 18 K in the heat exchanger (from 20 °C to 2 °C), the potential maximum heat recovery is 275 kWh/day. A storage system for GW that can function as a buffer is implemented, as illustrated in Figure 4. The indirect solution is beneficial as the water impurities are limited to the GW tank, which represents a standard solution.

2.3 Main heat pump and refrigeration concept

The CO_2 system is designed for operations at low pressure (LP), medium pressure (MP) and a regulative parallel pressure level that is dependent on ambient temperature, as illustrated in Figure 5. The system concept aims to incorporate as many available heat sources as possible. The refrigerated rooms and freezers require continuous operation of the heat pump, resulting in 24/7 generation of heat, which is stored (e.g. DHW) for later use.

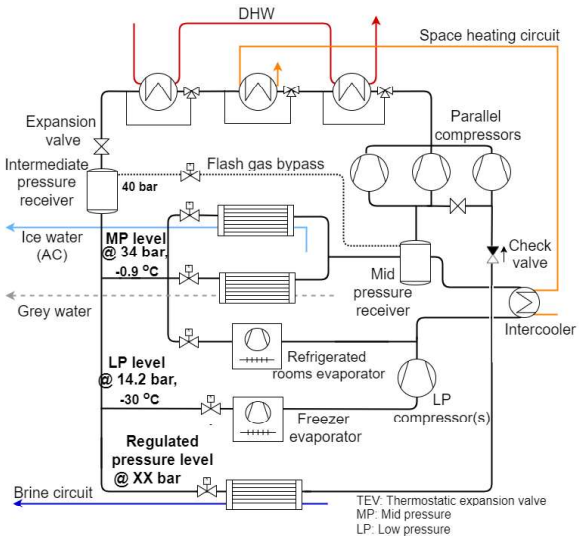

Figure 5: Integrated CO_2 heat pump and chiller unit with MT and LT cooling loads, DHW, space heating and AC with auxiliary regulative pressure level and GW heat recovery

The gas cooler configuration consists of three heat exchangers in series, which deliver heat to the DHW and space heating circuits. In the gas cooler, heat is rejected at relatively constant pressure until it reaches a temperature in the proximity of the inlet DHW. During seasons with no demand for space heat, the middle heat exchanger is bypassed and all the heat is applied for DHW. The high-pressure side is regulated for an optimum heat transfer, dependent on the gas cooler arrangement. From the gas cooler, the fluid is expanded from the high-pressure side to an intermediate pressure receiver at 40 bar. The receiver is a flash tank where vapor is removed through a bypass to the MP receiver. Hence, only fluid of low vapor quality is entering the various evaporators downstream.

The CO_2 cycle recovers thermal energy from the ice water, the refrigerated rooms and the GW at the MP level. After evaporation, the gas proceeds to the MP receiver, which serves several purposes, such as preventing liquid carryover to the second stage compressors. Consequently, it enables the possibility of running the evaporators flooded. The MP receiver functions as an intercooler for the gas from the LP stage, and assists in evaporating liquid present in the tank. When heat recovery from GW is not sufficient to cover the DHW demand, the interface to the brine circuit is employed and the parallel compressor is activated. The current parallel circuit implementation enables the possibility for the compressor to function in several ways. When the ambient temperature, and thus brine temperature, provides the means of evaporation close to the MP level, it is possible to run the parallel compressor incorporated in MP compressor arrangement. This is achieved by opening the valve on the suction manifold between the compressors. The compressors will then work in a single stage. Switching of different compressor suction lines could reduce investment cost and improve compactness in the CO_2 unit (Hafner et al., 2016).

During cold seasons, the ambient reaches a temperature close to or below that of the CO_2 MP level evaporating temperature (-0.9 °C), which makes it difficult to operate the parallel compressor integrated in the medium compressor arrangement. The valve between the compressors will then be closed and the parallel compressor is dismantled from the MP level. The brine evaporator circuit then operates with a parallel compressor to the rest of the system and thus enables evaporation at low ambient temperatures.

2.4 Dymola simulation setup and control strategy

The object-orientated simulation tool, *Dymola,* together with *TIL-Media* library*,* was applied for the construction and simulation of the energy system. The hotel energy system has been modeled in a single model structure and has been simplified in design for simulation purposes: PCM tanks have been modeled as hydronic tanks with equal energy storage capacity: the brine circuit interfaces have been modeled as direct-air heat exchange units. The following assumptions has been made for the overall system:

- No unintentional pressure loss in components
- No unintentional heat transfer between components and the ambient
- Constant heat transfer in all heat exchangers
- Constant speed, volumetric and isentropic efficiency of 0.70 in all compressors

Additional details regarding the model is described in Smitt (2017).

The system must be controlled according to both heating and cooling demands. This becomes especially challenging during parts of the year when neither heating nor AC demand is in vast dominance, but still of a certain magnitude. When this occurs, both the CO_2 and propane heat pumps are active. The operational strategy is then coordinated according to both contributions, due to the shared sources and sinks, e.g. space heating and AC. The CO_2 system produces maximum possible space heat within the temperature glide, but at the same time, the magnitude of heat produced is dependent on the cooling provided. Whether or not this heat is sufficient to meet the next peak demand is thus dependent on variables beyond the instantaneous charge in the thermal storage. The control strategy for the system is presented for the following three scenarios:

- Heating mode
  When the system is running in heating mode, all available sources are utilized for such a purpose. The CO_2 cycle collects heat from GW, in addition to the base load from refrigeration rooms and freezers. The brine circuit interface is activated as a backup source, should there be need for additional heating. If space heating demand predominates that of DHW, the gas cooler is controlled for maximum rejecting to this circuit. This is managed by controlling the water flow through the heat exchangers and reducing the pressure in the gas coolers, ensures a more leveled heat rejection curve. Similar to the CO_2 system, the propane heat pump will use the brine circuit as a heat source in case the ice water tanks are fully charged.
- Cooling mode
  During cooling mode, the space heating demand is insignificant and the thermal storage is fully charged. The CO_2 heat pump therefore only includes the necessary base load functions from refrigeration rooms and freezers, in addition to the ice water interface. The DHW buffer is utilized as a heat sink in the CO_2 circuit. Hence, the heat exchanger interface to the space heating circuit is bypassed. The GW heat recovery is bypassed in the CO_2 circuit, as the integrated systems is functioning as a chiller unit producing ice water for AC. The surplus heat from the propane system is rejected to the ambient via the secondary circuit, as this heat pump is working purely in refrigeration mode.
- Combined heating and cooling mode
  When neither heating nor cooling demands are excessive, only the CO_2 unit is employed. The system functions as a combined heat pump and chiller unit that provides DHW, space heat and AC. The ice water circuit provides the majority of heat to the system and is supplemented by GW heat recovery if necessary. Only when all other available heat sources have been exerted is the brine interface towards the ambient air at the regulative pressure level activated. The propane unit is employed if there are additional thermal demands and the integrated system will then be operating in either heating or cooling mode.

2.5 Results and discussion

The simulated results are given for three seasons, where all thermal demands are covered by the integrated energy system. The results are concentrated around CO_2 system performance for fall/spring simulations, as this scenario is representative for the largest period of the year. The main focus of the simulated results is to review the system performance under different operational conditions. The energy consumption in relation to pumps and fans is not considered in the results, only work from the compressors. Figure 6 depicts the CO_2 system and propane system efficiency for all seasons, respectively. The energy efficiencies are defined as all useful thermal contributions divided by the total compression work within the compression cycle, as stated in equations 1

$$CO_2\ energy\ efficiency = \frac{H_{Gas\ Cooler} + H_{Intercooler} + C_{Freezing\ Rooms} + C_{Refrigerated\ rooms} + C_{AC}}{W_{MP} + W_{LP} + W_{Regulated\ pressure\ level}} \quad \text{(eq. 1)}$$

where *H* and *C* represent heating and cooling contributions, respectively. The yearly average energy efficiency for the CO_2 system of 5.55 is calculated based on the average energy efficiency values for the simulated weeks, with the summer and winter results weighted at 25% each, while the fall/spring result is weighted 50%. Compared to a conventional hotel heat pump solution (coefficient of performance = 4) with 80% space heating coverage, electric generated DHW and no heat recovery, the purposed combined system would provide a 68% reduction in operational costs.

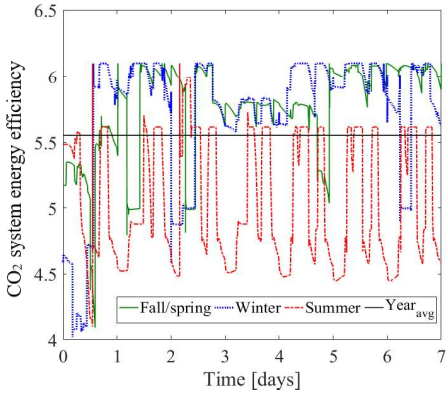

Figure 6: CO_2 system energy efficiency for all simulated seasons

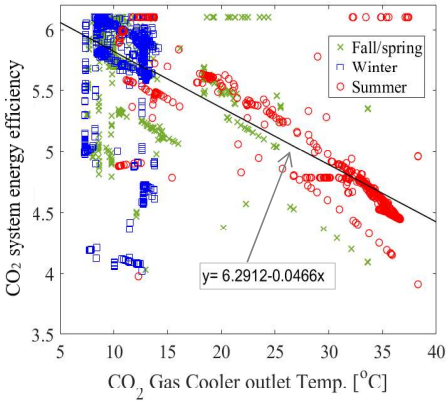

Figure 7: Energy efficiency related to CO_2 gas cooler outlet temperature

Figure 7 shows the CO_2 system energy efficiency related to gas cooler outlet temperature. The efficiency is considerably higher for winter conditions as the heating demand is larger and the gas cooler outlet temperature has a maximum of about 15 °C due to low ambient temperatures. Figure 8 illustrates the operation of the propane system. Due to the combined operation of heating and cooling, as well as large thermal buffers, the system is able to operate continuously for long periods of time.

A total of 1994 kWh is rejected thought the brine evaporator to the ambient during the simulated summer week. It is evident that there is a relation between heat rejection and total heating demand for the hotel as the amount of energy rejected to the ambient is at its lowest for the winter simulation, with

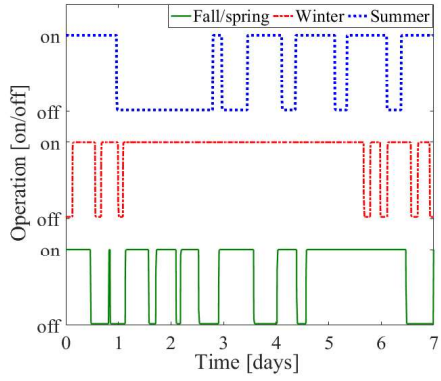

Figure 8: Operation of propane system for all simulated seasons

an average of 64 kWh per day. However small, the disregarded heat represents a loss in the system and should be assessed. As heat rejection accounts for approximately 9% of the annual operational costs, it should be investigated if simultaneous deployment of all three gas coolers at the same time is the best strategy. An alternative solution is to only supply heat to one subsystem at a time. The second gas cooler would then be bypassed during charging of the DHW tanks. Only when the tanks are fully charged would the first and third gas coolers be bypassed. The CO_2 pressure is regulated for optimal heat rejection to the space heating circuit, as this interface is reconnected. This procedure would repeat itself when the DHW tanks are close to empty. The separate heat rejection strategy and CO_2 pressure adaptation could potentially reduce the heat rejection a great deal.

For all simulations, the heat exchanger in the regulative pressure level is only utilized at the beginning of the simulated week. This is due to the fact that the DHW tanks are empty at the start of each simulation and need quick charging. If not taking this circumstance into consideration, it can be questioned whether or not this evaporator is dispensable under normal operational conditions. 410 kWh is recovered from the GW over a two-day period for the fall/spring simulated week. However, the GW could be employed in a different manner. A possibility is controlling the mass flow of GW, and thus heat recovery, according to the load variations in the CO_2 MP level. If regulating the mass flow of GW in order to stabilize this level, one can insure fewer variations in MP compressor mass flow. This will, however, require more or less continuous heat recovery and a certain GW storage capacity. Figures 9 and 10 show the instantaneous space heating and AC production versus the actual demands. For both cases, the load is reduced significantly due to the magnitude of the thermal storage. For space heating and AC, the maximum peaks are reduced with 22.3 kW and 31.4kW, respectively.

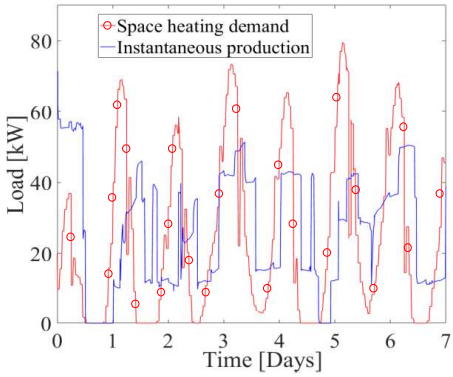

Figure 9: Space heating production versus actual demand for fall/spring scenario

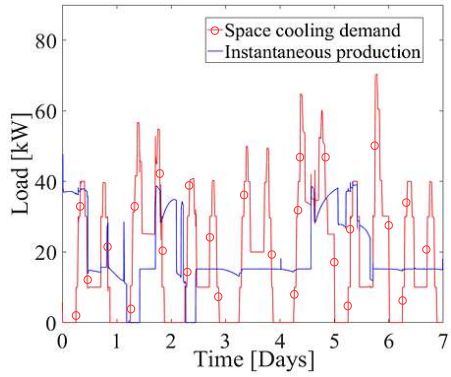

Figure 10: Space cooling production versus actual demand for fall/spring scenario

The heating system peak load is delayed with a few hours each day, representing the effects of the thermal buffer. Reduction and balancing of the heat demand variations would allow for a smaller installed heat pump unit working with a higher degree of continuous operations. In order to evaluate how the size of the space heating and cooling tanks influence the performance of the system, simulations with different storage volumes have been performed. Figure 12 depicts the space heating production load versus the actual demand over an interval of 24 hours. The storage volumes of both space heating and cooling have been evaluated for 50% and 8% of the original volumes. The base load case of 100% capacity is equivalent to the plot presented in Figure 9 (day 3), where the peak is considerably lower than the demand. As the sizes of the tanks decrease, the load required to cover the demand increases. For the 50% capacity case, the load is well above the actual space heating demand. This is due the low charge in the space heating tank, which triggers a high compressor displacement as the system attempts to cover the demand while charging the tank. The 8% capacity case illustrates the production load when there is nearly no thermal buffer. As the space heating demand is

approaching its peak, the compressor overcompensates the displacement, similar to the 50% capacity case. One major difference between the cases is that the peak load is not delayed when the volume is reduced to 8%. As the compressor attempts to cover the load, it turns on and off sporadically. In comparison with the original case of 100% capacity, the compressors and heat exchangers would have to be dimensioned for a higher load and the energy efficiency of the system would be reduced with at least 50%, as combined heating and cooling operations are highly limited.

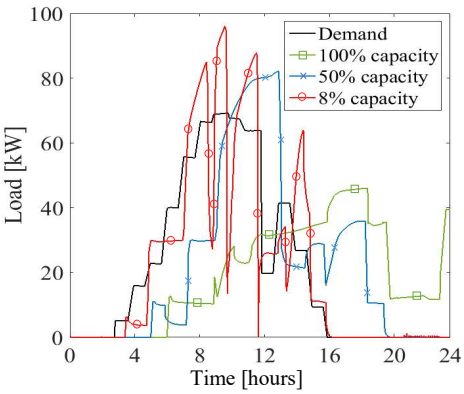

Figure 12: Space heat demand versus actual production load for different tank sizes

Another design aspect that should be assessed is the arrangement of the CO_2 MP level. In the current design, the refrigeration load of 5 kW and the room temperature requirement of 3 °C are governing the MP. As the space heating load is decidedly larger, the MP should be raised to a level where production of ice water is optimized. The refrigeration rooms could alternatively run on a separate lower pressure level with its own compressor. In addition, direct evaporation, rather than by use of ice water, should be considered for large and continuous AC loads, such as accumulated by the commercial kitchens and central HVAC units. Hence, a secondary energy transfer would be eliminated and ice water pump work would be reduced.

3. CONCLUSION

The results from the simulations reveals a high efficiency for the CO_2 unit, as the thermal buffers make it possible to utilize the heat pumps simultaneously for both heating and refrigeration. The CO_2 heat pump has an average energy efficiency of 5.55, due to combined operations and heat recovery from available sources. The purposed system is able to cover all thermal demands for the simulated scenarios. This includes DHW, space heating, AC and refrigeration of cold storage rooms. There is a strong relationship between ambient temperature and CO_2 energy efficiency. For optimal heat pump performance, the CO_2 gas cooler outlet temperature should be less than 15 °C. The magnitude of the storage tanks limits the number of compressor stops and enables a high energy efficiency for the system. By implementing thermal storage for space heating and cooling, the compression work is reduced considerably in comparison to actual demand. The consequence of this is that peak loads are delayed with a few hours, which was the same effect expected from the PCM modules. More stable operation with a 20-30 kW peak reduction is achieved in relation to both space heating and AC. The integrated energy system is more profitable in regards to operational costs, in comparison to more conventional hotel heat pump solutions. System improvements includes evaluating alternatives for heat production in order to reduce heat rejection; employing GW heat recovery according to load variations in the MP level; installation of refrigeration rooms on a separate pressure level, which enables elevation of the CO_2 suction pressure level of the MP compressors, in accordance to ice water temperature requirements.

NOMENCLATURE

AC	Air Conditioning	HFC	Hydrofluorocarbon
C	Cooling load (kW)	HVAC	Heating Ventilation Air Conditioning
CO_2	Carbon Dioxide	LP	Low Pressure (14.2 bar)
DHW	Domestic Hot Water	MP	Medium Pressure (34 bar)
GW	Grey Water	PCM	Phase Changing Materials
H	Heating load (kW)	W	Power input (kW)

REFERENCES

Fleischer, A., 2015. Thermal energy storage using phase change materials: fundamentals and applications. Springer, Cham.

Hafner, A., Banasiak, K., 2016: Full scale supermarket Laboratory R744 Ejector supported & AC integrated parallel compression unit. Proceedings of the 12th IIR Gustav Lorentzen Natural Working Fluid Conference, Edinburgh, Scotland.

Hafner, A., & Banasiak, K. (2016). R744 ejector technology future perspectives. Journal of Physics: Conference Series, 745(3), 13.

Heath, E. A., 2017. Amendment to the Montreal Protocol on Substances that Deplete the Ozone Layer (Kigali Amendment). International Legal Materials 56 (1), 193 – 205.

Polzot, D'agaro, & Cortella. (2017). Energy Analysis of a Transcritical CO2 Supermarket Refrigeration System with Heat Recovery. Energy Procedia, 111, 648-657.

Selvnes, H., 2017. Energy distribution concepts for urban supermarkets including energy hubs. Master thesis, Norwegian University of Science and Technology, Trondheim.

Stavset, O. Kauko, H., February 2015. Energy use in nonresidential buildings: possibilities for smart energy solutions. Tech. Rep. 1.1, SINTEF Energy Usage.

Smitt, S., 2017. Integrated energy concepts for high performance hotel buildings. Master thesis, Norwegian University of Science and Technology, Trondheim.

Stene, J., 2004. Residential CO2 Heat Pump System for Combined Space Heating and Hot Water Heating. Doctoral dissertation, Norwegian university of Science and Technology, Trondheim.

Paper II

S. Smitt, A. Hafner, E. Hoksrød (2019). "Presentation of the first combined CO_2 heat pump, air conditioning and hot tap water system for a hotel in Scandinavia." In: *Proceedings of the 8th IIR International Conference on Ammonia and CO_2 Refrigeration Technologies*, Ohrid, North Macedonia.

Presentation of the first combined CO_2 heat pump, air conditioning and hot tap water system for a hotel in Scandinavia

Silje Marie SMITT[1], Armin HAFNER[1] and Erik HOKSRØD[2]

[1]Norwegian University of Science and Technology,
Kolbjørn Hejes vei 1D, 7491 Trondheim, Norway,
silje.smitt@ntnu.no, armin.hafner@ntnu.no
[2]Kelvin AS, erik.hoksrod@kelvinas.no

ABSTRACT

Hotels are high-energy consuming buildings with numerous demands for heating and cooling at several temperature levels. The heating load is largely dominated by hot water production (28%: NVE, 2016) in order to meet the hot water consumption of the many guests. The current practice is to have several independent heating and cooling systems. Most of the hotels in northern Europe use thermally inefficient methods, such as electric boilers or district heating stations, which simultaneously provide high temperature heat for tap water and a high temperature space heating circuit. Currently, CO_2 technologies are widely used in Scandinavia at an industrial scale thanks to their high efficiency in cold climates. The first combined CO_2 heating, air conditioning and hot tap water system with an integrated thermal storage for a hotel is installed (2018) in Norway (Trondheim) and is presented in this paper. The working principal of the system is clearly described in this work and data obtained from the first test campaigns are presented. The heat pump has an installed capacity of 280 kW. If cooling is needed, chilled water for AC cooling is used as a heat source. Heat is rejected to two different circuits in the gas cooler in order to achieve high and medium temperature levels according to the setpoint of the different heating applications. The tap water system is mainly composed of a 6 m^3 buffer tank storage unit, in order to ensure continuous production of hot water to covers the peak demand period. Preliminary results show significant energy savings (59-68%) and peak power reductions (15-45%).

Keywords: CO_2 heat pump, energy savings, hotel buildings, HVAC, peak power reduction

1. INTRODUCTION

Energy for heating purposes is the greatest contributor to the overall energy consumption within the Nordic hotel sector. On an average basis, hotels in Norway use approximately 240 kWh/m^2 year, where the share of space heating and hot tap water needs is about 60 % of the total energy consumption (NVE, 2016). Commonly, the hot water consumption follows a specified schedule depending on the occupancy and the daily activities (showering) e.g. in the morning (from 6 to 8 a.m.) and the evening (from 7 to 9 p.m.), which generates large consumption peaks. Very few energy systems installed in Scandinavian hotels take actions to reduce the peak power consumption that occur following these time periods of large hot water consumption. Moreover, most hotels use electric boilers or district heating stations to provide high temperature heat (80°C) to both hot water and the hydronic space heating circuit, which is neither thermally nor exergy efficient compared to low temperature hydronic heating (Hesaraki and Holmberg, 2013).

During the last few years, the interest for environmentally friendly thermal energy systems is steadily growing within the Scandinavian hotels sector. One of the main factors being the governmental restrictions in building construction and operation, which encourages the building companies to adopt new, sustainable and more environmentally friendly solutions (Swedish Ministry of the Environment (2009), Norwegian Ministry of the Environment (2008)). Moreover, the competition is getting tougher between the hotel chains, which are continuously adopting new strategies in order to present the best quality service and increase their market share. Environmental awareness is now becoming a key element and one of the main concerns in hotel marketing and branding (Lee *et al.* (2010), Bohdanowicz (2005)).

CO_2 is an environmentally friendly and natural refrigerant, which has no ozone depleting potential (ODP) and a negligible global warming potential (GWP) comparing to synthetic refrigerants. CO_2 is widely available, inexpensive, and is neither toxic nor flammable. Due to its temperature glide in transcritical cycle, CO_2 as a refrigerant is excellent for heating tap water. The technology for residential water heaters is well established (Zhang *et al.*, 2015). However, the application of CO_2 heat pumps at an industrial scale, for a combined hot water and space heating systems remains very limited. Nekså (2002) and Stene (2004) were first to describe such concepts for transcritical CO_2 heat pump systems. In their approach, heat is delivered for different tasks (e.g. hot water and floor heating) at appropriate temperature levels through a series of gas coolers (two or three). Currently, CO_2 transcritical cycles with heat recovery are mainly applied within the supermarket sector. In order to achieve a higher energy efficiency, the excess heat obtained from the gas cooling process is used for space heating, air handling unit (AHU) and hot tap water production (Stavset and Kauko (2015), Hafner and Banasiak (2016)). In this work, the first combined CO_2 heat pump and chiller unit with an integrated thermal energy storage for hotels in Scandinavia is presented. The main system components and operations are described. First operational data are collected and analyzed and main conclusions are presented.

2. SYSTEM DESCRIPTION

Scandic Hell Hotel in Trondheim, Norway, was established in 1987. Until 2018, it has been equipped with a heating system consisting of an electric boiler (for base load coverage) and an oil boiler (to cover peak loads). Figure 1 shows the CO_2 system installed in June 2018, which provides the hotel with space heating, hot tap water and AC cooling. The heat pump design is based on a typical single-stage supermarket refrigeration unit equipped with heat recovery. The CO_2 unit is composed of four parallel compressors, ranging in sizes from 17.8 m^3/h to 21.2 m^3/h (50 Hz). Only one compressor is equipped with a variable speed drive (VSD) for low load operations and for adaptive load control between the activation steps of the non-variable compressors. In comparison to a large, single VSD compressor, the presented solution is advantageous as only one compressor, carrying part of the load, is operating below its optimal point. The high pressure and load control of the heat pump is based on feedback signals from the different thermal demands, such as hot tap water, ventilation and the radiators. These signals are supplied to the controller[1], which optimizes the high-pressure level within specific constraints, such as the different setpoint temperatures. The CO_2 heat pump uses up to four 50 kW air-evaporators. In case of simultaneous cooling and heating demands, it is possible to recover heat from a chilled water heat exchanger (HX) for AC cooling. The combination of the chiller unit and the heat pump will have a double benefit: Improve the overall system efficiency and satisfy the heating needs of the hotel.

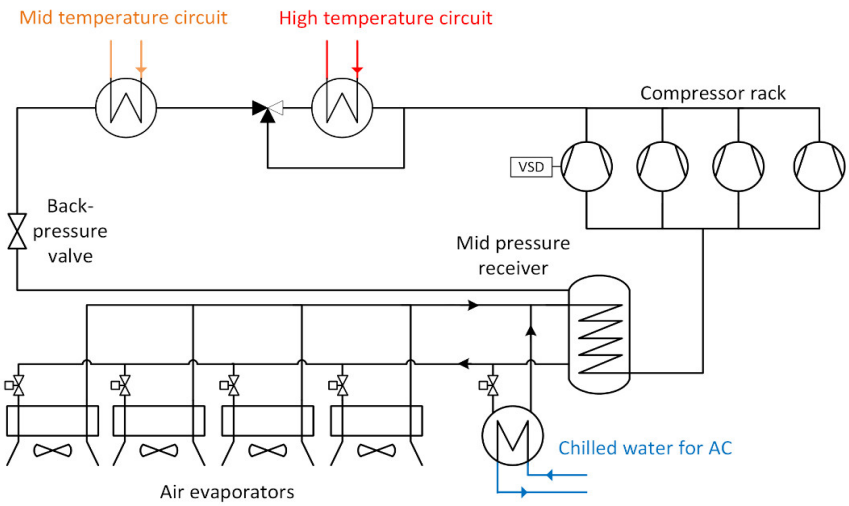

Figure 1: Layout of the combined CO_2 heat pump and chiller system

[1] Danfoss AK-PC 781

The heat pump is designed to maximize the benefit of the CO_2 temperature glide by allocating heat to adapted temperature levels and thus reduce the thermodynamic losses. The main strengths of the system lies in its operational flexibility during different seasons and with varying demands. The system rejects heat to two separate secondary hydronic circuits through a series of gas coolers (GC1 and GC2), as shown in figure 2. The mid temperature (MT) circuit provides heat primarily to ventilation batteries and a radiator circuit. The remaining heat is used to preheat the tap water from approximately 8–25°C through a heat exchanger (HX1). Next, the fluid is recirculated back to GC2. The CO_2 temperature is then further reduced and the efficiency of the cycle is thus considerably enhanced. For winter season operations, it is possible to employ the last HX in the series (HX2) for defrost of the air evaporators at temperatures close to or below 0°C.

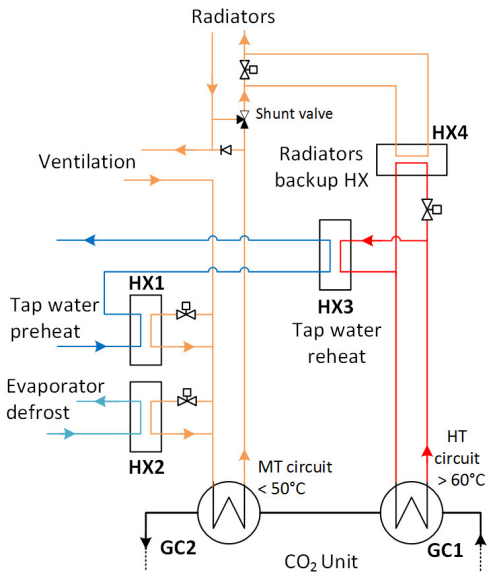

Figure 2: Layout of secondary hydronic circuits

The high temperature (HT) circuit is mainly used to reheat tap water through HX3, by the use of the recovered high temperature heat from GC1. A radiator backup interface (HX4) is also installed in the HT circuit and acts as an interface between the two secondary circuits. HX4 is only used if the radiator setpoint temperature is higher than the MT circuit setpoint temperature. In these instances, the fluid from the MT circuit is reheated past 50°C in HX4. When the fluid returning from the radiators is higher than the setpoint temperature of the MT circuit, the passage to the radiators is closed off. A shunt circuit is then established exclusively between the radiators and HX4, in order to insure a low temperature of the fluid returning to GC2.

Hot tap water is continuously produced in both the preheat and reheat HXs when there is demand for ventilation heating. A sufficiently large water storage is therefore a key factor to achieve a high system efficiency, as the heat pump to a lager extent can operate in optimal conditions. This configuration is especially advantageous in hotel facilities since the hot water consumption curve is characterized by peak hours. In case of hot water generation excess, the heat storage can represent an optimal solution as it represents two important benefits. First, it supplies the extra hot water during peak hours and secondly it allows for continuous accumulation of hot tap water, which stabilizes the compressor power input. Figure 3 describes the possibility to bypass the preheat HX and use the reheat interface for the entire heating operation in case of an instantaneous need for hot water. This configuration is also useful when there is low space heating demand, typically during summer operations. The heat pumps function is thus fully dedicated to the hot water production. The CO_2 heat pump is then controlled similarly to the traditional CO_2 residential water heaters. The high pressure of the heat pump is lifted from optimal pressure to 100 bar and is only reduced when the buffer storage system is fully charged.

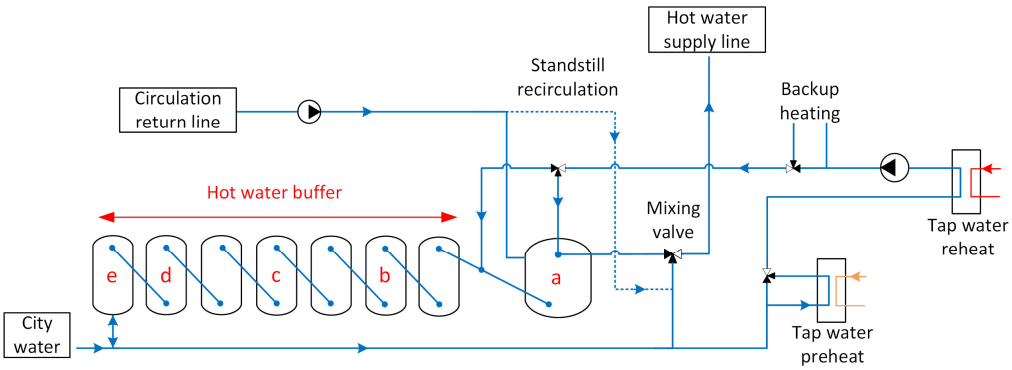

Figure 3: Hot water circuit and buffer storage system

The hot water storage system consists of a set of tanks in series, where the last seven containers of 4.2 m^3 represent the thermal buffer. The buffer storage should, as a minimum, be dimensioned to cover the entire peak demand for hot water. As most hotels are lacking an accurate overview of their water consumption, the option of integrating additional storage units should be considered during the design process.

During the charging process, the excess hot water is stored and moves through the series of tanks as the buffer is gradually charged from right to left. Water is drawn from the last tank ((*e)* in figure 3) and is directed towards HX1 and HX3 for heating. The thermal storage is fully charged when the normally stratified tanks have a high and uniform temperature throughout the buffer. During the discharging process, water is drawn from tank (*a)* and is mixed with city water to a setpoint temperature of 55°C before entering the supply line. The buffer will then become stratified as the high temperature boundary moves gradually to the right. Tank (*a*) has a storage volume of 1.8 m^3. It is designed to keep a higher temperature than the buffer in order to guarantee hot water, independent of the status of the buffer. In addition, an auxiliary electric boiler is used to cover additional heating demands.

3. RESULTS AND DISCUSSION

3.1. Hot tap water generation and storage

Temperature sensors are located at the center of each tank (a→e) (see Figure 3) to measure the bulk temperatures (Ta→Te), respectively. A typical charging and discharging cycle of the buffer over two-day period is shown in Figure 4. One may clearly note the presence of a thermal stratification inside the buffer is described by the gradual increase of temperature from tank (b) to tank (e). The storage cycle has a periodicity of 24 hours. The discharging cycles are characterized by a sudden temperature drop as the buffer is refilled with cold city water. The backup tank temperature (T_a) occasionally drops below its setpoint (55°C) and thus more heat is required from the heat pump to satisfy the set point conditions. In this case, the generated hot water flows directly to the mixing valve (see Figure 3) in order to satisfy the supply temperature requirement. This indicates that the storage volume of the buffer is not able to handle the whole hot water peaks. As a solution, either the buffer storage volume should be increased or the trigger signal for hot water production must be moved further down the buffer. The recommended position of the trigger signal should allow for the complete utilization of the buffer in the high hot water demand situations. The consequence of moving the trigger sensor down the buffer would be an increase in hot water generation at an earlier time, insuring the temperature integrity of tank *(a)*.

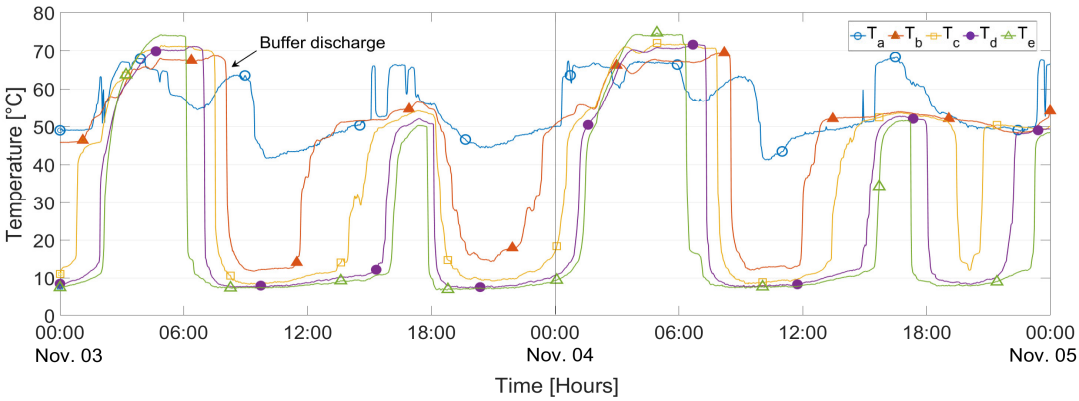

Figure 4: Thermal stratification in the thermal buffer over 48-hours (from 3.nov to 5.nov 2018)

Figure 5 shows the variation in the heat input from the CO_2 heat pump over the two-day period. It can be observed that hot water production occurs in periods of 7-8 hours. A total of 64 m^3 hot tap water is produced by the CO_2 system through the preheat and reheat HXs (HX1 and HX3), where an energy average of 1515 kWh/day is used for hot water heating. It can also be seen that the heat pump is operational for 85 % of the time over the two day period. In figure 5, 54% of the total heat output from the gas coolers is used for hot water generation. The average coefficient of performance (COP) of the entire heating system (compressors, pumps, fans) is 2.92 during the two-day period under an average ambient temperature of 7.4 °C.

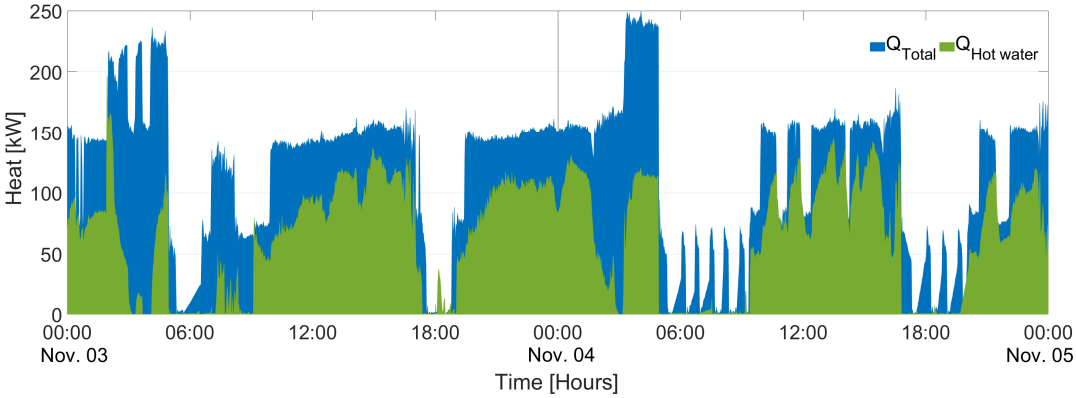

Figure 5: Heat output from CO_2 gas coolers (from 3.nov to 5.nov 2018)

3.2. First results on energy savings

Figure 6 shows the energy consumption used to satisfy the heating needs during the first six months operational period of the CO_2 heat pump and chiller system. The energy consumption in 2018 is related to data from 2015 and 2016, as complications with the heating system in 2017 rendered the energy data invalid. A significant reduction in energy consumption can be observed since the first month of operation. The relative energy savings of the system increases significantly during commissioning due to post-installation adjustments and improvements of control parameters. The inclusion of old components in the system, e.g. hydronic supply lines and ventilation heating batteries, can have a negative effect on the system efficiency in terms of pressure losses and flow assurance. The average COP of the entire heating system is 2.993 over the first six months of operation, and is being improved by replacing problematic components, such as ventilation batteries. The largest relative monthly savings occurs in October, where the energy consumption is reduced by 69 % (78,500 kWh) compared to 2016. The energy consumption stabilizes at a 59-69% reduction in the period from September to December.

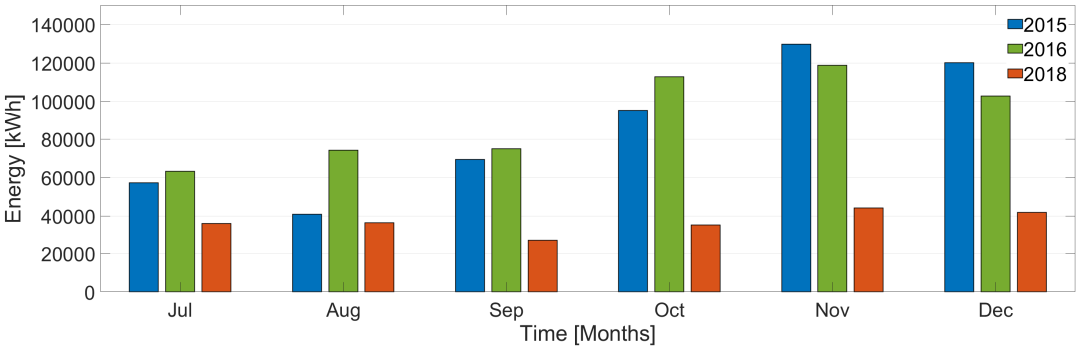

Figure 6: Heating energy consumption from July – December

Figure 7 depicts the monthly average and peak power consumption from July to December 2015, 2016 and 2018. The average power consumption is significantly reduced (59-75%) from September to December, compared to that of 2015 and 2016. A similar behavior of the peak power consumption of the system was observed. The reduction of peak power is small in July and August, but increases during the commissioning period. From October to December 2018, one may note that the entire heating systems has an average power consumption of 50-60 kW. The maximum power draw for the entire thermal system stabilizes over the same period to around 190 kW, or 54-84% compared to previous years. This is significant in terms of operational expenses, as a high peak power consumption coincide with peak power tariffs. Based on the six months of energy consumption, the specific heating energy consumption for the hotel is estimated to be 55-65 kWh/m^2 year for 2019. This is far below the Norwegian average of 144 kWh/m^2 year.

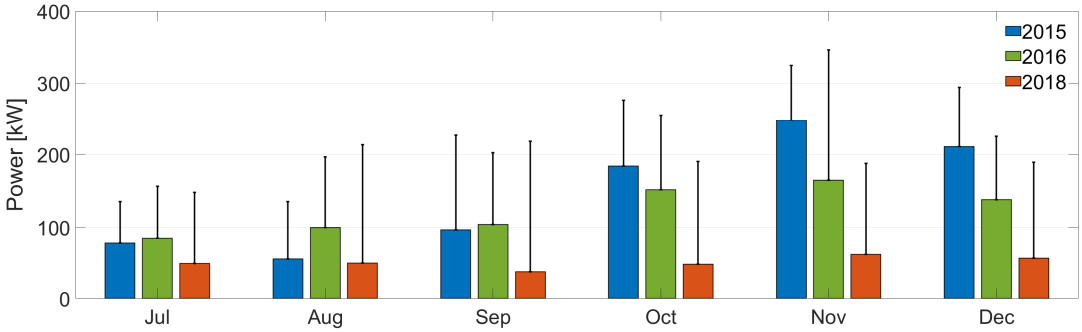

Figure 7: Power consumption in relation to heating from July - December

4. CONCLUSIONS

This paper presents the layout and working principle for the first CO_2 heat pump and chiller unit installed in a Scandinavian hotel. The system delivers heat to secondary hydronic circuits through two gas coolers in series, in order to reduce the thermodynamic losses by temperature adaptation towards the specific heating demands. Within the secondary system, heat is distributed to ventilation, radiators, hot tap water and alternatively an evaporator defrost loop. This is achieved by rejected heat in a configuration that insures a low CO_2 gas cooler outlet temperature before expansion. A large portion of the heat is allocated to hot tap water, and a large storage buffer is therefore essential in order to reduce fluctuation in operational load. The hotel has a total storage volume of 6 m^3, which handles large hot water consumption peaks in the mornings and evenings. The buffer system was charged with 64 m^3 hot water over a two day period, where production of hot water from the CO_2 system typically transpired in periods of 7-8 hours and with an intensity of 100 kW. An average of 1515 kWh/day is directed to hot tap water heating, which is about 54 % of the total heat output from the system over the period. The temperature in the first storage tank occasionally drops below its setpoint temperature and this should be corrected by moving the trigger signal for water generation. This would increase production at an earlier time and insure the temperature integrity of the hot water system.

The energy consumption and power outtake of the hotel is reduced significantly after the installation of the CO_2 heat pump and chiller unit. During the first six months of operation, a monthly maximum energy reduction of 78,500 kWh was achieved in October, describing a reduction of 69 % compared to previous years. The average COP of the CO_2 heat pump is 2.993 during the first six months, which includes the commissioning period. There is an increased interest for environmentally friendly thermal energy systems within the Scandinavian hotel sector. The solution presented in this paper presents a real potential to reduce energy and power consumption by the use of a safe, inexpensive and environmentally friendly natural working fluid.

NOMENCLATURE

AC	Air conditioning	HFC	Hydrofluorocarbons
AHU	Air handling unit	HT	High temperature
CO_2	Carbon dioxide	HX	Heat exchanger
COP	Coefficient of performance	LT	Low temperature
		VSD	Variable speed drive

REFERENCES

Bohdanowicz, P., 2005. European hoteliers' environmental attitudes: Greening the business. Cornell Hotel and Restaurant Quarterly 46, 188–204.

Hafner, A., & Banasiak, K., 2016. R744 ejector technology future perspectives. Journal of Physics: Conference Series, 745(3), 13.

Hesaraki, A. and Holmberg, S., 2013. Energy performance of low temperature heating systems in five new-built Swedish dwellings: A case study using simulations and on-site measurements. Building and Environment, 64, pp.85-93.

Stavset, O. and Kauko, H., February 2015. Energy use in non-residential buildings -possibilities for smart energy solutions. Tech. Rep. 1.1, SINTEF Energy Research.

Lee, J.-S., Hsu (Jane), L.-T., Han, H., Kim, Y., 2010. Understanding how consumers view green hotels: how a hotel's green image can influence behavioural intentions. Journal of Sustainable Tourism 18 (7), 901–914.

Norwegian Ministry of the Environment, 2008. Norwegian climate policy - Summary in English: Report No. 34 (2006–2007) to the Storting, Oslo. pp. 29 - 31.

Norwegian Water Resources and Energy Directorate (NVE), 2016. Analyse av energibruk i yrkesbygg. Report No. 24 (2016), Oslo. pp. 36 - 40.

Nekså, P., 2002. CO2 heat pump systems. International Journal of refrigeration, 25(4), 421-427.

Swedish Ministry of the Environment. A coherent climate and energy policy - climate. Government bill 2008/09:162. 2009. Stockholm.

Zhang, J. F., Qin, Y., & Wang, C. C., 2015. Review on CO2 heat pump water heater for residential use in Japan. Renewable and Sustainable Energy Reviews, 50, 1383-1391.

Paper III

S. Smitt, A. Hafner (2019). "Numerical performance investigation of a CO_2 heat pump and refrigeration system for a Nordic hotel." In: *Proceedings of the 25th IIR International Congress of Refrigeration.* Montréal, Canada.

Manuscript ID: 128
DOI: 10.18462/iir.icr.2019.128

Numerical performance investigation of a CO_2 heat pump and refrigeration system for a Nordic hotel

Silje Marie SMITT, Armin HAFNER
Norwegian University of Science and Technology,
Kolbjørn Hejes vei 1D, 7491 Trondheim, Norway,
silje.smitt@ntnu.no, armin.hafner@ntnu.no

ABSTRACT

This article evaluates the first adaptation of a CO_2 supermarket unit as an integrated solution for hotel applications. The system consists of a single unit for heating, ventilation, air conditioning (HVAC) and domestic hot water (DHW). The heat pump and chiller unit is installed in Northern Europe and has a heating and cooling capacity of 280 and 75 kW, respectively. Included in the thermal system is a 6 m^3 DHW storage for peak load shaving. A dynamic model of the system is developed in the *Modelica* programming language and the validity of the model is discussed. The model behavior is similar to actual system performance. The operational benefits of applying fixed-speed compressors are evaluated through simulations. The results show that the overall efficiency of the complete thermal system is improved by 3.8% when compared to using the current variable speed drive (VSD) control strategy.

Keywords: CO_2 heat pump and AC, combined heating and cooling systems, hot thermal energy storage, hot tap water production

1. INTRODUCTION

The interest for environmentally friendly thermal energy systems is steadily growing within the Nordic hotels sector and is becoming an important element in hotel branding (Lee *et al.* (2010), Bohdanowicz (2005)). Energy for heating purposes is the greatest contributor to the overall energy demand within the Nordic hotel sector. On an average basis, hotels in Norway require approximately 240 kWh/m^2 per year, where the share of DHW demand is about 16 % of the total energy demand (NVE, 2016). A study of water consumption in hotel chains in Europe show that 70 % of the hotel facilities use 151–250 liter of water/guest-night (Bohdanowicz *et al,* 2007). The hot water consumption follows a specified schedule depending on the occupancy and the daily activities (showering) e.g. in the morning (from 6 to 8 a.m.) and the evening (from 7 to 9 p.m.), which generates large consumption peaks (Deng *et al.* (2002), *Standard Norway* SN/TS 3031 (2016)). Very few energy systems installed in Nordic hotels take actions to reduce the peak power demand that occur following these time periods of large DHW consumption.

In order to satisfy future legislation and environmental goals, efficient and profitable energy systems must be implemented to reduce the large energy demand and environmental footprint of the sector. Integrated CO_2 heat pump and chiller systems is a solution that meets these standards and can cover all thermal needs of the hotel. CO_2 is an environmentally friendly and natural refrigerant, which has no ozone depleting potential (ODP) and a negligible global warming potential (GWP) compared to synthetic refrigerants. It is widely available, inexpensive, and is neither toxic nor flammable. Due to its temperature glide when operating in a transcritical cycle, CO_2 as a refrigerant is excellent for heating tap water and the technology for residential water heaters is well established (Zhang et al., 2015). Currently, CO_2 transcritical cycles with heat recovery are mainly applied within the supermarket sector, where excess heat obtained from the gas cooling process is used for space heating, air handling units (AHU) and DHW production (D'Agaro *et al* (2019), Hafner and Banasiak (2016)).

The first combined CO_2 heat pump and chiller unit for hotels in cold climates was installed in Norway in 2018 (Smitt *et al*, 2019). The system is equipped with 6 m^3 integrated thermal energy storage to reduce DHW consumption peaks. The buffer storage offers two important benefits as it supplies extra hot water during peak hours and enables continuous production and accumulation of DHW, which stabilizes the operation of the heat pump unit. There are generally large variations in the heating demand of the hotel during the spring/fall season. The current accumulation strategy in these instances is to charge for short periods, typically 6-8 hours, at high loads (~100 kW). When charging the storage over a longer period, however, the heat load could be reduced by taking advantage of the continuous accumulation that the storage provides. An alternative charging strategy is to accumulate based on available compressor load when operating the compressor at optimum conditions at fixed speed. Moreover, an on/off control of the compressors would reduce the inefficiencies associated with VSD regulation. This paper investigates the operational influence of using a fixed speed compressor compared to a VSD controlled device. System efficiencies are evaluated according to the optimal compressor operation and continuous DHW accumulation.

2. SYSTEM DESCRIPTION

The hotel building was established close to Trondheim, Norway, in 1987. Until 2018, it has been equipped with a heating system consisting of an electric boiler (for base load coverage) and an oil boiler (to cover peak loads). Fig. 1 shows the CO_2 heat pump and chiller unit, which provides the hotel with space heating, DHW and AC cooling. The heating capacity of the system is 280 kW. The heat pump design is based on a typical single-stage supermarket refrigeration unit equipped with heat recovery. The CO_2 unit is composed of four single-stage compressors arranged in parallel, where one compressor is equipped with a VSD. The high pressure and load control of the heat pump is based on feedback signals from the different thermal demands, such as hot tap water, heat towards ventilation- and radiators circuits. The building side supplies these signals to the heat pump controller, which optimizes the high-pressure level within specific constraints, such as the different setpoint temperatures.

The CO_2 heat pump is equipped with four 50 kW air/CO_2-evaporators, at -15 ºC evaporation temperature. In case of simultaneous cooling and heating demands, it is possible to recover heat from a 75 kW chilled water heat exchanger (HX) for AC cooling. The combination of the chiller unit and the heat pump is beneficial, as it reduces the overall operational cost for the hotel operators while satisfying the heating and cooling demands. Heat is delivered to two secondary hydronic circuits through the two gas coolers (GC1 and GC2) in series, where the appropriate temperature adaptation to each secondary circuit is achieved by the CO_2 temperature glide in the supercritical region. The high temperature (HT) circuit is mainly used to reheat tap water through the reheat HX by the use of the recovered high temperature heat from GC1. A radiator backup interface is also installed in the HT circuit and acts as an interface between the two secondary circuits. The mid temperature (MT) circuit provides heat primarily to ventilation heat exchanger batteries and a radiator circuit. The remaining heat is used to elevate the tap water temperature from approximately 8 to 25℃ through the preheat HX. Next, the MT fluid is recirculated back to GC2. The CO_2 temperature is thereby further reduced and the efficiency of the cycle is considerably enhanced. For winter season operations, it is possible to employ the defrost HX in the MT circuit for defrost of the air evaporators.

Hot tap water can be produced continuously in both preheat and reheat HXs when there is a need for ventilation heating. An optimum sized water storage is a key factor for a high system efficiency, as the working range in which the heat pump can operate in optimal conditions is larger. A hot water buffer configuration is especially advantageous in hotel facilities since the DHW consumption curve is characterized by enormous peaks during a few hours in the mornings and evenings. Yet, if DHW is continuously generated, it can be stored for later usage in order to handle these peaks. The hot water storage system consists of tanks in series with a storage capacity of 6 m^3. During charging, DHW is directed to the storage, where it moves through the series of tanks as the buffer is gradually charged from right to left. Cold water is drawn from the last tank (no. 8) and is sent through the heating process. The thermal storage is fully charged when the normally stratified tanks have a high and uniform temperature throughout the buffer.

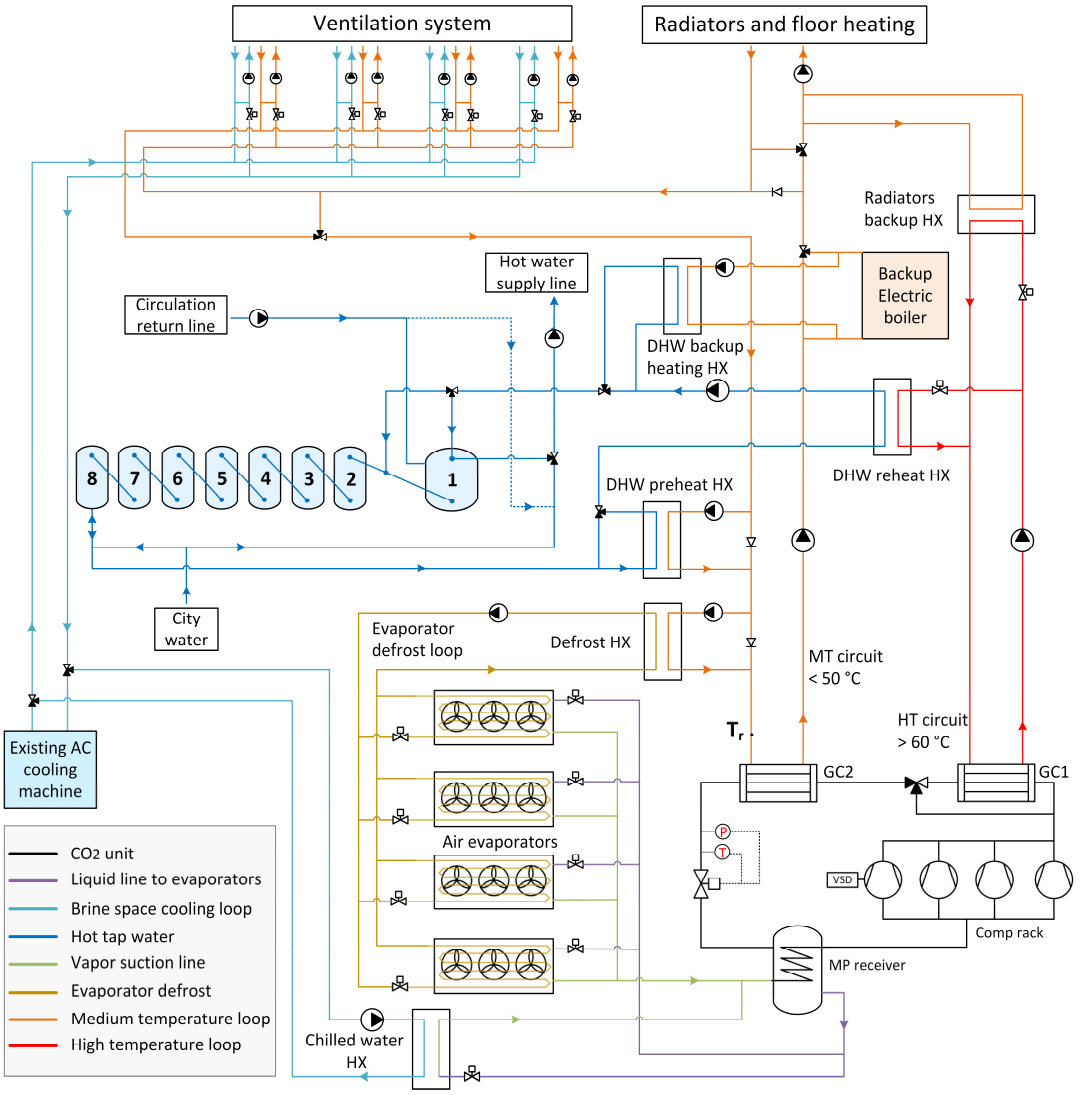

Figure 1: Circuit diagram of CO_2 unit with HVAC and DHW

3. SIMULATION MODEL

A model of the entire thermal system was created in the *Modelica* programming language. The programming environment *Dymola* was used to simulate the quasi-dynamic system with variations of 20 minutes intervals in the setpoint temperatures, heating and cooling loads and DHW usage. The model was built using components from the thermodynamic library, *TIL-Suite*, developed by TLK-Thermo GmbH**.** TIL-Suite is an advanced library for transient simulations of fluid systems and is especially applicable for heat transfer modelling purposes, i,e. heat pumps, refrigeration, cooling and heating systems. Among the components that are included in the library are compressors, pumps, valves and HXs. These can be connected in the oriented physical modeling interface, Dymola, to construct complex models. Each physical element in the diagram structure represent a real physical element in the system. When the component elements are connected in the model structure, the mathematical equations in all components constitute the behavior of the model. All components used in the simulation model of the heat pump and chiller system are specified according to manufacturer description. Plate HXs are used for all heat exchange between the different internal circuits. The VDI

heat transfer model in TIL-library (Martin, 2010) is used to describe the transfer properties of all single-phase liquids in the system. The pressure losses are assumed to be quadratic and mass flow dependent. Constant heat transfer coefficient of 3000 $W.m^{-2}.K^{-1}$ and 2500 $W.m^{-2}.K^{-1}$ are used for the CO_2-side of the gas coolers and evaporators, respectively. TIL-library correlations for quadratic pressure drop in pipes describe the pressure losses in the fin-and-tube evaporators (Wagner, 2001). TIL-Media library is applied for the simulation of the fluids used in the model, which includes refrigerant CO_2, water, glycol and dry air. External data for boundary conditions, heating and cooling loads are imported to the model with the program *TIL-FileReader*. All external data inputs to the model have the resolution of one hour. Dampening transitions are included to increase the stability of the model by reducing rapid changes. The set of model equations are solved with the *DASSL* algorithm.

3.1. Boundary conditions and controlling

The control of the components in the model is achieved according to the specification given by the manufactures of the CO_2 heat pump and chiller unit. PI-controllers operate all the active components in the model, such as compressors, pumps, fans and valves. Each component in the model is controlled according to setpoints in the system. All the important parameters in the hotel thermal system are measured and logged at irregular intervals. As the system is not operating in a controlled environment, irregular data points may occur. A 72-hour period of system operation (3^{rd} – 6^{th} November 2018) was chosen in order to validate the behavior of the Dymola model. This period was selected as it best reflects the specified and typical behavior of the system. Fig. 2 shows the ambient temperatures recorded at the hotel location during the correspondent period. The data was obtained from the Norwegian Meteorology Institute Database. Hourly mean ambient temperatures are applied as model input in evaporators and are used to define the setpoint temperatures of the hotel building (Fig. 3). Curve fittings are applied to the building setpoints that are used in the model.

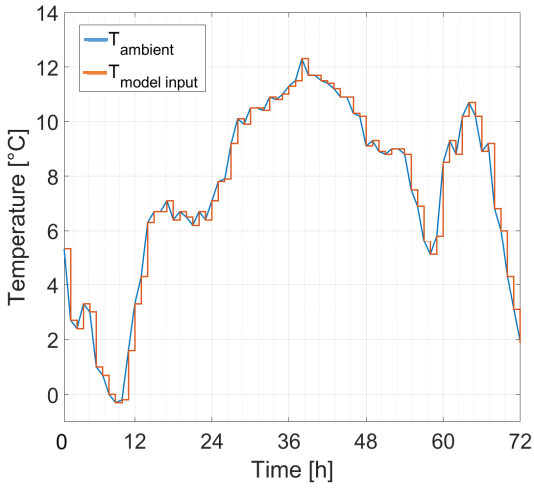

Figure 2: Ambient temperatures and model input

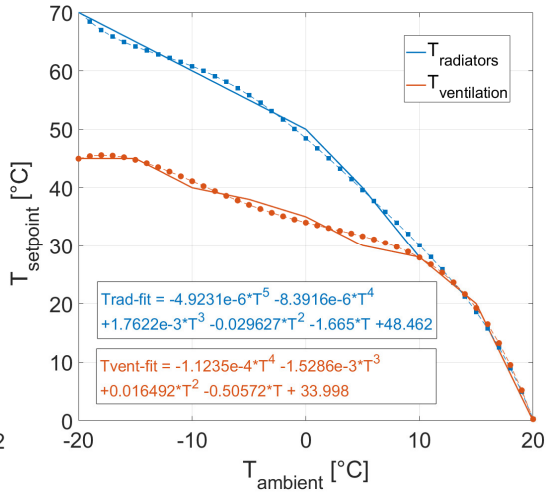

Figure 3: Hotel setpoint temperatures model fitting

The modeled requested compressor load is defined in Eq.(1), where the ratio is approximated based on logged data from the system. The VSD compressor is controlled from a frequency of 30 to 70 Hz, dependent on the required capacity. The three remaining compressors in the rack are controlled by on/off switching. The requested capacity of the model will be increased in steps of 0.05 (5% of total system capacity) if the required temperatures in the system are not reached. The displacement will continue until the temperature setpoints in Fig. 3 are satisfied. A similar strategy is used to reduce capacity should the ventilation supply temperature become considerably higher than the setpoint temperature. The compressors are turned off during low load operations if the setpoints in the model are satisfied.

$$\text{Requested compressor load ratio} = \frac{0.24708(Q_{vent} + Q_{rad} + 1.0335)}{100} + \text{state} * 0.16 \qquad \text{Eq. (1)}$$

State in Eq.(1) is a variable that is assigned values from 0 to 2 based on the energy remaining in the DHW storage. When the temperatures in the DHW storage becomes lower than a threshold, the requested heating capacity of the thermal system is increased as *state* is no longer zero. Fig. 5 shows the simplified control logic used in the Dymola model to recreate the charging behavior in the system. *State 1* is triggered by the requirements described in path *A*. If the demand for DHW is greater than what is supplied to the storage, more heat input is necessary. Path *C* is then activated resulting in *state 2*. Path *D* is included as a temperature restricting of the fluid returning to GC2 (T_r in fig. 1) to limit the CO_2 gas cooler outlet temperature. Only when the storage is fully charged is path *B* triggered and the system returns to normal operations. Fig. 5 shows the specific heat demands applied to the model over the 72 hour period. The data are calculated based on logged power output in the hotel thermal system, where the mean measured values per 20 minutes are used as input to the model. Momentary power peaks and rapid changes are therefore not included. However, the same sum amount of energy per 20 minutes is applied. No AC cooling demand occurred over this time period.

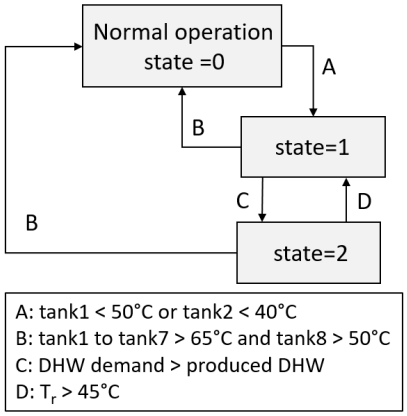

Figure 4: Simplified charging strategy for the DHW storage

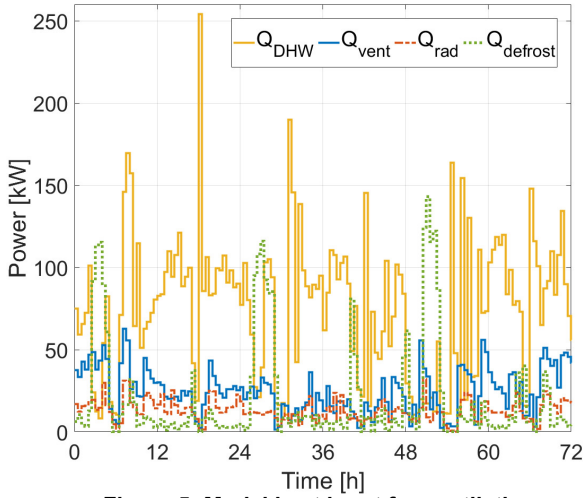

Figure 5: Model heat input for ventilation, radiators, DHW and defrost (hourly changes)

3.2. Model validation

A model of the entire thermal system is simulated for a 72-hour period with the input values described in the previous section. Fig. 6 shows the simulated and measured power input to the hot water subsystem, where the area represents the heat input. These values are equivalent to DHW heat input through the preheat and reheat HXs (see Fig. 1). The figure also displays the percentage energy charge in the storage. 50 and 400 kW are used to define the range between 0-100%. Fig. 7 shows the heat power input to the thermal system through the two gas coolers. The hourly root mean square deviation (RMSD) is 37.1 and 39.0 for the simulated values in Fig. 6 and Fig. 7, respectively. This would be considered high errors were the goal of the model to predict the exact system point values. However, the model behavior is similar to the actual system trends as the heat input (area) occurs at approximately the same time over the period. This is also reflected in the storage energy as chagrining and discharging are cooccurring during the period. A certain delay is observed in the simulated data, which has a large influence on the RMSD values. As the data is investigated over a long time interval, external factors might influence the system behavior. The largest deviation between the simulated and measured data is the magnitude of the power. As it can be seen in Fig. 6 and Fig. 7, the simulated data does not achieve the high power peaks that is observed in the measured data. The underprediction of power input could be explained by model simplification, i.e. neglecting heat losses. This behavior is of little consequence as it is undesirable, and can be explained by the interval length mean values used as model input (Fig. 5). A reduction of the interval would be a possible solution that would decrease the power error. However, the important aspect of the simulation results is that the model is able to fulfill all demand inputs during the period. In addition,

all minimum setpoint temperatures are satisfied during active model operation. The model responds similarly during the same occurrences, i.e. when there is demand for charging the DHW storage and during the low load operations.

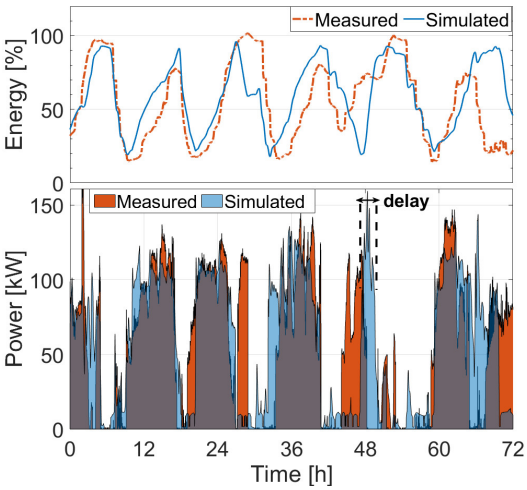

Figure 6: Storage charge, power and heat to the DHW system

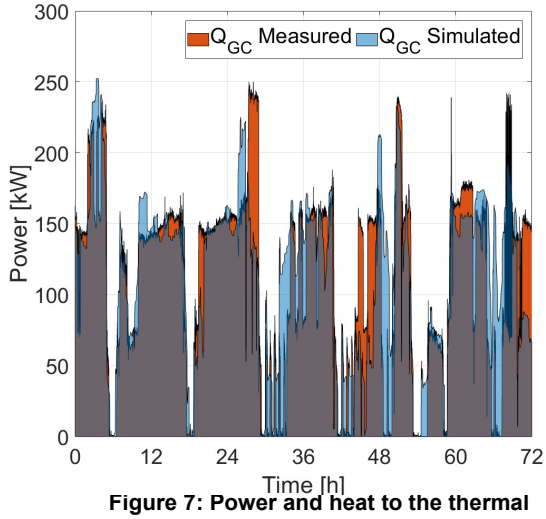

Figure 7: Power and heat to the thermal system through the gas coolers

Eq.(2) defines the energy efficiency of the system over the period as total amount of heat supplied to the thermal system divided by the sum of all power inputs. Table 1 lists the measured and simulated energy efficiency to be comparable. This is indicates that experimental and numerical results are in a good agreement. This is further confirmed when considering the total heat accumulations over the period. Table 1 depicts accumulated heat deviations between the numerical and experimental data of 5.1% (DHW subsystem, Fig.6) and 4.7% (entire thermal system, Fig.7).

Table 1: Measured and simulated produced heat and efficiencies

Parameter	Values	Period (72 h)
Total DHW heat input [kWh]	Measured	4079
	Simulated	4285
	% Error	5.1
Total thermal system heat input [kWh]	Measured	8041
	Simulated	8418
	% Error	4.7
Mean energy efficiency	Measured	2.94
	Simulated	2.92

$$\text{Energy efficiency (E. E.)} = \frac{Q_{GC1} + Q_{GC2}}{\sum W_{compressors} + \sum W_{fans} + \sum W_{pumps}} \qquad \text{Eq. (2)}$$

3.3. Alternative DHW accumulation and compressor control

Constant frequency of 50 Hz is applied to all compressors in the model and the control strategy of the system is modified in order to investigate possible operational benefits. The DHW storage is charged with available heat when the compressors are operating in optimum conditions. The requested capacity is defined by Eq.(1). However, *state* is zero at all times. The compressors will operate with the same off-conditions at low loads when setpoints are satisfied. If the setpoints temperatures in the system are not satisfied, a second compressor will be activated. This will also be the case if condition *A* (Fig. 4) is satisfied. If this is still not sufficient to charge the storage, a third compressor will be switched on as condition *C* is satisfied. Similar as the behavior presented in Fig. 4, the number of compressors activated by the storage is reduced to normal when the storage is fully charged, during which the number of active compressors again is defined by Eq.(1).

4. SIMULATION RESULTS AND DISCUSSION

A fixed-speed compressor control strategy is applied to the model and simulations are conducted for a 72-hour period. No additional model modifications are made. Setpoints, boundary conditions and input values are as stated in section 3.1. Fig. 8 shows the power and heat (area) to the DHW subsystem and the instantaneous energy charge (%) in the storage. Fig. 9 shows the power and heat to the entire thermal system. It is observed from both figures that the heat area and peak power values are reduced compared to the simulations with VSD regulation. The desired model behavior of heat recovery over a longer period at lower intensity is achieved. The buffer is charged over a longer period by using available load in the compressors. The storage capacity is higher for longer periods due to continuous DHW accumulation. The total heat energy accumulated over the period is 4275 kWh and 8420 kWh for the fixed-speed compressor case in Fig. 8 and Fig. 9, respectively. This is a slight increase compared to results from the simulation with VSD, which confirms that the fixed-compressor operational strategy is a functional alternative to VSD-regulation. All thermal demands are fulfilled and all minimum temperature setpoints are satisfied during the operating time of the system.

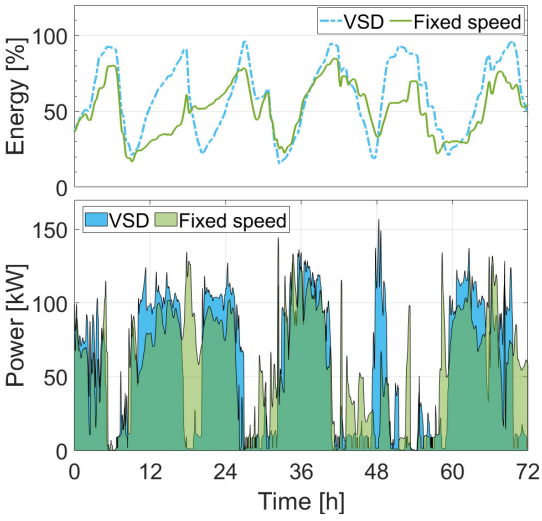

Figure 8: Storage charge, power and heat to the DHW system with fixed-speed compressors

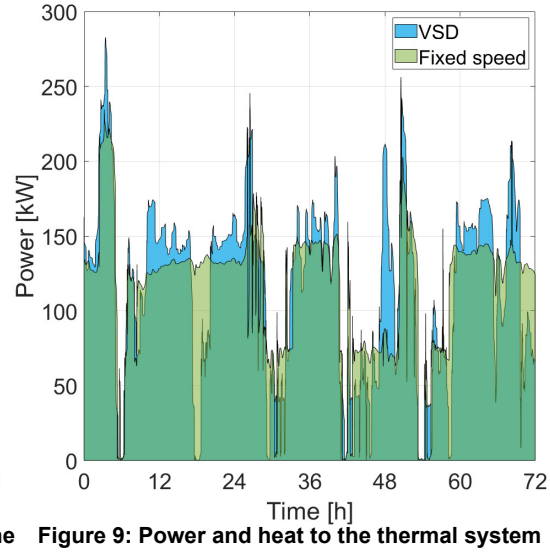

Figure 9: Power and heat to the thermal system through the gas coolers with fixed-speed compressors

The mean energy efficiency of the entire thermal system is 3.03 for the period, which is a 3.8% increase in relation to the reference validation case (E.E. = 2.92) with VSD controlled compressors. For both simulations, only three of the four compressors in the rack are activated during the 72-hours. However, the maximum compressor motor power input is reduced with 22.6 kW (from 99.2 kW to 76.6 kW) in the fixed-speed investigation. The overall energy input to the compressors are reduced from 2726 kWh to 2601 kWh, which is a difference of 125 kWh or about 4.6% for the entire period. A 108 kWh or 3.6% reduction in work energy input to the complete thermal system is achieved (from 3034 kWh to 2926 kWh) in relation to the VSD regulation results. The energy consumption of the entire thermal system is thus reduced whilst there is an increase in total heat output. The operating time of the compressors are increased from 91% to 94% or with about 3 hours over the interval. Heat recovery from the AC chiller unit is normally limited, as heating and cooling demands are generally not synchronized. However, fixed-speed compressor control allows for DHW accumulation over longer periods. A larger amount of heat could therefore potentially be recovered from the AC ice water as the operating period is increased. Combined heat pump and chiller mode is not investigated in this paper, as a cooling demand is not recorded in the selected time interval. This investigation only reveals the benefits of fixed-speed compressors for periods with similar system operation and behavior. A broader selection of operational scenarios should therefore be investigated to fully reveal the potential benefits of fixed-speed compressor control in systems with thermal storage.

5. CONCLUSIONS

This work investigates the operational strategy and design of the first CO_2 heat pump and chiller unit installed in a Nordic hotel. A dynamic simulation model of the entire thermal system is constructed with the Modelica programming language. A 72-hour period of system operation is selected to validate the model behavior. Variations with 20 minute intervals in the ambient temperatures, setpoint temperatures, heating and cooling loads and DHW usage are applied to the model. The simulation results show high RMSD values, which are mainly caused by mismatch due to delay in model behavior. The model responds similarly to the system during events, which is the consequential aspect of the model validation. All demands and all minimum setpoint temperatures are satisfied with 4.7% error in total heat energy accumulated over the period.

The thermal storage enables accumulation of DHW based on available load when operating the compressors, which is currently applying VSD to one compressor. An alternative fixed-speed compressor control strategy is therefore evaluated. The mean energy efficiency of the complete thermal system increases by 3.8% to 3.03. The maximum compressor motor power input is reduced with 22.6 kW in the fixed-speed investigation. The overall energy demand (wihtin the investigated period of 72 h), to the compressors is reduced with 125 kWh or about 4.6%. For the model of the entire thermal system, a 3.6% reduction in energy input is observed. The energy consumption of the entire thermal system is reduced with a similtanous increase in the total heat output. The results show that a fixed-speed compressor control is beneficial and should be considered in future systems.

NOMENCLATURE

Q	Work Input (kW)	W	Heat Input (kW)

REFERENCES

Bohdanowicz, P., 2005. European hoteliers' environmental attitudes: Greening the business. Cornell Hotel and Restaurant Quarterly 46, 188–204.

Bohdanowicz, P., Martinac, I., 2007. Determinants and benchmarking of resource consumption in hotels - Case study of Hilton Int.ernational and Scandic in Europe. Energy and buildings, 39(1), 82-95.

D'Agaro, P., Coppola, M.A. and Cortella, G., 2019. Field tests, model validation and performance of a CO2 commercial refrigeration plant integrated with HVAC sustem. International Journal of Refrigeration, accepted manuscript, january 2019.

Deng, S. M., Burnett, J., 2002. Water use in hotels in Hong Kong. International Journal of Hospitality Management, 21(1), 57-66.

Lee, J.-S., Hsu (Jane), L.-T., Han, H., Kim, Y., 2010. Understanding how consumers view green hotels: how a hotel's green image can influence behavioural intentions. Journal of Sustainable Tourism 18 (7), 901-914.

Hafner, A., Banasiak, K., 2016. R744 ejector technology future perspectives. Journal of Physics: Conference Series, 745(3), 032157.

Martin, H., 2010. N6 pressure drop and heat transfer in plate heat exchangers. In VDI Heat Atlas. Springer, Berlin, Heidelberg, 1515-1522.

Norwegian Water Resources and Energy Directorate (NVE). Analyse av energibruk i yrkesbygg. Report No. 24 (2016), Oslo, 36-40.

Standard Norway SN/TS 3031, 2016. Energy performance of buildings – Calculation of energy needs and energy supply. Report No. 1 (2016), Oslo, 41-43.

Smitt, S. M., Hafner, A., Hoksrød, E., 2019. Presentation of the first combined CO2 heat pump, air conditioning and hot tap water system for a hotel in Scandinavia. IIR Conference on Ammonia and CO_2 Refrigeration Technologies. Ohrid, Republic of Macedonia, April 11-13, 2019.

Zhang, J. F., Qin, Y., Wang, C. C., 2015. Review on CO2 heat pump water heater for residential use in Japan. Renewable and Sustainable Energy Reviews, 50, 1383-1391.

Wagner, W., Strömung und Druckverlust, 5. Auflage, Vogel Buchverlag, 2001. d

Paper IV

S. Smitt, I. Tolstorebrov, A. Hafner (2020). "Integrated R744 unit for hotels: Analysis of field data." In: *Proceedings of the 13th IIR Gustav Lorentzen Conference on Natural Refrigerants*, Kyoto (Online), Japan.

PAPER ID: 1056
DOI: 10.182/iir.gl.2020.1056

Integrated R744 unit for hotels: Analysis of field data

Silje M. SMITT, Ignat TOLSTOREBROV, Armin HAFNER

Norwegian University of Science and Technology,
Kolbjørn Hejes vei 1D, 7491 Trondheim, Norway,
silje.smitt@ntnu.no, ignat.tolstorebrov@ntnu.no, armin.hafner@ntnu.no

ABSTRACT

This study investigates the performance of an integrated R744 HVAC and domestic hot water unit for a Norwegian hotel. The thermal system of the hotel is described and data from the first year of operation are analyzed. The heating and cooling capacities supplied by the integrated R744 unit are studied on a weekly and monthly basis to evaluate the seasonal behavior of the system. The hot water storage devices can hold an energy of 350 kWh at fully charged conditions and demonstrated peak demand reductions of more than 100 kW during a two-day period. The results show that the hot water usage accounts for 52 % of the annual heat load of the hotel. The energy efficiency analysis reveals an annual system COP of 2.90, and thus an untapped system improvement potential that can be exploited by re-evaluating the hot water charging strategy of the R744 unit.

Keywords: CO_2 heat pump and AC, combined heating and cooling systems, hot thermal energy storage, domestic hot water production, analysis.

1. INTRODUCTION

An increased focus on environmentally friendly heat pump solutions together with a global effort to reduce the application of F-gases is strengthening the position of natural refrigerants. In recent years, R744 heat pumps has been successfully implemented in buildings with high domestic hot water (DHW) demands, such as hotels, gyms and pool facilities (Rony et al., 2019). Integrated R744 units that provide DHW, heating and cooling can achieve efficiencies that are comparable to HFC systems, as demonstrated by Tosato et al. (2019), Byrne et al., (2009) and Cecchinato et al. (2005). However, different modes of R744 operation and control of DHW storage systems can highly influence efficiency (Tosato et al., 2019; Minetto et al., 2016). This paper presents the operation of an integrated R744 unit with 6 m^3 thermal storage for hotel application through long-term logged data, where the influence of different modes of operation are evaluated.

2. SYSTEM DESCRIPTION AND INSTRUMENTATION

The integrated R744 HVAC unit is installed in medium sized (9000 m^2) hotel in Trondheim, Norway. The system was installed as part of a refurbishment of the thermal system in 2018, replacing the existing electric- and oil boiler. After 6 months of operation a monthly energy-saving of 59-69 % was achieved (Smitt et al., 2019). The R744 unit is an adapted single-stage supermarket refrigeration unit with an installed heating and air conditioning (AC) cooling capacity of 280 kW and 75 kW, respectively. Heat production is achieved with the same strategy that is applied for heat recovery in transcritical R744 supermarket units (Danfoss, 2015), with the exception that the heating load, rather than the cooling load, is the controlling parameter. Four air evaporators (50 kW at -15 °C) are installed and applied dependent on the heating load. Alternatively, a heat exchanger (HX) interface (75 kW at 12/7 °C) to the chilled water circuit (HX6) can be used to recover heat if AC cooling is needed. The chilled water produced by the R744 system is used to supplement the existing AC chiller unit and is only applied as an auxiliary function during heat production. The R744 system provides heating and DHW for the hotel through two separate hydronic circuits, as shown in Figure 1. A mid temperature circuit (< 50 °C) provides heat through the second gas cooler (GC2) to space heating, DHW preheat and defrost of evaporators. The high temperature circuit (> 60°C) is supplied through GC1 and is primarily applied for DHW reheating through HX3. During winter operations, high-temperature heat can be supplied from this circuit to the hotel's radiators and floor heating systems through HX5.

The DHW subsystem consists of several tanks in series with a combined water volume of 6 m^3. The DHW system is supplied with heat from the R744 unit through HX2 and HX3, or from the backup electric boiler through HX4. The control of the R744 unit is characterized by two distinctive modes of operation; active charging of DHW tanks (charging mode) and non-charging mode. During the non-charging mode, most of the heating load is allocated to the mid-temperature circuit to cover the moderate temperature demands, e.g. radiators, floor and ventilation heating. Excess heat is allocated to the DHW subsystem, usually at a low load to achieve the required DHW temperature. The second mode of operation occurs during charging of the DHW storage and is activated when the temperatures in foremost tanks (1-3) fall below a threshold. During the charging process, excess hot water is stored and moves through the series of tanks as the buffer is gradually charged from tank 1 to tank 10. Water is drawn from the last tank, tank 10, and is sent through the heating process, in the same manner as described by Minetto (2011). The thermal storage is fully charged when the normally stratified storage reaches a high and uniform temperature.

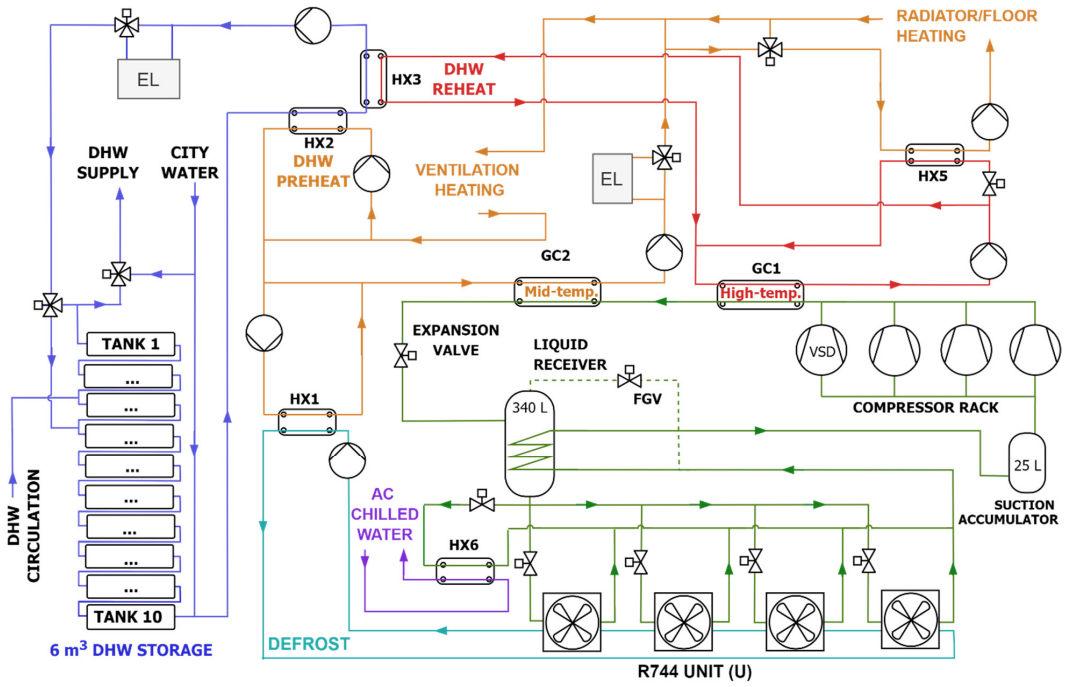

Figure 1: System layout

2.1. Data acquisition method

The evaluation of the system performance under different modes of operation is carried out by means of sensors that are used to calculate key performance indicators. All hydronic fluid branches are instrumented with temperature sensors (NTC10 thermistors, ± 0.2 K) and mass flow meters (oscillator mass flow sensor, class 2). Temperature sensors in the DHW tanks and secondary systems have been validated to operate within a range of ± 0.1 K. Heat flow meters for secondary fluids are installed at every HX (PT500 temperature sensors, oscillator mass flow sensor, class 2) and electrical power supply monitors (energy analyzer in control unit, ± 2%) are installed in the R744 unit. The real-time field measurements of the hotel have been obtained via the web-monitoring software IWMAC (IWMAC, 2009). All the recorded data have been resampled and synchronized to the same time step, using the weighted average of the time intervals. The DHW loads were calculated as described by Smitt et al. (2020), due to the lack of an energy meter in the DHW supply line. The data used in this analysis were collected and processed for the period from September 2018 to September 2019.

2.2. Performance indicators

The following parameters are calculated to assess the performance of the thermal system. Collected measurements for heating capacities, AC capacities and power consumption are used to calculate the seasonal coefficient of performance (SCOP) of the R744 system. The SCOP of the R744 unit and secondary systems, referred to as $SCOP_{sys}$, is defined as the ratio of useful thermal load to the total electricity consumption, using Eq. (1). The average value of calculated measurement uncertainty is included in the equation.

$$SCOP_{sys} = \frac{\sum(\int \dot{Q}_{GC1} + \int \dot{Q}_{GC2} + \int \dot{Q}_{\mathrm{AC}})}{\sum(\int \dot{W}_{\mathrm{compressors}} + \int \dot{W}_{\mathrm{fans}} + \int \dot{W}_{\mathrm{pumps}} + \int \dot{W}_{\mathrm{aux,el}})} \pm 6.2\ \% \qquad \text{Eq. (1)}$$

$\dot{W}_{\mathrm{compressor}}$, $\dot{W}_{\mathrm{fans}}$, and $\dot{W}_{\mathrm{pumps}}$ [kW] represent the combined electricity consumption for all compressors, evaporation fans and pumps, respectively. $\dot{W}_{\mathrm{aux,el}}$ [kW] is the electricity consumption for auxiliary systems, such as control and monitoring equipment. Q_{GC1} and $\dot{Q}_{GC2}$ [kW] is the heat supplied through the gas coolers as shown in Figure 1, while $\dot{Q}_{\mathrm{AC}}$ is the AC load that is supplied through HX6.

The SCOP for the entire thermal system is used to evaluate the overall performance of the thermal system in the hotel. $SCOP_{sys+el}$ is calculated using Eq. (2) and includes heat and work from the electric boiler.

$$SCOP_{sys+\mathrm{el}} = \frac{\sum(\int \dot{Q}_{GC1} + \int \dot{Q}_{GC2} + \int \dot{Q}_{\mathrm{AC}} + \int \dot{Q}_{\mathrm{EL}})}{\sum(\int \dot{W}_{\mathrm{compressors}} + \int \dot{W}_{\mathrm{fans}} + \int \dot{W}_{\mathrm{pumps}} + \int \dot{W}_{\mathrm{aux,el}} + \int \dot{W}_{\mathrm{EL}})} \pm 10.5\ \% \qquad \text{Eq. (2)}$$

where $\dot{Q}_{\mathrm{EL}}$ and $\dot{W}_{\mathrm{EL}}$ is the heat and power associated with the operation of the electric boiler, respectively.

3. RESULTS

Field results from the operation of the thermal system in the hotel is presented in this section. The focus of the results is surrounding how DHW charging and non-charging mode influence the system performance. Figure 2 shows parameters essential to the operation of the DHW system over a two-day period, demonstrating both charging and non-charging mode. Figure 2A shows the temperature stratification across the storage, which is illustrated by the temperatures in tanks 1, 5 and 10. The storage load and the corresponding energy in the storage over the period are shown in Figures 2B and 2C, respectively. Figure 2D shows the temperature of water that is returned to gas cooler 2 for reheating.

The water temperature of the storage fluctuates between 8 and 78°C during the period. The state of the storage can be determined by studying the temperatures in tank 1 and tank 10. As the last tank in the series, tank 10 is sensitive to change in DHW mass flow rates entering and exiting the DHW subsystem. Supply water at 8 °C enters tank 10 during discharge and is gradually pushed through the storage as hot water is drawn from tank 1. The sudden drop in all temperatures in Figure 2A illustrates the discharge of the storage and corresponds to peaks in the DHW usage, as can be observed in Figure 2B. The energy potential of the storage is fully exploited when tank 1 reaches its minimum water temperature. The charging of the storage is illustrated by the increase in the temperatures across the buffer. Hot water is supplied to the storage via tank 1 and is circulated through the buffer. The temperature boundary between hot and cold moves through the storage, as tank temperatures are lifted. As a consequence, the temperature of the water returning from mid temperature circuit to the second gas cooler increases, which elevates both the gas cooler outlet temperature and pressure.

As seen from Figures 2A to 2D, there is a 24-hour pattern to the behavior of the DHW storage temperatures. The storage energy is fully exerted and is recharged twice a day. This is reflected in Figure 2B, which shows that the storage is typically charged for 7 to 10 hours. The sudden drop in storage temperature can be seen in reference to the behavior of DHW usage. As shown in Figures 2A and 2B, large values of DHW usage peaks in the range of 200 kW cause a rapid decrease in the storage temperatures. The storage buffer provides a beneficial reduction of peak loads, which is represented by the difference between DHW usage and DHW storage heat supply, which is more than 100 kW during peak hours. At fully charged conditions, the storage reaches an energy potential of approximately 350 kWh. Another benefit of the large storage volume is higher flexibility in DHW production, which allows for low-intensity DHW generation over longer time intervals.

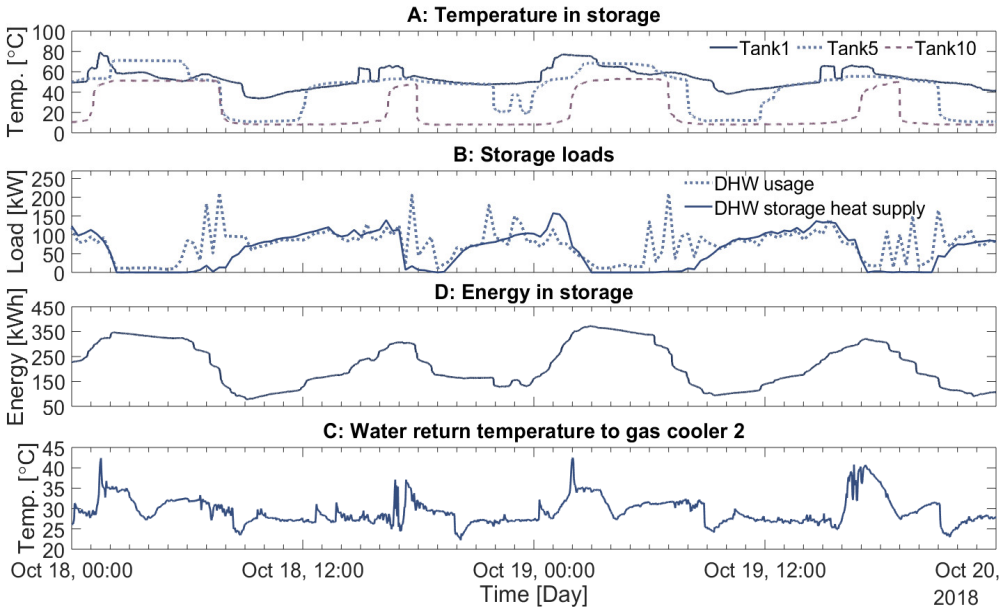

Figure 2: Operation of the DHW system over a 2-day period showing (A) storage temperature, (B) storage loads, (C) energy in the storage and (D) water return temperature to gas cooler 2 (GC2).

The hot water consumption in hotel buildings is characterized by large consumption peaks for a few hours during the mornings and evenings. Figure 3 shows the hot water average daily consumption profile, DHW usage [kWh], and the profile of heat supplied by the heat pump to the storage [kWh], over a period of one year. The average DHW daily usage during this period is 1104 kWh/day. However, significant variations in daily consumption were recorded with maximum and minimum values of 2480 and 480 kWh/day. On average, 2.3% of the DHW usage is covered by the electric boiler. As seen in Figure 3, most of the DHW usage occurs between hour 8 and midnight. The peaks in DHW usage occur during hours 9 and 23 at values around 70 kWh. However, the heat supply to the storage does not exceed 58 kWh due to the buffer effect granted by the storage, which demonstrates how the system handles power peaks on an average basis. On an annual basis, DHW usage account for 52 % (403,000 kWh) of the annual heat consumption in the hotel, which is within the normal value of 40-70% for this type of building (Su, 2012; Deng and Burnett, 2000).

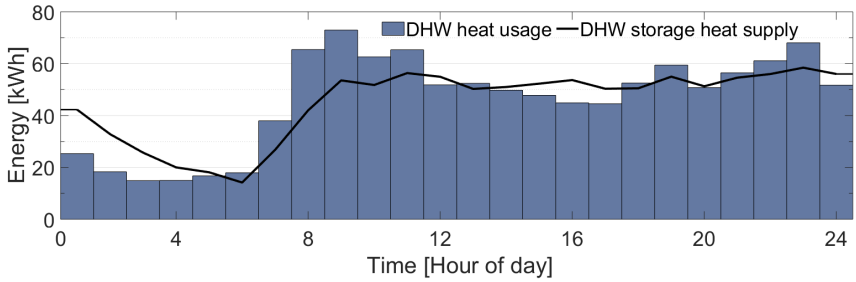

Figure 3: Hourly-average DHW usage and DHW storage heat supply from Sep. 2018 – Sep. 2019.

The seasonal SCOPs and annual values are listed in Table 1. The average ambient temperature, T_a, for the specified intervals are included in the table. All SCOPs are highly dependent on T_a and increase with approximately 0.4 from the winter to the summer season. The somewhat low value of annual $SCOP_{sys}$ of 2.90 for the integrated system is partially due to the limited recovery of cold energy to the AC cooling circuit. On an annual basis, approximately 5% of the total heat to the hotel is supplied by the electric boiler. As a result, $SCOP_{sys+el}$ is reduced by 9% when compared to $SCOP_{sys}$. It is expected that the boiler is applied during the

winter season to cover peak heating. However, the low value of $SCOP_{sys+el}$ during the summer season indicates excessive use of the boiler for DHW heating. This is explained by the high return temperature of water to GC2, as shown in Figure 2D. Excessive gas cooler exit temperature triggers a signal to reduce the compressor capacity, due to compromised efficiency. Consequently, DHW production by the heat pump is reduced and the required load is then compensated by the boiler.

Table 1: Seasonal and annual COP from Sep. 2018 to Sep. 2019

Season	Period	$SCOP_{sys}$	$SCOP_{sys+el}$	T_a [°C]
Spring, Fall	September-November, April-June	2.99 ± 0.19	2.73 ± 0.29	8.4
Winter	November-April	2.78 ± 0.17	2.57 ± 0.27	0.4
Summer	June-September	3.20 ± 0.20	2.75 ± 0.29	15.0
Annual	September-September (2018-2019)	2.90 ± 0.18	2.64 ± 0.28	6.8

The mean COP_{sys} for transcritical operations (>73.9 bar), within specific temperature intervals are shown in Figure 4. The COPs are categorized by whether DHW charging is taking place. Situations when the DHW storage is being actively charged, and the system is controlled according to both SH and DHW loads, are identified by the subscript *ch*. The subscript *nch* includes circumstances when the heat supply to the hotel is controlled by SH demands, and no active charging of the DHW storage is taking place. The analysis of variance (ANOVA: single factor) was applied to analyze the efficiency of the system under different modes of operations. The difference is considered significant at $p < 0.05$.

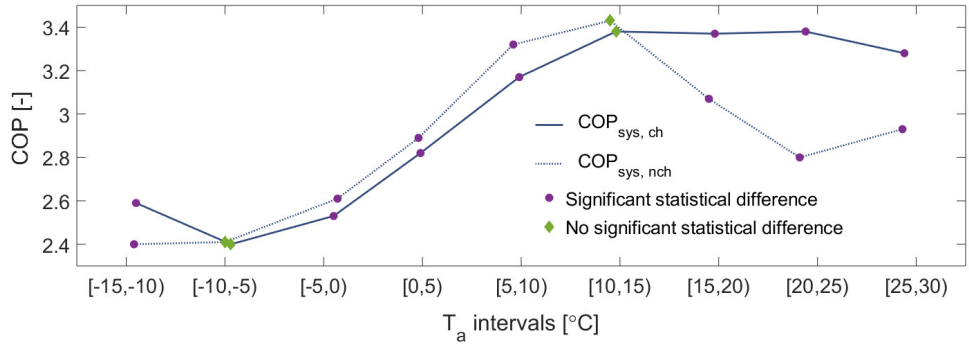

Figure 4: COP during DHW charging and non-charging for specific temperature intervals.

Figure 4 exhibits significant difference between charging and no charging values of COP_{sys} for all intervals, with the exception of -10 to -5°C and 10 to 15°C. The mean COP_{sys} during no DHW charging, $COP_{sys,nch}$, is generally higher than charging mode COP_{sys}, $COP_{sys,ch}$, at low temperatures. However, both $COP_{sys,ch}$ is considerably higher than $COP_{sys,nch}$ at ambient temperature above 15°C. This unusual relationship between the two modes of operation can be explained by the magnitude of the space heating load and the temperature of the water returning to the second gas cooler. The temperature of the fluid returning from the secondary system is generally higher at high values of space heating, as the setpoints of space heating and thus the return temperatures are elevated at low values of T_a. Additionally, DHW charging provides a temperature lift in the return circuit, which was also illustrated by Tosato et al. (2019). They noted a reduction in COP of 18 % during the final part of the DHW charging process, which was caused by high return temperatures from the storage. Hence, during seasons with low T_a, high space heating and thus generally high return fluid temperature, the heating load of the R744 unit is limited due to high gas cooler outlet temperatures. This problem diminishes when space heating is limited, as can be observed in Figure 4 at T_a above 15°C.

4. CONCLUSIONS

This work investigated key operating parameters for an R744 heating and AC cooling unit installed in a Norwegian hotel. The system is integrated with HVAC, DHW and a 6 m^3 thermal storage. Field measurements

from the hotel were analyzed for a one-year period and essential parameters to evaluate the system performance under different modes of operation were discussed. The DHW load accounts for 52% of the annual heat load supplied to the hotel and follows a particular 24-hour pattern, with low consumption between midnight and hour 6. The peak DHW load occurs around hour 9 and reaches an hourly-averaged value of 73 kWh. The DHW storage holds an energy capacity of 350 kWh at fully charged conditions and demonstrates peak demand compensation of more than 100 kW during a two-day period. The COPs during DHW charging mode are higher when compared with no charging mode at ambient temperatures above 15°C, due to limited space heating demands. The annual SCOP for the integrated R744 system was found to 2.90. Additionally, about 5% of the total heat to the hotel is supplied by the electric boiler, which decreases overall system SCOP by 9%. The application of the boiler is often a result of high return temperatures from the building during DHW charging, which limits the operation of the heat pump. Other factors that greatly influence the efficiency of the system are variations in the ambient temperatures and high temperatures at the gas cooler exit. Future work should therefore focus on increasing the system performance by charging the storage during longer periods at reduced capacities.

NOMENCLATURE

AC	Air Conditioning
DHW	Domestic Hot Water
GC	Gas Cooler
HVAC	Heating, Ventilation, Air Conditioning
HX	Heat Exchanger
$\dot{Q}$	Thermal load [kW]
SCOP	Seasonal Coefficient of Performance
$\dot{W}$	Power [kW]

subscripts

aux,el	Auxiliary electrical equipment
ch	Charging mode
EL	Electric boiler
nch	Non-charging mode
sys	R744 unit and secondary systems
sys+el	R744 unit, secondary systems and boiler

REFERENCES

Byrne, P., Miriel, J., Lenat, Y., 2009. Design and simulation of a heat pump for simultaneous heating and cooling using HFC or CO_2 as a working fluid. International Journal of Refrigeration 32, 1711–1723.

Cecchinato, L., Corradi, M., Fornasieri, E., Zamboni, L., 2005. Carbon dioxide as refrigerant for tap water heat pumps: a comparison with the traditional solution. International Journal of Refrigeration 28, 1250–1258.

Danfoss, 2015. Application guide: Heat Reclaim in Transcritical CO_2 Systems. URL: https://assets.danfoss.com/documents/DOC167786419094/DOC167786419094.pdf. Application guide DKRCE.PA.R1.F1.22.

Deng, S.M., Burnett, J., 2000. A study of energy performance of hotel buildings in Hong Kong. Energy and Buildings 31, 7–12.

IWMAC, 2019. Centralized Operation and Surveillance by Use of WEB Technology. URL: https://www.iwmac.com.

Minetto, S., 2011. Theoretical and experimental analysis of a CO_2 heat pump for domestic hot water. International Journal of Refrigeration 34, 742–751.

Minetto, S., Cecchinato, L., Brignoli, R., Marinetti, S., Rossetti, A., 2016. Water-side reversible CO2heat pump for residential application. International Journal of Refrigeration 63, 237–250.

Rony, R.U., Yang, H., Krishnan, S. and Song, J., 2019. Recent advances in transcritical CO2 (R744) heat pump system: a review. Energies, 12(3), p.457.

Smitt, S., Tolstorebrov, I., Hafner, A., 2020. Integrated CO_2 system with HVAC and hot water for hotels: Field measurements and performance evaluation. International Journal of Refrigeration 116, 59-69.

Smitt, S., Hafner, A., Hoksrød E., 2019. Presentation of the first CO_2 heat pump, air conditioning and hot tap water system for a hotel in Scandinavia. Proceedings of the 8th Conference on Ammonia and CO_2 Refrigeration Technologies. 11-13 April 2019. Ohrid, Republic of Macedonia.

Su, B., 2012. Hotel design and energy consumption. World Academy of Science, Engineering and Technology 72, 1655–1660.

Tosato, G., Girotto, S., Minetto, S., Rossetti, A., Marinetti, S., 2019. An integrated CO_2 unit for heating, cooling and DHW installed in a hotel. Data from the field., in: 37th UIT Heat Transfer Conference.